UNIVERSITY OF CALIFORNIA, SAN DIEGO

Absorption, Metabolic Incorporation, and Inflammation Engendered by the Non-human Sialic Acid, *N*-glycolylneuraminic Acid

A dissertation submitted in partial satisfaction of
the requirements for the degree of Doctor of Philosophy
in

Biomedical Sciences

by

Christopher John Gregg

Committee in Charge:

Professor Ajit Varki, Chair
Professor Jeffrey D. Esko
Professor Gary S. Firestein
Professor Chris K. Glass
Professor Joseph L. Witztum

2011

The dissertation of Christopher John Gregg is approved, and it is acceptable in quality and form for publication on microfilm and electronically:

Chair

University of California, San Diego

2011

DEDICATION

This dissertation is dedicated to the scientists whose work formed its foundations.

TABLE OF CONTENTS

LIST OF FIGURES

CHAPTER 1

CHAPTER 2

CHAPTER 3

CHAPTER 5

APPENDIX I

LIST OF TABLES

ACKNOWLEDGEMENTS

This disseration would not be possible without the work of many scientists resulting in the publications of which I am so proud. Chapter 1, in part, is a reprint of the material as it appears in *Varki NM, Anderson D, Herndon JG, Pham T, Gregg CJ, Cheriyan M, Murphy J, Strobert E, Fritz J, JG E, & Varki A, Evolutionary Applications 2:101-112, 2009*. Chapter 2, in full, is based on a pre-final manuscript, *Banda K*, Gregg CJ*, Chow RE, Varki NM, Varki A, in preparation Journal of Biological Chemistry* (* denotes equal authorship). Chapter 3, in full, is a reprint of the material as it appears in *Pham T*, Gregg CJ*, Karp F, Chow R, Padler-Karavani V, Cao H, Chen X, Witztum JL, Varki NM, & Varki A, Blood Journal, 114:5225-5235, 2009* (* denotes equal authorship). Chapter 4 and Appendix I, in part, are reprints of the material as it appears in *Taylor RE, Gregg CJ, Padler-Karavani V, Ghaderi D, Yu H, Huang S, Sorensen RU, Chen X, Inostroza J, Nizet V, & Varki A, J Exp Med 207:1637-1646, 2010*.

Ajit Varki is an amazing mentor. I have been incredibly lucky to stumble into a training opportunity with Ajit at UCSD. Ajit combines his incredible scientific aptitude with an infectious work ethic, boundless curiousity, and a love of good people. Thank you, Ajit for helping me stay the course. Your eyes were always on the goal and you steered my work straight through the lefts & the rights, through the ups & the downs. I will always reflect the intellectual breadth you bring to bear on glycobiology. Although it is difficult to synthesize immunology, evolution, microbiology, medicine, chemistry, and glycobiology, I understand that the difficulty is rewarded with novel perspective.

To my distinguished committee members and other mentors, thank you for making UCSD a world class, biomedical research facility with all the best and none of

worst features of world-renowned research universities. To Jeffrey Esko, thank you for dedicating your time to serving on my committee. You are an amazing scientist and you hold rigorous science in the highest regard. I have tried to emulate your skepticism and critical thinking in my projects. I also need to thank you for your commitment to training the very best students, whether in your lab or in the graduate program in general. To Gary Firestein & Christopher Glass, thank you for sitting on my thesis committee and providing me with guidance as my project matured. To Nissi Varki, I can't thank you enough, both as a colleague and for supporting our lab when you have so very much on your plate. Thank you for helping me understand pathology and teaching me how to approach looking for a needle in a haystack. To Pascal Gagneux, I am very fortunate to have crossed paths with you. I have enjoyed every one of our conversations and you have taught me to never stop learning. Thank you for the opportunity to participate in the early incarnations of CARTA.

Sandra Diaz should be canonized, if she ever retires. Thank you a million times, Sandra, for carrying the lab. If a method seemed foreign and daunting, you had mastered it in the early '80s. If an experiment was more intense than expected, you would jump in to support the cause without asking. If you were busy, you would always take time to listen to questions or concerns. If you weren't at work, you'd answer the phone when we called. If you quit, the lab might fall apart and that is frightening.

Varki Lab (2005-2009), thank you. To Tho Pham, you are wise beyond your years. Thank you for showing me what a true scientist is and for our amazing collaboration. To Darius Ghaderi & Jonas Löfling, you guys were amazing colleagues. By being immersed in your antics, you taught me how to tenaciously attack projects to wade through the failures of experimental science. To Rachel Taylor, you taught me that the experiment is in the controls. Your attention to detail forced me to slow down

and actually plan better experiments. To Vered Padler-Karavani, you deserved tenure track long ago. You are a brilliant scientist and you set an amazing example both professionally and personally. If we just keep going, we will be paid our dues some day. To Nancy Hurtado, thank you for teaching me so much about cytometry. When I took over the cytometer from you, I had no idea it would be one of the most intellectually fruitful, yet simultaneously cursed endevours of graduate school. To Miriam Cohen, thank you for your expertise in microscopy. Your images are beautiful and you are invaluable as a resource to those around you wherever you are. To Lance Stein, thank you for the laughs and for helping with the truly digusting aspects of studying Neu5Gc. To Pascal Lanctot, thank you for the back hand. Our pick-up throwing sessions will always be “a San Diego memory”.

Varki Lab (2009-present), thank you. To Kalyan Banda, you’ve got a brilliant mind and I have really enjoyed struggling through our project with ample doses of work and play. I couldn’t have done this without you. To Oliver Pearce, I have really enjoyed our musings about biology, sialic acids, evolution, ethics, experiments, controls, and everything else. You have been an amazing colleague and friend. I have learned much from you, Chemist. To Leela Davies, it is curious how things happen. I never expected the person who relentlessly questioned me at my poster about Neu5Gc and human evolution to join the lab and become such a fast friend. It has been amazing working side-by-side with you and watching you grow. Don’t worry, you’ve got this. To Paula Soto, you have been a great colleague and neighbor. I just wish we had gotten the Neu1 story to unfold easily on our way out. To Patrick Secrest, you ran the show. Without your tireless dedication, I would have had to cast off complicated animal experiments, like the Aging Study, as impossible. To Anne Bergfeld, you are an amazing scientist, generous person, and good friend. In your short time with us, you

have been invaluable to the lab. I hope that you have found everything you were looking for when moving to San Diego. To Melanie Neize, thank you so much for administering our work. We would all (Ajit included) fall apart without you. To Fang Ma, I have enjoyed tackling similar problems together while pursuing different projects. You have absorbed everything that I have taught you and, in turn, are becoming the expert for those around you. To Xiaoxia Wang, you have come unbelievably far. You now span the void between the wet bench and the dry bench. You are poised to do amazing research and I am glad to call you a trusted colleague.

To the Esko Lab, you have been good colleagues and great friends. To Omai Garner, Rusty Bishop, & Manuela Schuksz, you set the bar for me. Thank you for the mouse work tutorials that were riddled with wit, laughter, and mild derision. To Erin Foley and Jon Gonzales, thank you for comiserating about the realities of our job.

To everyone who had a hand in this work when I asked for help, this is as much your accomplishment as it is mine. To Felix Karp, Renee Chow, and Andrea Garcia, thank you for supporting our projects with beautiful, yet rigorously controlled histology. Histolgy is perhaps fraught with more failure than any other scientific method, and I thank you for your tireless efforts to get it right. To Avelino Farinas, Michelle Chung, and Michelle Abueg, thank you for not just doing the support work, but for being good enough to take on the science too. I have tried to teach as much as possible and I hope that you all have learned something lasting.

To the UCSD Biomedical Sciences Graduate Program, thank you for the environment that puts the students first. Thank you current and past Program Chairs for your work. Thank you Gina Butcher and Leanne Nordeman for making our program one of the best graduate programs in the country. BMS past & present, you all have created a great environment to relax in when we lay down our experiments.

Finally, I would like to thank my family and friends. My wife, Nichole, is the most supporting person I have. Nichole, you understand my work and the time that it takes. You don't get mad when I'm late. You don't make me feel guilty. I owe you everything because you have kept me sane. To John & Sandra Gregg, thank you for raising me exactly the way you did. It was perfect. To Chip, Caroline, & Cameron Gregg, thank you for your support and love. I love you all. To my friends, thank you for keeping me close even though I was often late getting out of work, couldn't get out of work, or was too tired from work to hang out. This is what I was doing throughout the days, nights, and weekends.

VITA

EDUCATION

2005 – 2011 **Ph.D. Biomedical Sciences**,
University of California, San Diego

2001 – 2005 **B.S. Biomedical Engineering**,
Chemical Engineering Concentration,
Johns Hopkins University, Whiting School of Engineering

ORIGINAL RESEARCH ARTICLES

*denotes equal author contribution

Steppan J, Ryoo S, Schuleri KH, **Gregg CJ**, Hasan RK, White AR, Bugaj LJ, Khan M, Santhanam L, Nyhan D, Shoukas AA, Hare JM, Berkowitz DE. Arginase Modulates Myocardial Contractility by a Nitric Oxide Synthase 1-dependent Mechanism. Proc Natl Acad Sci U.S.A. 103(12):4759-64, 2006.

Varki NM, Anderson D, Herndon J, Pham T, **Gregg CJ**, Cheriyan M, Murphy J, Strobert E, Fritz J, Elise J, & Varki A. 2009. Heart Disease is Common in Humans and Chimpanzees but is Caused by Different Pathological Processes. Evol. Appl. 2: 101-112, 2009

Pham T*, **Gregg CJ***, Karp F, Chow RE, Padler-Karavani V, Cao H, Chen X, Witztum JL, Varki NM, & Varki A. Evidence for a Novel Human-Specific Xeno-auto-antibody Response Against vascular Endothelium. Blood. 114(25): 5225-5235, 2009

Taylor RE, **Gregg CJ**, Padler-Karavani V, Ghaderi D, Yu H, Sorensen RU, Chen X, Inostroza J, Nizet V, & Varki A. A Novel Mechanism for the Generation of Human Xeno-auto-antibodies Against the Non-human Sialic Acid N-glycolylneuraminic Acid. J. Exp. Med. 207(8): 1637-1646, 2010

Gregg CJ, Steppan J, Gonzalez DR, Champion HC, Phan A, Barouch LA, Nyhan D, Shoukas AA, Hare JM, & Berkowitz DE. β_2 Adrenergic Receptor-Coupled PI3K Constrains cAMP-dependent Increases in Cardiac Inotropy Through PDE4 Activation. Anesth Analg. 111(4): 870-877, 2010

Banda K*, **Gregg CJ***, Chow RE, Diaz SL, Varki NM, & Varki A. On the Metabolism and Fate of N-glycolyl groups of Vertebrate Amino Sugars: Mechanisms Underlying the Gastrointestinal Incorporation of the Non-Human Sialic Acid Xenoautoantigen, N-glycolylneuraminic Acid (submitted to J. Biol. Chem)

RESEARCH EXPERIENCE

2006 – Present Graduate Researcher, University of California, San Diego

2004 Provost Undergraduate Research Fellow, Johns Hopkins University

2003 – 2005 Undergraduate Researcher, Johns Hopkins University (under Dan E Berkowitz, MD)

ORIGINAL RESEARCH ABSTRACTS & MEETINGS

*denotes equal author contribution

2010 **Poster Presentation,** *San Diego Glycobiology Symposium*

2009 **Poster Presentation,** *Society for Glycobiology Annual Meeting*
Banda K*, **Gregg CJ***, Chow RE, Diaz SL, Varki NM, & Varki A. Investigating the Dietary Fate of the Non-human Sialic Acid, Neu5Gc. Annual Meeting of the Society for Glycobiology 2009. San Diego, CA.

2009 **Poster Presentation,** *American Society for Experimental Medicine Annual Meeting*
Taylor RE, **Gregg CJ**, Padler-Karavani V, Ghaderi D, Yu H, Sorensen RU, Chen X, Inostroza J, Nizet V, & Varki A. A Novel Mechanism for the Generation of Human Xeno-auto-antibodies Against the Non-human Sialic Acid N-glycolylneuraminic Acid

2009 **Poster Presentation,** *San Diego Glycobiology Symposium*

2008 **Poster Presentation,** *San Diego Glycobiology Symposium*

2008 University of California, San Diego *CARTA, Anthropogeny: Defining the Agenda.*
Gregg CJ & Ayala FJ. Evolutionary Origin & World Expansion of *Plasmodium falciparum*, the Agent of Malignant Malaria

2007 **Poster Presentation,** *Society for Glycobiology Annual Meeting*
Gregg CJ, Pham T, Karp F, Padler-Karavani V, Varki NM, & Varki A. A Human Specific Mechanism for the Dietary Exacerbation of Atherosclerosis.

2006 University of California, San Diego CARTA, The Origin & Fate of the Neanderthals

2005 **Oral Presentation,** *American College of Cardiology Annual Meeting*
Gregg CJ, Champion HC, Phan A, Steppan J, Barouch LA, Nyhan D, Shoukas AA, Hare JM, & Berkowitz DE. 2005. β_2 Adrenergic Receptor-Coupled PI3K Constrains cAMP-dependent Increases in Cardiac Inotropy Through PDE Activation.

2005 **Poster presentation,** *American Society of Critical Care Medicine Meeting*

2004 **Poster Presentation,** *American Heart Association Scientific Sessions*
Gregg CJ, Champion HC, Phan A, Steppan J, Barouch LA, Nyhan D, Shoukas AA, Hare JM, & Berkowitz DE. 2005. β_2

Adrenergic Receptor-Coupled PI3K Constrains cAMP-dependent Increases in Cardiac Inotropy Through PDE Activation.

AFFILIATIONS, AWARDS, & HONORS

2010	Best Talk Award at the UCSD Biomedical Sciences Retreat
2007 – 2009	Member Society for Glycobiology
2008	University of California, San Diego, Biomedical Sciences Graduate Student Admissions Committee
2007	Howard Hughes Medical Institute Med-into-Grad Fellow
2004	Provost Undergraduate Research Award
2002 – 2005	Johns Hopkins University Dean's List

ABSTRACT OF THE DISSERTATION

Absorption, Metabolic Incorporation, and Inflammation Engendered by the Non-human Sialic Acid, *N*-glycolylneuraminic Acid

by

Christopher John Gregg

Doctor of Philosophy in Biomedical Sciences

University of California, San Diego, 2011

Professor Ajit Varki, Chair

All human adults have circulating antibodies against *N*-glycolylneuraminic acid (Neu5Gc), a sialic acid that can't be produced in humans. However, dietary Neu5Gc (particularly from red meat) can be metabolically incorporated into human tissues and expressed on self glycans, as if made endogenously. We hypothesize that dietary Neu5Gc (xenoantigen) and Neu5Gc-specific antibodies (xenoautoantibodies) interact in a mechanism generating chronic inflammation, perhaps contributing to human-specific risk of diseases associated with red meat consumption.

Chapter 2 presents evidence that supports a role for dietary Neu5Gc as the source of human tissue Neu5Gc through a gastrointestinal study of dietary Neu5Gc in the Neu5Gc-deficient *Cmah*$^{-/-}$ mouse model. In this model, Neu5Gc-containing glycoproteins are digested by intestinal enterocytes and trafficked through the blood to the liver and other peripheral tissues. Long term feeding of Neu5Gc-containing glycoproteins leads to tissue incorporation in a human-like pattern, establishing this feeding paradigm as a means to mimic the human condition *in vivo*.

Appendix I presents studies aimed at generating a human-like Neu5Gc-specific antibody response in mouse. Although humans develop spontaneous Neu5Gc-specific antibodies early in life, *Cmah*$^{-/-}$ mice need to be immunized. Several immunization strategies are compared, but erythrocyte ghost- and mucin-based antigens have attractive properties. This section also presents work towards control immunizations, as well as discussing important aspects about detecting immune responses at the bench.

Chapter 3 demonstrates incorporation of dietary Neu5Gc in human vasculature, a site that interacts with circulating Neu5Gc-specific antibodies to generate chronic inflammation in humans. *In vitro* studies show that Neu5Gc-specific antibodies generate inflammation in vascular endothelium exhibiting Neu5Gc incorporation.

Chapter 4 synthesizes information from Chapters 2 and 3 and Appendix I in a mouse model of atherosclerosis where groups were defined by dietary Neu5Gc and Neu5Gc immunization. Initial studies indicate that Neu5Gc-specific antibodies negatively correlate with atherosclerosis, potentially disagreeing with results from Chapter 3 and suggesting an unexplored role(s) for Neu5Gc in lesion pathophysiology. Alternatively, the erythrocyte ghost immunization may not mimic the human condition, which could underlie this unexpected result.

CHAPTER 1

Introduction: Sialic Acids & the Human Condition

A background on glycans and their diversity. Beyond the central role for sugars in cellular metabolism, monosaccharides and linear/branched oligosaccharides that are covalently attached to proteins and lipids, collectively called glycans, play important roles in complex biological functions. Glycans largely exist on extracellular proteins (glycoproteins, proteoglycans) and lipids (glycolipids), although intracellular glycans are also prominent[1]. Although glycans can be physically dwarfed by protein carriers, their copy number per cell is enormous. Wile there can exist 10^2-10^3 copies of a common transmembrane proteins per cell (e.g., TNF Receptor on HL60 cells[2]), there can be 10^8-10^9 copies of sialic acid per cell[3]. Cell-surface glycans are ubiquitous throughout all taxa of life suggesting that evolution has maintained a selective pressure for organisms coated in a dense forest of carbohydrates[4]. Glycans function to mask underlying structures from pathogens and to create opportunities for new carbohydrate-based functions. Glucose, *N*-acetylglucosamine, galactose, *N*-acetylgalactosamine, mannose, fucose, uronic acids, and sialic acids are common components of mammalian glycans, though these components are quite different in other taxa (e.g., in plants).

DNA, RNA, and proteins fall into the category of template-derived biological molecules. Modifications to the DNA template will affect downstream RNA and protein structure in a predictable way. On the other hand, glycans (and lipids) are not template-based biological molecules. Although the enzymes for glycan synthesis are encoded in the genome, actual biosynthesis constitutes an emergent system whose behavior is not possible to predict based on relevant DNA sequences alone[5]. This is as a result of the organization of glycosylation in the endoplasmic reticulum and golgi apparatus. Relevant glycosyltransferases and glycosidases reside in these

compartments and work in sequence and in parallel to engender and modify nascent glycans on specific protein and lipid acceptor sites[5].

In the case of a nascent glycoprotein, glycosylation can occur at specific asparagine residues as the polypeptide is folded in the endoplasmic reticulum and/or at specific serine/threonine residues as the nascent glycoprotein transits through the Golgi apparatus to its target microdomain. However, of the many possible glycosylation sites in a given protein sequence, few sites are guaranteed glycosylation each time that sequence is translated[6], illustrating one mechanism underlying the diversity of glycans. Other mechanisms underlying glycan diversity include cellular expression patterns of glycosyltransferases and glycosidases, their relative expression levels, the levels of each precursor monosaccharide (e.g., sialic acid) and their activated forms (CMP-sialic acid, which is required for glycosylation), as well as the 'glycosylation load' borne by the system as a whole[5]. Moreover, a single glycosylation site on a given protein will exhibit micro-heterogeneity between other copies of the same protein from the same cell[6]. Thus, glycosylation can generate structural diversity that is just not possible from a finite genome encoding proteins alone. This diversity does not lend itself to 1:1 receptor:ligand interactions, common in protein-protein interactions. Instead, uncommon structures, common structures in uncommon places, uncommon modifications of common structures, and patterns of glycans have clued researchers into interesting biological functions of glycans in biology[7]. At this time, many glycan structures have no distinct function, although this is not surprising given the emergent nature of glycan biosynthesis and the limited information currently available.

Diversity of the sialic acids and modifications at the C-5 position. Sialic acids are a family of over 50 alpha-keto acidic monosaccharides found primarily in the deuterostome lineage of animals[8], and secondarily in the micro-organisms that colonize or invade them[9]. Most monosaccharides found in mammalian glycans are hexoses/hexosamines, however sialic acids are formed by the condensation of *N*-acetylmannosamine (hexose) with pyruvate (3 carbons) to form a 9-carbon monosaccharide, *N*-acetylneuraminic acid (Neu5Ac)[10]. Sialic acids are typically the capping monosaccharide that terminates a glycan chain on glycoproteins and glycolipids, thus sialic acids conferr a negative charge density at the extracellular frontier. Sialic acids are involved in many endogenous cell-cell and cell-matrix interactions, are essential for early development *in vivo*[11], yet are commonly exploited by pathogens, such as influenza virus[12] and bacterial toxins[13,14]. In mammals, sialic acids can be modified with functional groups at every carbon[8] and we hypothesize that the breadth of modifications represent an evolutionary response to pathogen exploitation in the face of the need to preserve endogenous biological functions of sialic acids.

Although there are numerous sialic acid modifications, the hydroxylation of the *N*-acetyl group at the C-5 position of Neu5Ac is especially notable. This reaction is only carried out by the hydroxylase *CMAH* to generate CMP-*N*-glycolylneuraminic acid (CMP-Neu5Gc) from CMP-Neu5Ac[15]. Thus, Neu5Gc and Neu5Ac differ by a lone oxygen atom at the C-5 position. *N*-glycolyl groups are notable for their rarity in nature, although the significance of this is not appreciated. In nature, the only organisms that have mastered the biochemistry required to generate an *N*-glycolyl group are mammals with Neu5Gc and *Mycobactera* with *N*-glycolylmuramic acid[16,17].

Neu5Gc is also notable because it, like Neu5Ac, is a scaffold for further modifications at other carbons. Neu5Gc and modifications thereof are expressed widely throughout mammals, however there is complex interspecies and intraspecies variation in expression patterns. There is variable Neu5Gc expression levels within an organism, aside from a common lack of Neu5Gc expression in mammalian brains[18], as well as an unpublished line of observations regarding Neu5Gc expression in the blood (e.g., if Neu5Gc is high on erythrocytes, then it is likely low on serum proteins, and vice-versa). Tissue specific regulation of *CMAH* must occur to account for these observations although little work has focused here thus far.

Uniquely human loss of the sialic acid, Neu5Gc. Although Neu5Ac and Neu5Gc are the dominant sialic acids in many mammals, humans cannot produce Neu5Gc due to an *Alu*-mediated insertion into the *CMAH* open-reading frame that caused a premature truncation of *CMAH*[19]. Humans cannot carry out the conversion of CMP-Neu5Ac into CMP-Neu5Gc, thus produce only Neu5Ac and modifications thereof. Genomic sequences from humans of diverse geographic origins showed that this mutation was fixed in the human population 2 million years ago (MYA), though the mutation likely arose about 3 MYA. Subsequent generation of a *Cmah* knockout (*Cmah*$^{-/-}$) mouse confirmed that *Cmah* is required for Neu5Gc expression in mammals.

Humans are unusual in that we cannot produce Neu5Gc. Our closest evolutionary cousins, the chimpanzees and all other hominids express Neu5Gc. Moreover, common mammals (cow, lamb, sheep, pig) all express Neu5Gc to varying extents, making human sialic acid biology apparently unique among mammals.

Consequences of Neu5Gc loss for human physiology and disease I: Aftershocks from the loss of Neu5Gc. Although the actual evolutionary pressures that selected for the human loss of *CMAH* function are unknown, exploitation of Neu5Gc epitopes by an relevant pathogen is a prime candidate[20]. Sialic acids are widely exploited as binding targets by pathogens during infection. This includes the protozoal parasite *Plasmodia*, which causes malaria. *Plasmodia* are an extremely successful group of parasites that have co-evolved to parasitize nearly every mammal living in tropical and sub-tropical ecosystems, including primates, where infections cause extreme fevers and mortality[21]. Many *Plasmodia* use a sialic acid-binding protein as the initial ligand to facilitate the mechanism of invasion into host erythrocytes. Interestingly, *Plasmodia* that infect humans and those that infect chimpanzees exhibit restricted host tropism that is likely to be sialic acid dependent. The human pathogen (*Plasmodium falciparum*) binds selectively to Neu5Ac, while the chimpanzee pathogen (*Plasmodium reichenowii*) prefers Neu5Gc[22]. Genomic comparison of *P. falciparum* isolates show that they are most closely related to *Plasmodia* that parasitize (Neu5Gc-expressing) gorilla[23] indicating that *P. falciparum* likely had to adapt infect Neu5Gc-free hominids. This example represents an important paradigm that pathogens, as well as self, had to adapt to life without Neu5Gc.

Although the loss of Neu5Gc could have been transiently good or even necessary for survival of the hominid population, any self-biological functions that required Neu5Gc would have lost their ligand. Three important classes of sialic acid binding receptors are the Selectins, Factor H, and the **s**ialic acid binding **i**mmuno**g**lobulin-like **lec**tins (Siglecs). Although there is little evidence for preference of Neu5Ac versus Neu5Gc with Selectins or Factor H, Siglecs have been affected by the loss of Neu5Gc[24,25]. Siglecs play important roles within the immune system in self-

recognition and can dampen subsequent immune responses upon sialic acid binding[26]. Analysis of hominin Siglec's and their human homologues has shown that Neu5Gc was the ancestral ligand for many Siglecs, thus human Siglecs lost their ligand 2-3 MYA and had to adapt to regain function. While some human Siglecs did adapt to Neu5Ac (Siglec-7, -9), others lost their sialic acid binding function (Siglec-12), were deleted from the genome or were pseudogenized (Siglec-13, -14, -16), or exhibit altered expression patterns (Siglec-1, -5, -6, -11)[25]. For example, human lymphocytes have reduced Siglec expression, including undetectable levels of Siglec-5, which is robustly expressed on lymphocytes of chimpanzees, orangutans, and gorillas[27]. Emerging work has shown that human lymphocytes are hyper-reactive compared to chimpanzee lymphocytes for a variety of stimulations at a variety of doses[28]. Also, humans exhibit a preponderance of hyper-reactive lymphocyte-mediated diseases, such as type-1 diabetes, psoriasis, bronchial asthma, and HIV progression to AIDS. These immune-related phenotypes are correlated with the reduction of Siglec levels on human lymphocytes, however the causal link is yet to be established.

Consequences of Neu5Gc loss for human physiology and disease II: Dietary Neu5Gc and incorporation into human cells and tissues. Despite the fact that humans cannot produce Neu5Gc, some human tissues paradoxically contain Neu5Gc. Classic work described the Hanganutziu-Deicher antigen, a Neu5Gc-containing ganglioside[29], as an onco-antigen in certain carcinomas[30]. Recent work used a polyclonal Neu5Gc IgY antibody (αNeu5Gc IgY) to confirm that Neu5Gc is present in some human carcinomas, as well as human placental villi[31], and epithelium lining hollow organs, such as the intestines[13].

The paradox that Neu5Gc can be found in some human tissues is somewhat resolved when one recognizes that Neu5Gc is rich in our diet. Neu5Gc levels are highest in foods such as beef, pork, lamb and, to a lesser extent, dairy products. Neu5Gc is conspicuously low in poultry, eggs, and fish, while sialic acids are absent in fruits and vegetables[31]. Estimations based on the USDA recommended daily dietary allowances and Neu5Gc content of common foods indicates that humans can ingest ~10 mg_{Neu5Gc}/day. To test the hypothesis that human tissue Neu5Gc is from dietary sources, human volunteers ingested 1 mg of Neu5Gc monosaccharide, which could be detected at low levels in salivary mucins and hair[31].

Studies in human cells showed that cellular biosynthesis does not discriminate between Neu5Ac and Neu5Gc and will utilize both for glycosylation[32]. When Neu5Gc is supplemented *in vitro*, it is taken up by macropinocytosis, a large scale endocytic process where extracellular fluid is engulfed in membrane ruffles and internalized as a macropinosome[33]. Thereafter macropinosomes fuse with the lysosomal compartment, which contains sialidases, other glycosidases, and monosaccharide transporters. The lysosome contains the endogenous catabolic pathways for re-uptake of sialic acids (for example, during autophagy of cell-surface glycoproteins)[32]. Glycosidically-linked Neu5Gc can be released by lysosomal sialidases, thereby allowing free Neu5Gc to be transported into the cytoplasm via *Sialin*, the lysosomal sialic acid transporter[32]. Once in the cytoplasm, Neu5Gc is apparently treated like Neu5Ac and can enter the nucleus where it is activated to CMP-Neu5Gc for subsequent glycosylation. Furthermore if transferred onto self glycans, Neu5Gc can be efficiently recycled through the lysosomal compartment and added onto other self glycans, perpetuating its half-life[32]. This metabolic loophole whereby Neu5Gc can enter into self-glycans is an important one and is necessary for dietary incorporation *in vivo*.

Consequences of Neu5Gc loss for human physiology and disease III: All humans express Neu5Gc-specific antibodies. Although the Hanganutziu-Deicher antigen (Neu5Gc-GM2 ganglioside) was originally recognized for its incorporation into human carcinomas, it was later found to be the epitope recognized by heterophile (so called H-D) antibodies in humans[29]. It was only recently appreciated that all humans have a polyclonal Neu5Gc-specific antibody response and the H-D antibodies were just the 'tip of the iceberg'[34-36]. Thus, while cellular biosynthetic pathways cannot recognize the single oxygen atom difference between Neu5Gc and Neu5Ac during glycosylation, the adaptive immune system successfully detects this difference. Human Neu5Gc-specific antibodies can be detected at some level in all humans and exist in multiple isotypes (IgM, IgG, and IgA)[34]. These antibodies exhibit polyclonal binding specificity to the structural diversity in which Neu5Gc could be found *in vivo*, yet are exquisitely specific for Neu5Gc over Neu5Ac despite the difference of a lone oxygen atom. Although the Neu5Gc-specific antibody response is quite variable from person to person, some individuals can have very high antibody levels, with Neu5Gc-specific IgG levels approaching ~0.2% of total[34]. Although epidemiological studies are underway, there is currently scant evidence to correlate Neu5Gc antibody levels with dietary Neu5Gc intake in humans.

Neu5Gc-specific antibodies arise early in the first year of life in humans[37]. Sera from infants were analyzed by ELISA for Neu5Gc-specific IgM and IgG antibodies. Endogenous Neu5Gc-specific antibodies appeared at 6 months and achieved adult levels at 12 months in infants who had ingested cow's milk based formula and solid foods that included beef, pork and lamb. Neu5Gc-specific IgM were absent in cord sera from these infants suggesting that Neu5Gc-specific antibodies are not germ-line

encoded “natural antibodies”[38], and instead require a post-natal antigenic stimulus. The early appearance and class switching of these antibodies indicate that humans are exposed to that antigenic stimulus early in life.

Consequences of Neu5Gc loss for human physiology and disease IV: Neu5Gc-specific antibodies and carcinoma progression. The presence of multiple Neu5Gc-specific antibody isotypes, including IgMs and certain subclasses of IgGs suggest that these antibodies can deposit complement and engender a cell-independent inflammatory response upon binding Neu5Gc in self tissues. The data demonstrating the presence of Neu5Gc in some human carcinomas indicate that the antibodies may have relevance for cancer progression in humans[30,31]. Recent work[39] tested the relevance of Neu5Gc-specific antibodies in promoting Neu5Gc-expressing tumor growth *in vivo*. Both human and murine affinity-purified Neu5Gc-specific antibodies promoted growth of syngeneic Neu5Gc-expressing tumors in *Cmah*$^{-/-}$ mice in a dose dependent manner by increasing vascularization through low-grade inflammation in the tumor[39]. This result supports the relevance of Neu5Gc and Neu5Gc-specific antibodies *in vivo* and suggests that human tumors may be exploiting our unique sialic acid biology for a growth advantage.

Little is known about the gastrointestinal handling of dietary sialic acids. Although dietary Neu5Gc has medical relevance and is consistently consumed by humans eating red meat and dairy products, very little is known about how glycans are handled by the gastrointestinal tract. Although much work has addressed how dietary glucose and glucose polymers (starch) are digested and transported into the body, this work likely has little relevance here for multiple reasons. Whereas secreted amylases

are important in digesting glucose polymers into monomers for import through the GLUT family of neutral monosaccharide transporters, sialidases and applicable anionic monosaccharide transporters are located in the lysosomal compartments[32], suggesting that a glycan must be endocytosed to be metabolized, akin to lysosomal glycan recycling discussed earlier (pg. 8). Seminal work by Nöhle & Schauer used radioactive sialic acids to trace gastrointestinal fate in fed mice and rats[40,41]. They found that free Neu5Ac monosaccharide was rapidly absorbed from the gastrointestinal tract upon feeding, with nearly 90% absorbed 2 hours after feeding. Most of the radioactivity appeared intact in the urine and only 2% of the radioactivity remained in the body at 6 hours after feeding. On the other hand, sialic acid-containing glycoproteins are handled very differently and the radioactivity is absorbed much more slowly. Interestingly, substantial (60%) radioactivity remains in the body after 24 hours including some respired radioactivity, suggesting that dietary sialic acid-containing glycans can be metabolized and/or delivered to peripheral tissues. Thus, it is important to understand in what form (glycoprotein, glycolipid, free glycan, free monosaccharide) Neu5Gc exists in our diet. Moreover, it is important to understand the gastrointestinal kinetics of Neu5Gc and to recapitulate the human condition in a mouse model where dietary Neu5Gc incorporates into mouse tissues in a human-like pattern.

Previous attempts in our lab have failed to incorporate Neu5Gc into *Cmah*$^{-/-}$ mouse tissues through the diet or injections (Table 1-1). Most attempts involved high levels of free Neu5Gc (monosaccharide) chronically fed through the drinking water. Several studies, some for as many as 16 weeks, failed to incorporate Neu5Gc into target tissues at convincing levels with the sole exception of low levels of incorporation into mammary tumors of *Cmah*$^{-/-}$ mice on free Neu5Gc in the drinking water. Moreover, studies where the gastrointestinal tract was bypassed by injecting animals

with high doses of free Neu5Gc did not lead to incorporation similar to that seen in humans. In fact, injections of free Neu5Gc only led to incorporation of the kidney tubules, consistent with Nöhle & Schauer's result that free Neu5Gc is rapidly excreted from the body in the urine.

Other failed strategies (Table 1-1) included intravenous injection of micelles enriched for the ganglioside, Neu5Gc-GM3, carried out with high doses for several weeks, which resulted in a weak staining in the lungs. Also passive transfer of wildtype, Neu5Gc-expressing serum into *Cmah*$^{-/-}$ animals introduced Neu5Gc-containing glycans into circulation for weeks, but did not lead to Neu5Gc incorporation into tissues. Finally, *Cmah*$^{-/-}$ animals rapidly breakdown Neu5Gc *in vivo*. Experiments where Neu5Gc-deficient pups were birthed to a Neu5Gc-expressing (*Cmah*$^{+/-}$) dam showed that although *Cmah*$^{-/-}$ and *Cmah*$^{+/-}$ pups phenocopy each other in tissue Neu5Gc levels at birth, *Cmah*$^{-/-}$ pups are completely devoid of Neu5Gc two weeks of age. This suggests that endogenous metabolic pathways unidirectionally metabolize Neu5Gc in the absence of *Cmah*. This finding, as well as a lack of consideration for the physiologic form of delivery, offers some explanation why many strategies yielded unconvincing results.

The pathological cause of heart disease is different between humans and great apes. Although humans and great apes are closely related and exhibit many similarities, their common disease susceptibilities are surprisingly different. For example, while both humans and chimpanzees frequently die of 'heart disease', the underlying pathological processes are quite different. Humans are predisposed to severe atherosclerosis of the vasculature, which is an unresolved inflammation of the peri-vascular space that can be driven by high circulating LDL cholesterol[42,43]. High

circulating LDL can accumulate at sites of inflammation in the vasculature, where macrophages unsuccessfully attempt to metabolize the cholesterol. High levels of LDL or LDL that has been oxidatively modified by free radicals released during inflammation are pro-inflammatory and can promote lesion growth by attracting more monocytes into the lesion to perpetuate vascular inflammation[44]. Inflammation progresses and the lesion grows to the point where it begins to obstruct circulation or until the lesion bursts, releasing its thrombogenic contents into the bloodstream to obstruct distal circulation. Human atherosclerosis tends to develop in the coronary, the carotid, the renal, and femoral arteries leading to event such as heart attack, stroke, kidney damage, and peripheral numbness. Interestingly, emerging epidemiological evidence from several groups has found significant positive correlations between red meat intake and biomarkers of inflammation in Iranian women[45], cardiovascular disease-related mortality in American women[46] and mortality in American elderly[47].

On the other hand, chimpanzees succumb to a myocardial pathology that does not affect the arteries. Instead, chimpanzee myocardial sections demonstrate extensive fibrosis and collagen deposition within the heart muscle itself, while their coronary arteries are relatively healthy (Fig. 1-1A). Although comparisons between sedentary humans and captive chimpanzees are difficult, chimpanzees had higher circulating cholesterol than age- and sex-matched human cohorts (Fig. 1-1B). Other data suggests that chimpanzees have similar lipoprotein profiles as humans (e.g., relative levels of LDL, IDL, HDL, etc.) and that chimpanzees also have the ApoE4 allele, which predisposes humans to hypercholesterolemia, thus is also associated atherosclerosis[48]. Despite these observations, advanced atherosclerosis and its clinical presentations (heart attack, stroke) are virtually absent in chimpanzees[49].

Hypotheses and Organization. This dissertation has been guided by an overarching hypothesis that dietary Neu5Gc can be incorporated into self-tissues and interacts with circulating Neu5Gc-specific antibodies to engender chronic inflammation, potentially explaining unusual human disease predispositions associated with red meat consumption. We hypothesize that dietary Neu5Gc incorporates into human blood vessels and interacts with Neu5Gc-specific antibodies to engender vascular inflammation and that this mechanism helps explain human predilection for vascular inflammation. This dissertation presents work to establish a mouse model of the human condition, which required understanding dietary kinetics and exploiting delivery of Neu5Gc *in vivo* (Chapter 2), required investigating the inflammatory properties of human Neu5Gc-specific antibodies in vascular cells *in vitro* (Chapter 3), required trying different methods to generate a human-like antibody response in the *Cmah*$^{-/-}$ mouse (Appendix I), and initial attempts are then made to put these variables together in a mouse model of atherosclerosis (Chapter 4).

ACKNOWLEDGEMENTS

Chapter 1, in part, reproduces figures from a manuscript as it appears, *Varki N, Anderson D, Herndon, JG, Pham T, Gregg CJ, Cheriyan M, Murphy J, Strobert E, Fritz J, Else JG, & Varki A., Evolutionary Applications, 2:101-112, 2009*. The dissertation author was a co-author and Dr. Ajit Varki directed and supervised the research that is included in this chapter.

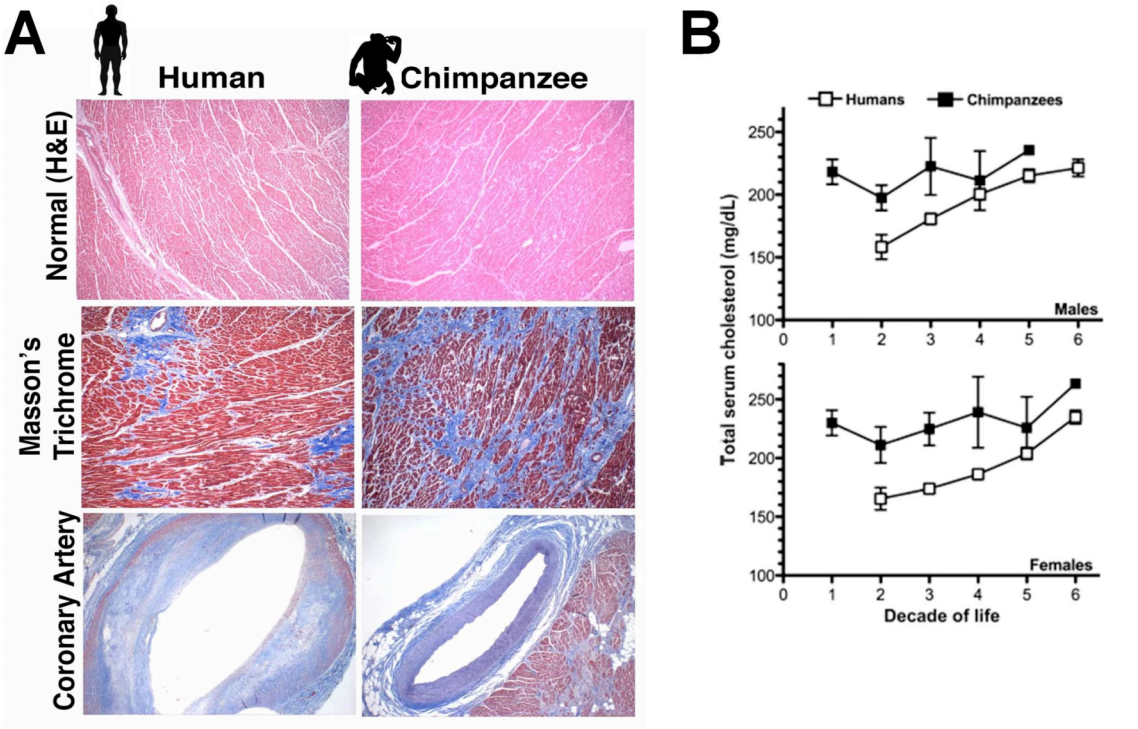

Figure 1-1. The Pathological Cause of Heart Disease is Different between Humans and Great Apes[49]**. A.** Histology of human (left column) and chimpanzee (right column) myocardium shows species-dependent pathological differences. Although overall myocardial structure seems similar in Hematoxylin and Eosin staining (top row), Masson's Trichrome staining (middle row) reveals extensive collagen deposition (blue staining) in the peri-vascular space in humans, while staining throughout the myocardium in chimpanzees. Histology of coronary arteries (bottom row) show atherosclerosis of the human vessel that is characterized by sub-endothelial thickening, lipid-based lesions, and general tissue disorganization, whereas the chimpanzee counterpart is clean and well-organized. **B.** Longitudinal comparison of total serum cholesterol in human and captive chimpanzee populations. Chimpanzee data[50] and human data[51] were taken from 2 independent, original articles and plotted here, on the same axis, for comparison. Total serum cholesterol data from both publications was grouped by sex and age in decades. Human data was acquired from 6757 participants in the Framingham Heart Study, aged 15-79. Chimpanzee data was acquired from 252 chimpanzees, aged 0-60, living in captivity at the Yerkes Primate Foundation in Atlanta, GA, USA. Chimps "were fed a commercial primate chow, supplemented with fruits and vegetables". Error bars are not shown for the oldest chimps (5th decade in males, n=1; 6th decade in females, n=3) due to small sample size. Data are plotted as mean ± 95% C.I. The Total serum cholesterol axis starts at 100 mg/dL.

Table 1-1. Lessons from Past Neu5Gc Animal Loading Experiments

IHC – Immunohistochemistry; **HPLC** – High Performance Liquid Chromatography.

**Hedlund, M., et al.: N-glycolylneuraminic Acid Deficiency in Mice: Implications for Human Biology and Evolution. Mol. Cell. Biol., 27:4340-4346, 2007.

Loading Strategy	Dose	Duration (weeks)	Detection Methods	Notes
Cmah$^{+/-}$ dams pregnant with *Cmah*$^{-/-}$ pups	N/A	3	HPLC, IHC	*Cmah*$^{-/-}$ & *Cmah*$^{+/-}$ born to *Cmah*$^{-/-}$ sire & *Cmah*$^{+/-}$ dam. Neu5Gc content of littermate tissues was identical *in utero*.
Cmah$^{-/-}$ pups born to *Cmah*$^{+/-}$ dams	0 (after birth)	N/A	HPLC, IHC	*Cmah*$^{-/-}$ pups born to *Cmah*$^{+/-}$ dams lost Neu5Gc content rapidly after birth, with levels nearly undetectable at postnatal day 10.
Cmah$^{-/-}$ pups born to *Cmah*$^{-/-}$ dams fed Neu5Gc in the drinking water	1 mg_{Neu5Gc}/mL	3		Free Neu5Gc in the drinking water (*ad libitum*) did not load *Cmah*$^{-/-}$ pups *in utero***.
Cmah$^{-/-}$ mice are fed Neu5Gc in the drinking water long term	• 1 mg_{Neu5Gc}/mL •1.5 mg_{Neu5Gc}/mL	• 10, 16 • 4	IHC only	• Free Neu5Gc in the water (*ad libitum*) led to very weak loading in Cmah$^{-/-}$ mice, only at very long timepoints in skeletal muscle, cardiac muscle, and some glands. • Mammary tumors from Cmah$^{-/-}$ animals on a spontaneous mammary tumor forming background (MMTV-PyMT transgenic) incorporated Neu5Gc from the drinking water**.
Cmah$^{-/-}$ mice injected IP with free Neu5Gc	40 mg_{Neu5Gc}/kg* day	3	IHC only	Animals injected with free Neu5Gc intraperitoneally exhibited loading only of the tubules of the kidney, reminiscent of excretion into the urine.
Cmah$^{-/-}$ mice injected IV with GcGM3 micelles	28.6 mg_{Neu5Gc}/kg* day	3	IHC only	Animals injected with GcGM3 ganglioside intravascularly exhibited loading in the lungs, a first pass organ after IV injection.
Passive serum transfer of wildtype (*Cmah*$^{+/+}$) into *Cmah*$^{-/-}$ mice	100 uL_{serum}/inj	1, 2	HPLC, IHC	Neu5Gc containing, wildtype (*Cmah*$^{+/+}$) serum was injected IP into *Cmah*$^{-/-}$ mice. Neu5Gc on wildtype serum persisted in circulation (45% remaining 4 days after transfer), but resulted in no detectable peripheral tissue loading.

REFERENCES

1. Varki, A. et al. *Essentials of Glycobiology* (Cold Spring Harbor Laboratory Press, Plainview, NY, 2009).
2. Brockhaus, M. et al. Identification of two types of tumor necrosis factor receptors on human cell lines by monoclonal antibodies. *Proc Natl Acad Sci U S A* **87**, 3127-3131 (1990).
3. Kraemer, P. M. Sialic acid of mammalian cell lines. *J Cell Physiol* **67**, 23-34 (1966).
4. Varki, A. Nothing in glycobiology makes sense, except in the light of evolution. *Cell* **126**, 841-845 (2006).
5. Varki, A., Esko, J. D. & Colley, K. J. in *Essentials of Glycobiology* (eds Varki, A., Cummings, R. D., Esko, J. D., Freeze, H. H., Stanley, P., Bertozzi, C. R., Hart, G. W. & Etzler, M. E.) 37-46 (Cold Spring Harbor Laboratory Press, Cold Spring Harbor, NY, 2009).
6. Rudd, P. M. & Dwek, R. A. Glycosylation: Heterogeneity and the 3D structure of proteins. *Crit Rev Biochem Mol Biol* **32**, 1-100 (1997).
7. Cummings, R. D. & Esko, J. D. in *Essentials of Glycobiology* (eds Varki, A., Cummings, R. D., Esko, J. D., Freeze, H. H., Stanley, P., Bertozzi, C. R., Hart, G. W. & Etzler, M. E.) 387-402 (Cold Spring Harbor Laboratory Press, Cold Spring Harbor, NY, 2009).
8. Angata, T. & Varki, A. Chemical diversity in the sialic acids and related alpha-keto acids: an evolutionary perspective. *Chem Rev* **102**, 439-469 (2002).
9. Lewis, A. L. et al. Innovations in host and microbial sialic acid biosynthesis revealed by phylogenomic prediction of nonulosonic acid structure. *Proc Natl Acad Sci U S A* **106**, 13552-13557 (2009).
10. Schauer, R. Chemistry, metabolism, and biological functions of sialic acids. *Adv Carbohydr Chem Biochem* **40**, 131-234 (1982).
11. Schwarzkopf, M. et al. Sialylation is essential for early development in mice. *Proc Natl Acad Sci U S A* **99**, 5267-5270 (2002).
12. Gagneux, P. et al. Human-specific regulation of Alpha2-6 linked sialic acids. *J Biol Chem* **278**, 48245-48250 (2003).
13. Byres, E. et al. Incorporation of a non-human glycan mediates human susceptibility to a bacterial toxin. *Nature* **456**, 648-652 (2008).
14. Varki, A. Multiple changes in sialic acid biology during human evolution. *Glycoconj J* **26**, 231-245 (2009).
15. Hedlund, M. et al. N-glycolylneuraminic acid deficiency in mice: implications for human biology and evolution. *Mol Cell Biol* **27**, 4340-4346 (2007).
16. Brennan, P. J. Structure, function, and biogenesis of the cell wall of Mycobacterium tuberculosis. *Tuberculosis (Edinb)* **83**, 91-97 (2003).
17. Vollmer, W. Structural variation in the glycan strands of bacterial peptidoglycan. *FEMS Microbiol Rev* **32**, 287-306 (2008).

18. Varki, A. Loss of N-glycolylneuraminic acid in humans: Mechanisms, consequences, and implications for hominid evolution. *Am J Phys Anthropol* **Suppl 33**, 54-69 (2001).

19. Chou, H. H. et al. A mutation in human CMP-sialic acid hydroxylase occurred after the Homo-Pan divergence. *Proc Natl Acad Sci USA* **95**, 11751-11756 (1998).

20. Varki, A. & Gagneux, P. Human-specific evolution of sialic acid targets: explaining the malignant malaria mystery? *Proc Natl Acad Sci U S A* **106**, 14739-14740 (2009).

21. Ayala, F. J. & Coluzzi, M. Chromosome speciation: humans, Drosophila, and mosquitoes. *Proc Natl Acad Sci U S A* **102 Suppl 1**, 6535-6542 (2005).

22. Martin, M. J., Rayner, J. C., Gagneux, P., Barnwell, J. W. & Varki, A. Evolution of human-chimpanzee differences in malaria susceptibility: relationship to human genetic loss of N-glycolylneuraminic acid. *Proc Natl Acad Sci U S A* **102**, 12819-12824 (2005).

23. Liu, W. et al. Origin of the human malaria parasite Plasmodium falciparum in gorillas. *Nature* **467**, 420-425 (2010).

24. Varki, A. Glycan-based interactions involving vertebrate sialic-acid-recognizing proteins. *Nature* **446**, 1023-1029 (2007).

25. Varki, A. Colloquium paper: uniquely human evolution of sialic acid genetics and biology. *Proc Natl Acad Sci U S A* **107 Suppl 2**, 8939-8946 (2010).

26. Crocker, P. R. & Redelinghuys, P. Siglecs as positive and negative regulators of the immune system. *Biochem Soc Trans* **36**, 1467-1471 (2008).

27. Nguyen, D. H., Hurtado-Ziola, N., Gagneux, P. & Varki, A. Loss of Siglec expression on T lymphocytes during human evolution. *Proc Natl Acad Sci U S A* **103**, 7765-7770 (2006).

28. Soto, P. C., Stein, L. L., Hurtado-Ziola, N., Hedrick, S. M. & Varki, A. Relative over-reactivity of human versus chimpanzee lymphocytes: implications for the human diseases associated with immune activation. *J Immunol* **184**, 4185-4195 (2010).

29. Merrick, J. M., Zadarlik, K. & Milgrom, F. Characterization of the Hanganutziu-Deicher (serum-sickness) antigen as gangliosides containing N-glycolylneuraminic acid. *Int Arch Allergy Appl Immunol* **57**, 477-480 (1978).

30. Kawachi, S. & Saida, T. Analysis of the expression of Hanganutziu-Deicher (HD) antigen in human malignant melanoma. *J Dermatol* **19**, 827-830 (1992).

31. Tangvoranuntakul, P. et al. Human uptake and incorporation of an immunogenic nonhuman dietary sialic acid. *Proc Natl Acad Sci U S A* **100**, 12045-12050 (2003).

32. Bardor, M., Nguyen, D. H., Diaz, S. & Varki, A. Mechanism of uptake and incorporation of the non-human sialic acid N-glycolylneuraminic acid into human cells. *J Biol Chem* **280**, 4228-4237 (2005).

33. Doherty, G. J. & McMahon, H. T. Mechanisms of endocytosis. *Annu Rev Biochem* **78**, 857-902 (2009).

34. Padler-Karavani, V. et al. Diversity in specificity, abundance, and composition of anti-Neu5Gc antibodies in normal humans: potential implications for disease. *Glycobiology* **18**, 818-830 (2008).

35. Nguyen, D. H., Tangvoranuntakul, P. & Varki, A. Effects of natural human antibodies against a nonhuman sialic acid that metabolically incorporates into activated and malignant immune cells. *J Immunol* **175**, 228-236 (2005).

36. Zhu, A. & Hurst, R. Anti-N-glycolylneuraminic acid antibodies identified in healthy human serum. *Xenotransplantation* **9**, 376-381 (2002).

37. Taylor, R. E. et al. Novel mechanism for the generation of human xeno-autoantibodies against the nonhuman sialic acid N-glycolylneuraminic acid. *J Exp Med* **207**, 1637-1646 (2010).

38. Ochsenbein, A. F. & Zinkernagel, R. M. Natural antibodies and complement link innate and acquired immunity. *Immunol Today* **21**, 624-630 (2000).

39. Hedlund, M., Padler-Karavani, V., Varki, N. M. & Varki, A. Evidence for a human-specific mechanism for diet and antibody-mediated inflammation in carcinoma progression. *Proc Natl Acad Sci U S A* **105**, 18936-18941 (2008).

40. Nohle, U. & Schauer, R. Metabolism of sialic acids from exogenously administered sialyllactose and mucin in mouse and rat. *Hoppe Seylers Z Physiol Chem* **365**, 1457-1467 (1984).

41. Nohle, U., Beau, J. M. & Schauer, R. Uptake, metabolism and excretion of orally and intravenously administered, double-labeled N-glycoloylneuraminic acid and single-labeled 2-deoxy-2,3-dehydro-N-acetylneuraminic acid in mouse and rat. *Eur J Biochem* **126**, 543-548 (1982).

42. Lundberg, A. M. & Hansson, G. K. Innate immune signals in atherosclerosis. *Clin Immunol* **134**, 5-24 (2010).

43. Glass, C. K. & Witztum, J. L. Atherosclerosis. the road ahead. *Cell* **104**, 503-516 (2001).

44. Steinberg, D. & Witztum, J. L. Oxidized low-density lipoprotein and atherosclerosis. *Arterioscler Thromb Vasc Biol* **30**, 2311-2316 (2010).

45. Esmaillzadeh, A. et al. Dietary patterns and markers of systemic inflammation among Iranian women. *J Nutr* **137**, 992-998 (2007).

46. Bernstein, A. M. et al. Major dietary protein sources and risk of coronary heart disease in women. *Circulation* **122**, 876-883 (2010).

47. Sinha, R., Cross, A. J., Graubard, B. I., Leitzmann, M. F. & Schatzkin, A. Meat intake and mortality: a prospective study of over half a million people. *Arch Intern Med* **169**, 562-571 (2009).

48. Hanlon, C. S. & Rubinsztein, D. C. Arginine residues at codons 112 and 158 in the apolipoprotein E gene correspond to the ancestral state in humans. *Atherosclerosis* **112**, 85-90 (1995).

49. Varki, N. et al. Heart disease is common in humans and chimpanzees, but is caused by different pathological processes. *Evolutionary Applications* **2**, 101-112 (2009).

50. Herndon, J. G. & Tigges, J. Hematologic and blood biochemical variables of captive chimpanzees: cross-sectional and longitudinal analyses. *Comp Med* **51**, 60-69 (2001).

51. Abbott, R. D. et al. Joint distribution of lipoprotein cholesterol classes. The Framingham study. *Arteriosclerosis* **3**, 260-272 (1983).

CHAPTER 2

Mechanisms Underlying the Gastrointestinal Incorporation of the Non-Human Sialic Acid Xenoautoantigen, *N*-glycolylneuraminic Acid

ABSTRACT

While *N*-acetyl groups are common in nature, *N*-glycolyl groups are rare. Mammals express two major sialic acids, *N*-acetylneuraminic acid (Neu5Ac) and *N*-glycolylneuraminic acid (Neu5Gc). Humans cannot produce Neu5Gc, yet metabolically incorporate Neu5Gc from mammalian foods, with accumulation in the epithelial lining of hollow organs, endothelial lining of the vasculature, fetal tissues and carcinomas. This accumulation has relevance for diseases associated with such foods, via interaction with the Neu5Gc-specific antibodies, yet little is known about how ingested sialic acids in general and Neu5Gc in particular are metabolized in the gastrointestinal tract. We studied the gastrointestinal and systemic fate of Neu5Gc-containing glycoproteins (Neu5Gc-glycoproteins) or free Neu5Gc in the Neu5Gc-free *Cmah*$^{-/-}$ mice. Ingested free Neu5Gc exhibited rapid absorption into the circulation and fast urinary excretion. In contrast, ingestion of Neu5Gc-glycoproteins led to uptake of Neu5Gc into the small intestinal wall, appearance of Neu5Gc in circulation at a steady-state level for several hours, and led to metabolic incorporation into multiple peripheral tissue glycoproteins and glycolipids. Feeding Neu5Gc-glycoproteins but not free Neu5Gc mimics the human condition, causing tissue incorporation into human-like sites in *Cmah*$^{-/-}$ fetal and adult tissues, as well as developing tumors. Thus, glycosidically-linked, Neu5Gc-containing glycoproteins, rather than the free monosaccharide, are the likely dietary source for human tissue accumulation. This human-like mouse model of dietary Neu5Gc accumulation can now be used to further elucidate specific mechanisms of Neu5Gc delivery from the gut to tissues, as well as the general mechanisms of metabolism of ingested sialic acids.

INTRODUCTION

Sialic acids are acidic capping sugars on glycan chains, found on cell surface glycans and secreted glycans in animals of the *Deuterostome* lineage (vertebrates, and so-called "higher" invertebrates)[1]. The localization and ubiquity of sialic acids underscores their importance in mediating numerous cellular and extra-cellular interactions. The core 9-carbon structure of sialic acids can be extensively modified to fine-tune these interactions, for example at C-5 where hydroxylation of the *N*-acetyl group of *N*-acetylneuraminic acid (Neu5Ac) by the enzyme Cytidine Monophosphate *N*-acetylneuraminic Acid Hydroxylase (CMAH) generates *N*-glycolylneuraminic acid (Neu5Gc)[2-4]. Neu5Ac and Neu5Gc are the major sialic acids expressed in most mammals.

Despite the ubiquity of Neu5Gc in most mammals, CMAH is non-functional in all humans due to an *Alu*-mediated deletion of *CMAH* exon 6, causing premature truncation of the open reading frame[5]. Thus, humans cannot produce Neu5Gc only Neu5Ac. Neu5Gc was also absent in human-like *Cmah*$^{-/-}$ mouse[6], showing there exists no alternate pathway for Neu5Gc biosynthesis in mammals.

Interestingly, intracellular sialic acid biosynthetic enzymes do not discriminate between Neu5Gc and Neu5Ac, and exogenous Neu5Gc can exploit a metabolic "loophole" to be used for sialylation of human cells[7]. This finding is important in light of existing evidence for the presence of Neu5Gc in human carcinomas and fetal tissues. More recently, histology of human tissues using an affinity-purified Neu5Gc antibody (αNeu5Gc IgY) has demonstrated several human tissues where Neu5Gc is characteristically present, such as endothelial cells lining the micro- and macro-vasculature[8], carcinomas[9], placental tissues[10], and epithelial cells lining hollow organs[11,12]. Given that humans who eat red meats and other animal-associated food

products consume milligram quantities of Neu5Gc each day[11], it is reasonable to propose that the Neu5Gc detected in human tissues originates from dietary sources. Indeed, previous human volunteer studies showed that orally ingested Neu5Gc appears in the urine, and that small amounts might be incorporated into salivary mucins[11]. Dietary-derived Neu5Gc in human tissue has also been confirmed by mass spectrometry[11].

While human sialic acid biosynthetic enzymes do not discriminate between Neu5Ac and Neu5Gc, the human humoral immune system does, and all humans tested have circulating Neu5Gc-specific immunoglobulins (Ig) at variable (sometime high) levels[11,13,14]. These antibodies are known to arise during the first year of life[15]. Recent work has explored the potential pathological role of Neu5Gc in human carcinomas[9], atherosclerosis[8], and susceptibility to dietary shiga-like toxins[12]. These studies suggest that Neu5Gc is actively exacerbating these diseases, in most cases through interactions with circulating Neu5Gc-specific Ig[8,9]. Thus, there is a need to understand mechanisms underlying tissue incorporation of ingested Neu5Gc and to conclusively prove that dietary Neu5Gc can be accumulated in a manner mimicking human-like tissue distribution.

Although sialic acids are produced intracellularly, recycling pathways can liberate cell surface and extracellular sialic acids for intracellular re-utilization. Cell surface glycoproteins and glycolipids from the cell surface are endocytosed in the process of autophagy or other regulated internalization mechanisms[16]. In addition, cells sample their external environment through macropinocytosis and capture extracellular sialylated glycans into intracellular vesicles[16]. It is largely unclear to what extent cells balance endogenous sialic acid production and sialic acid recycling/scavenging to satisfy cellular needs for sialylation. However, it is known that mammalian infants

require dietary sialic acid supplementation for optimal brain development[17]. Dietary sialic acid improves memory formation, learning metrics, and brain sialic acid content in piglet[18] and rat[19] models. Moreover, evidence has shown that breast milk as opposed to formula is much richer in sialic acid content[20,21] and that breastfed children develop higher IQ levels than formula-fed children[22].

Despite these observations, remarkably little is known about the fate of ingested sialic acids in mammals. Aside from one observation of sialidase activity in intestinal fluids[23], the only studies on this topic were performed by Nöhle & Schauer. They showed that while radioactive free sialic acid fed to mice and rats appears largely intact in the urine[24,25], radioactive sialylated mucin-type glycoproteins were absorbed more slowly from the intestine. Moreover the radioactive glycoproteins seemed to be metabolized, as evinced by radioactive CO_2 respired by the animals[26]. Beyond this, little else is known about the fate of ingested sialic acids in mammals.

In this study, we have used a Neu5Gc-deficient mouse with a human-like defect in *Cmah* as a model where ingested Neu5Gc can be followed like a radioactive tracer in a Neu5Gc-free environment. Two complimentary reagents, a polyclonal chicken anti-Neu5Gc IgY antibody (αNeu5Gc IgY) and fluorescent tagging of free sialic acids with DMB for HPLC (see methods) play a prominent role in this work and deserve an introduction to help the reader understand their respective utilities. As shown in Fig. 2-1A, Neu5Gc-containing glycoproteins can be detected by αNeu5Gc IgY because αNeu5Gc IgY recognizes Neu5Gc in the α conformation. The glycosidic linkage that covalently links Neu5Gc to the underlying glycan holds Neu5Gc in this conformation, while free Neu5Gc monosaccharide is primarily (~90%) in the β-conformation and is not recognized by αNeu5Gc IgY. On the other hand DMB requires the α-keto acid moiety of sialic acid to be free to react and form the fluorescent adduct that is followed

in HPLC. The α-keto acid moiety is not available when sialic acids are glycosidically linked. Thus, DMB will only react with free Neu5Gc monosaccharide. Glycosidically linked sialic acids can be released from glycans using an acid hydrolysis (2M acetic acid at 80°C for 3 hrs). Thus carrying out acid hydrolysis on a sample allows constitutes the difference between detecting total Neu5Gc (with acid hydrolysis) and detecting free Neu5Gc (without hydrolysis) of a sample.

The *Cmah*$^{-/-}$ mouse and these reagents (Fig. 2-1A) allowed us to study the gastro-intestinal kinetics of ingested Neu5Gc *in vivo*, the appearance of dietary metabolites in the blood and urine, and ascertain the tissues where dietary Neu5Gc is metabolically incorporated *in vivo*. Given that Neu5Gc is the first example of a foreign immunogenic molecule that is incorporated in human tissues and likely responsible for exacerbating chronic inflammatory conditions, the study of its gastro-intestinal kinetics and metabolic incorporation is also of importance to human health and disease.

RESULTS & DISCUSSION

Ingested free Neu5Gc is only minimally recovered from organs of fed mice. We initially compared the total recovery of Neu5Gc from organs of *Cmah*$^{-/-}$ mice at multiple time points following equimolar gavage of free Neu5Gc or Neu5Gc-containing glycoproteins (Neu5Gc-glycoproteins = porcine submaxillary mucin, PSM). As shown in Table 2-1, the recovery of Neu5Gc (from the entire gastrointestinal tract, the blood, the liver, and the kidneys; excluding urine and feces) was different when comparing the two feeding paradigms. Less than 20% of free Neu5Gc was recovered two hours after feeding compared to 60.4 ± 4.8% in Neu5Gc-glycoprotein fed mice. Percentage recoveries drop by a factor of ~10 every two hours, regardless of feeding paradigm, and Neu5Gc is difficult to recover 4 and 6 hours after free Neu5Gc feeding. We

hypothesize that the disparity in our recovery of Neu5Gc from free Neu5Gc and Neu5Gc-glycoprotein fed mice could be due to two factors: Neu5Gc might be metabolized such that we cannot track using DMB-HPLC; Neu5Gc might be rapidly excreted from the body, as suggested by Nöhle and Schauer[25].

Ingested Free Neu5Gc is rapidly absorbed from the gastrointestinal tract and with no evidence of metabolic incorporation into tissues. To understand the minimal recovery of free Neu5Gc after feeding, we looked for recoveries in multiple individual organs, intestinal contents, blood, and urine. Fig. 2-1B depicts visually how we segmented the gastrointestinal tract and other organs for these studies. Two hours after feeding, Neu5Gc in gastrointestinal (stomach, small and large intestinal) contents (Fig. 2-1C) of free Neu5Gc fed mice were markedly lower than in Neu5Gc-glycoprotein fed mice (10.9 ± 10.1% compared to 45.8 ± 3.8% of total Neu5Gc recovered, respectively). This confirms rapid disappearance of free Neu5Gc from the intestines due to absorption from and/or degradation within the gut. Intestinal wall segments and other tissues (liver, kidney and blood) (Fig. 2-1D) did not act as a sink for free Neu5Gc, indicating minimal metabolic incorporation *in vivo*.

Ingested Free Neu5Gc is transiently seen in blood and is efficiently excreted in urine. In keeping with the rapid absorption of free Neu5Gc from the intestines, free Neu5Gc levels in blood (Fig. 2-1F, solid black circles) peaked 1 hour after feeding, quickly declining thereafter. A similar pattern of excretion was seen in urine (open gray circles) with a peak around 30-60 min and minimal amounts by the end of 5 hours. These data qualitatively mirror each other and mimic the excretion kinetics of radioactive sialic acids[24,25]. The high recovery of free Neu5Gc in urine accounts for the poor recovery of Neu5Gc from tissues of free Neu5Gc fed mice. No Neu5Gc was detected in feces of free Neu5Gc fed mice (not shown). Importantly, studies with

methylene blue (not shown) indicate that ingested materials reach the ceco-ileal junction only at 6 hours after feeding, with blue-stained feces appearing sometime between 9-12 hours. Thus, the *C57bl6* mouse gastrointestinal kinetics discount the idea that the monosaccharide passes undigested through the gastrointestinal tract. We propose that the residual unaccounted for Neu5Gc is either degraded in the gut lumen (perhaps by the gut microbiome) or by endogenous metabolic pathways.

Feeding Neu5Gc-glycoproteins exhibits different intestinal metabolism, circulatory kinetics, and urine excretion compared to free Neu5Gc feeding. In striking contrast to free Neu5Gc feeding, which was entirely found as a free monosaccharide *in vivo* (intestines/blood/urine), Neu5Gc from Neu5Gc-glycoprotein fed mice was largely detected on glycans (e.g., Neu5Gc glycosidically linked to underlying sugars and presumably a carrier protein/lipid). In the blood, Neu5Gc detection by DMB-HPLC (Fig. 2-1E) required acid hydrolysis for DMB tagging, and in intestines and liver, we were able to track Neu5Gc using αNeu5Gc IgY (Fig. 2-2), all suggesting that Neu5Gc-glycoprotein-derived Neu5Gc is trafficked as a glycan.

In the blood of Neu5Gc-glycoprotein fed mice, glycosidically-bound Neu5Gc appears in circulation on unknown molecules and maintains a near steady state for several hours (Fig. 2-1E, solid black circles). Interestingly, Neu5Gc-glycoprotein fed mice exhibit no excretion of Neu5Gc in urine (Fig. 2-1E, open gray circles), up to 48 hours after feeding (not shown). Thus, reduced recovery of Neu5Gc in Neu5Gc-glycoprotein fed mice at later time points (Table 2-1) is likely a result of metabolism, not excretion. Two hours after feeding, a high percentage of Neu5Gc can be recovered from the small intestinal walls (Fig. 2-1D). In particular, the terminal part of the small intestine was enriched for Neu5Gc (Fig. 2-1D, white and gray bars). Detection required acid hydrolysis, indicating that Neu5Gc was still carried on a glycan within the

intestinal wall. We derive confidence from the assertion Neu5Gc is in the intestinal wall because we also tracked a bacterial nonulosonic acid, Kdo, by DMB-HPLC to control for our intestinal lavage. Because >99.5% of Kdo was present in the intestinal contents fraction, we reasoned that our intestinal wall fraction was well lavaged and any Neu5Gc detected here was internalized by the wall or stably associated.

We confirmed our HPLC results using αNeu5Gc IgY in immunohistological analysis of Neu5Gc-glycoprotein fed intestinal rolls. In Fig. 2-2A, the upper row shows enriched staining in the middle (SI2) and terminal sections (SI3) of the small intestine and minimal staining in the proximal small intestine (SI1) and large intestine (LI), agreeing with our DMB-HPLC analysis. This staining appears within intestinal villi and does not appear to be associated with the luminal border, rather on the basolateral side of the intestinal enterocytes. To control for this staining, we employed a Control (pre immune) IgY on the Neu5Gc-glycoprotein fed tissues (Fig. 2-2A, middle row) and used αNeu5Gc IgY on non-fed *Cmah*$^{-/-}$ tissues (Fig. 2-2A, bottom row), both of which yield no staining. To further demonstrate the specificity of our staining, we blocked αNeu5Gc IgY with 10% chimpanzee serum (a rich source of Neu5Gc-containing glycans), which abrogated the intestinal staining (Fig. 2-2B). Thus we conclude that the majority of ingested Neu5Gc-glycoproteins are trafficked through the terminal half of the small intestine, roughly equating to the ileum in humans.

Feeding Neu5Gc-glycoproteins is physiologically relevant I. Dietary Neu5Gc-glycoproteins are bioavailable for glycosylation in the intestines. Because feeding Neu5Gc-glycoproteins exhibited different gastrointestinal kinetics than feeding free Neu5Gc, and because we reasoned that Neu5Gc-glycoproteins mimic red meat more so than a free monosaccharide, we hypothesized that Neu5Gc derived from a meal containing Neu5Gc-glycoproteins would be bioavailable. The small intestines are a

major site of digestion, exhibiting post-prandial metabolic activity to distribute dietary metabolites from the intestines, through the general circulation to peripheral tissues. The intestines secrete many proteins and lipids that are commonly sialylated, including the apolipoproteins, hormones, and gangliosides[27]. Because glycosylation is occurring in postprandial intestines, we hypothesized that a Neu5Gc-rich meal could contribute to intestinal glycosylation[7]. If correct, then we predict that a Neu5Gc-glycoprotein-rich meal could contribute to ganglioside synthesis as well as glycoprotein synthesis. As the presence of Neu5Gc-containing gangliosides would offer strong evidence for our hypothesis, we used repetitive 10:10:1::CH_3Cl:MeOH:sample extraction of intestinal wall homogenates 2 hrs after bound Neu5Gc feeding. From the lipid fraction, we purified gangliosides and were able to identify Neu5Gc by DMB-HPLC (Fig. 2-3A, red trace), which runs at the same time as a Neu5Gc containing standard (black trace). Notably, the majority of Neu5Gc in this intestinal fraction remained in the protein pellet (not shown). Control extractions using non-fed intestinal homogenates spiked with Neu5Gc-GM3 demonstrated the reliability of our methods by recovering Neu5Gc only in the lipid fraction (Fig. 2-3B, bright red trace), and not the protein faction (dark red trace). Control blanks were fractions of non-spiked, *Cmah*$^{-/-}$ homogenates (bright and dark green traces), which showed no Neu5Gc peaks.

Feeding Neu5Gc-glycoproteins is physiologically relevant II. Neu5Gc derived from Neu5Gc-glycoprotein feeding is bioavailable for glycosylation in the liver. To determine if dietary Neu5Gc-glycoproteins can be delivered to peripheral tissues in the *Cmah*$^{-/-}$ mice, we harvested livers at various times for immunohistology with αNeu5Gc IgY, which revealed staining in the portal vein endothelium at 2 hrs (Fig. 2-2C) then spread out into the peri-portal hepatocytes at 4 hrs (Fig. 2-2D). Western blot analysis of identical samples shows incorporation of Neu5Gc in many endogenous liver

glycoproteins (Fig. 2-4A) and the signal increases over time. We control for the specificity of αNeu5Gc IgY in western using a mild periodate treatment of the (PDVF) blotting membrane, which specifically destroys the C8-C9 side chain of sialic acids[28], a structural feature required for αNeu5Gc IgY binding (see Fig. 2-4A, column "*Cmah* +/+ Serum Control", and data not shown). Note that mild periodate treatment of blotted membranes does not non-specifically interfere with epitope recognition as conventional protein antigens are still recognized with or without treatment (see "Control IgY" lane in Fig. 2-4B). Importantly, this staining seen in the livers in Fig. 2-4A is not similar to native PSM run on SDS-PAGE and probed with αNeu5Gc IgY (Fig. 2-4B), indicating that the staining seen in postprandial liver homogenates is not just PSM fragments that have somehow made it to the liver.

Moreover, western blots of the liver samples after PNGaseF treatment (Fig, 2-4C) showed a shift in apparent molecular weight of some (black arrow heads), but not other bands (two-sided black arrows). Native PSM control lanes exhibited no shifts nor loss of bands upon PNGaseF treatment, indicating that the Neu5Gc-glycoprotein meal was not sensitive to PNGaseF (Fig. 2-4C) and that bands seen in peripheral tissues are not fragments of PSM that have been delivered to these tissues. The fact that PNGaseF treatment did not remove obvious bands in Neu5Gc-glyocprotein-fed liver homogenates, but instead shifted migration behavior in SDS-PAGE, could indicate that dietary Neu5Gc temporarily dominates cellular sialic acid pools in post-prandial glycosylation scenarios and nascent glycoproteins are sialylated with multiple Neu5Gc residues on N- and O-linked glycans. We conclude from these experiments that, Neu5Gc-glycoprotein feeding is bioavailable for self-glycan synthesis in multiple tissues.

Fasting and addition of dietary fat increases plasma Neu5Gc levels. We attempted to investigate dietary conditions that might increase the incorporation of Neu5Gc. Addition of fat (corn oil) in the gavage of Neu5Gc-glycoproteins significantly increased Neu5Gc levels in plasma at several time points (Fig. 2-10A). We recognized that this increase was directly linked to the absorption and transport of dietary fat and hypothesized that chylomicrons could be a mechanism of transport for Neu5Gc through the blood. Many apolipoproteins are glycosylated and apolipoprotein synthesis is stimulated in post-pradial enterocytes to nucleate chylomicron formation[29]. To test if Neu5Gc is present on chylomicrons secreted by the intestines, we analyzed sialic acids from isolated plasma lipoprotein fractions of Neu5Gc-glycoprotein fed mice. However, no Neu5Gc was detected in any of the lipoprotein fractions (not in chylomicrons, Fig. 2-10B; nor in LDL, Fig. 2-10C; nor in IDL, Fig. 2-10D; nor HDL, Fig. 2-10E). Instead, we detected Neu5Gc in the remnant plasma fraction after lipoprotein extraction. Increased Neu5Gc levels in plasma following fasting and addition of corn oil thus seems to be a result of alteration of gastrointestinal kinetics, likely by slowing food clearance from the stomach via constriction of the pyloric sphincter and increasing transit time to the intestines, and perhaps by stimulating small intestinal metabolism in general. In this regard, it is interesting to note that most Neu5Gc-rich foods consumed by humans (red meats) also happen to have a high fat content.

Long term Neu5Gc-glycoprotein feeding results in human-like incorporation of Neu5Gc in endothelial and epithelial tissues. Multiple attempts to load *Cmah*$^{-/-}$ mice with free Neu5Gc monosaccharide failed to recapitulate the human condition of incorporation into vasculature[8], carcinomas[9], placental tissues[10], or epithelium[12]. Our failed attempts are tabulated in Table 1-1. They include long term (4-16 wks) free Neu5Gc in drinking water, which did not yield convincing incorporation by

immunohistology with αNeu5Gc IgY, and 4 weeks of bi-weekly intraperitoneal injections of free Neu5Gc, which only lead to incorporation of the tubules of the kidney. In hindsight, this result agrees with the finding (Fig. 2-1F) that ingested free Neu5Gc is rapidly excreted into the urine. Four week free Neu5Gc in the drinking water did achieve minimal incorporation in spontaneous mammary tumors *in vivo*, but never into normal tissues[6].

We hypothesized that long term Neu5Gc-glycoprotein feeding is physiologic and might recapitulate human-like Neu5Gc incorporation. Indeed, immunohistology with αNeu5Gc IgY of 3 week Neu5Gc-glycoprotein fed mice revealed detectable levels of Neu5Gc incorporation into multiple organs (Fig. 2-5, three right columns). In particular, vasculature from the aorta (Fig. 2-5A, black arrow), spleen (Fig. 2-5B, black arrow) and kidney (Fig. 2-5C) showed staining. As expected, the small intestinal villi showed diffuse staining (Fig. 2-5D), indicative of its role in dietary trafficking. Importantly, we did not detect Neu5Gc staining in any organs from non-fed *Cmah*$^{-/-}$ animals (Fig. 2-5, two left columns)

At 4 weeks of Neu5Gc-glycoprotein feeding, we analyzed Neu5Gc incorporation by flow cytometry using single cell suspensions from heart, aorta, and small intestine (Fig. 2-6). In these experiments, cells from Neu5Gc-glycoprotein fed mice (red dots/traces) were compared to genotype controls in which cell suspensions from non-fed *Cmah*$^{-/-}$ mice (blue dots/traces) and *Cmah*$^{+/+}$ mice (green dots/traces) were isolated in parallel. Neu5Gc-glycoprotein fed mice showed increased Neu5Gc staining above levels detected in non-fed *Cmah*$^{-/-}$ cells (blue dots/traces), although not approaching levels of wildtype, *Cmah*$^{+/+}$ cells (green dots/traces). Interestingly, cells from aorta, heart, and small intestine of Neu5Gc-glycoprotein fed mice that were Neu5Gc^{+} largely co-expressed CD31, an endothelial cell marker (Fig. 2-6A). This was

not the case in the liver where Neu5Gc^{+} events were CD31^{-}. Similar assays at 10 weeks of Neu5Gc-glycoprotein feeding showed increased Neu5Gc incorporation in cells from aorta, heart, and small intestine (Fig. 2-6C), compared to 4 week feeding. CD31^{+} co-staining of Neu5Gc^{+} cells was seen again in aorta, heart, and small intestine, but not in liver (not shown). Subsequent intracellular staining for albumin (Alb) in hepatocytes showed that Neu5Gc^{+} events were Alb^{+} (Fig. 2-6B), which agrees with our short term Neu5Gc-glycoprotein feeding immunohistology (Fig. 2-2D) where Neu5Gc was detected in a pattern consistent with peri-portal hepatocytes. The endothelial (CD31^{+}) localization of Neu5Gc tissue incorporation is very similar to that seen in human tissues[8], thus these results (Figs. 2-5, 2-6) strongly support the hypothesis that human tissue Neu5Gc is the result of dietary Neu5Gc incorporation from glycosidically-bound, not free sources.

Our lab has long hypothesized that dietary Neu5Gc tissue incorporation and the prevalent Neu5Gc-specific antibody response[14] represents a human specific mechanism for inflammation. With apparent success loading *Cmah*$^{-/-}$ animals with dietary Neu5Gc, we were interested to test if mouse Neu5Gc-specific antibodies could recognize tissue incorporation within the context of self. To do this, we used serum of mice immunized against Neu5Gc-loaded *Haemophilus influenzae* as a source of mouse Neu5Gc-specific antibodies. This immunization strategy is physiologically possible in humans, and yields Neu5Gc-specific antibodies of multiple isotypes in *Cmah*$^{-/-}$ mice[15]. Sera generated from Neu5Gc-loaded *H. influenzae* stain *Cmah*$^{+/+}$, but not *Cmah*$^{-/-}$ heart tissue (Fig. 2-7A), demonstrating the Neu5Gc specificity of these sera. Interestingly, these sera recognized Neu5Gc incorporated into aortic cross sections of 3 week Neu5Gc-glycoprotein fed *Cmah*$^{-/-}$ mice (Fig. 2-7B, middle row). This staining could be blocked by 10% chimpanzee serum (Fig. 2-7B, bottom row),

similar to αNeu5Gc IgY, and co-localized entirely with the endothelial marker CD31 (Fig. 2-7C). These results indicate that serum Neu5Gc-specific antibodies can recognize the dietary derived, metabolically incorporated "xenoautoantigen" Neu5Gc.

Feeding Neu5Gc-glycoproteins to pregnant dams result in *in utero* incorporation into fetal tissues. Past studies reported the presence of Neu5Gc in human fetal meconium[30], then in human fetal tissues and placenta[11]. We suspected that the Neu5Gc detected in fetal tissues was the result of incorporation from the maternal diet.

In prior studies, 1 mg/mL free Neu5Gc in drinking water failed to load fetuses[6]. To model a physiologic pregnancy scenario in the mouse, *Cmah*$^{-/-}$ dams were fed Neu5Gc-glycoprotein chow from fertilization and throughout pregnancy with *Cmah*$^{-/-}$ pups. Tissue homogenates from post natal day 1 organs show Neu5Gc incorporation into many glycoproteins, including in small intestine (Fig. 2-8A). Immunohistology of post natal day 1 animals with αNeu5Gc IgY showed Neu5Gc staining in nearly every tissue tested (Fig. 2-8B), except the brain (Fig. 2-8C). *Cmah*$^{-/-}$ pups were maintained on a Neu5Gc-glycoprotein chow after weaning and were studied 4 weeks after birth by immunohistology with αNeu5Gc IgY. These animals showed similar patterns of staining, indicating that Neu5Gc was still accumulating through the diet after birth. Neu5Gc staining was not restricted to endothelial and epithelial tissues in pre-natal/post-natal loaded *Cmah*$^{-/-}$ mice and we could detect Neu5Gc at sites like smooth muscle bundles (not shown), skeletal muscle fibers (not shown), and in the endocardium (Fig. 2-8B), patterns not yet seen in human tissues. Throughout our experiments, we have seen a consistent enrichment for Neu5Gc incorporation in endothelial and epithelial cells. This is an unexplained phenomenon. Understanding the delivery mechanism by which dietary Neu5Gc is trafficked through the bloodstream will explain these patterns. This is the subject of current studies.

Neu5Gc-glycoprotein feeding results in incorporation into developing tumors. The presence of Neu5Gc in human carcinomas has been reported several times, and Neu5Gc was previously hypothesized to be an onco-fetal antigen in human cancer[30]. However, human carcinoma cells that are cultured in Neu5Gc-free media become Neu5Gc free over time[7], and oncogene-induced breast carcinomas in *Cmah*$^{-/-}$ mice were Neu5Gc free, until free Neu5Gc feeding in the drinking water at 1.5 mg_{Neu5Gc}/ml over 4 weeks yielded weak incorporation in the tumors[6].

We hypothesized that we could load tumors *in vivo* with Neu5Gc-glycoproteins. We injected 10^6 syngeneic MC38 carcinoma cells sub-cutaneously into the flanks of *Cmah*$^{-/-}$ mice. The mice were then split into 3 groups: 1, maintained on Neu5Gc-free soy chow; 2, moved to free Neu5Gc in the drinking water; 3, moved to Neu5Gc-glycoprotein chow. Tumor growth was not statistically different between the groups over the 3 week course (not shown). We used our flow cytometry-based assay to detect Neu5Gc levels on MC38 cells isolated from the flank tumor. Similar to previous results with free Neu5Gc feeding and cancer[6], free Neu5Gc feeding in this model led to increased Neu5Gc incorporation in MC38 cells compared to tumor cells grown in animals on the Neu5Gc-free soy chow (Fig. 2-9, left panel, black trace). However, MC38 cells from Neu5Gc-glycoprotein fed mice exhibited substantially increased Neu5Gc compared to both free Neu5Gc fed and soy chow fed mouse tumor cells (Fig. 2-9, right panel, black trace). It was interesting that Neu5Gc-glycoprotein feeding did not led to increased intensity of staining, compared to free Neu5Gc feeding, but instead led to a larger proportion of cells being Neu5Gc$^+$. This aspect indicates that both free Neu5Gc and Neu5Gc-glycoprotein feeding can load developing tumors, but Neu5Gc-glycoprotein feeding gains access to a greater proportion of the tumor. This may be

due to the poorly understood delivery mechanism of Neu5Gc-glycoprotein to peripheral tissues.

Once again, cancer was the only scenario where free Neu5Gc feeding resulted in some detectable Neu5Gc incorporation *in vivo*. If reliable in humans, this observation could be exploited to deliberately load tumors. Because ingested free Neu5Gc is poorly incorporated into physiologic tissues, tumor cells could be selectively labeled. Introduction of a Neu5Gc-specific toxin or inflammation associated with recognition by the human Neu5Gc-specific antibody response could then target the tumor for cytologic or immunologic attack, respectively. Regardless of these speculations, the onco-fetal characteristics of Neu5Gc in humans can likely be attributed to metabolic incorporation of Neu5Gc-glycoproteins from the diet.

CONCLUSIONS & PERSEPCTIVES

We have previously found trace amounts of Neu5Gc in a characteristic incorporation pattern in human tissues, despite the fact that humans are genetically unable to produce Neu5Gc. These tissues are endothelium of small and large blood vessels, intestinal epithelium (epithelium lining hollow organs), placenta, fetal tissues, and some carcinomas. We hypothesized that Neu5Gc in human tissues is metabolically incorporated from the diet, but many failed experiments in the mouse (Table 1-1) indicated that simple presence of free Neu5Gc *in* vivo was not sufficient. The current data have shown for the first time that dietary Neu5Gc-containing glycoproteins (PSM) are metabolically incorporated *in* vivo in a human-like tissue distribution (Fig. 2-5, 2-6). The striking contrast (Fig. 2-1) of Neu5Gc-glycoprotein feeding with the negative results of free Neu5Gc feeding indicates that there must exist a novel pathway for intestinal processing of glycosidically-bound Neu5Gc, with

subsequent delivery and incorporation into peripheral tissues. Free Neu5Gc is rapidly absorbed from the intestines, appears rapidly in blood, only to end up in urine in short term feeding studies. Long term loading studies agree well that free Neu5Gc does not work (Table 1-1). On the other hand, Neu5Gc-glycoprotein feeding exhibits different handling in the small intestine and throughout the body, disappearing more slowly from the intestine with a prolonged appearance in the blood and in the liver. Further studies are needed to elucidate the transport mechanism underlying this pathway.

It seems unlikely that humans and mice have evolved this system purely to scavenge dietary Neu5Gc. Given the striking differences in kinetics of free Neu5Gc and Neu5Gc-glycoprotein "meals", the ability of Neu5Gc-glycoproteins to result in metabolic incorporation in specific tissues, and the need for dietary sialic acids at critical periods of mammalian growth, it is likely that we are actually studying a general pathway for incorporation of dietary sialic acids. The bloodstream transport molecule for Neu5Gc has eluded us thus far. It does not seem to be a typical glycoprotein that can be resolved by Western Blot using αNeu5Gc IgY (not shown). It is also somewhat confounding that previous work (bottom row of Table 1-1) repeatedly injected Neu5Gc-containing serum proteins and achieved prolonged circulation (up to 8 days post injection) into *Cmah*$^{-/-}$ mice, yet there was no incorporation detected in peripheral tissues. It is possible that dietary Neu5Gc is not trafficked on conventional glycoprotein from the intestine through the bloodstream to peripheral tissues. For example, Neu5Gc could be trafficked in the bloodstream on a GPI-anchored carrier protein, which would not be seen on a conventional western but would require acid hydrolysis to detect Neu5Gc by DMB-HPLC. We are very interested to understand the *in vivo* transport mechanism for dietary Neu5Gc. We predict that understanding this

mechanism will shed light on the heretofore unexplained pattern of dietary Neu5Gc tissue incorporation seen in humans and now in *Cmah*$^{-/-}$ mice.

In conclusion, we are beginning to understand how humans metabolically incorporate dietary Neu5Gc. This information has important ramifications for human health and underscores the importance of minimizing dietary intake of Neu5Gc, presumably to reduce the body burden of Neu5Gc (although we have little data regarding the turnover of incorporated Neu5Gc in humans). Reducing dietary Neu5Gc should also minimize the risk for Neu5Gc-binding Shiga-like toxins[12] as well as minimize the interaction of Neu5Gc-specific antibodies and dietary Neu5Gc in promoting vasculitis[8] or carcinoma progression[9]. However, the ability of free Neu5Gc to load subcutaneous carcinomas (Fig. 2-9) presents an interesting possibility to selectively incorporate Neu5Gc into tumors for therapeutic reasons. We are pursuing this tumor labeling strategy, but it will be important to assure that free Neu5Gc does not load physiologic tissues *in vivo*, even at low levels.

MATERIALS & METHODS

Mice and Chow. *Cmah*$^{-/-}$ mice have been described previously [6]. Mice were housed in an AAALAC (Association for Assessment and Accreditation of Laboratory Animal Care)-approved vivarium with 12-hour diurnal lighting and access to food and water *ad libitum*. *Cmah*$^{-/-}$ mice were maintained on a Neu5Gc-deficient soy chow (110951/110751, Dyets, Inc.) to ensure that animals consumed no Neu5Gc prior to experiments. We confirmed that this chow is free of Neu5Gc by DMB-HPLC and is also free of sialic acids by the TBA reaction (data not shown). The Institutional Animal Care & Use Committee at UCSD approved all researchers and animal procedures.

Other Reagents. All reagents and chemicals were purchased from Fisher Scientific, unless otherwise specified.

Free Neu5Gc and Neu5Gc-glycoproteins for Feeding Studies. Free Neu5Gc was either purchased commercially (Inalco) or synthesized in-house according to published methods[31]. Porcine submaxillary mucin[32] was used as a source of mucin-type, Neu5Gc-containing glycoproteins (Neu5Gc-glycoproteins). Porcine submaxillary glands (Pelfreeze Biologicals) were chopped finely and homogenized in 5 volumes of water. Homogenates were centrifuged at 8000 rcf for 15 minutes, and the supernatant then filtered through glass wool. The mucin was precipitated by acidification (pH 3.5) and mixed overnight at 4˚C, then left to settle. Once settled, the supernatant was removed by siphoning and the precipitated mucin was centrifuged at 400 rcf for 15 minutes, washed with water, and centrifuged again. Mucin pellets were neutralized to pH 8.0 and dialyzed using a 10,000 MWCO CE membrane (Spectrum Labs) in 20 volumes of water, at least 5 volume changes. This preparation, called Porcine Submaxillary Mucin (PSM), was then dried by lyophilization and its Neu5Gc content was characterized by DMB-HPLC.

Neu5Gc-rich glycopeptides were also prepared from syngeneic mouse plasma from wild-type *C57bl6/J* mice (Harlan Teklad). Plasma was digested with 5 mg/mL proteinase K (Invitrogen) at 56˚C overnight, more proteinase K added to 10 mg/mL and digested at 56˚C for another night. After boiling for 20 minutes, glycopeptides were enriched by Sephadex G-25 Column Chromatography. Briefly, Sephadex G-25 Fine resin (GE Healthcare) was swelled and de-fined thrice in phosphate-buffered saline (PBS), pH 7.4, and packed into a column. The bed was equilibrated with 5 bed volumes of H_2O. One mL of 1:1 Digested plasma:H_2O was loaded onto the column and washed in with 500 µL H_2O and 1.5 mL fractions were collected. Sialic acid rich

fractions were identified by TBA and pooled. The Neu5Gc content of pools was quantified by DMB-HPLC.

Short Term and Long Term Feeding of Neu5Gc. *Cmah*$^{-/-}$ mice were gavaged with 1 mg_{Neu5Gc} using gavage needles (Braintree Scientific). At the appropriate time after feeding, animals were anesthetized using Isoflurane (VetOne), blood was collected by cardiac puncture. Next, we made a ventral, midline incision that exposed the peritoneal cavity, then isolated and cannulated the proximal duodenum on blunt-end needle. The small intestine was secured to the needle using 6.0 silk sutures (Braintree Scientific). We then isolated and clamped the distal ileum at the ceco-ileal junction and detached the small intestine from the cecum. The entire small intestine was flushed out with 6 mL PBS via the cannulation and the contents were collected from distal ileum into a glass conical tube. The small intestinal contents were dried down and resuspended in 1 mL H_2O. The small intestine (~30 cm) was divided into 3 equal segments. The cecal and large intestinal contents were lavaged similarly using PBS and similarly collected. The cecum and large intestinal wall were saved as one fraction. The stomach contents were emptied by large incision and subsequent dunking in lavage solution and collected. The stomach wall, liver and one kidney were collected. All tissue/intestinal content sections were then homogenized in 1 mL H_2O plus Type III protease inhibitor cocktail (EMD Biosciences). All samples were then snap-frozen in a dry ice/ethanol bath and stored at -80˚C. Fig. 2-1B depicts visually how we segmented the gastrointestinal tract and other organs for these studies.

Long-term feeding studies were carried out by homogenously mixing purified porcine submaxillary mucin into powdered soy chow (pg. 38) at a dose of 100-250 $\mu g_{Neu5Gc}/g_{chow}$. Chow powder was sterilized prior to feeding. Alternatively, custom chow was prepared professionally (Dyets, Inc.) by mixing mucin into the soy chow

ingredients before formulation. We measured body weight of the animals to ensure they thrived on the experimental chows.

Blood and Urine Kinetic Studies. Animals were gavaged, as above. To sample blood, we used the submandibular bleeding technique where blood is sampled from a conscious animal by puncturing the submandibular cheek pouch with a 5.0 mm lancet (Goldenrod Animal Lancets). Minimum blood volume (25-50 µL) was collected in plain glass capillary tubes and allowed to clot in Serum Microtainers (Becton Dickenson). Serum was isolated by spinning tubes at 10,000 rcf for 2 minutes and stored at -20˚C. Animals were bled at most 3 times before sacrifice. Urine was collected by restraining a conscious animal and taking advantage of spontaneous urination. If necessary, animals were gently massaged from the sternum in the caudal direction to induce urination. Urine was collected in plain capillary tubes and stored at -80˚C.

Quantification of Free- and Glycosidically-linked Neu5Gc by DMB-HPLC. Neu5Gc in tissue, blood, and urine samples was quantified by high performance liquid chromatography (HPLC) on a LaChrom Elite HPLC (Hitachi) using chemically-synthesized standards for Neu5Ac and Neu5Gc, as well as known biological standards for O-acetylated sialic acids (purified bovine submaxillary mucin sialic acids) at 0.9 mL/min in 85% H_2O, 7% MeOH, 8% CH_3CN. Fluorescent signals were excited at 373 nm and acquired at 448 nm.

Specific volumes of tissue homogenates were taken to maintain total sample sialic acid amounts below a 4 nmol threshold: stomach/small/large intestinal wall samples (100 $\mu L_{homogenate}$), stomach/small/large intestinal contents (100 $\mu L_{homogenate}$), liver (20 $\mu L_{homogenate}$), kidney (20 $\mu L_{homogenate}$), serum (5 $\mu L_{homogenate}$), urine (5 $\mu L_{homogenate}$).

To quantify free sialic acids in these samples, homogenates were diluted and spun in a Microcon-10, 10,000 MWCO centrifugal filter at 14,000 rcf for 15 minutes.

The retentate was washed with 400 µL H_2O and spun again. Free sialic acids in the run through were dried down (Eppendorf Vacufuge), resuspended in H_2O, and were derivatized with a 2x DMB solution, which contained 7 mM 1,2-diamino-4, 5-methylenedioxybenzene (DMB), 1.4 M acetic acid, 0.75 M β-mercaptoethanol, 18 mM sodium hydrosulfite. Samples were derivatized in the dark at 50˚C. for 2.5 hours[33].

To quantify total sialic acids, sialic acids were first de-O-acetylated in 0.1 M NaOH for 30 minutes at 37˚C. Next, glycosidically-linked sialic acids were released by acid hydrolysis in 2 M acetic acid at 80˚C for 3 hours. Samples were spun through a Microcon-10, washed, dried down, resuspended and derivatized as above.

Detection of Neu5Gc by Western Blot. Tissue homogenates were loaded on 10% polyacrylamide mini gels (Bio-Rad), then electrophoresed and electrotransferred to PDVF membranes (Bio-rad) using a Fastblot Semi-dry Transfer system (Biometra). Periodate treatment of membranes was used to confirm specificity of Neu5Gc signals and was performed by thrice washing PDVF membranes quickly in H_2O, then by thrice washing membranes in PBS pH 6.5 for 5 minutes, then exposing membranes to freshly made 2 mM $NaIO_4$ in PBS pH 6.5 for 30 minutes in the dark (or PBS control), then by thrice washing membranes quickly in H_2O, and finally by thrice washing membranes in H_2O for 5 minutes. Blocking, antibody incubations, and washes were then performed on the Snap-ID Vacuum Incubation System (Millipore). Membranes were blocked with 30 mL 0.5% Neu5Gc-free cold water fish gelatin (Sigma-Aldrich) in Tris-buffered saline containing 0.1% Tween (TBST+FG). Membranes were then incubated with 30mL chicken anti-Neu5Gc antibody (αNeu5Gc IgY, Sialix, Inc.), diluted 1:25,000 in TBST, washed 6 times with 30 mL TBST+FG, and then incubated with 30 mL HRP-anti-chicken-IgY (Jackson Immunoresearch), diluted 1:10,000. Signals were visualized by

Immobulon Chemiluminesce (Millipore), followed by exposure to Kodak BioMax XAR film for 5-30 s.

Detection of Neu5Gc by Histology. Tissues from animals were taken and either flash frozen in OCT (Sakura) or fixed in 10% neutral buffered formalin for 24 hours, then paraffin embedded. In the case of the small intestinal segments, each segment was cut open lengthwise and rolled up from the proximal end to the distal end with the mucosal side facing outwards. The rolls were fixed in 10% neutral buffered formalin for 24 hours, then paraffin processed and embedded. The rolls were sectioned at 5μm, then deparaffinized in xylene, followed by rehydration in graded ethanol dilutions and submersion in phosphate buffered saline with 0.1% Tween (PBST). The slides were overlaid with blocking buffer (0.5% cold water fish gelatin in PBST) and blocked for endogenous biotin (Vector Laboratories, Burlingame, CA) and peroxidase. Slides were incubated overnight at 4ºC with the αNeu5Gc IgY (1:5,000) and Control IgY (1:5,000; Jackson ImmunoResearch, West Grove, PA). Slides were then washed and incubated with the biotinylated donkey anti-chicken IgY (1:500; Jackson ImmunoResearch), then with Cy3-streptavidin (1:500; Jackson ImmunoResearch) for 30 minutes each. Cell nuclei were stained by incubation with DAPI (1:200,000; Sigma-Aldrich). Slides were then mounted in VectaMount (Vector Laboratories) and visualized by fluorescence microscopy.

For cryopreserved liver and postnatal day 1 specimens, frozen sections were cut from the OCT blocks rehydrated in PBST. Next, the slides were blocked for non-specific binding, blocked for endogenous biotin/peroxidase, and post-fixed in 10% neutral buffered-formalin (Fisher Scientific). Slides were incubated with antibodies as above, except that the secondary was followed by peroxidase-streptavidin (1:500; Jackson ImmunoResearch), developed with AEC substrate (Vector Laboratories), and

counterstained with Mayer's hematoxylin (Sigma-Aldrich). Slides were then mounted in VectaMount (Vector Laboratories) and visualized by brightfield microscopy.

Lipoprotein Isolation. Lipoprotein fractions were isolated according to previous reports[34]. Briefly, lipoproteins were prepared from murine blood drawn using sequential preparative ultracentrifugation. TRLs (δ = 1.006 g/ml) were prepared from pooled plasma samples (*n* = 10 mice; volume, 5 ml) by centrifugation for 12 hours at 135,000 *g* in a Beckman 50.3Ti rotor. VLDL remnants and IDL were then collected as the δ = 1.006–1.019 g/ml fraction. LDL and HDL were subsequently collected as the δ = 1.019–1.063 and δ = 1.063–1.21 g/ml fractions, respectively. Sialic acids were extracted from samples and quantified by DMB-HPLC, as described above.

Total Lipid Extraction and Ganglioside Purification. Total lipids were extracted from 200 μL of tissue homogenates using a 10:10:1::Chloroform:Methanol:Sample. Samples were vortexed to mix, then bubbled for 30 seconds with N_2, and sealed. Extraction proceeded at room temperature for 16 hours while shaking. Non-lipid materials were pelleted by centrifugation at 2,000 rcf for 15 minutes. Total lipids were then dried down on a Buchler Evapomix and resuspended by sonication (Fisher Sonic Dismembrantor) in 1.5 mL of 50mM KH_2PO_4, pH 7.3. Phospholipids were destroyed by treatment with Phospholipase C (Sigma), 5 mU/mg_{tissue}, for 6 hours at 37˚C. Samples were dried down on a Buchler Evapomix and resuspended in 1 mL methanol. We used anion exchange chromatography to purify gangliosides (sialo-glycolipids) from the remaining lipids. Sephadex A25 resin (GE Healthcare) was swelled in methanol and de-fined thrice with successive washes in 60:30:8::Methanol:Chloroform:0.8M Sodium Acetate by mixing, then aspirating the supernatant after the bulk resin had settled. Next the de-fined resin was washed thrice 60:30:8::Methanol:Chloroform:Water. The activated, de-fined resin was then prepared as a 50% slurry in methanol. Single-use

columns were prepared in 5" Pasteur pipettes by tamping a small plug of glass wool near the tip, such that the eventual flow rate of the column was ~1 drip/sec. Columns were packed with 50% DEAE A25 resin slurry, such that the bed was 3-4 cm in height or ~1mL bed volume. Columns were then washed with 6 bed volumes of 60:30:8::Methanol:Chloroform:Water, then with 6 volumes of methanol. 1 mL samples were applied to the column and allowed to run through. The columns were then washed with 6 bed volumes of methanol. Mono-, di-, tri-sialogangliosides were eluted together with 6 bed volumes of 0.5 M sodium acetate in methanol. Eluates were dried down and resuspended in 4 mL 1:1::Methanol:Water. Eluates were de-salted using C18 cartridges (Analtech). To desalt, these cartridges were equilibrated with 2 x 10 mL methanol washes, then 2 x 10 mL 1:1::Methanol:Water. Eluates from anion exchange were applied to the cartridge slowly. Cartridges were washed with 4 x 10 mL of water, then eluted with 2 x 10 mL 1:1::Chloroform:Methanol and 1 x 10 mL 2:1::chloroform:methanol. Eluates were dried down. Sialic acids were extracted from samples and quantified by DMB-HPLC, as above.

Long-term Neu5Gc Loading Studies. We fed adult *Cmah*$^{-/-}$ animals continuously with professionally formulated soy chow containing porcine submaxillary mucin (100-250 $\mu g_{Neu5Gc}/g_{chow}$) *ad libitum*. On day 28 of feeding, overnight fasted animals were euthanized and perfused via left ventricular puncture. In addition to fed animals, we also performed genotype controls in every experiment (a non-fed *Cmah*$^{-/-}$ mouse and a wildtype *Cmah*$^{+/+}$ mouse). The lobes of the liver were flipped up to identify hepatic veins and a minor branching vein off the largest hepatic vein was cut to create an outlet for perfusion. The basic perfusion solution was Krebs-Ringers (122 mM NaCl, 5.6 mM KCl, 5.5 mM D-glucose, 20 mM HEPES, 25 mM $NaHCO_3$, pH to 7.4 and filter sterilized). The animals were perfused with 20 mL of warmed Krebs-Ringer Solution

plus 10 mM EDTA at 7 mL/min. Next, animals were perfused with 20 mL of Krebs-Ringers Solution plus 150 μM $CaCl_2$,, plus 0.5 mg/mL Collagenase Type I (from Clostridium Hemolyticum, Sigma). Target organs (heart, aorta, jejunum, liver) would become opaque upon collagenase digestion with good perfusion. The organs were dissected out of the animal and placed into an iced 6 well plate and minced briefly, dissociated using a transfer pipette and the suspensions passed through cell strainers (100 μm, 70 μm, 70 μm, 40 μm, respectively, all from BD Biosciences). The resulting cell suspensions were washed twice in Krebs-Ringer solution plus 150 uM $CaCl_2$ by centrifugation at 300 rcf for 5 min at 4˚C. The final pellets were resuspended in 1mL of Krebs-Ringer solution and counted on an automated cell counter (Beckman Coulter).

Detection of Cell Surface Neu5Gc by Flow Cytometry. An equal number of cells were stained for flow cytometry. All cells were stained with αNeu5Gc IgY and with a rat-anti-mouse-CD31 (BD Biosciences). All cells were washed by centrifugation and incubated with a donkey-anti-chicken-IgY-Cy5 F'ab fragment (Jackson Immunoresearch) and with a goat-anti-mouse-IgG-AlexaFluor488 (Invitrogen). All cells were washed by centrifugation and resuspended for flow cytometry in PBS. To stain intracellularly for albumin, hepatocytes were stained for Neu5Gc, as above. After staining, cells were fixed and permeabilized according to the Cytofix/Cytoperm Kit (Becton Dickenson), stained with 1 μg rabbit-anti-albumin (IgG enriched, Accurate Chemical Co.), then stained with donkey-anti-rabbit-AlexaFluor488 (Invitrogen). Staining was controlled by performing intracellular staining with 1 μg pre-immune rabbit serum as the primary antibody. Cytometry was performed on a BD Facscalibur (BD Biosciences) and the data analyzed using Flowjo (Treestar).

ACKNOWLEDGEMENTS

This work was supported by NIH grants R01-GM32373, R01-CA38701 and a Meriaux Alliance Grant to Ajit Varki.

Chapter 2, in full, is based on a pre-final manuscript, *Banda K*, Gregg CJ*, Chow RE, Varki NM, Varki A, in preparation Journal of Biological Chemistry* (* denotes equal authorship). This manuscript is the result of a very fruitful collaboration a post-doctoral colleague, Kalyan Banda. The dissertation author will be the primary author and Dr. Ajit Varki directed and supervised the research that forms the basis of this chapter.

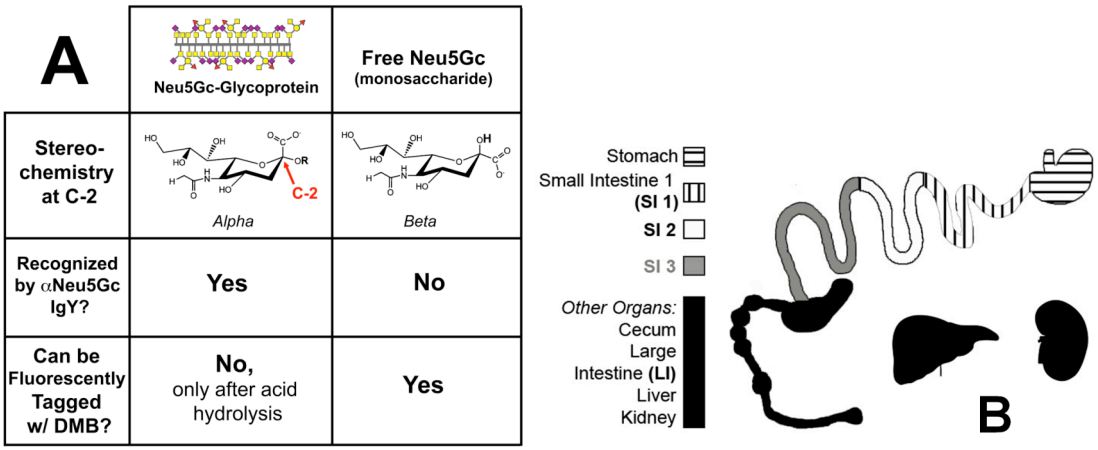

Figure 2-1. Different Gastrointestinal Handling of Neu5Gc in Free Neu5Gc or Neu5Gc-glycoprotein Feeding. A. This figure shows the two feeding strategies compared in this study (Neu5Gc-glycoprotein, left column; free Neu5Gc, right column) and with two key reagents used in this study. αNeu5Gc IgY can recognize glycosidically-linked Neu5Gc, such as on porcine submaxillary mucin (PSM, "Neu5Gc-glycoprotein" in this study). DMB is a fluorogenic tag that can react only with free Neu5Gc monosaccharide for quantification in HPLC. Acid hydrolysis can be used to release glycosidically-linked Neu5Gc from glycans so that it can be tagged by DMB and is an important process step for quantifying total Neu5Gc (with acid hydrolysis) and free Neu5Gc (without acid hydrolysis). **B.** Schematic of tissues studied in this paper. Stomach, small and large intestinal contents were collected. The small intestine was divided into 3 isometric sections (SI1, SI2, SI3), along with the stomach, large intestine (LI), liver and kidney and collected. Urine and feces were also collected.

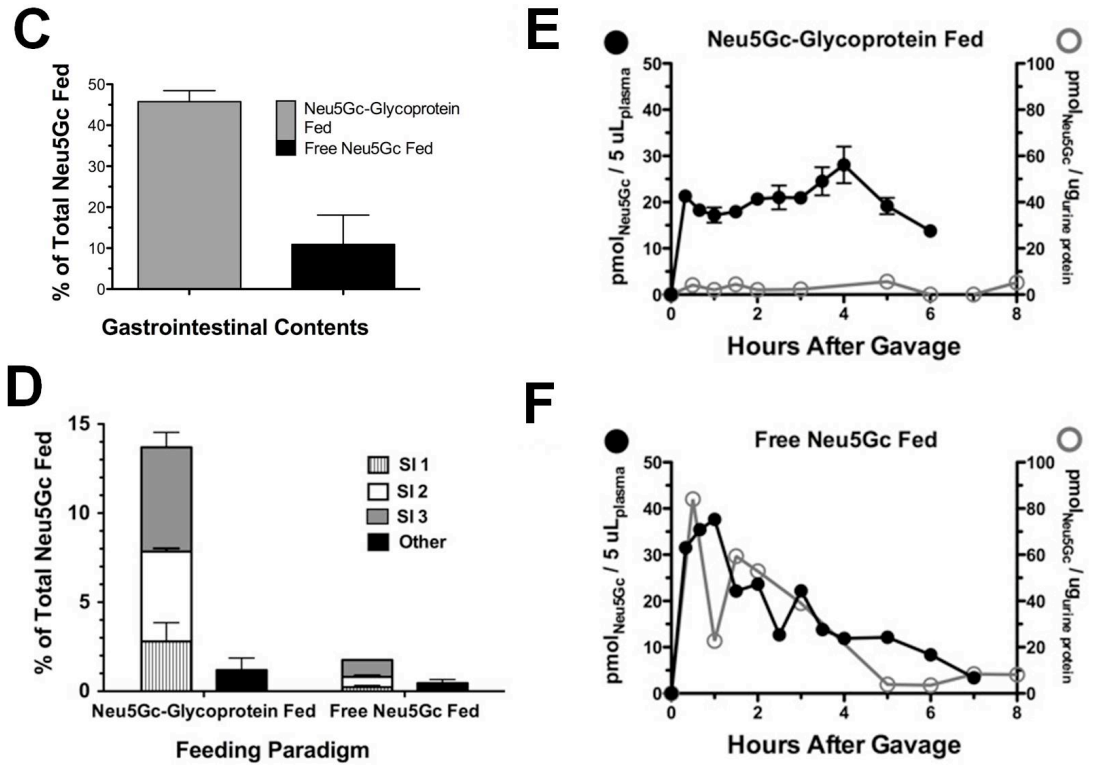

Figure 2-1, cont'd. Different Gastrointestinal Handling of Neu5Gc in Free Neu5Gc or Neu5Gc-glycoprotein Feeding. **C.** Neu5Gc recovered from contents of the gastrointestinal tract (Stomach, small and large intestinal contents) expressed as a percentage of amount gavaged (0.3 $mmol_{Neu5Gc}$). We recovered significantly more Neu5Gc from the content of Neu5Gc-glycoprotein fed mice than free Neu5Gc fed mice. **D.** Marked differences between Neu5Gc recovered from organs of free Neu5Gc and Neu5Gc-glycoprotein fed mice at 2 hours after feeding. SI1 (hatched bar), SI2 (white bar), SI3 (gray bar), other (black bar): liver, kidney, cecum/LI. Neu5Gc-glycoprotein feeding leads to Neu5Gc being retained in the intestines longer, compared to rapid absorption of free Neu5Gc from the intestinal contents. Neu5Gc from Neu5Gc-glycoprotein feeding is particularly enriched in the terminal small intestine (SI3, gray bar). **E.** The blood and urinary excretory kinetics of Neu5Gc in Neu5Gc-glycoprotein fed mice. Neu5Gc maintains a near steady state for up to 6 hours after feeding in blood (solid black circles) and is minimally excreted in urine (open gray circles) even at the end of 48 hours (data not shown). Neu5Gc was very minimally detected in feces from Neu5Gc-glycoprotein fed mice, ruling it out as major means of excretion. Neu5Gc derived from glycoprotein sources is unlikely to be excreted in large amounts unchanged. **F.** Free Neu5Gc fed mice show a spike and rapid disappearance of Neu5Gc from blood (solid black circles), indicating that it is rapidly absorbed from the gastrointestinal tract. Neu5Gc in urine from these mice shows similar kinetics, a spike and rapid disappearance (open gray circles). The scale of the y-axes in **E,F** is the same. Very minimal amounts of free Neu5Gc were detected in feces of free Neu5Gc fed mice.

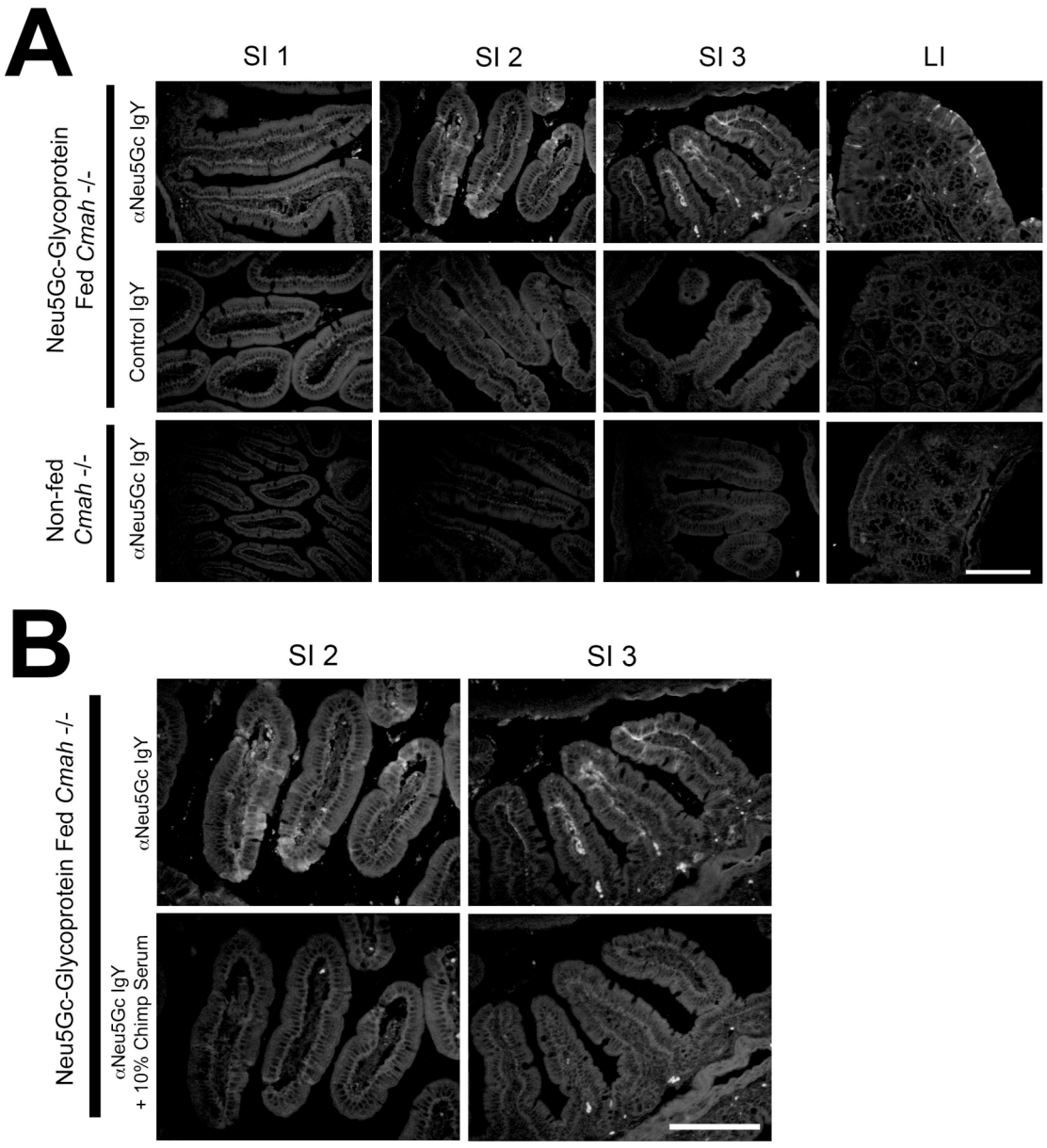

Figure 2-2. Intestinal Uptake of Neu5Gc only in Neu5Gc-glycoprotein-fed Mice. A. Frozen sections of indicated intestine from Neu5Gc-glycoprotein fed mice 2 hours after feeding. Sections are stained with 1:5000 αNeu5Gc IgY (top row) showing prominent uptake in the middle (SI2) and terminal (SI3) part of the small intestine, agreeing with Fig. 2-1C. Control IgY shows absence of staining on same tissues (middle row). Importantly, tissues from non-fed *Cmah*$^{-/-}$ mice show absence of staining with αNeu5Gc IgY (bottom row). **B.** To control for the staining in A., we repeated staining in SI2, SI3 with and without 10% chimpanzee serum during the primary antibody incubation step. Chimpanzee serum is a rich source of Neu5Gc-containing glycoproteins and blocked staining seen by αNeu5Gc IgY in the SI segments (bottom row). Scale bar = 100 μm.

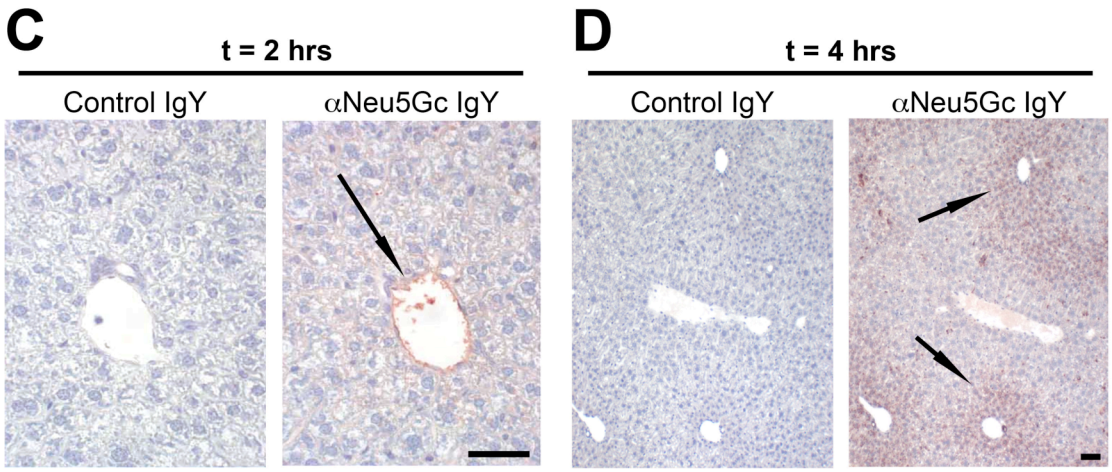

Figure 2-2, cont'd. Intestinal Uptake of Neu5Gc only in Neu5Gc-glycoprotein-fed Mice. C,D. Uptake of Neu5Gc in Neu5Gc-glycoprotein fed mice by the liver. To determine if Neu5Gc derived from Neu5Gc-glycoprotein feeding is trafficked to peripheral tissues, we harvested livers of fed mice at 2 hours (C) and 4 hours (D). Immunohistochemistry using αNeu5Gc IgY revealed staining in the portal vein at 2 hours (C), peri-portal hepatocytes at 4 hours (D) and increasingly diffuse peri-portal hepatocytes at 6 hours (figure not shown). Scale bar = 100 μm.

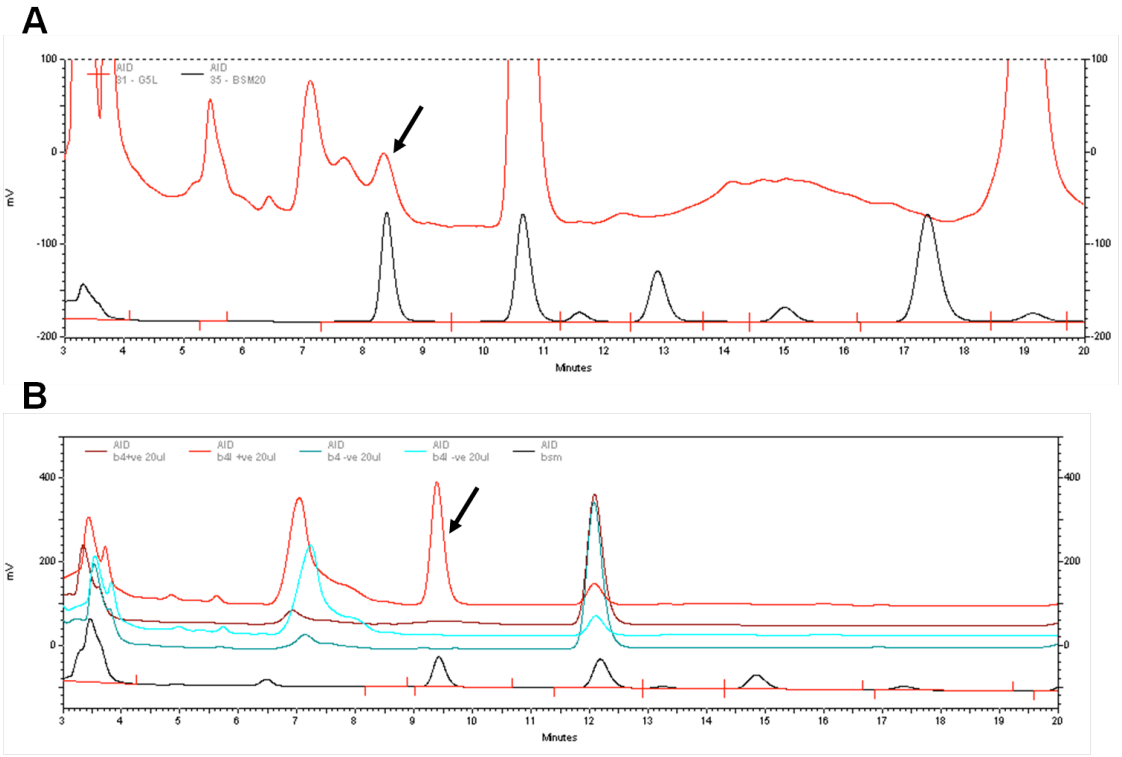

Figure 2-3. Neu5Gc from Neu5Gc-glycoprotein Feeding is Bioavailable for Endogenous Glycan Synthesis. A. Total tissue lipids were extracted according to the methods and Neu5Gc was detected by DMB-HPLC. Neu5Gc was detected on the endogenous glycolipids of mouse intestinal wall (bright red trace, marked with a black arrow). Neu5Gc containing standards are shown (black trace) at the bottom of the chromatogram. **B.** Lipid extraction controls. To control for the lipid extraction procedure, we spiked non-fed *Cmah*$^{-/-}$ mouse intestinal segments with a Neu5Gc containing lipid (GcGM3 ganglioside). We were able to recover the spiked Neu5Gc-containing ganglioside, GcGM3, only in the lipid phase (bright red trace, marked with a black arrow), not the protein pellet (dark red trace). Non-spiked, non-fed *Cmah*$^{-/-}$ intestinal homogenates showed no Neu5Gc in either lipid (bright green trace) or protein (dark green trace). Neu5Gc containing standards are shown (black trace) at the bottom of the chromatogram. These controls indicate the efficacy of our lipid extraction.

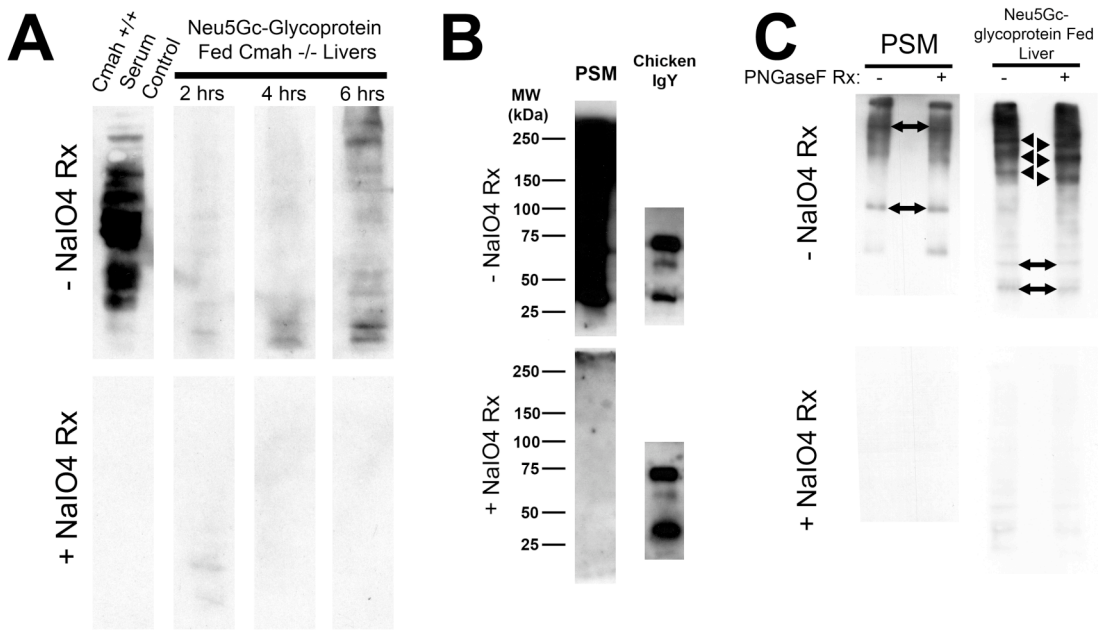

Figure 2-4. Immunoblots with αNeu5Gc IgY Confirm that Neu5Gc from Neu5Gc-glycoprotein Feeding is Incorporated into Self-liver Glycans. A. Immunoblot of Neu5Gc-glycoprotein fed *Cmah*$^{-/-}$ liver homogenates (25 µg/lane) at the indicated time point with αNeu5Gc IgY with (bottom) and without (top) periodate treatment (+/- $NaIO_4$ Rx) of PDVF blotting membrane. Neu5Gc is present on many endogenous liver glycoproteins and signal increases over time. To control for staining we treated control PVDF membranes with mild periodate (2mM), which makes Neu5Gc unrecognizable to αNeu5Gc IgY. The positive control, "Cmah +/+ Serum Control" (left lane), is strong, but 100% sensitive to mild periodate treatment (bottom blot). **B.** Immunoblot of native Porcine Submaxillary Mucin (PSM, called "Neu5Gc glycoprotein", 100 ng/lane) with αNeu5Gc IgY, with (bottom) and without (top) mild periodate treatment (as in A). PSM runs as a high molecular weight smear, with no apparent, distinct bands. Chicken IgY (100 ng) was included to show that mild periodate treatment does not interfere with epitope recognition of proteins in SDS-PAGE. **C.** Immunoblot of Neu5Gc-glycoprotein fed *Cmah*$^{-/-}$ liver at 6 hours with αNeu5Gc IgY with (bottom) and without (top) periodate treatment. To show that Neu5Gc is bioavailable for endogenous glycan synthesis, we used PNGaseF treatment of liver homogenates. PNGaseF treatment did not remove bands, but instead lead to a shift towards a lower apparent molecular weight for several bands (black arrow head) in +PNGaseG lanes, compared to –PNGaseF lanes. Migration of other bands within the same homogenate was not affected by PNGaseF treatment (two-sided black arrows). PSM controls exhibited no apparent shift with PNGaseF treatment, commensurate with mucin-type O-GalNAc glycans on PSM (B).

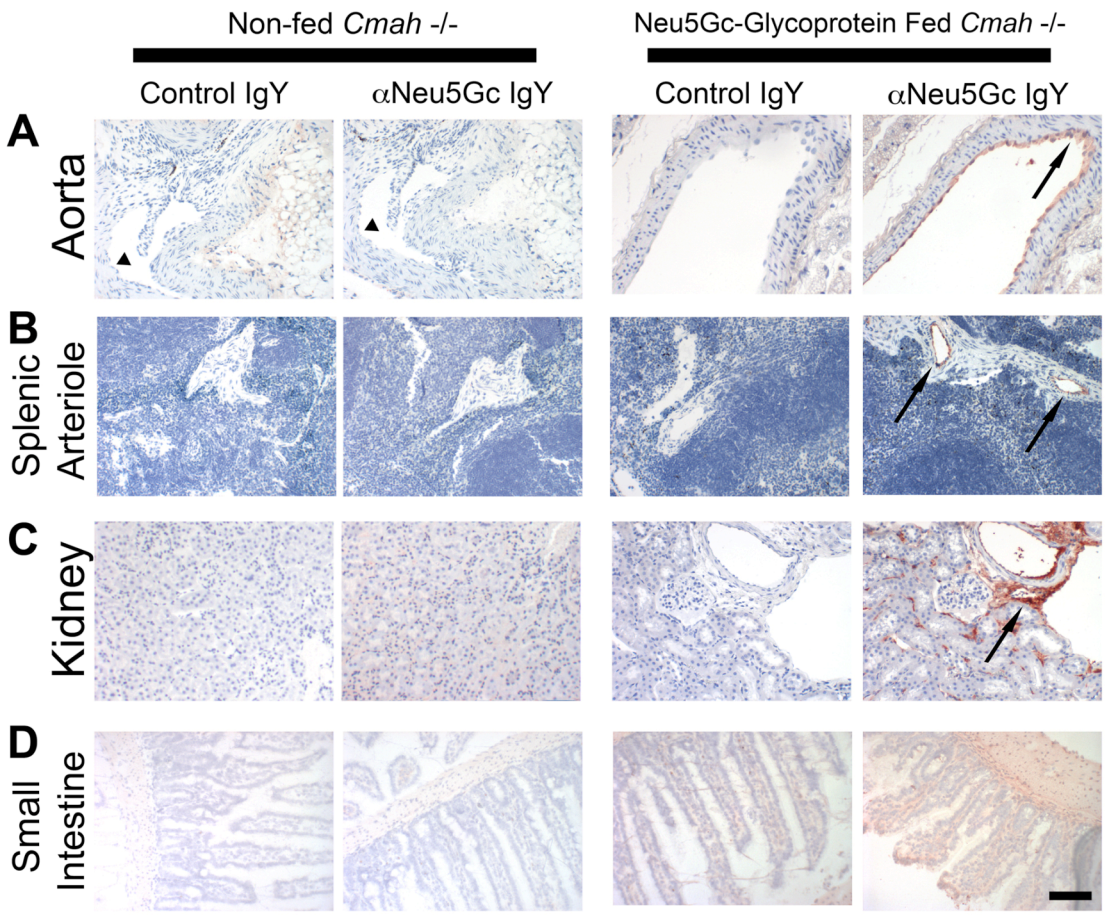

Figure 2-5. Long term Neu5Gc-glycoprotein Feeding Leads to Metabolic Incorporation of Neu5Gc with a Human-like Tissue Distribution I. A-D. Paraffin embedded sections of Aorta (A), Spleen (B), Kidney (C), and Small Intestine (D) of 3 week Neu5Gc-glycoprotein fed mice were stained with 1:5000 Control IgY or αNeu5Gc IgY (2 right columns). Brown staining (see black arrows) with αNeu5Gc IgY, not seen Control IgY indicates that Neu5Gc is incorporated into these tissues. Similar sections from non-fed *Cmah*$^{-/-}$ tissues were also stained with Control IgY or αNeu5Gc IgY (2 left columns), which showed no staining. Collapsed lumen of non-fed aorta (A, left columns) is marked (see black arrowhead). Scale bar = 100 μm.

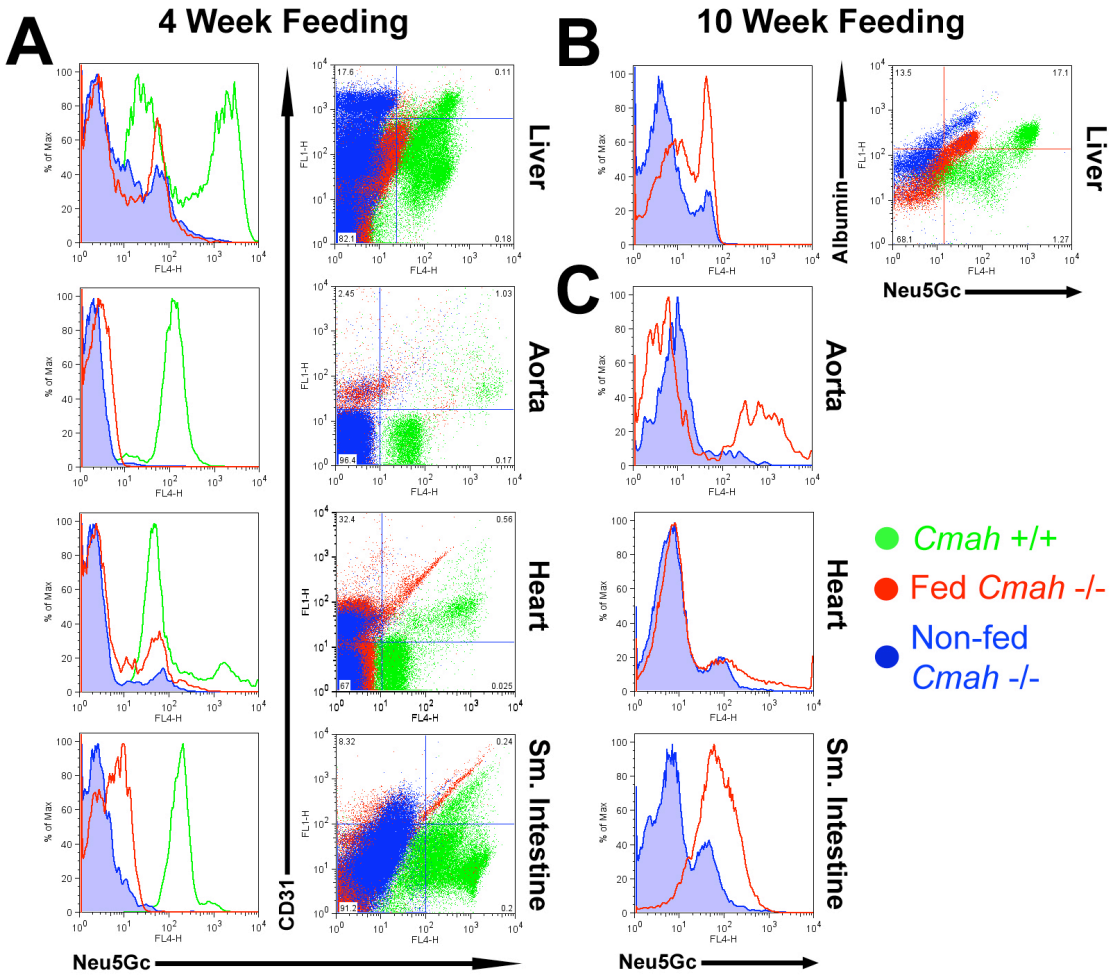

Figure 2-6. Long term Neu5Gc-glycoprotein Feeding Leads to Metabolic Incorporation of Neu5Gc with a Human-like Tissue Distribution II. A-C. *Cmah*$^{-/-}$ mice were fed with Neu5Gc-glycoprotein for 3 weeks (A) or 10 weeks (B,C). At sacrifice, the animals were perfused with collagenase, organs dissociated and stained with αNeu5Gc IgY (A-C), anti-CD31 IgG (A,C), or anti-albumin IgG (B). Flow cytometric analysis showed positive staining for Neu5Gc in Neu5Gc-glycoprotein fed mice (red dots/traces) above levels seen with non-fed *Cmah*$^{-/-}$ controls (blue dots/traces) at 4 weeks of feeding (A) and increased further at 10 weeks of feeding (C). Most Neu5Gc positive events from heart, aorta, and small intestine co-stained with a marker for endothelium (CD31), while Neu5Gc positive events in the liver (B) co-stained with a marker for hepatocytes (albumin). Tissues from *Cmah*$^{+/+}$ mice were used as positive controls and for comparison (green dots/traces). These results are representative results from staining that were carried out on multiple occasions with 3 Neu5Gc-glycoprotein fed mice per occasion.

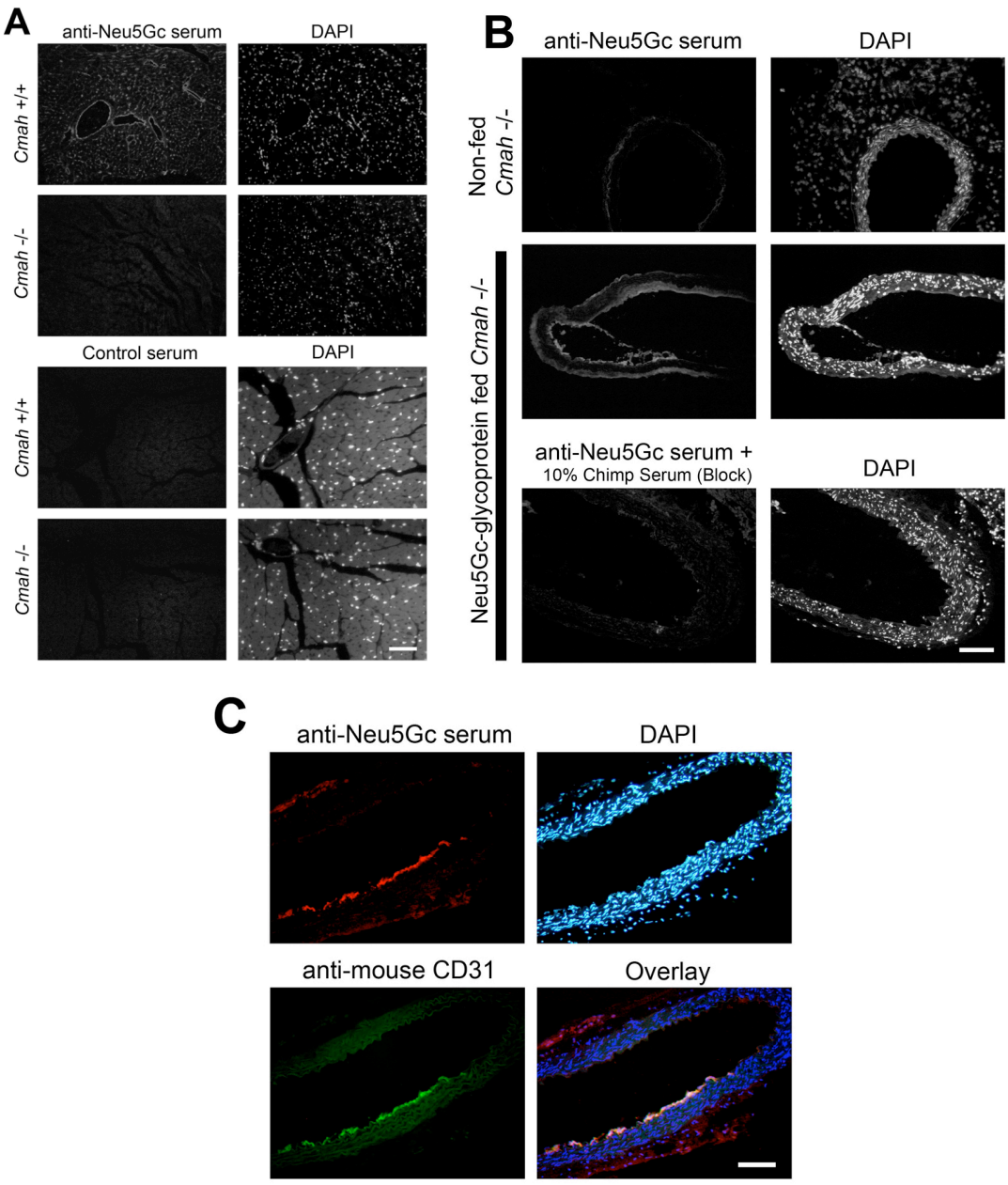

Figure 2-7. Metabolically Incorporated Neu5Gc can be Recognized by Neu5Gc-specific Antibodies. A. *Cmah*$^{-/-}$ mice were immunized against Neu5Gc to generate Anti-Neu5Gc serum using previously published methods[15]. This serum was used to recognize Neu5Gc in heart sections from *Cmah*$^{+/+}$ mice (top pair), but not in *Cmah*$^{-/-}$ heart tissues (bottom pair in top quartet) or when these tissues were incubated with control serum from *Cmah*$^{-/-}$ mice immunized with Neu5Gc-free bacteria (lower quartet). **B.** Anti-Neu5Gc serum was then incubated with aortic cross sections from non-fed (top pair) and Neu5Gc-glycoprotein fed mice, which yielded luminal staining only in fed mice only(middle pair). This staining was sensitive to blocking with 10% chimpanzee serum (bottom pair), which confirmed the specificity of this serum for Neu5Gc. **C.** Fluorescence colocalization microscopy showed colocalization (yellow) between aortic Neu5Gc (red), and the endothelial marker (CD31, green), which can be clearly seen in the 3 color fluorescence overlay at the bottom right. Scale bar = 100 µm.

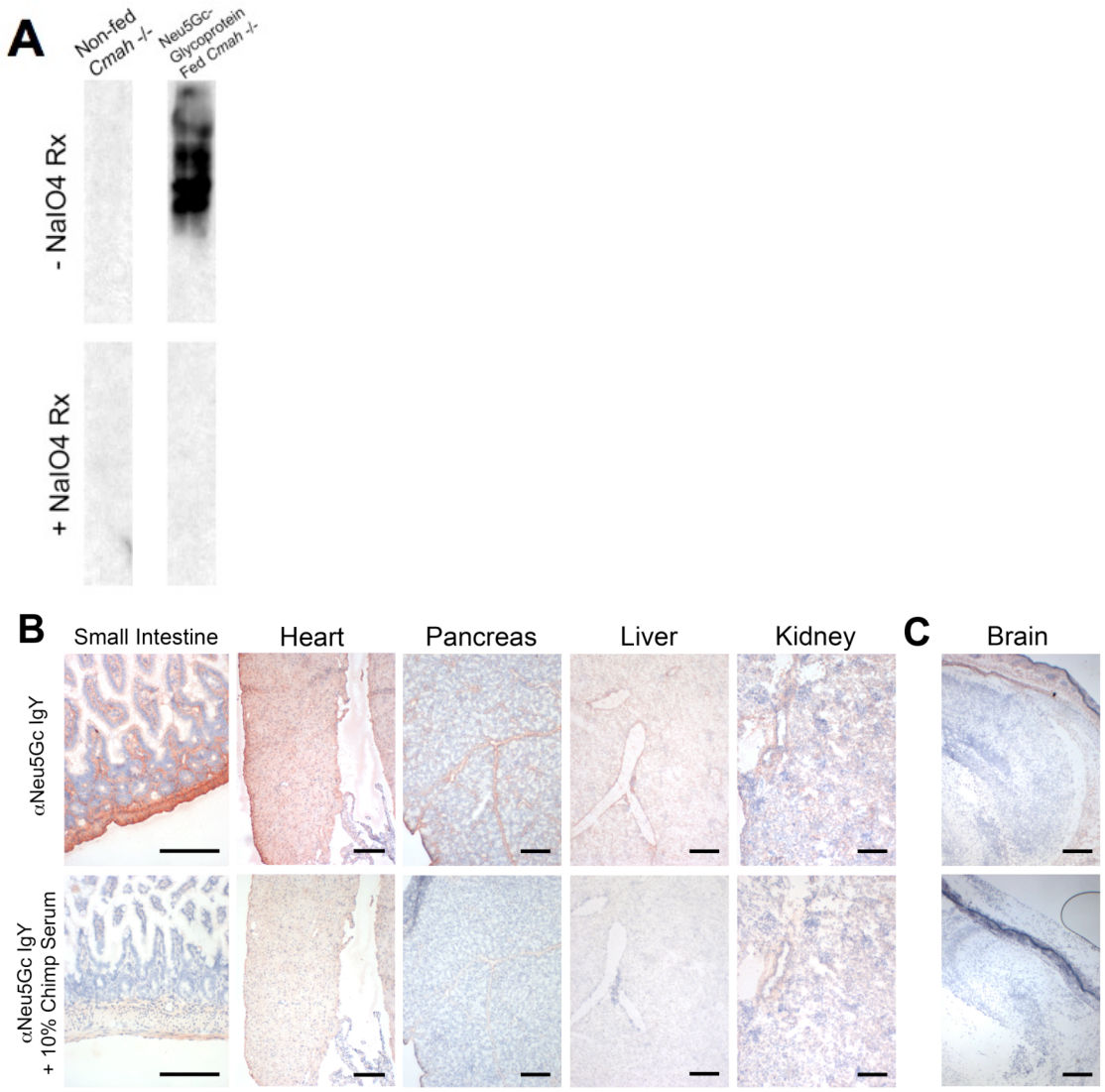

Figure 2-8. Maternal Dietary Neu5Gc is Metabolically Incorporated *In Utero* into Newborn Tissues. **A.** Western blot analysis with αNeu5Gc IgY demonstrates Neu5Gc on multiple glycoproteins of fetal small intestinal homogenates (top) that is sensitive to periodate treatment (+$NaIO_4$-rx, bottom). **B.** Immunohistochemistry with αNeu5Gc IgY of multiple tissues from *in utero* loaded *Cmah*$^{-/-}$ newborns indicated widespread incorporation of dietary Neu5Gc, in patterns that exceed those seen with adult feeding. *In utero* loaded mice demonstrate staining with αNeu5Gc IgY many tissues including heart, smooth muscle (surrounding intestinal villi), pancreas, liver, and kidney (top row). Staining was controlled with 10% chimpanzee serum block (bottom row). **C.** Consistent with the human condition, we were still unable to load Neu5Gc into the brain, although the cranial and dermis tissue surrounding the brain show staining with αNeu5Gc IgY (top row) that is sensitive to block with chimpanzee serum (bottom row). Scale bar = 100 μm.

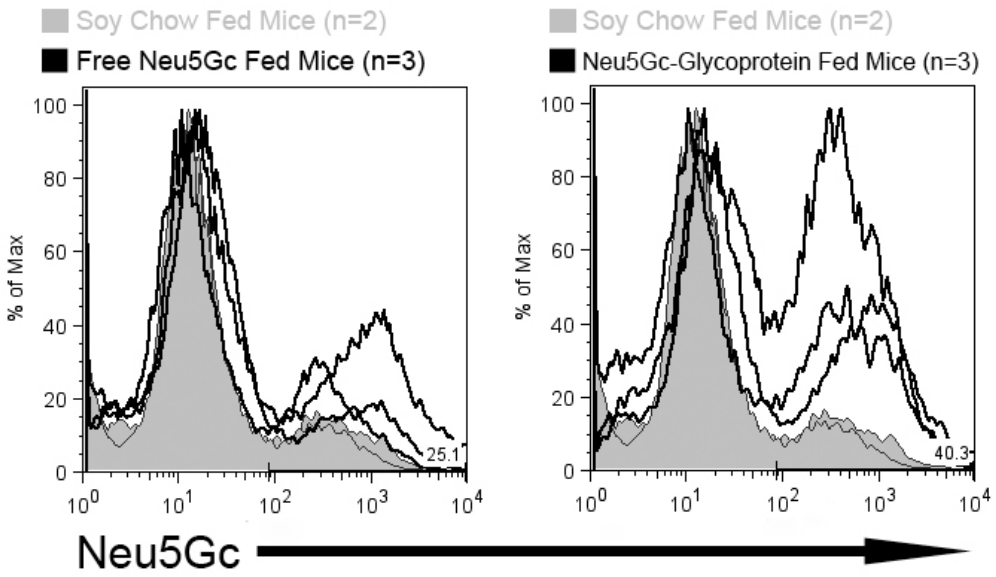

Figure 2-9. Dietary Neu5Gc is Incorporated into Developing Tumors *In Vivo*. To determine if dietary Neu5Gc can be incorporated in tumors *in vivo*, adult *Cmah*$^{-/-}$ mice were injected sub-cutaneously with 0.5*10^6 MC38 cells and fed no Neu5Gc (soy chow fed, tinted gray histograms, n=2), fed free Neu5Gc (solid line in the left histogram, n=3), or fed bound Neu5Gc (solid line in right histogram, n=3) for 3 weeks. Tumors were removed and digested into single cell suspensions using collagenase. 10^6 tumor cells from each mouse were stained αNeu5Gc IgY for flow cytometric analysis. Neu5Gc was incorporated into tumor cells from Neu5Gc-glycoprotein fed mice and free Neu5Gc fed mice, though at lower levels as indicated by the lower intensity of staining.

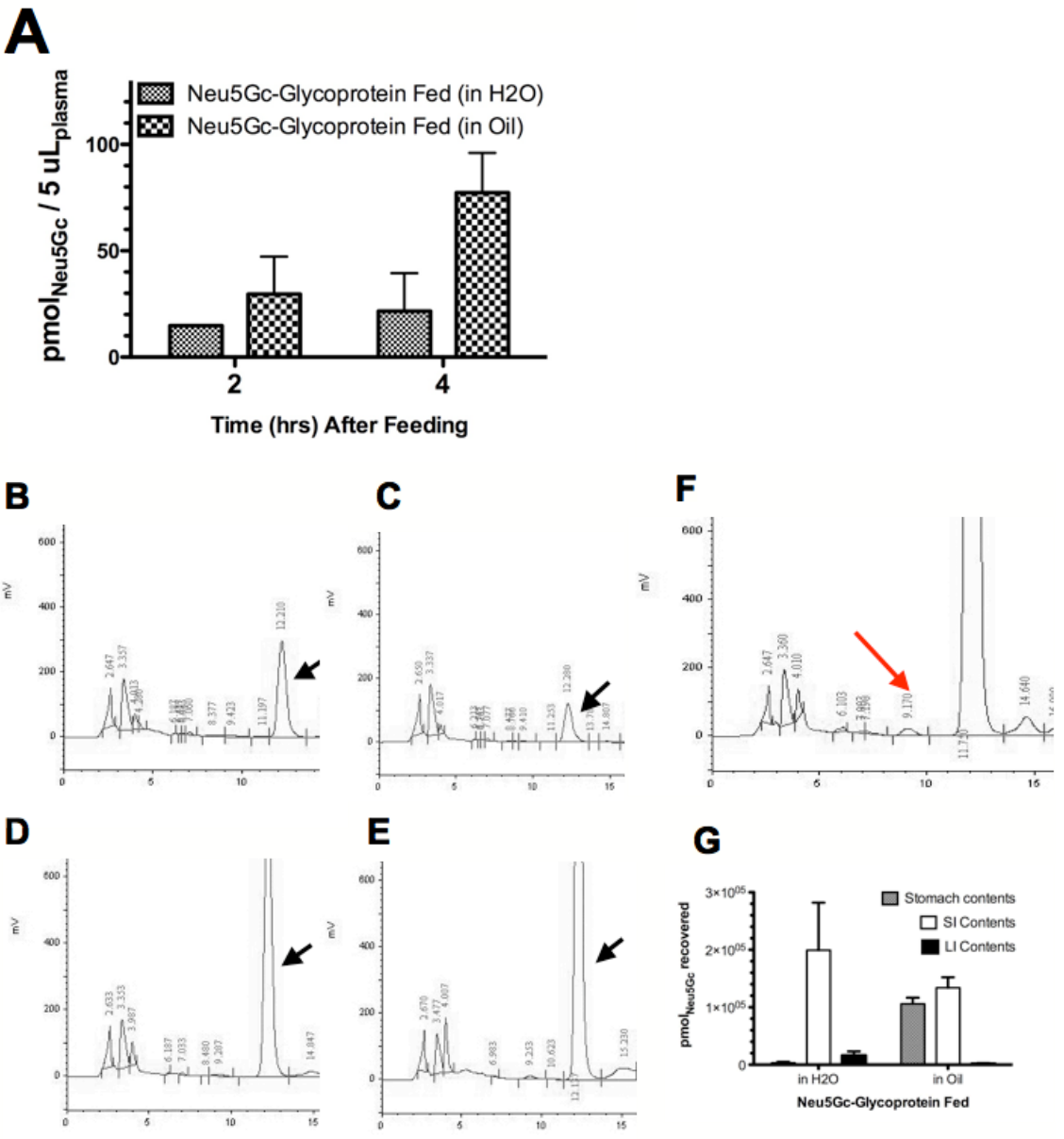

Figure 2-10. The Bloodstream Carrier Molecule for Neu5Gc is Not Lipoproteins. A. *Cmah*$^{-/-}$ mice were gavaged with Neu5Gc-glycoprotein in corn oil or water. Increased bloodstream Neu5Gc levels were associated with corn oil (and fasting), shown here 2 and 4 hours after feeding. **B-F.** Neu5Gc could not be detected from glycans of lipoproteins derived from chylomicrons (B), IDLs (C), LDLs (D), or HDLs (E), but instead was present in the remnant serum fraction (F). Neu5Ac is marked by a black arrow and Neu5Gc is marked by a red arrow (as determined in DMB-HPLC of known standards). **G.** Increased Neu5Gc levels in plasma following fasting and addition of corn oil seems to be a result of alteration of gastrointestinal kinetics, likely by slowing food clearance from the stomach, thereby increasing transit time through the small intestines. This is indicated by large amount of Neu5Gc recovered from the stomach contents in mice fed Neu5Gc-glycoproteins in corn oil (gray bar).

Table 2-1. Total Recovery of Neu5Gc after Feeding of Free Neu5Gc or Neu5Gc-glycoproteins. We gavaged equimolar amounts of free Neu5Gc or Neu5Gc-glycoprotein into *Cmah*$^{-/-}$ animals. At the indicated time points we isolated tissues (stomach, intestines, liver, and blood) and intestinal contents (stomach, small intestine, large intestine) and quantified the total Neu5Gc that could be recovered as a percentage of the total Neu5Gc fed (0.3 $mmol_{Neu5Gc}$). These recovery values omit any Neu5Gc in the urine (studied separately, Fig. 2-1E,F) due to the practicalities of urine collection. Fecal material was not collected at these time points as previous studies showed the digestive front barely reaches the cecum/large intestine at 6 hours after feeding.

	Hours After Feeding	2	4	6
% Neu5Gc Recovered	Neu5Gc-Glycoprotein Fed	60.44 ± 4.8	5.99 ± 2.1	0.40
	Free Neu5Gc Fed	18.37	1.50	< 0.01

REFERENCES

1. Varki, A. Sialic acids in human health and disease. *Trends Mol Med* **14**, 351-360 (2008).
2. Kelm, S. & Schauer, R. Sialic acids in molecular and cellular interactions. *Int Rev Cytol* **175**, 137-240 (1997).
3. Angata, T. & Varki, A. Chemical diversity in the sialic acids and related alpha-keto acids: an evolutionary perspective. *Chem Rev* **102**, 439-469 (2002).
4. Varki, A. Colloquium paper: uniquely human evolution of sialic acid genetics and biology. *Proc Natl Acad Sci U S A* **107 Suppl 2**, 8939-8946 (2010).
5. Chou, H. H. et al. A mutation in human CMP-sialic acid hydroxylase occurred after the Homo-Pan divergence. *Proc Natl Acad Sci USA* **95**, 11751-11756 (1998).
6. Hedlund, M. et al. N-glycolylneuraminic acid deficiency in mice: implications for human biology and evolution. *Mol Cell Biol* **27**, 4340-4346 (2007).
7. Bardor, M., Nguyen, D. H., Diaz, S. & Varki, A. Mechanism of uptake and incorporation of the non-human sialic acid N-glycolylneuraminic acid into human cells. *J Biol Chem* **280**, 4228-4237 (2005).
8. Pham, T. et al. Evidence for a novel human-specific xeno-auto-antibody response against vascular endothelium. *Blood* **114**, 5225-5235 (2009).
9. Hedlund, M., Padler-Karavani, V., Varki, N. M. & Varki, A. Evidence for a human-specific mechanism for diet and antibody-mediated inflammation in carcinoma progression. *Proc Natl Acad Sci U S A* **105**, 18936-18941 (2008).
10. Diaz, S. L. et al. Sensitive and specific detection of the non-human sialic Acid N-glycolylneuraminic acid in human tissues and biotherapeutic products. *PLoS ONE* **4**, e4241 (2009).
11. Tangvoranuntakul, P. et al. Human uptake and incorporation of an immunogenic nonhuman dietary sialic acid. *Proc Natl Acad Sci U S A* **100**, 12045-12050 (2003).
12. Byres, E. et al. Incorporation of a non-human glycan mediates human susceptibility to a bacterial toxin. *Nature* **456**, 648-652 (2008).
13. Nguyen, D. H., Tangvoranuntakul, P. & Varki, A. Effects of natural human antibodies against a nonhuman sialic acid that metabolically incorporates into activated and malignant immune cells. *J Immunol* **175**, 228-236 (2005).
14. Padler-Karavani, V. et al. Diversity in specificity, abundance, and composition of anti-Neu5Gc antibodies in normal humans: potential implications for disease. *Glycobiology* **18**, 818-830 (2008).
15. Taylor, R. E. et al. Novel mechanism for the generation of human xeno-autoantibodies against the nonhuman sialic acid N-glycolylneuraminic acid. *J Exp Med* **207**, 1637-1646 (2010).
16. Doherty, G. J. & McMahon, H. T. Mechanisms of endocytosis. *Annu Rev Biochem* **78**, 857-902 (2009).

17. Wang, B. Sialic acid is an essential nutrient for brain development and cognition. *Annu Rev Nutr* **29**, 177-222 (2009).

18. Wang, B. et al. Dietary sialic acid supplementation improves learning and memory in piglets. *Am J Clin Nutr* **85**, 561-569 (2007).

19. Bode, L. Human milk oligosaccharides: prebiotics and beyond. *Nutr Rev* **67 Suppl 2**, S183-91 (2009).

20. Wang, B., Brand-Miller, J., McVeagh, P. & Petocz, P. Concentration and distribution of sialic acid in human milk and infant formulas. *Am J Clin Nutr* **74**, 510-515 (2001).

21. Morgan, B. L. & Winick, M. A possible relationship between brain N-acetylneuraminic acid content and behavior. *Proc Soc Exp Biol Med* **161**, 534-537 (1979).

22. Anderson, J. W., Johnstone, B. M. & Remley, D. T. Breast-feeding and cognitive development: a meta-analysis. *Am J Clin Nutr* **70**, 525-535 (1999).

23. Dickson, J. J. & Messer, M. Intestinal neuraminidase activity of suckling rats and other mammals. Relationship to the sialic acid content of milk. *Biochem J* **170**, 407-413 (1978).

24. Nohle, U., Beau, J. M. & Schauer, R. Uptake, metabolism and excretion of orally and intravenously administered, double-labeled N-glycoloylneuraminic acid and single-labeled 2-deoxy-2,3-dehydro-N-acetylneuraminic acid in mouse and rat. *Eur J Biochem* **126**, 543-548 (1982).

25. Nohle, U. & Schauer, R. Uptake, metabolism and excretion of orally and intravenously administered, 14C- and 3H-labeled N-acetylneuraminic acid mixture in the mouse and rat. *Hoppe Seylers Z Physiol Chem* **362**, 1495-1506 (1981).

26. Nohle, U. & Schauer, R. Metabolism of sialic acids from exogenously administered sialyllactose and mucin in mouse and rat. *Hoppe Seylers Z Physiol Chem* **365**, 1457-1467 (1984).

27. Tso, P. & Balint, J. A. Formation and transport of chylomicrons by enterocytes to the lymphatics. *Am J Physiol* **250**, G715-26 (1986).

28. Norgard, K. E. et al. Enhanced interaction of L-selectin with the high endothelial venule ligand via selectively oxidized sialic acids. *Proc Natl Acad Sci USA* **90**, 1068-1072 (1993).

29. Rutledge, A. C., Su, Q. & Adeli, K. Apolipoprotein B100 biogenesis: a complex array of intracellular mechanisms regulating folding, stability, and lipoprotein assembly. *Biochem Cell Biol* **88**, 251-267 (2010).

30. Hirabayashi, Y., Higashi, H., Kato, S., Taniguchi, M. & Matsumoto, M. Occurrence of tumor-associated ganglioside antigens with Hanganutziu-Deicher antigenic activity on human melanomas. *Jpn J Cancer Res* **78**, 614-620 (1987).

31. Pearce, O. M. & Varki, A. Chemo-enzymatic synthesis of the carbohydrate antigen N-glycolylneuraminic acid from glucose. *Carbohydr Res* **345**, 1225-1229 (2010).

32. Gottschalk, A. *The chemistry and biology of sialic acids and related substances* (Cambridge University Press, Cambridge, 1960).

33. Hara, S., Yamaguchi, M., Takemori, Y., Nakamura, M. & Ohkura, Y. Highly sensitive determination of N-acetyl- and N-glycolylneuraminic acids in human serum and urine and rat serum by reversed-phase liquid chromatography with fluorescence detection. *J Chromatogr* **377**, 111-119 (1986).

34. Stanford, K. I. et al. Syndecan-1 is the primary heparan sulfate proteoglycan mediating hepatic clearance of triglyceride-rich lipoproteins in mice. *J Clin Invest* **119**, 3236-3245 (2009).

CHAPTER 3

Evidence for a Novel Human-specific Xenoautoantibody Response Against Vascular *N*-glycolylneuraminic Acid

ABSTRACT

Humans are genetically unable to synthesize the common mammalian sialic acid *N*-glycolylneuraminic acid (Neu5Gc). However, Neu5Gc can be metabolically incorporated and covalently expressed on cultured human cell surfaces. Meanwhile, humans express varying and sometimes high titers of polyclonal Neu5Gc-specific antibodies. Here, a survey of human tissues by immunohistochemistry with both a mono-specific chicken anti-Neu5Gc antibody and with affinity-purified human Neu5Gc-specific antibodies demonstrates endothelial expression of Neu5Gc, likely originating from Neu5Gc-rich foods like red meats. We hypothesized that the combination of Neu5Gc incorporation and Neu5Gc-specific antibodies can induce endothelial activation. Indeed, incubation of high-titer human sera with Neu5Gc-fed endothelial cells led to Neu5Gc-dependent antibody binding, complement deposition, endothelial activation, selectin expression, increased cytokine secretion and monocyte binding. The pro-inflammatory cytokine TNF-alpha also selectively enhanced human Neu5Gc-specific antibody reactivity. Neu5Gc-specific antibodies affinity-purified from human serum also directed Neu5Gc-dependent complement deposition onto cultured endothelial cells. These data indicate a novel human-specific mechanism in which Neu5Gc-rich foods deliver immunogenic Neu5Gc to the endothelium, leading to Neu5Gc-specific antibody-binding and complement-dependent activation, and potentially contributing to human vascular pathologies. In the case of atherosclerosis, Neu5Gc is present both in endothelium overlying plaques and in sub-endothelial regions, providing multiple pathways for accelerating inflammation in human vascular pathologies.

INTRODUCTION

Sialic acids are monosaccharides typically found at the outer ends of glycan chains covering the surface of all vertebrate cells[1]. The most commonly-expressed sialic acid is *N*-acetylneuraminic acid (Neu5Ac), which is the precursor for *N*-glycolylneuraminic acid (Neu5Gc) synthesis, via action of the CMP-*N*-acetylneuraminic acid hydroxylase (CMAH) enzyme[1]. While both Neu5Ac and Neu5Gc are expressed in many mammals (including our closest evolutionary cousins, the chimpanzees), the single-copy human *CMAH* gene was pseudogenized ~2-3 million years ago[2]. As mice with a human-like *Cmah* defect have no detectable Neu5Gc[3, 4], there is apparently no alternate mammalian pathway for Neu5Gc synthesis.

Although Neu5Gc is foreign to humans, our intracellular biochemical pathways cannot distinguish between Neu5Ac and Neu5Gc, which differ by one oxygen atom. Thus, exogenous Neu5Gc is taken up and metabolically incorporated into human cells, eventually being expressed on the cell surface as if it were made in the same cell[5-7]. Furthermore, orally ingested Neu5Gc is taken up into the human body[8], and small amounts of Neu5Gc are present in normal human tissues[8]. Interestingly, the Neu5Gc-rich foods identified to date are red meats—which have been associated with circulating inflammatory markers indicating endothelial dysfunction[9-12].

Although Neu5Ac and Neu5Gc seem biochemically indistinguishable to human intracellular biosynthetic pathways, the latter is immunogenic in humans, leading to Neu5Gc-specific antibody responses. While such antibodies had been reported in some diseases[13-15], it was only recently recognized that all adult humans express them[6, 7, 16]. Indeed, normal humans can express high titers of circulating Neu5Gc-specific IgG and IgM antibodies against a variety of Neu5Gc-containing epitopes commonly found on endothelial cells (see Fig. 1B of ref 17). Given this finding and the

presence of diet-derived Neu5Gc in human tissues, we consider the effects of this combination on human endothelial cells in this chapter.

Endothelial activation is a common feature of many diseases, including those associated with inflammation and reperfusion injury[18,19]. Antibody-mediated endothelial damage has also been described in many diseases, including primary autoimmune vasculitides[20, 21]; systemic autoimmune diseases with vascular involvement[22, 23]; as well as the early and late stages of atherosclerosis. Among primary autoimmune vasculitides such as Wegener's granulamatosis, Kawasaki disease, and Henoch-Schonlein purpura, there is an association between anti-endothelial cell antibodies (AECA) and disease status[22-27]. Systemic lupus erythematosus (SLE) also shows a relationship between AECA prevalence and disease status[28, 29]. Indeed, transfer of AECA into rabbits results in SLE-like nephritis[30]. It is likely that such antibodies act in concert with other immunological factors to exacerbate vascular damage[20, 24].

A humoral immunological contribution to atherosclerosis is also recognized. Antibodies against oxidized LDL epitopes are associated with coronary artery disease, are found in lesions, and are key players in endothelial damage and lesion progression[31, 32]. Infections can also generate a humoral response to bacterial HSP60, and the circulating anti-HSP60 antibodies can cross-react with stressed human aortic endothelial cells expressing modified autologous HSP60, causing an arteritis[33-36].

The AECA epitopes thus far identified are either proteins constitutively expressed by endothelial cells or upregulated by endothelial activation or inflammation[22, 26, 27, 37, 38]. Here we hypothesize that metabolic incorporation of dietary Neu5Gc into human endothelial cell surface glycoproteins leads to an immunogenic endothelial epitope that reacts with circulating human Neu5Gc-specific antibodies, causing complement deposition, endothelial activation and increased leukocyte

binding. In contrast to previous examples, the Neu5Gc-containing antigens are dependent on the endothelial cell's ability to metabolically incorporate Neu5Gc, which originates from food. To our knowledge, this is the first example of a "xenoautoantigen" that biochemically incorporates into human glycans and directs immunologic attack against "self". Additional novel features are that it is diet-induced and human-specific, and can potentially account for increases in circulating inflammatory markers associated with consumption of red meats [9-12].

RESULTS

Immunohistochemical detection of Neu5Gc on endothelium of large and small human vessels. Immunohistochemistry was performed on human tissue sections using a chicken polyclonal antibody (αNeu5Gc IgY) that is highly specific and sensitive for Neu5Gc-containing glycans. The specificity of this antibody for Neu5Gc was previously demonstrated by multiple methods[4], and was further controlled using a pre-immune IgY preparation. Examples are shown of results from frozen sections of many tissues. The αNeu5Gc IgY detected Neu5Gc on aortic endothelial cells from autopsy samples (Fig. 3-1A, left panel). Specificity of staining is demonstrated by a lack of background signal with Control IgY (Fig. 3-1A, middle panel), by a lack of signal when αNeu5Gc IgY was adsorbed out by Neu5Gc-rich chimpanzee serum (Fig. 3-1A, right panel), and by a lack of signal when tissue sections were sialidase pretreated (data not shown). Double-label staining with the endothelial marker CD31 (Fig. 3-1B) confirmed that Neu5Gc accumulation occurs primarily on the endothelium. As discussed later, we also showed accumulation of Neu5Gc in endothelium overlying atherosclerotic plaques.

Neu5Gc is also readily detected in the microvasculature of many human tissues. Examples such as placenta and colon are shown in Fig. 3-1C (left panels). Again, negligible background was demonstrated with Control IgY (Fig. 3-1C, right panels). Thus, Neu5Gc is present *in vivo* on the endothelium of both human large and small vessels, in a position to interact with circulating Neu5Gc-specific antibodies.

Affinity-purified human Neu5Gc-specific antibodies bind to endothelium in human tissue sections. To show that the human Neu5Gc-specific antibodies can also bind these endothelial antigens, we used a recently devised novel affinity-purification of Neu5Gc-specific antibodies from human sera[17]. The specificity of this enriched immunoglobulin (Ig) preparation for Neu5Gc was previously demonstrated by showing its failure to bind tissues of Neu5Gc-deficient *Cmah*$^{-/-}$ *mice*[17]. As shown in Fig. 3-2A (upper panels), the purified and biotinylated human Neu5Gc-specific antibodies stained endothelial cells of the human aorta, similar to the pattern seen with αNeu5Gc IgY in Fig. 3-1. Antibody binding was again Neu5Gc-dependent, as the staining was abrogated by pre-incubation with Neu5Gc-rich chimpanzee serum (middle panels), or when the tissue was pretreated with sialidase (lower panels). To further confirm Neu5Gc-specificity of the human antibodies, we studied the ability of methyl alpha-glycoside analogs of Neu5Gc (Neu5Gc2Me) or Neu5Ac (Neu5Ac2Me) to block the human Ig binding to endothelium. This synthetic mimic of glycosidically-linked Neu5Gc can effectively block the binding of human Neu5Gc-specific antibodies to Neu5Gc-containing glycans in ELISA assays[17]. Antibody binding to endothelium could be competed by Neu5Gc2Me but not by Neu5Ac2Me, confirming specificity for Neu5Gc-containing antigens on human aortic endothelium (Fig. 3-2B). Interestingly, endothelial Neu5Gc expression was also detected in the *vasa vasorum*, the small vessels within the wall of the aorta. Again, Neu5Gc2Me but not Neu5Ac2Me was able to abolish this

signal (Fig. 3-2B). Thus, Neu5Gc present on endothelium lining large and small vessels was detected by affinity-purified human Neu5Gc-specific antibodies.

Neu5Gc-specific antibodies from normal human sera bind to Neu5Gc-loaded human endothelial cells *in vitro*. To explore the pathogenic role of these human antibodies under more controlled conditions, we recapitulated the *in vivo* situation with an *in vitro* model system. We previously demonstrated that human cells in culture can take up free Neu5Gc and metabolically incorporate it onto self-glycans[5, 6]. Human endothelial cells also exhibited this ability in a dose- and time-dependent manner, with up to one-third of the cell surface Neu5Ac being replaced by Neu5Gc after a 3-day exposure to Neu5Gc in culture medium (data not shown, confirmed using αNeu5Gc IgY, as well as HPLC analysis). With this *in vitro* system to model accumulation of Neu5Gc into human vasculature *in vivo*, we tested the reactivity of Neu5Gc-loaded endothelial cells against a panel of human sera collected from random healthy humans. Cells loaded with Neu5Ac were included to provide the optimal control for background reactivity, allowing Neu5Gc-dependent phenomena to be specifically determined.

The level of antibody binding assessed by flow cytometry ranged from no binding to levels far above the background with Neu5Ac feeding (see representative profiles with four human sera in Fig. 3-3A, a more quantitative analysis of Neu5Gc-specific titers in the same healthy humans has been reported elsewhere[17]). We next observed variable Neu5Gc-specific reactivity in 14 random human sera for both IgG and IgM binding to intact cells, with human serum 34 (S34) giving the highest IgG binding and S35 giving the highest IgM binding. Arbitrarily normalizing IgG and IgM signals as a percent of the signal given by S34 in the same experiment (Fig. 3-3B), we find that most individuals (12/14) give relatively low IgG signals (defined as less than

33% of the IgG signal given by S34) while S34 and S37 give the highest IgG signal. For IgM, we found that more individuals (4/12) gave high Neu5Gc-specific IgM signals (at least 70% of the signal given by S34, Fig. 3-3B).

As an additional control, we assessed the ability of Neu5Gc2Me to block Neu5Gc-specific antibody binding. Using S37 as an example, we showed that Neu5Gc2Me inhibited Neu5Gc-specific IgG (Fig. 3-3C) and IgM (not shown) binding to Neu5Gc-loaded endothelial cells in a dose-dependent manner. In contrast, we observed little inhibition by Neu5Ac2Me. Thus, antibodies from normal human sera bind specifically to Neu5Gc-fed endothelial cells, and this interaction is Neu5Gc-dependent.

Human sera containing Neu5Gc-specific antibodies deposit complement onto Neu5Gc-loaded human endothelial cells. For further studies**,** we selected sera defined as “low-titer” or “high-titer” based on reactivity against Neu5Gc-loaded endothelium (S30 and S34 from Fig. 3-3B, respectively). Incubation of Neu5Gc-loaded endothelial cells with low-titer serum resulted in no complement deposition above levels seen with Neu5Ac-loaded endothelial cells (Fig. 3-3D, left panel). In contrast, high-titer serum gave a high level of Neu5Gc-specific complement deposition (Fig. 3-3D, right panel). Thus, the observed complement deposition is dependent on the Neu5Gc-specific antibody-antigen interaction. To confirm this, the high-titer serum S34 was heat-inactivated to deplete complement, yet retains immunoglobulin activity[6]. Heat-inactivated, high-titer sera failed to fix complement on endothelial cells (Fig. 3-3D, right panel, shaded curve). However, when heat-inactivated, high-titer serum was supplemented with fresh low-titer serum containing active complement, we again observed complement deposition in a Neu5Gc-dependent manner (Fig. 3-3E).

Neu5Gc-specific antibody-mediated complement deposition results in endothelial activation and increased leukocyte adhesion to Neu5Gc-loaded endothelial cells. Sublytic levels of complement deposition onto endothelial cells can induce cellular activation and up-regulation of surface adhesion molecules[43-45]. We therefore examined Neu5Gc-loaded endothelial cells exposed to human serum containing Neu5Gc-specific antibodies. Five-hour incubations with 50% high-titer serum gave an increase in surface E-Selectin expression in Neu5Gc-loaded endothelium over that in Neu5Ac-loaded cells (Fig. 3-4A, top left panel). As with antibody and complement deposition, there was some background with Neu5Ac-loaded cells, presumably due to other unrelated activating factors in the sera. Prior complement depletion by heat-inactivation abrogated the difference in E-Selectin expression between Neu5Gc- and Neu5Ac-loaded endothelium (Fig. 3-4A, bottom left panel). No differences in E-selectin expression were observed when cells were incubated with 50% low-titer serum (Fig. 3-4A, right panels).

In contrast to the transcriptionally-regulated E-Selectin surface expression upon activation, P-selectin surface expression occurs by mobilizing Weibel-Palade bodies to the plasma membrane[46]. Shorter (15-minute) incubations of HUVECs with high-titer serum elicited cell surface P-selectin expression that was Neu5Gc-dependent and also sensitive to serum heat inactivation (Fig. 3-4B). Thus, antibody-antigen binding with complement deposition is sufficient to induce cell surface P-selectin presentation. Background P-selectin presentation was not evident in Neu5Ac-loaded cells, nor in Neu5Gc-loaded cells exposed to low-titer or heat-inactivated serum.

We also studied cell lysates from such activated endothelial cells, looking for changes in cytokine production. Many cytokines were upregulated in cells loaded with Neu5Gc and stimulated with fresh high titer of Neu5Gc-specific serum, in comparison

to cells fed Neu5Ac and stimulated with the same fresh serum, or with cells loaded Neu5Gc but exposed to heat-inactivated serum (see Table 3-1). Many of the upregulated cytokines were involved in monocyte recruitment (e.g., CCL1/I-309, CCL8/MCP-2, CCL3/MIP-1α, CCL4/MIP-1β, CCL15/MIP-1δ, ICAM-1), leukocyte recruitment or differentiation (e.g., M-CSF, GM-CSF, GCSF), or in the generation of a pro-inflammatory state (e.g., IL-12 p70, IL-12 p40, IL-1α, IFNγ).

The above data confirm that binding of Neu5Gc-specific antibodies to Neu5Gc-containing glycans on endothelial cells and subsequent complement fixation causes endothelial activation. Recruitment of leukocytes to inflamed endothelium is a common pathway in endothelial damage, regardless of etiology. We therefore asked if the high-titered Neu5Gc-specific antisera could specifically enhance binding of monocytes to Neu5Gc-loaded endothelial cells. Human peripheral blood mononuclear cells (PBMCs, 10^5 per well) were added to Neu5Ac- or Neu5Gc-loaded endothelial cells, which had been exposed to high-titer (S34), low-titer (S30) serum, or heat-inactivated serum for 4 hours. The cell layer was stained with a Cy3-anti-CD14 antibody to detect monocytes, and binding events quantified by counting cells in ten random 400x power fields. Results are summarized in Fig. 3-4C. As a positive control, TNFα stimulated (10 ng/mL) endothelial cells demonstrated enhanced PBMC binding compared to cells not incubated with serum (28.1±2.0 vs 2.1±0.7 cells/field, respectively, $p<0.001$). Incubation with low-titer serum did not significantly increase PBMC binding to Neu5Ac (1.8±0.8 cells/field) or Neu5Gc-loaded endothelial cells (2.0±1.0 cells/field). However, high-titer serum significantly enhanced PBMC binding to Neu5Gc-loaded cells over that seen with Neu5Ac-loaded cells (19.1±3.1 vs 2.0±0.7 cells/field, respectively, $p<0.001$). Similar to the Selectin and cytokine production data, enhanced PBMC binding to Neu5Gc-loaded endothelium induced by S34 was sensitive to heat inactivation

(4.6±1.0 cells/field, $p<0.001$ vs. fresh S34, n.s. vs. No Serum control). Thus, we observed a significant increase in PBMC binding only to Neu5Gc-loaded endothelium that was exposed to fresh serum with high levels of Neu5Gc-specific antibodies.

Furthermore, PBMC binding to Neu5Gc-loaded endothelial cells, activated by high-titer serum was sensitive to blocking by 1mM Neu5Gc2Me, but not 1 mM Neu5Ac2Me (Fig. 3-4D). Representative immunofluorescence microscopy images of CD14-positive monocyte binding are also shown in Figure 3-8. We observed leukocyte binding and CD14 staining when endothelial cells are loaded with Neu5Gc and incubated with S34. There is substantially less leukocyte binding and CD14-positive binding on Neu5Gc-loaded endothelium when high-titered serum was pre-incubated with Neu5Gc2Me (bottom right panel), but not with Neu5Ac2Me (bottom left panel). These results further confirm that Neu5Gc antigen-antibody interaction is necessary for inducing subsequent leukocyte adhesion, and that the human Neu5Gc-specific antibodies are exquisitely specific for the single oxygen atom difference between Neu5Gc and Neu5Ac.

Endothelium overlying human atherosclerotic plaques contains Neu5Gc. Of the many human diseases associated with endothelial inflammation, the most prevalent is atherosclerosis, which involves intimal accumulation of LDL cholesterol and oxidized LDL epitopes and is exacerbated by many additional factors (see introduction and discussion). We therefore asked if Neu5Gc accumulation occurs in atherosclerotic plaques. As shown in Figure 3-5A, Neu5Gc is expressed in the endothelium overlying atherosclerotic plaques, as evidenced by colocalization with the endothelial marker CD31. Plaques are detected not only by their characteristic appearance, but also by their accumulation of $CD68^{+}$ macrophages and the lipid peroxidation epitope

malondialdehyde (MDA, Fig. 3-5B). This is shown more explicitly in Fig. 3-5C, where fluorescent images are double-stained for Neu5Gc and CD68.

Sub-endothelial expression of Neu5Gc within atheromas. Whereas Neu5Gc expression in healthy aortic sections was localized to the endothelium of micro- and macro-vasculature, areas of atherosclerotic human aorta exhibited novel sub-endothelial staining in addition to the typical endothelial staining (note the punctate, sub-endothelial Neu5Gc within the plaque in Fig. 3-5A). In another example (Fig. 3-5D), extensive and specific sub-endothelial Neu5Gc can be detected in the plaques. Thus, unlike the case in other blood vessels, Neu5Gc accumulation within atheromas provides an additional mechanism for Neu5Gc-specific antibodies to accelerate inflammation.

An inflammatory cytokine enhances human Neu5Gc-specific antibody binding to Neu5Gc-loaded endothelium. Many immune processes involving the vasculature manifest flares of exacerbation, and this is accompanied by a pathological production of inflammatory cytokines, notably TNFα. This cytokine can also significantly alter the display patterns of surface sialic acids on human endothelial cells by up-regulating expression of the sialyltransferase ST6Gal-I[47]. Thus, we hypothesized that local TNFα production might enhance the Neu5Gc-specific antibody binding profile to endothelial surfaces by altering the quantity and/or quality of Neu5Gc expression.

Endothelial cells were treated with or without TNFα during 18 hours of Neu5Gc or Neu5Ac feeding, and human serum antibody binding then assessed by flow cytometry. As shown in Fig. 3-6, TNFα-treatment increased binding of human Neu5Gc-specific antibodies. In contrast, no difference was observed between treated and non-treated Neu5Ac-loaded endothelium, confirming that augmented antibody binding is Neu5Gc-specific. Interestingly, TNFα treatment did not actually cause an obvious

increase in total Neu5Gc content as detected HPLC analysis (data not shown). Thus, the TNFα-induced increase in antibody binding represents a qualitative change in Neu5Gc antigen expression. We also studied IL-1β, IL-4, IL-6, IL-13, and IFNγ. Unlike TNFα none of these cytokines induced an increase in antibody binding to Neu5Gc-loaded endothelial cells, compared to mock-stimulated controls (data not shown). Thus, the TNFα effect involves additional unknown factors, perhaps perpetuating a vicious cycle in the endothelium overlying atherosclerotic lesions.

Affinity-purified human Neu5Gc-specific antibodies from human sera bind to specific glycoproteins in Neu5Gc-loaded endothelial cells and direct complement deposition. We further characterized the interplay amongst purified human Neu5Gc-specific antibodies, Neu5Gc-expressing endothelium, and complement. Using the purified human Neu5Gc-specific antibodies, we first investigated the nature of the endothelial glycoproteins containing Neu5Gc. Membrane proteins were isolated from Neu5Ac and Neu5Gc-loaded endothelium and subjected to Western Blotting. As shown in Fig. 3-7A, the purified human Neu5Gc-specific antibodies recognized only membrane glycoproteins isolated from Neu5Gc-loaded cultures. Interestingly, they bound only to a subset of the Neu5Gc-expressing glycoproteins detected by the broad-spectrum αNeu5Gc IgY. This result further indicates that specific linkages and/or conformational presentations of Neu5Gc on endothelial cell glycans are selective targets for circulating human antibodies.

Finally, we asked whether purified human Neu5Gc-specific antibodies could also initiate complement deposition. Neu5Gc-loaded endothelial cells were incubated with low-titer serum, affinity-purified Neu5Gc-specific antibodies, or both, and then double-labeled for complement deposition and IgG binding (Fig. 3-7B). As expected, incubation with a low-titer serum on Neu5Gc- or Neu5Ac-loaded endothelial cells

resulted in a majority of cells being double-negative (Fig. 3-7B, left column). In contrast, incubation of the purified Neu5Gc-specific antibodies on Neu5Gc-loaded endothelium resulted in 79% of cells becoming positive for IgG binding, while 86% of Neu5Ac-loaded cells remained double-negative (Fig. 3-7B, middle column). Moreover, incubation of Neu5Gc-loaded endothelium with a low-titer serum in the presence of the purified Neu5Gc-specific antibodies resulted in 71% of cells becoming positive for both IgG and complement binding (Fig. 3-7B, top panel of right column). These data confirm that human Neu5Gc-specific antibody binding to Neu5Gc-expressing endothelium directs complement deposition, and thus also likely drives Neu5Gc-dependent leukocyte adhesion *in vivo*.

DISCUSSION

Taken together, these findings suggest a mechanism whereby Neu5Gc-specific antibodies can initiate, perpetuate, and/or exacerbate an inflammatory response at the endothelium, potentially playing a role in disease states where vascular inflammation is involved, such as atherosclerosis,. Neu5Gc is a novel dietary and human-specific "xenoautoantigen" that may exacerbate a variety of vascular pathologies. Diets recommended by the United States Department of Agriculture lead one to ingest approximately 10 mg_{Neu5Gc}/day[8]. The primary dietary sources appear to be red meat (lamb, pork, and beef) and milk products, with Neu5Gc being conspicuously low in poultry and fish and absent from plants. Thus, long-term Neu5Gc intake and metabolic incorporation can explain our immunohistochemical finding of a strong Neu5Gc signal in the endothelial lining of blood vessels of human tissues. The proposed scenario is confirmed *in vitro* by demonstrating that Neu5Gc in cell media is sufficient for its incorporation into cell surface glycans in a time- and concentration-dependent manner.

We and others have previously shown that Neu5Gc is immunogenic in humans[6, 7, 16, 17]. Although it was previously thought that high antibody titers were only found in human diseases, we have recently found that the Neu5Gc-specific antibody response is quite prevalent[17], and have confirmed here that these antibodies can bind Neu5Gc-loaded human endothelial cells (Fig. 3-2A,B). Moreover we show that the purified Neu5Gc-specific human antibodies bound to Neu5Gc in human endothelial cells in tissue sections (Fig. 3-2), similar to that seen when using the Neu5Gc-specific chicken αNeu5Gc IgY (Fig. 3-1).

We hypothesized that the combination of Neu5Gc-containing glycans on endothelial cells and Neu5Gc-specific antibodies in circulation leads to antibody deposition on endothelial surfaces and subsequent complement deposition. This would promote a pro-inflammatory state in the vasculature and cell surface expression of adhesion molecules (Fig. 3-4). The nearly immediate upregulation of P-selectin and longer-term *de novo* presentation of E-selectin provide a means for selectin-initiated rolling adhesion of leukocytes on the vessel wall. Moreover, upregulation of cytokines by activated endothelial cells (see Table 3-1) that are involved in monocyte recruitment (CCL1, GM-CSF, M-CSF) and generation of a pro-inflammatory state (IL-12 p70, IL-12 p40, IL-1α, IFNγ) suggest mutually reinforcing mechanisms for facilitating monocyte extravasation at sites of endothelial Neu5Gc incorporation.

Indeed, *in vitro* evidence confirmed that PBMCs adhered to endothelial cells in a Neu5Gc-dependent fashion only in the presence of Neu5Gc-specific antibodies (Fig. 3-4C). Because leukocyte recruitment via endothelial interactions is central to many inflammatory vascular diseases, this human-specific mechanism for leukocyte binding could significantly contribute to endothelial damage. Furthermore, the presence of TNFα, a proinflammatory cytokine known to be upregulated during flares of vascular

damage, can enhance the impact of the human Neu5Gc-specific antibodies (Fig. 3-6). Finally, complement binding can have direct toxic effects on the endothelium, further contributing to endothelial damage. Such processes could be involved in exacerbating both the early stages of atherosclerosis and the late ulcerating phases, as both are facilitated by endothelial inflammation.

Of note, the Neu5Gc is covalently bound to and expressed on surface glycoproteins of the endothelial cells. Thus, any shedding of Neu5Gc on glycoproteins would be minor, and generalized immune complex formation is unlikely to be significant. However, this possibility needs to be considered. Also, we have previously reported that circulating blood cells do not express Neu5Gc, even after human volunteer ingestion of a large amount of Neu5Gc[8]. The reason for the difference between endothelial cells and blood cells is unknown, but it may have to do with differences in intracellular handling of exogenous Neu5Gc. Regardless, it is clear that the primary target of Neu5Gc-specific antibodies in circulation are endothelial cells.

In contrast to many other examples of AECAs, the humoral response to Neu5Gc is unique to humans, as compared to standard mammalian models. Interestingly, the Neu5Gc content of human tissues is likely to be chiefly dependent on dietary consumption of red meats, a food associated with increases in circulating markers of chronic inflammation[9-12]. In this regard, we recently showed that incorporation of dietary Neu5Gc into malignant cells can help explain the exacerbating effects of red meat consumption on carcinoma progression, a process also associated with chronic inflammation[48].

Of course, more information is needed about how dietary Neu5Gc is absorbed and distributed and what regulates its incorporation into tissues. It is also necessary to learn which endothelial glycan epitopes are the primary carriers of metabolically

incorporated Neu5Gc, and which specific Neu5Gc-specific antibodies are likely to be implicated in various pathological conditions involving vascular inflammation. The broad spectrum and variable prevalence of the Neu5Gc-specific antibodies in humans raises the possibility that not all subpopulations of antibodies are equally pathogenic. For example, as detailed recently[17], the Neu5Gc-specific antibody response is more pronounced for certain presentations of Neu5Gc, such as Neu5Gcα2-6Galβ1-4Glc-, a sequence found in endothelium *in vivo* and upregulated by inflammatory cytokines such as TNFα. Moreover, individuals with similar Neu5Gc-specific IgG levels did not give similar levels of complement deposition or cell activation, potentially reflecting differences in IgG subclass composition. Understanding the presentation(s) of Neu5Gc (both the linkage type and underlying glycoprotein structure) that are targeted by Neu5Gc-specific antibodies *in vivo* would also define relevant antigens that could be used to define pathogenic Neu5Gc-specific antibodies.

Finally, other investigators[49] have shown that conjugating a protein antigen to a foreign sugar can lead to enhanced production of antibodies against the protein itself, without the need for adjuvant. This response was dependent on the presence of antibodies against the foreign glycan, with the resulting immune complexes apparently acting as an adjuvant. Thus, antibodies that bind Neu5Gc on endothelial proteins could even prime a secondary immune response against these self-protein antigens themselves.

In conclusion, our studies describe a novel human-specific xenoautoantigen mediated immunologic mechanism that could contribute significantly to human vascular pathologies, such as atherosclerosis. It is interesting that subendothelial Neu5Gc deposition also appears within atherosclerotic lesions, perhaps due to permeability changes in chronically inflamed endothelium. Regardless of the reason, the

appearance of Neu5Gc within the lesions provides another potential mechanism to exacerbate inflammation via Neu5Gc-specific antibodies. Although much work is required to demonstrate relevance to human disease, this hypothesis would support novel therapeutic approaches to reducing or dampening flares of immunological responses against the endothelium. Such interventions could include reduction of dietary Neu5Gc intake and accumulation through simple diet-based interventions, enhanced elimination of Neu5Gc from humans, and/or reduction of Neu5Gc-specific antibodies titers.

MATERIALS & METHODS

Human serum samples. Normal human sera were from apparently healthy adult volunteers at the University of California, San Diego, with approval from the Institutional Review Board and written informed consent. Samples were de-identified, assigned a coded number, aliquoted, stored at -80°C and thawed only once, to preserve complement. For this study, we randomly used 14 of 37 prior donors[17], based solely only on their availability to re-donate blood.

Cell culture. Human Umbilical Vein Endothelial Cells (HUVECs, Lonza) were cultured in low serum (2% FBS) media supplemented with growth/serum factors as per manufacturer's instructions (EGM-2; Lonza). Cells were cultured in 24-well plates (BD Biosciences) in 5% CO_2 at 37^{o}C. To load with sialic acids, 3 mM Neu5Gc or Neu5Ac (Inalco) were diluted in EGM-2 media and incubated with cells for 3 days. While there were low levels of Neu5Gc-containing glycans in cells grown in FBS, these were competed out by 3 mM Neu5Ac feeding (data not shown). Cells were lifted with 10 mM EDTA solution without trypsin.

Detection of antibody binding and complement deposition on HUVECs by flow cytometry. HUVECs loaded with Neu5Ac or Neu5Gc were incubated with human sera diluted in media (without growth factors or FBS, EBM-2) at 1:5 (vol:vol) for IgG/IgM studies or 1:1 (vol:vol) for complement studies for 1 hour at 37^{o}C. Cells were gently washed twice with cold PBS and incubated on ice for 30 minutes with either FITC-mouse-anti-human IgG, FITC-mouse-anti-human IgM (Zymed Labs), or FITC-rabbit-anti-human C3b antibody (Dako), diluted 1:100 in PBS containing 20 mM EDTA. Cells were released by pipeting and fixed in 1% paraformaldehyde for 30 minutes on ice, and resuspended in PBS containing 10 mM EDTA for flow cytometry using a FACSCalibur (BD Biosciences).

Detection of cell adhesion molecule expression on HUVECs by flow cytometry. Neu5Ac or Neu5Gc loaded cells were incubated in human sera diluted 1:1 in EBM-2 for 0.25 hr (P-selectin) or 5 hr (E-selectin) at 37^{o}C. As a control, complement activity in serum was heat inactivated at 57^{o}C for 30 minutes. After incubation, cells were released and incubated in either mouse-anti-human CD62P or CD62E (BD Pharmingen), diluted 1:100 in EBM-2, for 30 minutes on ice. Antibody binding was detected with Alexa-488 goat-anti-mouse IgG (BD Pharmingen), diluted 1:100 in PBS containing 10 mM EDTA, quantified by flow cytometry.

Peripheral Blood Mononuclear Cell (PBMC) Isolation. Whole blood was isolated into BD Vacutainers (+EDTA, BD Biosciences) by venipuncture from healthy donors, and PBMCs isolated using Ficoll-Paque PLUS (GE Healthcare). PBMCs were plated onto 10 cm tissue culture plates (BD Biosciences) and cultured in RPMI plus 10% FBS overnight[39, 40].

PBMC Binding to HUVECs. Immunofluoresence microscopy of CD14-positive PBMC binding to HUVEC cultures were visualized with Alexa488-mouse anti-human CD14

antibody (BD Pharmingen), incubated for 1 hour on ice, mounted with SlowFade Gold containing DAPI (Invitrogen), and visualized with a Zeiss Axiolab (Zeiss) microscope. Digital photomicrographs were taken with a Sony DKC-5000 3CCD camera using NIH image software, analyzed using Adobe Photoshop, and overlaid to obtain double color images. Minor adjustments to brightness or contrast done to recapitulate the appearance to the human eye under the microscope were always done identically within each set of results. Most of the DAPI staining shows nuclei of endothelial cells and the morphological differences between endothelial (large, dim signal, ovular) and leukocyte (small, bright signal, circular) nlucei was helpful in discriminating binding events.

Cytokine Production by HUVECs. Cells were washed once with PBS, harvested with EDTA, counted, pelleted, and resuspended in cold Cell Lysis Buffer (Ray Biotech) plus protease inhibitor cocktail III (Calbiochem). Cell suspensions were kept on ice, sonicated with a Sonic Dismembranator 550 (Fisher) on ice, snap-frozen in an isopentane-dry ice slurry, and stored at -80C. Protein content was determined by the Bicinchoninic Acid Kit (BCA, Pierce) and equivalent protein amounts from all lysates used to detect cytokines with the Human Inflammation 3 kit (Ray Biotech), according to manufacturer's instructions. Chemiluminescent signals from all samples were exposed to film (Kodak) and developed. The film was photographed and the colors of the digital photograph were inverted in Photoshop (Adobe) for quantitative analysis. Signal intensities on the arrays were quantitatively analyzed using GenePix 6.0 (Molecular Devices).

Affinity purification of Neu5Gc-specific antibodies from human serum. Neu5Gc-specific antibodies were purified from human sera on sequential affinity columns with

immobilized human or chimpanzee sialoglycoproteins (rich with Neu5Ac or Neu5Gc, respectively) as described[4, 17].

Western Blots. Biotinylated, affinity-purified human Neu5Gc-specific antibodies were studied by Western blotting against surface membrane glycoproteins of Neu5Ac (Ac) or Neu5Gc (Gc)-loaded endothelial cells, and the banding pattern was compared to that generated with the αNeu5Gc IgY. HUVECs loaded with either Neu5Ac or Neu5Gc were lifted with 100 mM EDTA and sonicated. Membrane fractions were prepared, 3 μg denatured by boiling in SDS separated on 12.5% polyacrylamide mini gels (Bio-Rad), and electrotransferred to nitrocellulose membranes. Membranes were blocked overnight at 4°C with 0.5% Neu5Gc-free cold water fish gelatin (Sigma) in Tris-buffered saline containing 0.1% Tween (TBST). Primary antibodies were incubated for 5 hours at 4˚C with either biotinylated Neu5Gc-specific antibodies purified from individual human sera, diluted 1:100 in TBST, or chicken αNeu5Gc IgY, diluted 1:50,000 in TBST. Purification of the αNeu5Gc IgY is described elsewhere[4]. Membranes were washed 4 times for 5 minutes in TBST then incubated with Strepavidin-HRP (Bio-Rad), diluted 1:50,000, or HRP-anti-chicken-IgY (Jackson Immunoresearch), diluted 1:10,000, at room temperature (RT) for 45 minutes. Proteins were visualized by chemiluminescence detection (Pierce), followed by exposure to Kodak BioMax XAR film for 5-30 s.

Immunohistochemistry. Anonymous autopsy tissue samples of eleven normal and diseased human aortas were obtained from the Co-operative Human Tissue Network, with approval from the Institutional Review Board of UCSD. Tissue was frozen in OCT (Sakura) using isopentane-dry ice slurry and the tissue blocks kept at -80°C. Blocks were sectioned at 5 microns onto glass slides, and allowed to dry overnight. Washing buffer was PBS containing 0.1% Tween (PBST, Sigma), which was used between

each step of the procedure, and 0.5% fish gelatin/PBST was the diluting buffer. Frozen sections were blocked for endogenous biotin (Vector Laboratories), followed by fixation with 10% neutral buffered formalin (Fisher) for 20 minutes. Sections were then incubated at RT for 1 hour with the αNeu5Gc IgY at 1:500, and then with biotinylated donkey-anti-chicken IgY antibody (Jackson Immunoresearch) at 1:200, and then with Cy3-strepavidin (Jackson Immunoresearch) at 1:500 and then, if HRP was the label, color was developed using AEC (Vector labs), nuclei counterstained and the slides were mounted with an aqueous mounting media. Diseased aortic sections were also incubated with anti-CD68 antibodies (macrophage marker, BD Biosciences), anti-MDA antibody MDA2[41](oxidized-LDL marker) or the endothelial markers anti-human CD31 (Dako) and VWF (Dako). Nuclei were sometimes revealed with DAPI (Vector laboratories). Brightfield slides were viewed using an Olympus BH2 microscope and photographs taken for panels using the Olympus Magnafire software and Photoshop (Adobe).

Controls included pooled pre-immune chicken IgY substituted for αNeu5Gc IgY; pretreatment of sections with 250 mU of *Arthrobacter ureafaciens* sialidase (EY Laboratories Inc.) in 100 mM sodium acetate, pH 5.5 for 2.5 hours at 37^{o}C prior to fixation; or, dilution of 1:500 αNeu5Gc IgY in blocking solution containing 10% chimpanzee serum (a source of Neu5Gc-containing glycoproteins[42]) and applied over tissue sections.

Frozen sections of aorta were also probed with biotinylated Neu5Gc-specific antibodies purified from human serum[17] diluted 1:3 in blocking solution, and detected with rabbit anti-biotin, diluted 1:500 in blocking solution, followed by Cy3-anti-rabbit (Jackson Immunoresearch) diluted 1:500 in blocking solution, mounted with an

aqueous mounting media containing DAPI (Vector laboratories), and viewed at 400x and 1000x magnification as described above.

ACKNOWLEDGEMENTS

Supported by NIH grants R01-GM32373 and R01-CA38701 to A.V. T.P. was a Medical Student fellow of the Howard Hughes Medical Institute (HHMI).

Chapter 3, in full, is a reprint of the material as it appears, *Pham T*, Gregg CJ*, Karp F, Chow R, Padler-Karavani V, Cao H, Chen X, Witztum JL, Varki NM, & Varki A, Blood Journal, 114:5225-5235, 2009* (* denotes equal authorship). This paper is the result of another fruitful collaboration with a good friend and excellent scientist, Tho Pham. The dissertation author was the primary author and Dr. Ajit Varki directed and supervised the research that forms the basis of this chapter.

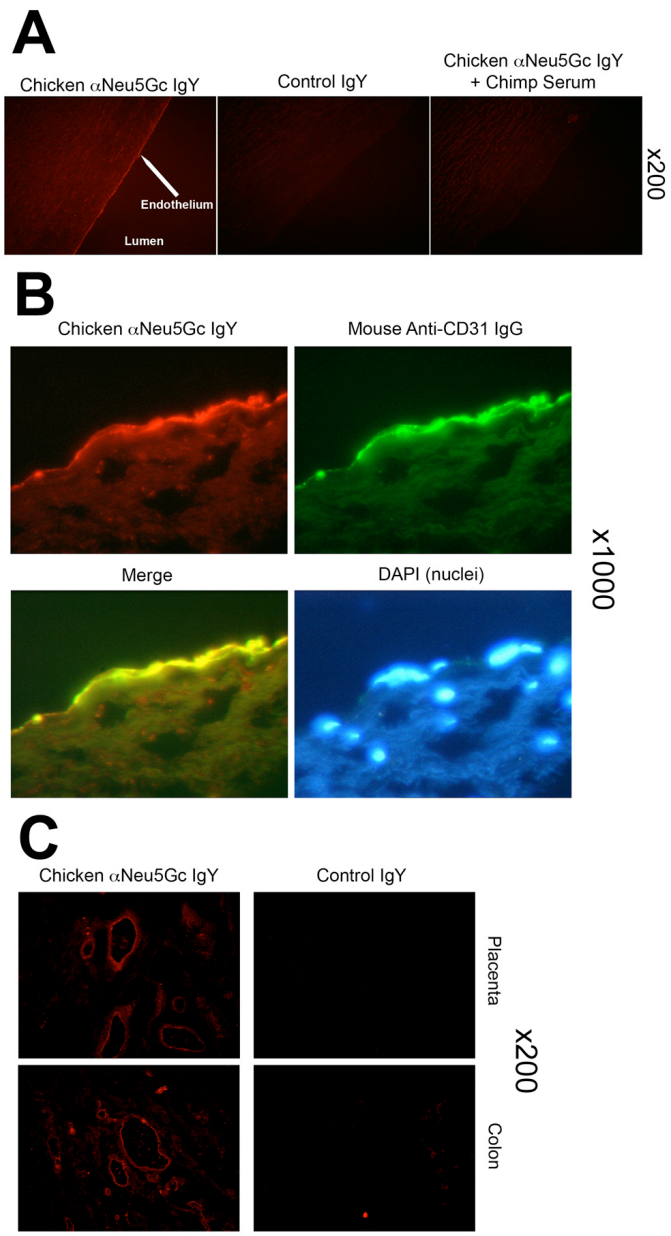

Figure 3-1. Detection of Neu5Gc in Aortic Endothelium of Human Autopsy Samples and Microvasculature of Colon and Placenta. The chicken anti-Neu5Gc antibody (αNeu5Gc IgY) was used to detect the presence of Neu5Gc on the endothelium of autopsy samples of normal-appearing human aorta. Typical representatives of 8 autopsy samples studied are shown. The red (Cy3) fluorescence represents labeling of Neu5Gc on endothelial cells of the aorta. **A.** Specificity of the antibody was demonstrated by the lack of signal with the non-immunized control chicken IgY (middle panel) and the abrogation of signal by adsorption with Neu5Gc-rich glycoproteins of chimpanzee serum (right panel). (Magnification 200x) **B.** Sections were double-stained with anti-CD31 for endothelial cells, and counterstained with DAPI to visualize nuclei (magnification 1000x). **C.** Sections of placenta (top panels) and colon (bottom panels) stain for Neu5Gc along microvasculature endothelial lining using αNeu5Gc IgY. Control IgY (right column) demonstrates specificity of signal (magnification 200x).

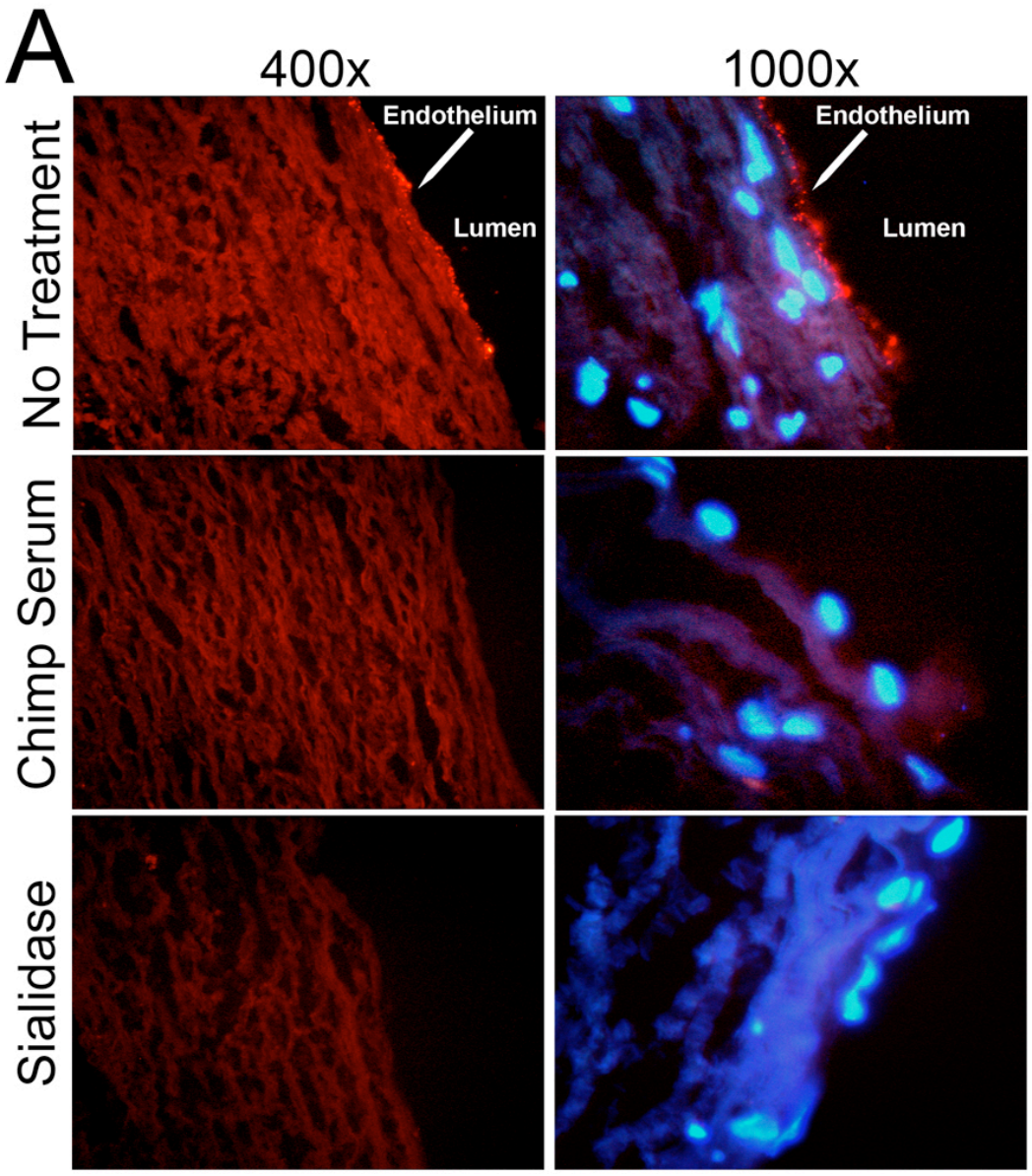

Figure 3-2. Affinity-purified Human Neu5Gc-specific Antibodies Bind Specifically to Neu5Gc on Endothelial Cells of Aorta and *Vasa Vasorum*. Affinity-purified human Neu5Gc-specific antibodies were used as a primary reagent on cryosections of autopsy samples of aorta. **A.** Sections were incubated with the biotinylated, affinity-purified human Neu5Gc-specific antibodies followed by rabbit anti-biotin and then Cy3-anti-rabbit, with nuclear counterstaining using DAPI (top panels). Antibody staining was abrogated by adsorption with chimpanzee serum (middle panels) or by prior sialidase pretreatment (bottom panels). A representative example of 5 independent experiments is shown.

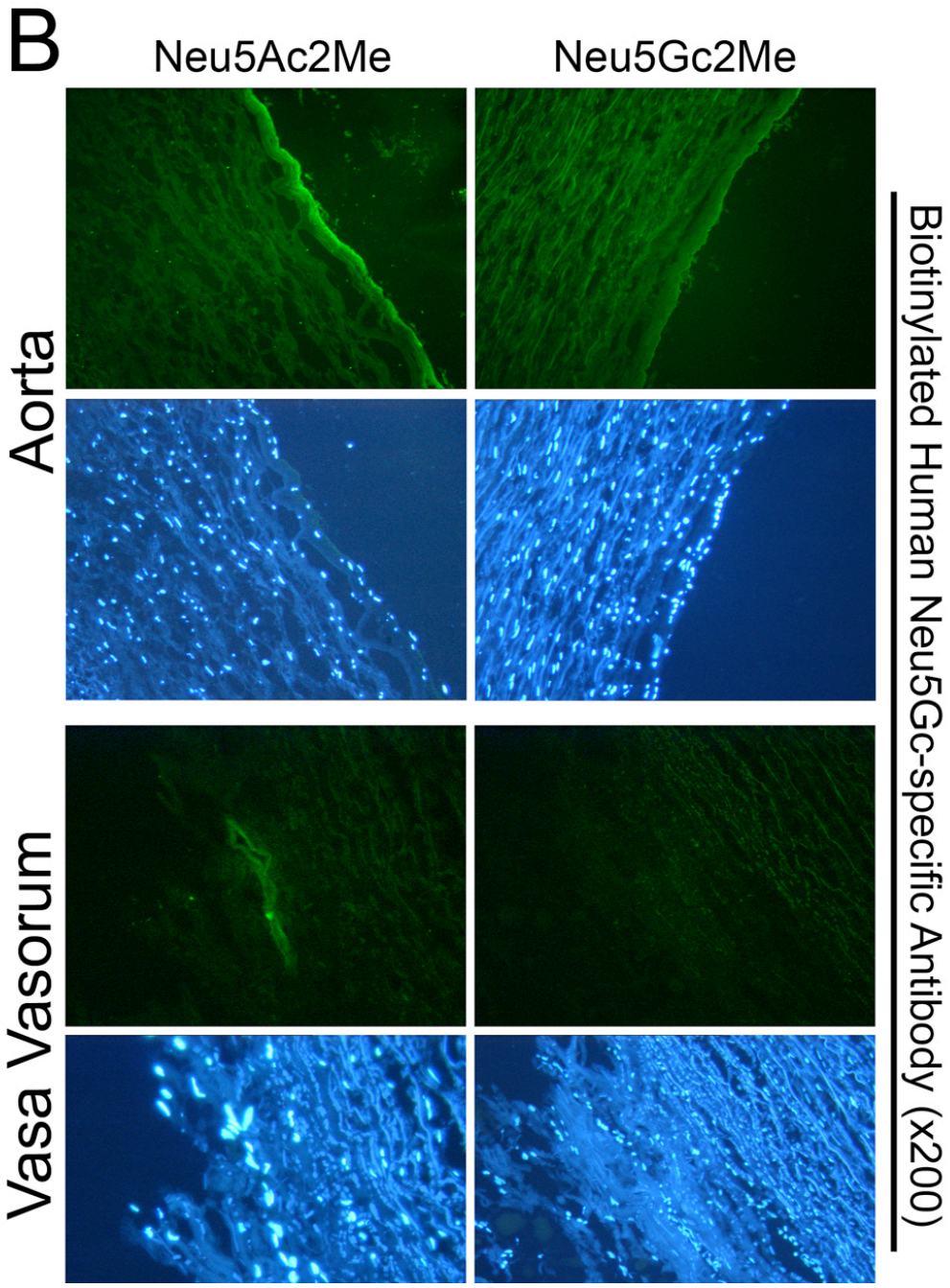

Figure 3-2, cont'd. Affinity-purified Human Neu5Gc-specific Antibodies Bind Specifically to Neu5Gc on Endothelial Cells of Aorta and *vasa vasorum*. Affinity-purified human Neu5Gc-specific antibodies were used as a primary reagent on cryosections of autopsy samples of aorta. **B.** Sections were incubated with biotinylated, affinity-purified human Neu5Gc-specific antibodies followed by mouse anti-biotin and FITC anti-mouse antibody and nuclear counterstaining with DAPI. Primary antibody staining was abrogated by addition of Neu5Gc2Me, but not by Neu5Ac2Me (both 1 mM). The staining pattern is appreciated in both aorta and vasa vasorum. A representative example of 3 independent experiments on 8 individuals is shown (magnification 400x).

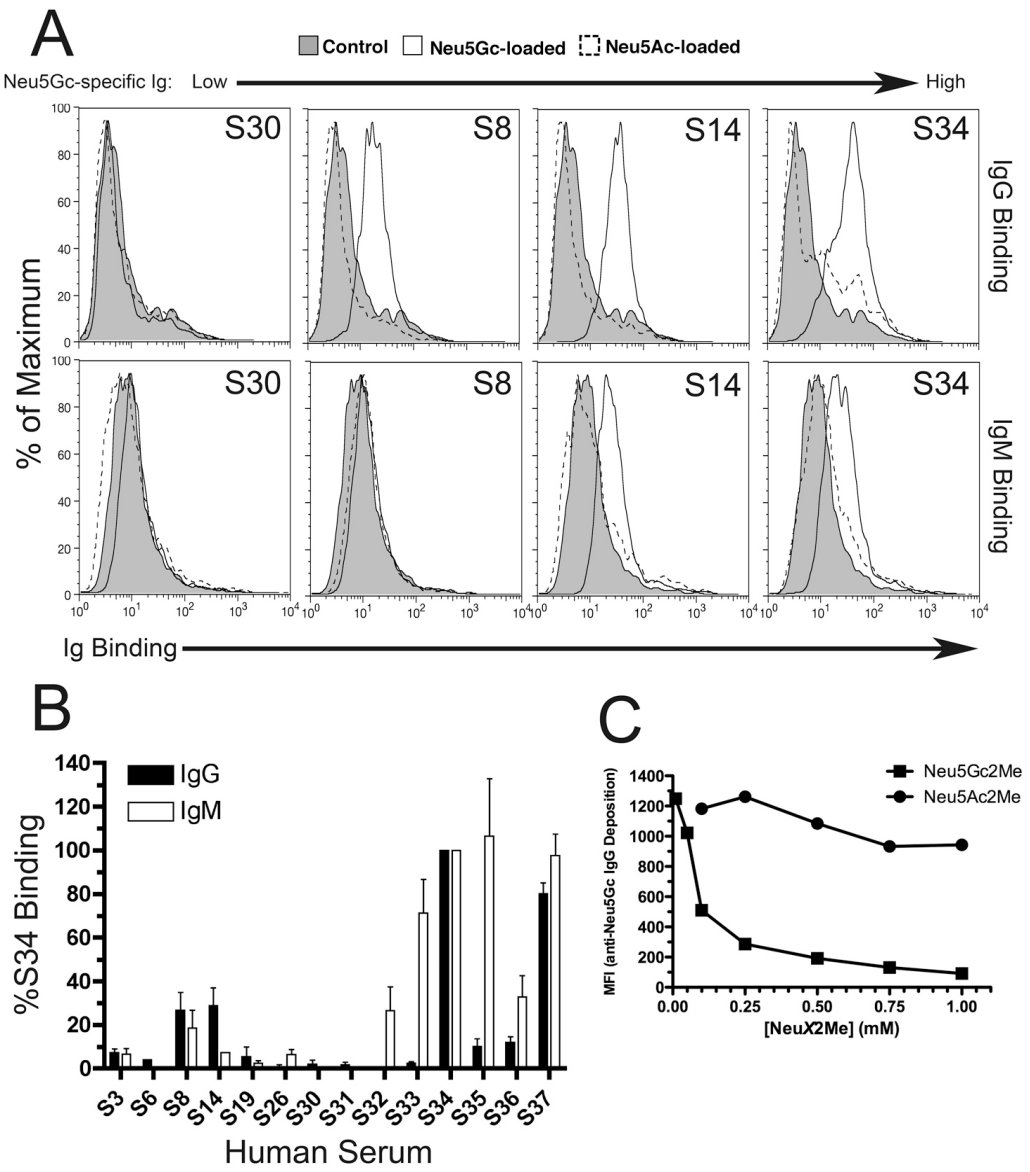

Figure 3-3. Human Serum Antibodies React Against Neu5Gc-loaded Endothelium. Human sera (S#), diluted 1:5, were assayed for their ability to bind HUVECs in a Neu5Gc-dependent manner. **A.** Binding of human serum IgG (top) or IgM (bottom) to loaded HUVEC's was assayed by flow cytometry. Neu5Gc-loaded cells (solid line), Neu5Ac-loaded cells (dotted line) and Neu5Gc-loaded cells stained with secondary antibody only (shaded curve). Representative individual human sera are shown. **B.** IgG and IgM binding were normalized as a percentage value of the signal obtained with S34. The data are presented as means+SEM (n=3). **C.** Binding of Neu5Gc-specific IgG antibodies from S37 to Neu5Gc-loaded HUVEC was inhibited with the alpha-methyl glycoside, Neu5Gc2Me in a dose-dependent manner, and not by Neu5Ac2Me.

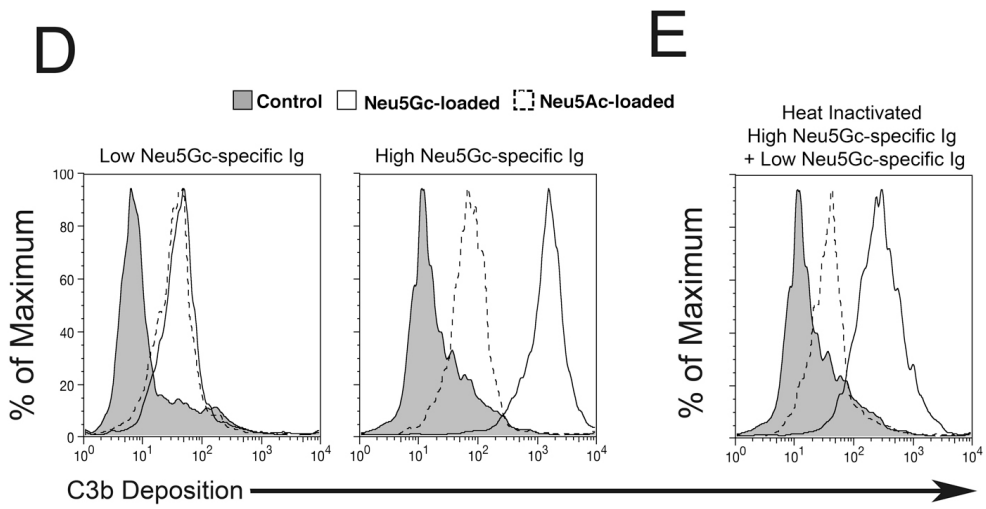

Figure 3-3, cont'd. Human Serum Antibodies React Against Neu5Gc-loaded Endothelium. Human sera (S#), diluted 1:1, were assayed for their ability to deposit complement on HUVECs in a Neu5Gc-dependent manner. **D.** Classical complement, C3 convertase (C3b), was deposited onto Neu5Gc-loaded HUVEC (solid lines) only when incubated with high-titered Neu5Gc-specific serum (S34, right panel) and not low-titered Neu5Gc-specific serum (S30, left panel). Non-specific complement was deposited onto Neu5Ac-loaded HUVEC (dotted lines) in a variable manner dependent on which sera was used, presumably due to unrelated serum factors. As a negative control, heat inactivated serum was incubated with Neu5Gc-loaded HUVECs (shaded curve). **E.** Heat inactivated S34 alone did not deposit complement in Neu5Gc-loaded HUVECs (shaded curve). Supplementation of S30 with heat-inactivated S34 shows Neu5Gc-dependent complement deposition in Neu5Gc-loaded (solid line) and not Neu5Ac-loaded HUVECs (dashed line). This indicates that Neu5Gc-specific antibodies are necessary and sufficient to mediate Neu5Gc-dependent complement deposition. All results presented in this figure were performed at least 3 times.

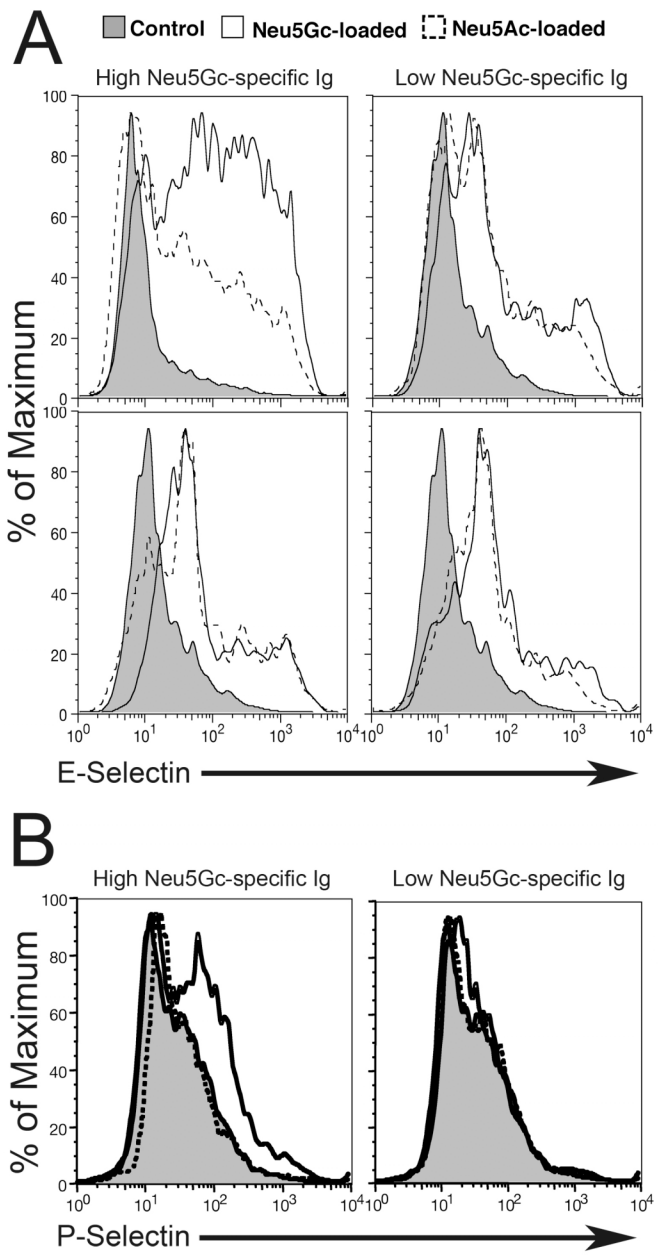

Figure 3-4. Human Serum Antibodies Enhance Adhesion Molecule Expression and PBMC Binding on Neu5Gc-loaded Endothelium. A. A representative example of surface E-selectin expression determined on Neu5Ac and Neu5Gc-loaded HUVECs after 5 hours of activation by low-titered serum (S30, right column) or high-titered serum (S34, left column) or heat-inactivated forms thereof (bottom row). Control peaks (shaded curve) represent E-selectin expression on endothelial cells not activated by serum. **B.** As described in (a) except HUVECs were exposed to serum for 15 minutes only. Heat Inactivated serum controls are included as a negative control (shaded curve). Short serum incubations show a Neu5Gc-dependent expression of P-selectin that requires Neu5Gc-specific antibodies and is sensitive to heat inactivation of serum. This response was most evident in low passage HUVECs ($p<3$), consistent with the observed (data not shown) and reported passage-dependent loss of P-selectin expression *in vitro*[50].

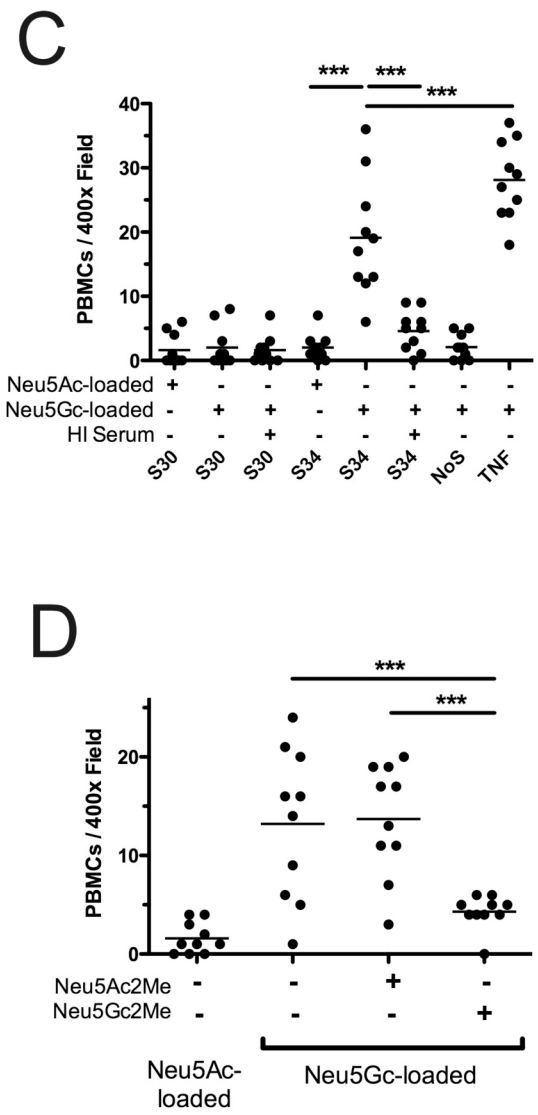

Figure 3-4, cont'd. Human Serum Antibodies Enhance Adhesion Molecule Expression and PBMC Binding on Neu5Gc-loaded Endothelium. C. HUVECs were cultured on 12 mm glass coverslips (Fisher) in 24 well plates and loaded with either Neu5Ac or Neu5Gc as above. Loaded cells were incubated with 50% human sera in EBM-2 for 4 hours at 37^{o}C or with heat-inactivated serum as a control. A negative control was not exposed to human serum (NoS) and a positive control was exposed to TNFα (10ng/mL) for stimulation. At 4 hours, 10^5 PBMCs were added to each well and incubated at 37^{o}C on an orbital shaker at 100 revolutions/min for 1 hour. Cells were washed thrice in PBS and fixed in PBS containing 3% paraformadehyde. Bound PBMC were counted in 10 randomly chosen fields at 400x magnification. Data were averaged and expressed as cells/field. Data are presented as mean with the scatter. This panel is a representative example of 5 similar replicates. ***p<0.001. **D.** Same as C except that the α-methyl-glycosides (1 mM) were incubated with the S34 prior to HUVEC stimulation. All groups were Neu5Gc loaded. We observed inhibition of PBMC binding in S34 stimulated HUVECs with Neu5Gc2Me, but not Neu5Ac2Me ***p<0.001. Examples of fluorescent images from the experiment in 4d are shown in Figure 3-8. All results presented were performed at least 3 times.

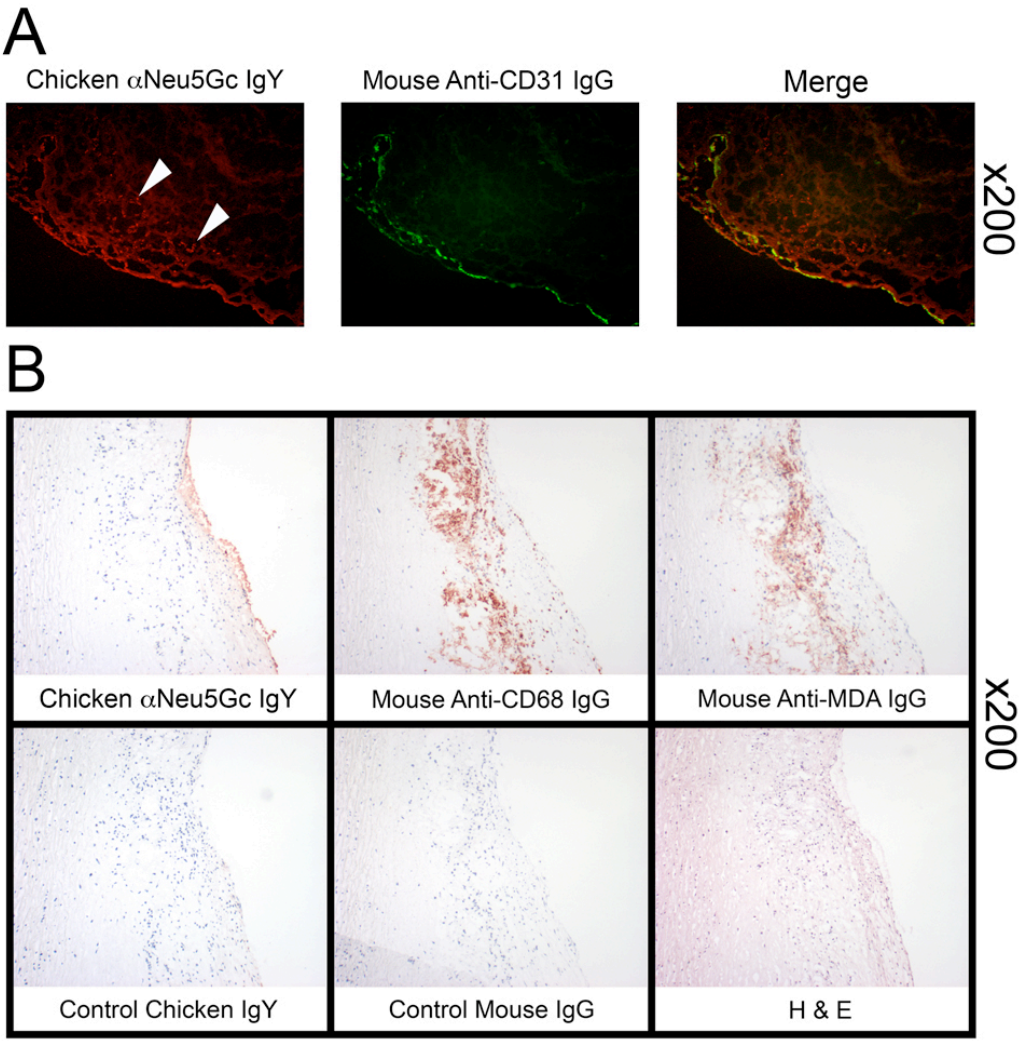

Figure 3-5. Neu5Gc in the Endothelium and Sub-endothelium of Atherosclerotic Plaques. **A.** Expression of Neu5Gc in endothelium overlying human aortic atherosclerotic plaques is shown by double labeling with the αNeu5Gc IgY (left panel) the endothelial marker CD31 (center panel, see merge, right panel). White arrows indicate sub-endothelial Neu5Gc within lesions (left panel). **B.** Samples of human aortic atherosclerotic plaques were identified by their characteristic appearance (H&E, lower right panel). Accumulation of macrophages (stained with anti-CD68, upper middle panel) and oxidized-LDL (stained with MDA2, upper right panel) are shown. The αNeu5Gc IgY (upper left panel) was used to detect the presence of Neu5Gc on the endothelium of the plaques. Control IgY and mouse IgG (lower right and middle panels) demonstrates specificity of the staining. **C.** Human aortic atherosclerotic plaque sections were double-stained with anti-CD68 (left panel) for macrophages and αNeu5Gc IgY (middle panel) for Neu5Gc. The merged fluorescent image (right panel) indicates that macrophages are recruited to the Neu5Gc-lined endothelium. **D.** Endothelium was labeled with anti-vWF antibody (center panel, note that there is also some subendothelial green auto-fluorescence due to macrophages and/or necrotic foci). In addition to typical endothelial-colocalized Neu5Gc staining, extensive sub-endothelial labeling with the αNeu5Gc IgY (red channel, left panel) is seen in this lesion (see yellow in the merged image, right panel). All pictures in this figure are representative examples of multiple independent analyses on multiple samples from multiple individuals.

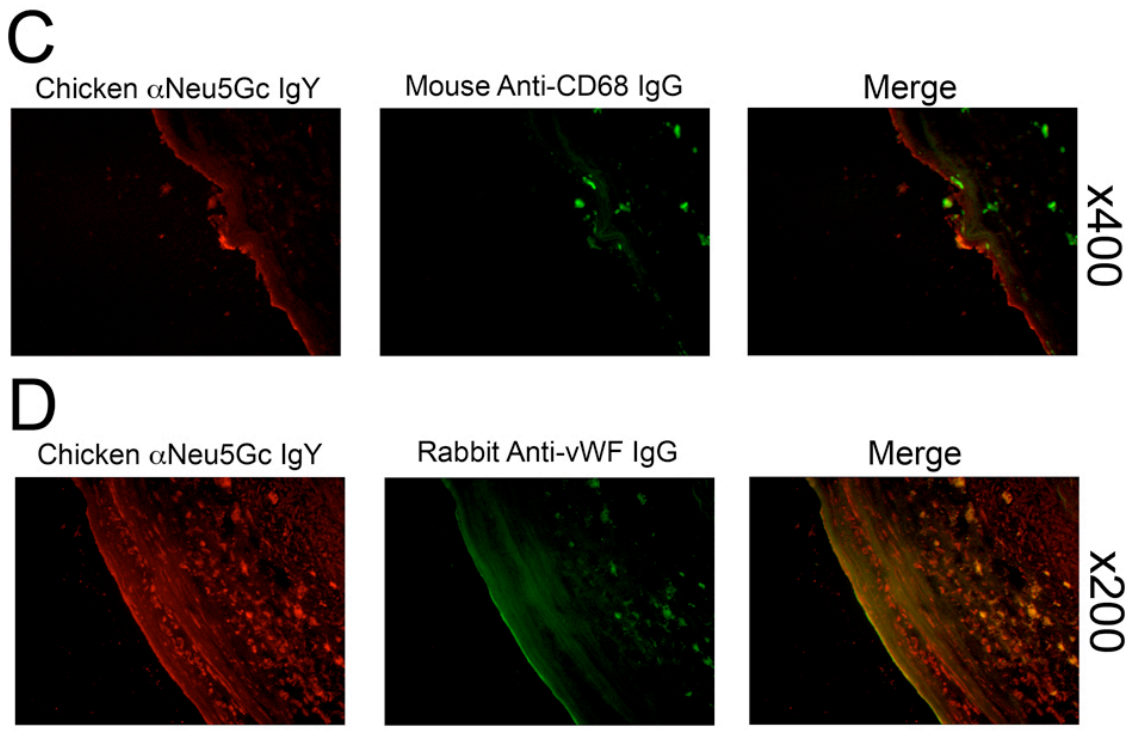

Figure 3-5, cont'd. Neu5Gc in the Endothelium and Sub-endothelium of Atherosclerotic Plaques. C. Human aortic atherosclerotic plaque sections were double-stained with anti-CD68 (left panel) for macrophages and αNeu5Gc IgY (middle panel) for Neu5Gc. The merged fluorescent image (right panel) indicates that macrophages are recruited to the Neu5Gc-lined endothelium. **D.** Endothelium was labeled with anti-vWF antibody (center panel, note that there is also some subendothelial green auto-fluorescence due to macrophages and/or necrotic foci). In addition to typical endothelial-colocalized Neu5Gc staining, extensive sub-endothelial labeling with the αNeu5Gc IgY (red channel, left panel) is seen in this lesion (see yellow in the merged image, right panel). All pictures in this figure are representative examples of multiple independent analyses on multiple samples from multiple individuals.

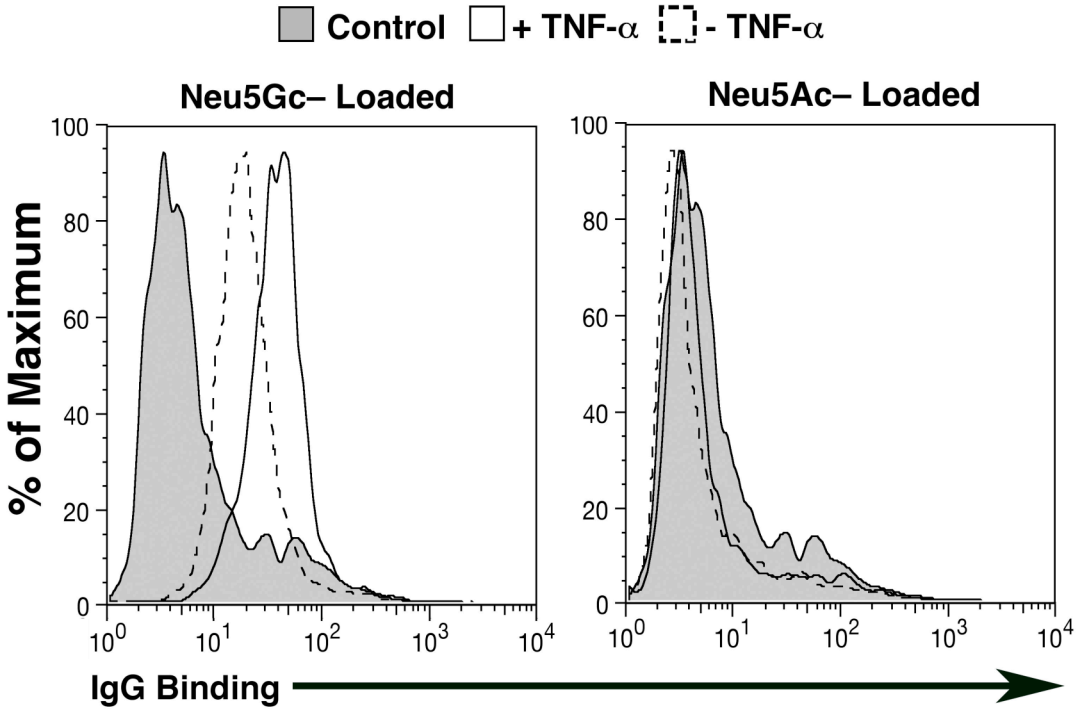

Figure 3-6. TNFα Augments Human Antibody Reactivity Against Neu5Gc-loaded Endothelium. Endothelial cells were treated with TNFα (10 ng/ml) during the last 18 hours of Neu5Gc loading. Antibody binding was assessed for both treated and non-treated cells after incubating with high-titered human serum (S34). Control peaks represent staining with FITC-conjugated secondary antibody alone. The experiment was performed multiple times and representative examples are shown. Several other cytokines studied (IL-1β, IL-4, IL-6, IL-13, and IFNγ) did not show this enhancing effect (not shown).

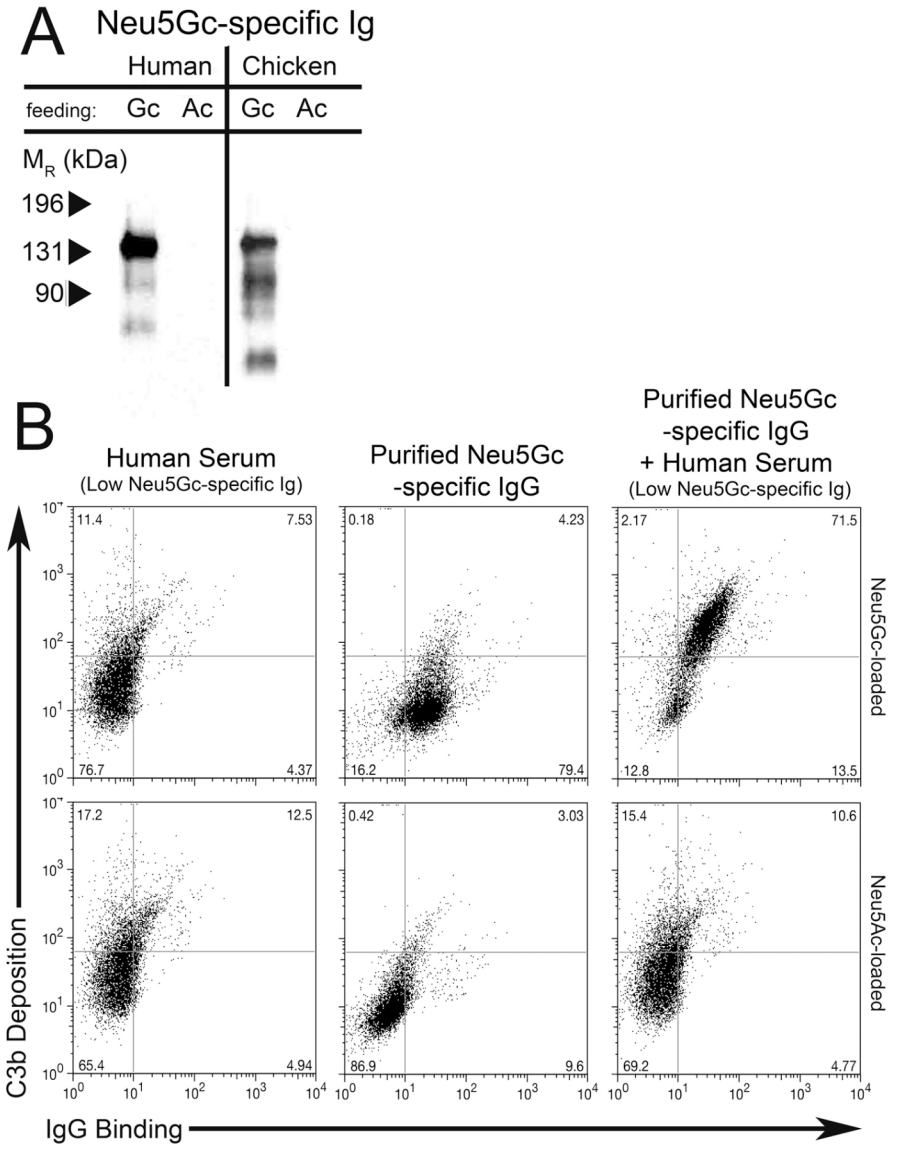

Figure 3-7. Affinity-purified Human Neu5Gc-specific Antibodies Bind Specifically to Neu5Gc-Loaded Endothelial Cells and Induce Complement Deposition. A. Biotinylated, affinity-purified human Neu5Gc-specific antibodies were studied by Western blotting against membrane glycoproteins of Neu5Ac (Ac) or Neu5Gc (Gc)-loaded endothelial cells, and the banding pattern was compared to that generated with the αNeu5Gc IgY. **B.** Neu5Gc-specific IgG binding (x-axis) and complement deposition (C3b, y-axis) were simultaneously assessed on Neu5Ac- and Neu5Gc-loaded endothelium. Affinity-purified Neu5Gc-specific antibodies, low-titered human serum (S30), or both were incubated with Neu5Gc-loaded (top panels) or Neu5Ac-loaded (bottom panels) HUVECs. While the low-titered human serum does not bind HUVECs in a Neu5Gc-dependent fashion (left column), the affinity purified Neu5Gc-specific antibodies are necessary and sufficient to bind Neu5Gc-loaded HUVECs in a Neu5Gc-dependent fashion (middle column). Supplementing the low-titered serum with the purified Neu5Gc-specific antibodies allows complement deposition on HUVECs in a Neu5Gc-dependent manner (right column). These are representative results of 3 independent experiments.

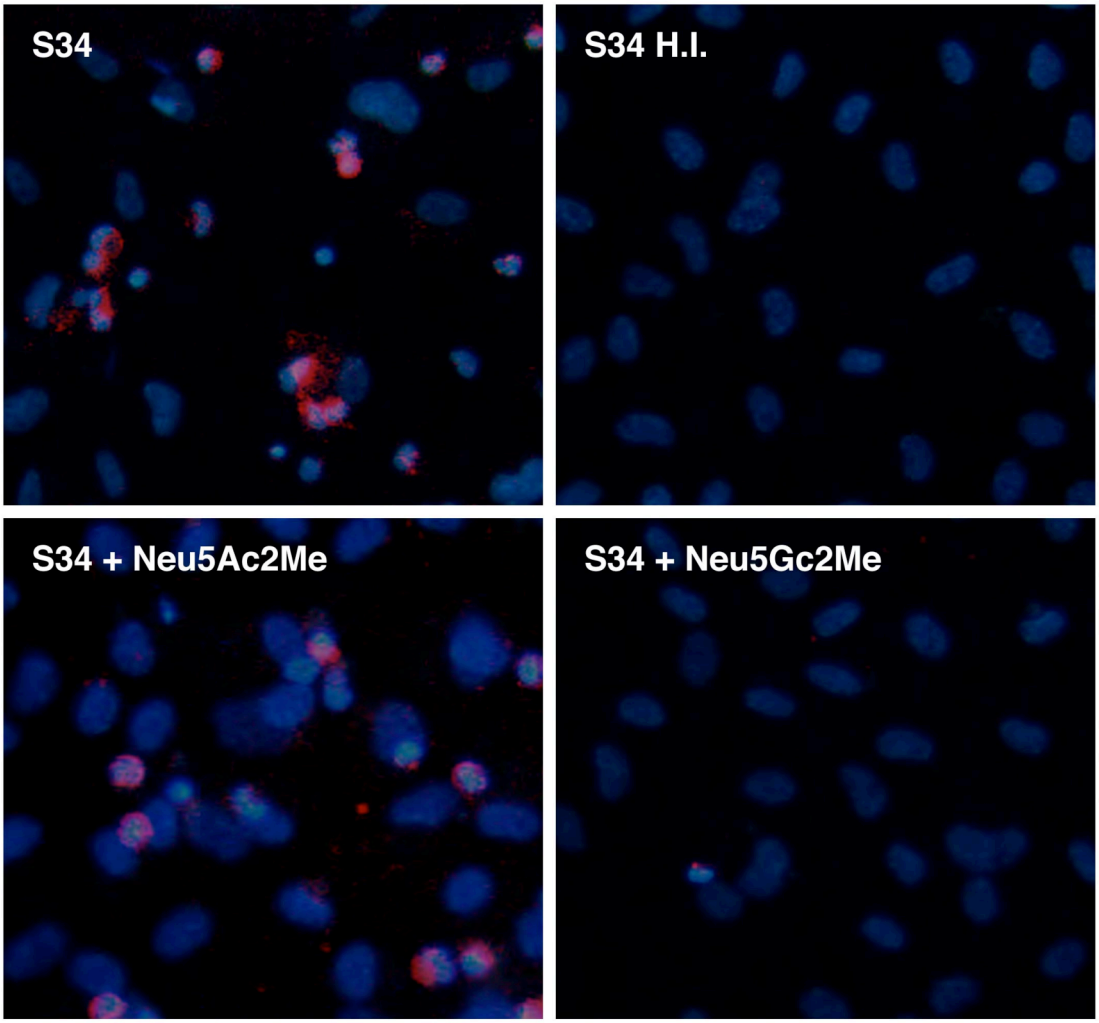

Figure 3-8. Immunofluorescence Confirms CD-14 Positive Monocytes Bind to Neu5Gc-loaded Endothelial Cells Stimulated with Neu5Gc-specific Antibodies. Slides were incubated with Alexa488-conjugated mouse anti-human CD14 antibody (BD Pharmingen) for 1 hour on ice, mounted with SlowFade Gold containing DAPI (Invitrogen), and visualized with a Zeiss Axiolab (Zeiss) microscope. We saw PBMC nuclei binding and CD14-staining of those nuclei when Neu5Gc-loaded HUVECs were activated with S34 (top left panel). We observed very little CD14-staining/PBMC binding when Neu5Gc2Me, but not Neu5Ac2Me was incubated with S34 prior to HUVEC activation.

Table 3-1. Changes in Cytokine Production by Neu5Gc-loaded Endothelial Cells Stimulated with Human Neu5Gc-specific Antibodies. Cytokine levels in endothelial cell lysates were studied in Neu5Ac- or Neu5Gcloaded HUVECs that were stimulated Neu5Gc-specific serum, with (left column) or without (right column) heat inactivation of seum. Data are presented as the average cytokine signal detected in lysates HUVECs normalized to the average cytokine signal detected in lysates from Neu5Ac-loaded, serum incubated HUVECs (e.g., normalized baseline for all cytokines = 1). Two cytokines, IL-12 p70 and CCL15 (MIP-1δ), were not detected in Neu5Ac-loaded/fresh serum stimulated cells, but were detected in Neu5Gc-loaded/fresh serum stimulated cells, thus the data were not amenable to presentation as fold increase over Neu5Ac-loaded cells. Of note, TGFβ1 showed a slight decrease in serum stimulated Neu5Gc-loaded HUVECs (0.9 ± 0.04 fold).

	Fold Change Over Levels in Neu5Ac-loaded Controls	
Cytokine	**Fresh Serum**	**Heat-Inactivated Serum**
CCL1 (I-309)	332.3 ± 40.5	Not detected
IL-10	36.4 ± 11.1	2.3 ± 1.0
IL-11	33.7 ± 4.2	2.0 ± 0.1
IL-7	31.6 ± 2.1	0.3 ± 0.1
IL-1α	31.5 ± 1.6	6.0 ± 1.8
IL-12 p40	19.2 ± 2.0	3.3 ± 0.8
IFNγ	10.0 ± 0.3	1.7 ± 0.3
GM-CSF	12.6 ± 0.1	0.7 ± 0.8
CCL3 (MIP-1α)	6.0 ± 0.4	1.7 ± 0.03
CCL8 (MCP-2)	5.4 ± 0.2	0.9 ± 0.1
GCSF	4.3 ± 0.2	0.7 ± 0.6
CCL4 (MIP-1β)	3.2 ± 0.2	1.7 ± 0.2
CXCL9 (MIG)	2.6 ± 0.2	1.2 ± 0.2
M-CSF	1.9 ± 0.1	0.9 ± 0.01
sTNF R1	1.7 ± 0.3	0.8 ± 0.01
PDGF-BB	1.5 ± 0.2	1.1 ± 0.01
ICAM-1	1.4 ± 0.04	1.1 ± 0.01
sTNF R2	1.4 ± 0.2	1.0 ± 0.02
TIMP-2	1.3 ± 0.1	1.1 ± 0.02
CXCL10 (IP-10)	1.3 ± 0.1	0.7 ± 0.02
TNFβ	1.2 ± 0.1	0.8 ± 0.1

REFERENCES

1. Varki A. Glycan-based interactions involving vertebrate sialic-acid-recognizing proteins. *Nature*. 2007;446:1023-1029.
2. Hayakawa T, Satta Y, Gagneux P, Varki A, Takahata N. Alu-mediated inactivation of the human CMP-N-acetylneuraminic acid hydroxylase gene. *Proc Natl Acad Sci USA*. 2001;98:11399-11404.
3. Hedlund M, Tangvoranuntakul P, Takematsu H et al. N-glycolylneuraminic acid deficiency in mice: implications for human biology and evolution. *Mol Cell Biol*. 2007;27:4340-4346.
4. Diaz SL, Padler-Karavani V, Ghaderi D et al. Sensitive and specific detection of the non-human sialic Acid N-glycolylneuraminic acid in human tissues and biotherapeutic products. *PLoS ONE*. 2009;4:e4241.
5. Bardor M, Nguyen DH, Diaz S, Varki A. Mechanism of uptake and incorporation of the non-human sialic acid N-glycolylneuraminic acid into human cells. *J Biol Chem*. 2005;280:4228-4237.
6. Nguyen DH, Tangvoranuntakul P, Varki A. Effects of natural human antibodies against a nonhuman sialic acid that metabolically incorporates into activated and malignant immune cells. *J Immunol*. 2005;175:228-236.
7. Yin J, Hashimoto A, Izawa M et al. Hypoxic culture induces expression of sialin, a sialic acid transporter, and cancer-associated gangliosides containing non-human sialic acid on human cancer cells. *Cancer Res*. 2006;66:2937-2945.
8. Tangvoranuntakul P, Gagneux P, Diaz S et al. Human uptake and incorporation of an immunogenic nonhuman dietary sialic acid. *Proc Natl Acad Sci U S A*. 2003;100:12045-12050.
9. Finch CE, Stanford CB. Meat-adaptive genes and the evolution of slower aging in humans. *Q Rev Biol*. 2004;79:3-50.
10. Lopez-Garcia E, Schulze MB, Fung TT et al. Major dietary patterns are related to plasma concentrations of markers of inflammation and endothelial dysfunction. *Am J Clin Nutr*. 2004;80:1029-1035.
11. Schulze MB, Hoffmann K, Manson JE et al. Dietary pattern, inflammation, and incidence of type 2 diabetes in women. *Am J Clin Nutr*. 2005;82:675-84; quiz 714-5.
12. Esmaillzadeh A, Kimiagar M, Mehrabi Y, Azadbakht L, Hu FB, Willett WC. Dietary patterns and markers of systemic inflammation among Iranian women. *J Nutr*. 2007;137:992-998.
13. Malykh YN, Schauer R, Shaw L. N-glycolylneuraminic acid in human tumours. *Biochimie*. 2001;83:623-634.
14. Beer P. The heterophile antibodies in infectious mononucleosis and after injection of serum. *J Clin Invest*. 1936;15:591-599.
15. Morito T, Kano K, Milgrom F. Hanganutziu-Deicher antibodies in infectious mononucleosis and other diseases. *J Immunol*. 1982;129:2524-2528.

16. Zhu A, Hurst R. Anti-N-glycolylneuraminic acid antibodies identified in healthy human serum. *Xenotransplantation*. 2002;9:376-381.

17. Padler-Karavani V, Yu H, Cao H et al. Diversity in specificity, abundance, and composition of anti-Neu5Gc antibodies in normal humans: potential implications for disease. *Glycobiology*. 2008;18:818-830.

18. Kinsey GR, Li L, Okusa MD. Inflammation in acute kidney injury. *Nephron Exp Nephrol*. 2008;109:e102-7.

19. Eltzschig HK, Collard CD. Vascular ischaemia and reperfusion injury. *Br Med Bull*. 2004;70:71-86.

20. Pall AA, Savage CO. Mechanisms of endothelial cell injury in vasculitis. *Springer Semin Immunopathol*. 1994;16:23-37.

21. Harper L, Savage CO. Pathogenesis of ANCA-associated systemic vasculitis. *J Pathol*. 2000;190:349-359.

22. Guilpain P, Mouthon L. Antiendothelial cells autoantibodies in vasculitis-associated systemic diseases. *Clin Rev Allergy Immunol*. 2008;35:59-65.

23. Navarro M, Cervera R, Font J et al. Anti-endothelial cell antibodies in systemic autoimmune diseases: prevalence and clinical significance. *Lupus*. 1997;6:521-526.

24. Meroni P, Ronda N, Raschi E, Borghi MO. Humoral autoimmunity against endothelium: theory or reality? *Trends Immunol*. 2005;26:275-281.

25. Gobel U, Eichhorn J, Kettritz R et al. Disease activity and autoantibodies to endothelial cells in patients with Wegener's granulomatosis. *Am J Kidney Dis*. 1996;28:186-194.

26. Jamin C, Dugue C, Alard JE et al. Induction of endothelial cell apoptosis by the binding of anti-endothelial cell antibodies to Hsp60 in vasculitis-associated systemic autoimmune diseases. *Arthritis Rheum*. 2005;52:4028-4038.

27. Yang YH, Wang SJ, Chuang YH, Lin YT, Chiang BL. The level of IgA antibodies to human umbilical vein endothelial cells can be enhanced by TNF-alpha treatment in children with Henoch-Schonlein purpura. *Clin Exp Immunol*. 2002;130:352-357.

28. Perry GJ, Elston T, Khouri NA, Chan TM, Cameron JS, Frampton G. Antiendothelial cell antibodies in lupus: correlations with renal injury and circulating markers of endothelial damage. *Q J Med*. 1993;86:727-734.

29. Song J, Park YB, Lee WK, Lee KH, Lee SK. Clinical associations of anti-endothelial cell antibodies in patients with systemic lupus erythematosus. *Rheumatol Int*. 2000;20:1-7.

30. Matsuo S, Fukatsu A, Taub ML, Caldwell PR, Brentjens JR, Andres G. Glomerulonephritis induced in the rabbit by antiendothelial antibodies. *J Clin Invest*. 1987;79:1798-1811.

31. Binder CJ, Shaw PX, Chang MK et al. The role of natural antibodies in atherogenesis. *J Lipid Res*. 2005;46:1353-1363.

32. Palinski W, Tangirala RK, Miller E, Young SG, Witztum JL. Increased autoantibody titers against epitopes of oxidized LDL in LDL receptor-deficient

mice with increased atherosclerosis. *Arterioscler Thromb Vasc Biol*. 1995;15:1569-1576.

33. Xu Q, Willeit J, Marosi M et al. Association of serum antibodies to heat-shock protein 65 with carotid atherosclerosis. *Lancet*. 1993;341:255-259.
34. Zhu J, Katz RJ, Quyyumi AA et al. Association of serum antibodies to heat-shock protein 65 with coronary calcification levels: suggestion of pathogen-triggered autoimmunity in early atherosclerosis. *Circulation*. 2004;109:36-41.
35. Wick G, Knoflach M, Xu Q. Autoimmune and inflammatory mechanisms in atherosclerosis. *Annu Rev Immunol*. 2004;22:361-403.
36. Perschinka H, Wellenzohn B, Parson W et al. Identification of atherosclerosis-associated conformational heat shock protein 60 epitopes by phage display and structural alignment. *Atherosclerosis*. 2007;194:79-87.
37. Praprotnik S, Blank M, Meroni PL, Rozman B, Eldor A, Shoenfeld Y. Classification of anti-endothelial cell antibodies into antibodies against microvascular and macrovascular endothelial cells: the pathogenic and diagnostic implications. *Arthritis Rheum*. 2001;44:1484-1494.
38. Del Papa N, Conforti G, Gambini D et al. Characterization of the endothelial surface proteins recognized by anti-endothelial antibodies in primary and secondary autoimmune vasculitis. *Clin Immunol Immunopathol*. 1994;70:211-216.
39. Brock TG, McNish RW, Coffey MJ, Ojo TC, Phare SM, Peters-Golden M. Effects of granulocyte-macrophage colony-stimulating factor on eicosanoid production by mononuclear phagocytes. *J Immunol*. 1996;156:2522-2527.
40. Delneste Y, Charbonnier P, Herbault N et al. Interferon-gamma switches monocyte differentiation from dendritic cells to macrophages. *Blood*. 2003;101:143-150.
41. Palinski W, Yla-Herttuala S, Rosenfeld ME et al. Antisera and monoclonal antibodies specific for epitopes generated during oxidative modification of low density lipoprotein. *Arteriosclerosis*. 1990;10:325-335.
42. Nguyen DH, Hurtado-Ziola N, Gagneux P, Varki A. Loss of Siglec expression on T lymphocytes during human evolution. *Proc Natl Acad Sci U S A*. 2006;103:7765-7770.
43. Zimmerman GA, McIntyre TM, Prescott SM. Adhesion and signaling in vascular cell-cell interactions. *J Clin Invest*. 1996;98:1699-1702.
44. Foreman KE, Glovsky MM, Warner RL, Horvath SJ, Ward PA. Comparative effect of C3a and C5a on adhesion molecule expression on neutrophils and endothelial cells. *Inflammation*. 1996;20:1-9.
45. Foreman KE, Vaporciyan AA, Bonish BK et al. C5a-induced expression of P-selectin in endothelial cells. *J Clin Invest*. 1994;94:1147-1155.
46. Geng JG, Bevilacqua MP, Moore KL et al. Rapid neutrophil adhesion to activated endothelium mediated by GMP-140. *Nature*. 1990;343:757-760.
47. Hanasaki K, Varki A, Stamenkovic I, Bevilacqua MP. Cytokine-induced beta-galactoside alpha-2,6-sialyltransferase in human endothelial cells mediates

alpha2,6-sialylation of adhesion molecules and CD22 ligands. *J Biol Chem*. 1994;269:10637-10643.

48. Hedlund M, Padler-Karavani V, Varki NM, Varki A. Evidence for a human-specific mechanism for diet and antibody-mediated inflammation in carcinoma progression. *Proc Natl Acad Sci U S A*. 2008;105:18936-18941.
49. Benatuil L, Kaye J, Rich RF, Fishman JA, Green WR, Iacomini J. The influence of natural antibody specificity on antigen immunogenicity. *Eur J Immunol*. 2005;35:2638-2647.
50. Takano M, Meneshian A, Sheikh E et al. Rapid upregulation of endothelial P-selectin expression via reactive oxygen species generation. *Am J Physiol Heart Circ Physiol*. 2002;283:H2054-61.

CHAPTER 4

N-glycolylneuraminic Acid in a Model of Chronic Vasculitis, Atherosclerosis

ABSTRACT

Given the evidence supporting Neu5Gc as a diet-derived antigen *in vivo* (Chapter 2) and the pro-inflammatory interplay between cellular Neu5Gc incorporation and Neu5Gc-specific antibodies in vascular endothelial cells (Chapter 3), we hypothesized that these variables could play a role in the aggravation of atherosclerosis through red meat consumption. To test this, we generated a novel, Neu5Gc-free murine model of atherosclerosis (*Cmah*, *Ldlr* double knockout mouse) in which we could induce Neu5Gc-specific immune responses (or not) and feed dietary Neu5Gc (or not). To generate the Neu5Gc-specific immune response, we investigated chimpanzee erythrocyte ghosts in a Freund's-based immunization, which generated a polyclonal response of IgM and IgG isotypes similar to that in humans. The antibodies generated using this antigen bound specifically to Neu5Gc, with no cross-reactivity to Neu5Ac, and required the intact 9-carbon sialic acid structure to bind. Animals that had been immunized against Neu5Gc and were eating dietary Neu5Gc also exhibited a robust IgG boosting response, an interesting finding given the widespread nature of human Neu5Gc-specific antibodies and the frequency of Neu5Gc in our diet. To control for this immunization strategy, we generated control chimpanzee erythrocyte ghosts with a chemically modified form of Neu5Gc. The control antigen generated a very robust control response against the chemically modified form of Neu5Gc with no evidence of cross reactivity. Surprisingly, after sixteen weeks of a Western Diet, the Neu5Gc-specific antibodies appeared to be atheroprotective, reducing atherosclerotic plaque burden in mice consuming high levels of dietary Neu5Gc.

INTRODUCTION

As discussed in the introduction, humans are predisposed advanced atherosclerosis, which is the leading cause of mortality in the western world[1]. This pathology does not affect the heart *per se*, but instead is a chronic vasculitis that endangers oxygen delivery to the heart muscle by compromising blood flow through the coronary vasculature. Atherosclerosis progresses due to continuous extravasation of monocytes and eventually lymphocytes into a developing lesion[2,3]. This inflammation results from many factors and has many auto-inflammatory characteristics[3], but the major inciting factor is cholesterol deposition in the sub-endothelial space due to high circulating LDL cholesterol[4].

Whereas an optimal inflammatory response will recognize damage/danger/infection, deal appropriately with that stimulus, and resolve by apoptosis or migration away from the site, leukocytes are effectively confounded by a continuous supply of cholesterol in atherosclerotic lesions. Monocyte-derived macrophages, the main leukocyte in developing lesions, will phagocytose cholesterol-rich lipoproteins in the lesion, leading to cholesterol accumulation in intracellular vacuoles and a cellular transition to a lipid-laden form of a macrophage, the foam cell[5]. In the context of the whole organism, excess cholesterol is readily absorbed into the gastrointestinal tract from the basolateral membrane of hepatocytes assisted by bile salts[6], but cholesterol and other oxy-sterols are the endpoint of complex lipid biosynthetic reactions and are poorly catabolized by cells themselves.

Cholesterol in lesions has important pro-inflammatory properties. LDL and oxidized LDL epitopes bind to pattern recognition receptors like TLR4 on leukocytes to engender a proinflammatory response[5]. Moreover, macrophages often deal with bacterial or parasitic infections where they use an oxidative burst to release high levels

of free radicals as a form of chemical attack. In the context of a developing lesion, oxidative bursts generate oxidized LDL epitopes, which independently contribute a proinflammatory component[2]. These mechanisms help propagate lesion development as the macrophages/foam cells within the lesion that secrete chemoattractants and cytokines to recruit more monocytes as well as lymphocytes in a vicious cycle that impairs resolution of inflammation within the lesion. Advanced lesions are large enough to affect the architecture of the blood vessel. For example, such lesions can obstruct blood flow, either partially or completely. Also, advanced lesions may or may not be stable. Unstable lesions can break down, releasing their contents into circulation, which will rapidly form clots and block distal circulation[7]. Because human atherosclerosis occurs dominantly in the large coronary and carotid arteries[1], these complications lead to catastrophic losses of blood flow for critical organs with high oxygen demand. Even partial loss of oxygen delivery can lead to heart and brain ischemia that has important functional consequences.

All lipids, including cholesterol, are transported through the circulation on amphipathic lipoproteins, which mask hydrophobic lipids like triglycerides in the core of the particle. Lipoproteins can be generated by the intestines (chylomicrons) and by the liver (very low density lipoproteins, VLDL; high-density lipoprotein, HDL) to deliver dietary lipids and hepatic cholesterol to peripheral tissues[8,9]. Lipoproteins are classified by their density, which increases during the life cycle of the molecule. For example, as VLDL particles circulate they encounter lipases on endothelium lining peripheral tissues, which break down triglycerides into free fatty acids. The free fatty acids can then escape the lipoprotein core and be taken up by the peripheral tissue in need of its energy content[8,10]. As a result of triglyceride metabolism, the density of the lipoprotein increases and it becomes enriched in cholesterol. This type of lipoprotein is

classified as LDL. Circulating LDL levels in humans have prognostic value for debilitating complications of advanced atherosclerosis, such as heart attack and stroke. Aggressively controlling LDL levels in patients through statins or other cholesterol lowering therapeutics reduces patient risk for complications of atherosclerosis[4].

Despite the therapeutic successes born from understanding the role of cholesterol in atherosclerosis, a significant percentage of human cardiovascular events arise in patients that exhibit no obvious risk factors for the disease[1]. This underscores that atherosclerosis is a multifactorial, inflammatory disease whose management could benefit from understanding other human-specific mechanisms for vascular inflammation. From an evolutionary perspective the widespread extent of atherosclerosis in humans is unexpected as severe atherosclerosis is not prevalent in primates, nor in hominins like the chimpanzee[11-13]. Such comparisons between humans and chimpanzees should be carefully weighted though. Diet and lifestyle are strikingly different between your average human at risk for atherosclerosis and a wild chimpanzee. However the data on the dearth of atherosclerosis in chimpanzees comes from captive animals. Though diet is difficult to reconcile, captive chimpanzees are sedentary and have life spans into the 50s in males and 60s in females[14]. Moreover captive chimpanzees have similar lipoprotein profiles as humans as well as extensive hypercholesterolemia (Fig 1-1B and [14]), potentially explained by the ancestral APOE4 allele that is persistent in chimpanzees and underlies hypercholesterolemia in humans[15]. Despite this, chimpanzee coronaries relatively free of advanced atherosclerotic lesions when examined by histology (Fig. 1-1A).

Chapters 2 and 3 have established Neu5Gc as a dietary risk factor that can interact with human Neu5Gc-specific antibodies in a human-specific mechanism for inflammation. Dietary Neu5Gc from red meat and dairy products are delivered to a

characteristic pattern of human tissues, importantly vasculature, by digestion of Neu5Gc-containing glycans. In addition, atherosclerotic lesions show a novel sub-endothelial accumulation of Neu5Gc, potentially suggesting other mechanisms by which Neu5Gc and the antibodies can affect lesion progression (Chapter 3, pg. 97). This incorporation and subsequent interaction with the Neu5Gc-specific antibodies offer a human-specific explanation for the ubiquity of human atherosclerosis, the sites susceptible to human atherosclerosis, and/or the development of advanced lesions. Indeed, evidence in vitro (Chapter 3) supports a role for human Neu5Gc-specific antibodies in generating vascular inflammation in a Neu5Gc-dependent manner. In this chapter, we ask whether the combination of dietary Neu5Gc and Neu5Gc-specific antibodies can interact to exacerbate atherosclerosis in a mouse model.

RESULTS

Modeling atherosclerosis in the *Cmah*, *Ldlr* double knockout mice (DKO). Mice are intrinsically resistant to atherosclerosis. To study the relevance of Neu5Gc and Neu5Gc-specific antibodies in murine atherosclerosis, we chose the *Ldlr* -/- background[16]. This model lacks the LDL receptor, primarily expressed in the liver to coordinate uptake of LDL particles. If challenged with a high-fat, high-cholesterol diet, these animals exhibit hypercholesterolemia and hypertryglyceridemia. Once bred onto the *Cmah*$^{-/-}$ background to make them Neu5Gc-free, we maintained animals on a low-fat/low-cholesterol/Neu5Gc-free diet to control the introduction of these variables. The *Cmah*, *Ldlr* DKO mouse is viable and Neu5Gc free, and exhibited typical diet-induced hypercholesterolemia.

In designing an experiment to model atherosclerosis, we identified several potential approaches. We were interested to test both short (8 wk.) and long (16, 20

wk.) time points, potentially reflecting a role for Neu5Gc/antibodies in initiation and overall progression of atherosclerosis, respectively. We were also interested to test if dietary Neu5Gc plays any role without an active antibody response, e.g., does incorporation of dietary Neu5Gc somehow dysregulate biological functions. In thie current study, we decided to pursue a 16 week course where animals were immunized prior to atherogenic chow or dietary Neu5Gc. After 16 weeks, the extent of atherosclerosis would be assessed in the aorta, as well as in the aortic valve.

Choice of an atherogenic chow to promote atherosclerosis and Neu5Gc incorporation. To promote atherogenesis and progression of disease, we chose the Western Diet as originally published[17] with and without added dietary Neu5Gc-containing glycoproteins (Neu5Gc-glycoproteins). This diet has the advantage of high fat content to generate hyperlipidemia, not just hypercholesterolemia. It is composed of 21%$_{weight}$ milk fat, yielding 42% calories from fat and 0.06%$_{weight}$ cholesterol. DMB-HPLC analysis showed that nearly all standard mouse chow (including chow from PicoLab, Dyets Inc., Harlan Teklad, Research Diets) contained Neu5Gc, likely due the protein ingredient, animal-derived casein. Sialic acid analysis of 4 standard mouse chow from multiple companies using DMB-HPLC showed that all standard chows contain Neu5Gc, averaging 3.0 ± 0.8 $\mu g_{Neu5Gc}/g_{chow}$, which translated to a bodily dose 0.39 ± 0.11 $mg_{Neu5Gc}/kg*d$ in mouse. There is potential uncertainty in this measurement because 3-separate milligram samples were tested in DMB-HPLC to estimate Neu5Gc content of 10 kilogram batches.

The Western Diet had more Neu5Gc than standard mouse chow, but was not Neu5Gc rich, with 7.6 $\mu g_{Neu5Gc}/g_{chow}$ (0.98 $mg_{Neu5Gc}/kg*d$). A custom formulation of Western Diet plus Neu5Gc-containing glycoproteins (Neu5Gc-glycoproteins) contains 278.4 $\mu g_{Neu5Gc}/g_{chow}$ (35.64 $mg_{Neu5Gc}/kg*d$). DMB-HPLC demonstrated that the chow

formulation process did not release any Neu5Gc from its glycoprotein carrier (not shown). Although the human dose is estimated to be around 0.16 mg_{Neu5Gc}/kg*d, mouse experiments have required substantially higher bodily doses to result in detectable Neu5Gc tissue incorporation (≥ 25 mg_{Neu5Gc}/kg*d). It is not certain why this is the case, but there are several likely explanations. First and foremost, we are trying to mimic the human condition and achieve decades of dietary Neu5Gc incorporation in a matter of weeks, thus requiring high doses. On the other hand, we have not been able to find incorporated Neu5Gc in *Cmah*$^{-/-}$ animals kept on a standard chow containing 0.341 mg_{Neu5Gc}/kg*d for 9-12 months, which indicates some threshold exists for detectable Neu5Gc incorporation in the mouse. Second, *Cmah*$^{-/-}$ animals were only generated a few years ago, thus they recently needed enzymes to metabolize Neu5Gc and recycle this metabolic dead end into more conventional monosaccharides[18]. Several pieces of information suggested that *Cmah*$^{-/-}$ mice rapidly metabolize Neu5Gc if present *in vivo*. For example, when *Cmah*$^{-/-}$ pups were born with *Cmah*$^{+/-}$ littermates to a *Cmah*$^{+/-}$ female, all pups phenotyped as Neu5Gc positive at birth. However within 14 days after birth, *Cmah*$^{-/-}$ animals were Neu5Gc free, indicating that the mice actively metabolized Neu5Gc in the absence of endogenous production. Despite the work described in Chapter 2, we may be fighting endogenous unidirectional metabolism to achieve Neu5Gc tissue incorporation *in vivo*, thus requiring higher bodily doses in mice than in humans.

Dietary Neu5Gc alone is insufficient to elicit Neu5Gc-specific antibodies in *Cmah*$^{-/-}$ mice. The temporal correlation between the appearance of Neu5Gc-specific antibodies and the introduction of animal-derived foods suggested that dietary Neu5Gc might represent the antigenic stimulus[19]. Despite 0.39 ± 0.11 mg_{Neu5Gc}/kg*d in regular

chow, *Cmah*$^{-/-}$ mice did not spontaneously generate Neu5Gc-specific IgM or IgG antibodies after 6–9 months (Fig. 4-1A, B).

In contrast, deliberate immunization with an Neu5Gc-rich antigen (chimpanzee erythrocyte ghosts with complete Freund's adjuvant) did elicit Neu5Gc-specific IgM (Fig. 4-1A) and IgG (Fig. 4-1B) antibodies in *Cmah*$^{-/-}$, but not wild-type mice. Despite the lack of spontaneously generated Neu5Gc-specific antibodies, *Cmah*$^{-/-}$ mice are capable of generating a humoral immune response against Neu5Gc upon active immunization (Fig. 4-1A, B).

Exploratory studies investigating Neu5Gc-specific antibody responses in the mouse are discussed in Appendix I. The interested reader is encouraged to read this section as many strategies have been attempted, but much work remains to be done.

Generating a well-controlled, human-like Neu5Gc-specific antibody response in the mouse for the atherosclerosis model. In light of work presented in Appendix I, chimpanzee erythrocyte ghosts were chosen as the optimal antigen for Neu5Gc immunization in mice. This is because the response is easily detectable in multiple isotypes, yields a high responder percentage (IgM: ~100%; IgG: ≥75%), and is polyclonal. As shown in Fig. 4-2B, averaged IgG responses from a cohort of *Cmah*$^{-/-}$ mice immunized with chimpanzee erythrocyte ghosts exhibit significant specific IgG that prefer Neu5Gcα2-6LacNAc, compared to Neu5Gcα2-3LacNAc. Although an individual either did (6/12 animals) or did not respond to Neu5Gcα2-3LacNAc, nearly all (11/12 animals) responded to Neu5Gcα2-6LacNAc. To control for the sialic acid-based specificity of antibody binding in ELISA, we used a mild periodate pre-treatment of the target ELISA glycans (in this case Neu5Gcα2-6LacNAc or Neu5Gcα2-3LacNAc). Mild (2 mM), short (10-20 min.) periodate treatments of sialic acids specifically attack the vicinal hydroxyls at C-8 and C-9 (see Fig. 4-2A for a schematic of this reaction).

The periodate oxidation truncates the C8-C9 side chain, releasing formaldehyde and formic acid, and generates an aldehyde at C-7. A strong reducing agent, $NaBH_4$, is used to reduce these reactive aldehydes into stable hydroxyls. Importantly, Neu5Gc-specific antibodies from chimpanzee erythrocyte ghost immunizations were periodate-sensitive (Fig. 4-2B, see white bars), indicating that Neu5Gc is necessary for these antibodies to recognize their antigen.

To control for a Neu5Gc immunization with a complex antigen (erythrocyte ghosts), it was important to design a control immunization with a similar complex antigen, but without the Neu5Gc response. Although human erythrocyte ghosts are a Neu5Gc-free antigen and are closely related to chimpanzee erythrocyte ghosts, both are xeno-antigens from the immunologic point of view of the mouse. These two xeno-antigens could potentially yield off-target immune responses in unpredictable (e.g., not systematic) ways.

We attempted two strategies to remove Neu5Gc from the chimpanzee erythrocyte ghosts before immunization, sialidase- and periodate-treatment. Sialidase treatment of ghosts with sialidase from *Artherobacter ureafaciens*[20] was able to remove 92% of the cell surface erythrocyte Neu5Gc, however we were unable to drive this reaction to completion, potentially reflecting the limited activity of sialidases on sialylated glycolipids[20]. The remaining Neu5Gc on sialidase-treated chimpanzee erythrocytes could generate weak responses in control groups. Moreover, sialidase treatment would expose terminal galactose, which could generate uncertain responses *in vivo*. Optimizing sialidase treatment of ghosts was thus not pursued.

Our second strategy was to truncate cell-surface Neu5Gc via a mild periodate oxidation of intact chimpanzee erythrocytes. We were able to track the success of erythrocyte periodate treatments using DMB-HPLC (Fig. 4-3A). In DMB-HPLC, an

organic solvent system elutes sialic acids from a reverse-phase column. Neu5Ac is retained on the column slightly longer than Neu5Gc due to the presence of the extra oxygen in Neu5Gc (oxygen → hydroxyl → potential for hydrophilic interactions). The truncation of the C8-C9 side chain and loss of these hydroxyls during the periodate oxidation made IO_4-rx-Neu5Gc (Fig. 4-3A, blue arrow) more hydrophobic than native Neu5Gc (Fig. 4-3A, red arrow), which resulted in a slight increase in retention time for IO_4-rx-Neu5Gc. Although initial reactions only truncated 90-95% of Neu5Gc on chimpanzee erythrocytes, we were able to drive this reaction to completion by manipulating the periodate:erythrocyte ratio. Increased ratios ≥ 400:1 resulted in destruction of 100% of erythrocyte Neu5Gc. Varying time, temperature, and concentration of the periodate oxidation did not improve oxidation performance. Samples oxidized under harsher periodate conditions (> 2 mM_{NaIO4}) exhibited undesirable side-affects, including precipitation/aggregation. Fresh sodium meta-periodate reagent was also an important component of a successful treatment.

Immunizing *Cmah*$^{-/-}$ mice with IO_4-rx-chimpanzee erythrocyte ghosts and mock-treated erythrocyte ghosts yielded a well controlled response. Importantly, the mock-treated erythrocyte ghosts generated a robust Neu5Gc-specific response (Fig. 4-3B) that was not statistically different in magnitude than that in untreated ghost immunization controls (not shown). Moreover the response against mock-treated ghosts was periodate-sensitive, which is to say that Neu5Gc-specific antibodies generated here required the native Neu5Gc structure (C8-C9) to bind. Analysis of the immune response generated against IO_4-rx-chimpanzee erythrocyte ghosts showed background-level responses to native Neu5Gc structures. However, the response to IO_4-rx-Neu5Gc was very strong (Fig 4-3B). Although unexpected at first, this result is

somewhat obvious given that IO_4-rx-chimpanzee erythrocyte ghosts carry an antigen (IO_4-rx-Neu5Gc) that is foreign *in vivo*.

Although sera from *Cmah*$^{-/-}$ mice immunized against IO_4-rx-chimpanzee erythrocyte ghosts did not bind to Neu5Gc-containing glycans in ELISA, we examined serum reactivity to mouse tissue sections as well as to LDL and oxidized LDL epitopes. While mock-treated ghost immunized sera stained kidney sections in a *Cmah*-dependent manner (e.g., staining *Cmah*$^{+/+}$, not *Cmah*$^{-/-}$ tissues), IO_4-rx-ghost immunized sera did not bind non-specifically, nor in a *Cmah*-dependent manner (Fig. 4-3C).

Periodate oxidation of an antigen has the potential to generate an off-target immune responses against oxidized epitopes. This is important because oxidized LDL and oxidized LDL antibodies have definite roles in atherosclerosis[21], thus we were interested to rule out that immune responses against IO_4-rx erythrocyte ghosts would cross-react with any of these epitopes and confound interpretation of the model. An ELISA approach using LDL, malondialdehyde-modified LDL (MDA-LDL), or Cu-oxidized LDL as targets demonstrated differences in binding between mock-rx ghost immunized sera and periodate-rx ghost immunized sera, however there was no preferential binding pattern of either sera against these targets (Table 4-1).

Finally, it is important to note that identical immunization regiments must be used in any atherosclerosis models. Adjuvant contains mycobacterial cell wall extract, which binds to leukocyte pattern recognition receptors like TLR2,4. Adjuvants have atheroprotective effects in mice[22,23], thus adjuvant exposure must be the same in all groups.

Neu5Gc-specific responses are boosted in *Cmah*, *Ldlr* DKO Mice consuming dietary Neu5Gc. As mentioned earlier, *Cmah, Ldlr* DKO mice did not express

spontaneous Neu5Gc-specific antibodies (pg. 114) and they responded similarly to immunizations that had been established in the *Cmah* single knockout background. Previous experiments using the *Cmah, Ldlr* DKO mice in a short term atherosclerosis model (8 weeks of Standard Chow + 1.25% Cholesterol with or without Neu5Gc-glycoproteinsa added) showed that naïve animals did not develop Neu5Gc-specific antibodies via dietary exposure (not shown). This is consistent with observations that correlate oral antigens with immunologic tolerance[24]. Nonetheless, it was interesting to see that even high doses dietary Neu5Gc are not sufficient to elicit Neu5Gc-specific antibody responses *in vivo*.

In this 19 week study of atherosclerosis (3 weeks for immunization followed by 16 weeks on Western Diet with or without Neu5Gc-glycproteins), Neu5Gc-specific antibody responses in *Cmah, Ldlr* DKO mice were quantified at week 0 (pre-immune), 3 (post-immune), 11 (8 weeks of diet), and 19 (16 weeks of diet). We were particularly interested in the magnitude of Neu5Gc-specific immune response before and after introduction of dietary Neu5c (week 3 versus week 11). Interestingly after 8 weeks of Western Diet + Neu5Gc-glycoproteins, animals that had been immunized against Neu5Gc exhibited a substantial boosting effect in Neu5Gc-specific IgG titers (Fig. 4-4A, top panel, compare gray solid bars to black solid bars) and to a lesser extent in Neu5Gc-specific IgM titers (Fig. 4-4B, bottom panel, same comparison). This boosting effect was quite strong, but was Neu5Gc-specific as evinced by the complete periodate knockdown of antibody binding (Fig. 4-4A, compared solid bars to open bars). 13/16 animals exhibited boosts in IgG levels between these two time points. It is notable that the 3/16 animals that showed no boost (ΔNO, ΔL, ΔR) were all littermates, exhibited very low IgG titers prior to the Western Diet + Neu5Gc-glycoproteins, and did not

demonstrate any boosts in IgMs. This suggested an overall lack of immune response against Neu5Gc that is correlated with this litter.

Because we observed the boosting phenomenon in animals that were ingesting dietary Neu5Gc and were immunized against Neu5Gc, we were interested to explore the specificity of this boosting phenomenon for Neu5Gc. To test this, we performed a longitudinal analysis of pooled serum from all groups at 0, 3, 11, 19 week timepoints (Fig. 4-4B). As expected only animals immunized against Neu5Gc (red diamonds) exhibited Neu5Gc-specific IgG (top panel), whereas animals immunized against IO_4-rx-Neu5Gc (blue squares) exhibited IO_4-rx-Neu5Gc-specific IgG (bottom panel). Although the post-immune response to IO_4-rx-Neu5Gc is stronger than the corresponding Neu5Gc response at 3 weeks, only Neu5Gc-specific IgG (top panel, red diamonds) exhibit a boosting response that is correlated with dietary Neu5Gc intake at 11 and 19 weeks. At these later timepoints, IO_4-rx-Neu5Gc-specific IgG (bottom panel, blue squares) have plateaued near post-immune levels and exhibit a modest decay over the 4 month study course.

Although the Western Diet contains 2.7% of the Neu5Gc content of the Western Diet + Neu5Gc-glycoproteins, Neu5Gc immunized animals on Western Diet alone exhibited a qualitatively similar boosting response (open red diamonds, ~20% reduced) compared to animals on a high Neu5Gc diet (closed red diamonds). This suggests that the dietary Neu5Gc content necessary to generate a boosting phenomenon *in vivo* is low (≤ 0.98 mg_{Neu5Gc}/kg*d). It should be noted that the bodily dose of Neu5Gc for mice on the Western Diet is 5.9 times greater than the estimated bodily dose of Neu5Gc in humans.

Based on these results, we would hypothesize that an individual could boost existing Neu5Gc-specific titers commensurate with their dietary Neu5Gc intake.

Because the Western Diet contains Neu5Gc as part of its standard formulation, dietary Neu5Gc is present in both diets, albeit 360 times less than in the Neu5Gc-glycoprotein formulation. Nonetheless, further investigation should verify that the boosting phenomenon does not occur in Neu5Gc immunized animals maintained on Neu5Gc-free, soy chow. One study to this end is currently underway (Chapter 5, pg. 157).

Finally, an analysis Neu5Gc- and IO_4-rx-Neu5Gc-specific IgG at week 19 (end of study) from animals on the Western Diet + Neu5Gc-glycoproteins showed that the magnitude of response between these immunization groups was not statistically different ($p=0.70$, Fig. 4-4C). This is in spite of the fact that Neu5Gc-specific IgG titers were an order of magnitude lower than the IO_4-rx-Neu5Gc-specific IgG titers just after the immunization regiment (Fig. 4-2B and Fig. 4-4B). That these titers are not statistically different speaks to the cumulative effects of the Neu5Gc-specific boosting phenomenon seen with dietary Neu5Gc.

Are Neu5Gc-specific antibodies and dietary Neu5Gc atheroprotective *in vivo*? Over the course of this study, we followed several metrics with atherosclerosis relevance. First, body weight at any given time point was not different between the groups, except at the end of the study where animals on Western Diet + Neu5Gc-glycoproteins exhibited a statistically significant increase in body weight compared to animals of Western Diet alone, a result that was independent of immunization (Fig. 4-5B). This statistically significant increase was the result of increased weight gain throughout the entire study as longitudinal plots of individual body weight show that animals on Western Diet alone gain weight slower than those on Western Diet + Neu5Gc-glycoproteins (Fig. 4-5A, compare closed shapes to open shapes).

We also followed fasting cholesterol and triglyceride levels. Based on what is known about dietary Neu5Gc and Neu5Gc-specific immune responses, we

hypothesized an effect on atherosclerosis independent of plasma lipid profiles. In support of this hypothesis, we found that there were no significant differences in fasting cholesterol or triglycerides at baseline or weeks 4 or 8 of diet (Fig. 4-6A). The exception being control immunized animals on Western Diet alone, which exhibited an atypical (statistically significant decrease) in fasting cholesterol levels at week 19, compared to all other groups (Fig. 4-6B), prompting exclusion of this group from further analysis. In spite of this outlier group, there was little difference in lipoprotein profiles between the groups at week 19 (Fig 4-6C). Taken together, these results indicate that any affect on atherosclerosis in this study would be independent of plasma lipid profiles.

Despite the overall similarity of physiologic variables between the groups, we found a statistically significant reduction in total atherosclerosis of the *en face* aorta in the Neu5Gc immunized animals on Western Diet + Neu5Gc-glycoproteins (Fig 4-7A, p=0.03). This surprising result was also borne out in the aortic valve where the Neu5Gc-specific antibodies and Western Diet + Neu5Gc-glycoproteins conferred an atheroprotective effect on cross-sectional atherosclerotic plaque burden, compared to control immunized groups on the same diet (Fig. 4-7B, p=0.029). The reduction of atherosclerosis at two separate vascular sites in this group suggested an overall reduction of plaque burden and an atheroprotective role for these Neu5Gc-specific antibodies *in vivo*, rather than a role in altering the sites as which lesions develop.

To understand the mechanisms underlying the reduction in atherosclerosis in Neu5Gc-specific immunized animals on the Western Diet + Neu5Gc-glycoproteins, we compared the relationship between cholesterol levels and atherosclerosis. Cholesterol levels exhibit a positive correlation with atherosclerosis in mice and in humans, thus we were interested to test if the immunizations affected this relationship. To develop a

cholesterol metric for this comparison, we calculated average cholesterol levels (|Cholesterol|) from fasting cholesterol values at 4, 8, and 16 weeks of Western Diet. |Cholesterol| has an advantage over cholesterol at a given timepoint as the average will more truly represent an animal's cholesterol burden throughout the entire study. In the aortic valve, we find that the slope of the relationship between |Cholesterol| and atherosclerosis is unchanged between the immunization groups, but the correlation is shifted downward in Neu5Gc immunized groups (Fig 4-7F). These results suggest that the Neu5Gc immunization does not affect the relationship between cholesterol and atherosclerosis in the aortic valve and that Neu5Gc-specific antibodies act to reduce atherosclerosis independent of affecting cholesterol. This notion agrees well with data that Neu5Gc immunization does not affect cholesterol biology (Fig. 4-5).

If the Neu5Gc-specific antibodies do indeed play an atheroprotective role, one would predict that titer should negatively correlate with disease. Natural inter-individual variability of Neu5Gc-specific immune responses offers an opportunity to plot such correlations. In fact, there is a negative correlation between Neu5Gc-specific IgG and lesion area in the *en face* aorta (Fig 4-7C), which is statistically correlated ($p=0.088$, as tested by simple correlation). On the other hand, there is little correlation ($p=0.70$) between IO_4-rx-Neu5Gc IgG and lesion area in the *en face* aorta (Fig. 4-7D), indicating that the periodate-rx ghost immunization, although strong, is not exacerbating disease *in vivo*. Moreover, the extent of disease in these animals is low compared to historical controls where *C57bl6 Ldlr* -/- animals on Western Diet for 16 weeks exhibited mean aortic lesion area of ~ 20% (JL Witztum, AC Li, unpublished observations). However we cannot rule out the possibility that the very strong initial response to the periodate-rx erythrocyte ghosts confounded our results by causing a generalized, non-specific

inflammation that exacerbated atherosclerosis in periodate-rx ghost immunized groups, such as happens in rheumatoid arthritis[25].

Animals expressing Neu5Gc-specific antibodies and ingesting Neu5Gc exhibit reduced biomarkers of endothelial damage. Based on data presented in Chapter 3, the combination of endothelial incorporation of Neu5Gc and Neu5Gc-specific antibodies promotes vascular inflammation. Endothelial damage is also associated with vascular inflammation, thus we predicted that the combination of dietary Neu5Gc and Neu5Gc-specific antibodies might generate biomarkers of endothelial damage that could be measured in circulation. Several biomarkers, such as soluble forms of VCAM1 (sVCAM) and ICAM1 (sICAM), have been implicated in endothelial damage[26]. Although sICAM levels did not vary between the groups (Fig. 4-8B), sVCAM was significantly reduced in the Neu5Gc-immunized group on Western Diet + Neu5Gc-glycoprotein (Fig. 4-8A) compared to the control-immunized group on Western Diet + Neu5Gc-glycoproteins ($p=0.004$), as well as compared to the Neu5Gc-immunized group on Western Diet alone ($p=0.014$), which were not significantly different from eachother. We were interested to observe that sVCAM levels were not different in control-imunized groups on Western Diet + Neu5Gc-glycoproteins and Neu5Gc-immunized groups on Western Diet alone, as this indicated that control-immunized groups did not lead to off-target endothelial damage.

DISCUSSION

These studies provided the first evidence that dietary Neu5Gc can boost existing Neu5Gc-specific immune responses over time. Previous studies showed that *Cmah*$^{-/-}$ mice on standard chow (0.39 mg_{Neu5Gc}/kg*d) [19] and Neu5Gc-glycoprotein-spiked chow (35.64 mg_{Neu5Gc}/kg*d, not shown) did not develop spontaneous Neu5Gc-

specific antibody responses. However, when animals that had been immunized against Neu5Gc were moved from a Neu5Gc-free chow to one rich in Neu5Gc, we observed a boosting response, particularly strong in the IgG isotype (Fig. 4-4A). This data suggests that dietary Neu5Gc passes through the gastrointestinal tract of naïve animals without a response, despite the presence of intestinal lymphocytes and antigen-presenting cells. However, after an immunization and the clonal expansion of antigen-specific B-lymphocytes, dietary exposure is recognized, causing a boost response.

It is important to verify our interpretation of this result because both formulations of the Western Diet contained Neu5Gc. Thus, we have designed an implemented an ongoing experiment to test this interpretation where animals are maintained on a Neu5Gc-free chow formulation that is used as the base for a Neu5Gc-rich diet. This study is discussed in Chapter 5 (pg. 157).

The results from the atherosclerosis model suggest an atheroprotective role for the Neu5Gc-specific antibodies. Although interesting, these data should be interpreted with caution. Although Neu5Gc-specific immune responses that we generate in the mouse are meant to mimic the human condition, the chimpanzee erythrocyte ghost immunization is used for its robust responder percentage. Although the chimpanzee erythrocyte ghost immunization is polyclonal and exhibits reactivity to a variety of Neu5Gc-containing targets in ELISA, we are currently unsure which, if any, human Neu5Gc-specific antibodies have cardiovascular relevance. In the mouse, we are unsure if the antibodies that we are generating are relevant for our model, thus we are unsure if this result has physiological relevance for humans. Are the same antibody specificities, which are generated in mouse, present in humans? Are we missing

antibodies with key specificities from the mouse that play roles in human atherosclerosis?

Questions notwithstanding, these data and the general, negative correlation of Neu5Gc-specific antibodies with atherosclerosis may have relevance *in vivo*. It will be important to understand the epidemiology of human antibodies to help guide future mouse studies. Also, it will be important to understand how the antibodies are acting to apparently reduce atherosclerotic plaque burden. *In vitro* evidence suggests that the antibodies should act to promote inflammation of the vasculature in accordance with dietary Neu5Gc incorporation. Data presented here show that biomarkers of endothelial damage, such as sVCAM, are actually reduced in Neu5Gc-immunized animals on dietary Neu5Gc (Fig. 4-8A). We have little information on how Neu5Gc and Neu5Gc-specific antibodies might affect macrophage and foam cell biology in the lesion. It is quite possible that the antibodies may exert a novel effect in lesions, thereby slowing disease progression. A few avenues for exploration might involve examining the interplay of Neu5Gc incorporation and Neu5Gc-specific antibodies on LDL uptake, oxLDL uptake, and the pro-inflammatory foam cell transition in *Cmah*, *Ldlr DKO* macrophages. A cellular mechanism supporting an atheroprotective effect of Neu5Gc-specific antibodies would be an important addition to this work before drawing firm conclusions on this study. Finally, if Neu5Gc antibodies do turn out to be atheroprotective, this would be at odds with the growing literature on the association between cardiovascular disease and red meat intake[27].

MATERIALS & METHODS

Detection of Neu5Gc-specific antibodies in human sera. Human Neu5Gc-specific antibodies were detected against Neu5Gcα2–6 or α2–3 linked to Galβ1–4Glcβ-HSA[28].

Briefly, 96-well microtiter plates (Costar 9018, Corning) were coated overnight at 4°C, in triplicate, with saturating concentrations of Neu5Gc containing glycoconjugates α2–6 or α2–3 linked to HSA (Sigma) alone or with saturating concentrations in 50 mM sodium carbonate-bicarbonate buffer, pH 9.5. To standardize antibody levels, each plate was also coated with serial dilutions of human IgG and IgM, (Jackson ImmunoResearch). Wells were blocked for 2 h at RT with 1% ovalbumin (Grade V, Sigma, free of Neu5Gc) in PBS, followed by incubation with serum samples diluted 1:100 in the same blocking solution for 2 h at RT. The plates were washed three times with PBS containing 0.1% Tween (PBST) and subsequently incubated for 1 h at RT with HRP-conjugated goat-anti-human IgM (Kirkegaard and Perry Laboratories), 1:4,000 diluted in PBS, or goat anti-human IgG (Bio-Rad) 1:6,000–1:7,000 diluted in PBS. After washing three times with PBST, wells were developed with *O*-phenylenediamine in a citrate-PO_4 buffer, pH 5.5, and absorbance was measured at 490 nm on a SpectraMax 250 (Molecular Devices). Neu5Gc-specific antibody values were defined by subtracting readings obtained from HAS alone from those obtained from the Neu5Gc-glycoconjugate-HSA antigens, and were quantified into ng/μl using the standard dilution curves of the corresponding purified human IgG or IgM.

Detection of Neu5Gc-specific antibodies in mouse plasma. To assess the Neu5Gc-specific response in this cohort, we performed an Enzyme-linked Immunosorbent Assay (ELISA), adapted from previously published methods[29]. 384 well ELISA plates (Pierce Maxisorp) were coated with 200 ng of target glycan/glycoprotein in 50 mM Sodium Carbonate/Sodium Bicarbonate buffer, pH 9.5. Targets included chemo-enzymatically synthesized glycans (Neu5Gcα2-6LacNAc and Neu5Gcα2-3LacNAc linked to human serum albumin, HSA), chimpanzee serum, purified porcine submaxillary mucin, and Neu5Gc covalently linked to poly-acrylamide,

PAA (Glycotech). Various targets were chosen to present Neu5Gc in ELISA in a few of the possible physiologic milieu that can be found *in vivo*, thus improving our understanding of the breadth of immune response generated by the chimpanzee erythrocyte ghost immunization.

To control for the Neu5Gc specificity of any signals against the targets, we utilized a mild periodate pre-treatment of glycans to specifically destroy Neu5Gc from the coated glycans/glycoproteins on the ELISA plate. Briefly, plates were thrice washed with PBS, pH 6.5. Next, wells that were periodate treated were incubated with 4 volumes of 2 mM fresh $NaIO_4$ in PBS pH 6.5 for 20 minutes in the dark at room temperature. Periodate reactions were quenched with 1 volume of 0.1 M $NaBH_4$ in PBS, pH 6.5, for 10 minutes in the dark at room temperature. Wells that were mock-periodate treated were incubated in premixed sodium periodate:sodium borohydride::4:1 solution to pre-quench the periodate and maintain native Neu5Gc. All wells were then washed thrice with 100 mM NaCl, 50 mM sodium acetate, pH 5.5 to remove borates. Wells were blocked with PBS + 0.5% cold water fish skin gelatin (Sigma), pH 7.3. Sera were diluted 1:100 to 1:2000 in PBS + 0.5% cold water fish skin gelatin, usually 4 hours at room temperature or overnight at 4°C. Both IgM and IgG isotypes were measured using Goat-anti-mouse-IgG/-IgM-Alkaline Phosphatase secondary antibodies (Jackson Immunoresearch), diluted 1:5,000 in PBS + 0.5% cold water fish skin gelatin. Signals were developed using *p*-nitrophenyl phosphate and read as an optical absorbance at 405 nm on a Spectramax 250 (Molecular Devices).

Chimpanzee erythrocyte ghost preparation. Fresh EDTA-anti-coagulated chimpanzee blood was shipped overnight from the Yerkes Primate Foundation (Emory University). The blood was spun down at 1,000 rcf for 10 minutes. The plasma and buffy coat layer were removed and the erythrocytes were resuspended in PBS with

Ca^{2+} and Mg^{2+}, then spun, then resuspended, and spun once more.

For periodate treatment, packed erythrocytes were added to fresh 2 mM $NaIO_4$ (Sigma) in PBS pH 6.5 at volume:packed erythrocyte::400:1. Samples were allowed to react, in the dark, at room temperature for 30 minutes, while gently stirring. Successful periodate treatments are associated with the faint browning of the erythrocyte solution. To quench the reaction, and equal volume of fresh 40 mM $NaBH_4$ (EMD Biosciences) in PBS pH 6.5 was added and allowed to react in the dark for 30 minutes. For mock treatment, the $NaIO_4$ and the $NaBH_4$ solutions were premixed for 5 minutes prior to adding the appropriate volume of packed erythrocytes. The samples were then spun down in a Sorvall Centrifuge (Beckman Instruments) at 1,000 rcf for 5 minutes.

2 mL of packed erythrocytes were aliquoted into 50 mL polycarbonate Sorvall Centriufuge tubes (Nalgene) and lysed with 28 mM TrisHCl, 1 mM EDTA, pH 7.4[30]. Erythrocytes were lysed on ice for 30 minutes, then spun down at least 10,000 rcf for 10 minutes with the brake on low. The supernatant was carefully aspirated and new lysis buffer was added. The tubes were spun and the cycle repeats until the supernatant is clear and the ghost pellet is opaque. Finally, samples were resuspended and spun down twice in 100 mM NaCl, 50 mM sodium acetate, before a final spin in water with the centrifuge break completely off. Preparations were characterized for protein and sialic acid content and stored in water + 0.01% butylated hydroxytoluene (to prevent lipid peroxidation) at 200 $\mu g_{protein}$/100 μL at -80°C.

Neu5Gc detection by DMB-HPLC. Sialic acids can be identified in samples using DMB-HPLC as described (Chapter 2, pg. 42, under **Quantification of…Neu5Gc by DMB-HPLC**). Periodate treated sialic acids are well-resolved on a Phenomenex C18 column in 85% H_2O, 75 MeOH, 8% acetonitrile, exhibiting ~1 minute increase in retention time compared to their respective native sialic acids.

Atherosclerosis study parameters. Male *Cmah, Ldlr DKO* littermates consumed the Western Diet (TD.98338, Harlan Teklad) for 16 weeks starting the experimental course at 8-10 weeks of age. Prior to beginning the Western Diet, animals were maintained on a strict Neu5Gc-free (sialic acid-free), soy chow diet (110951, Dyets, Inc.). Animals were immunized against Neu5Gc, using chimpanzee erythrocyte ghosts, or control immunized, using periodate-rx chimpanzee erythrocyte ghosts, in Freund's-based immunization. Animals were pre-bled for baseline serum samples using the submandibular technique, immunized, then boosted twice weekly thereafter. After the immunization course, the animals were begun on the Western Diet with or without Neu5Gc-containing glycoproteins. Animals were bled at 4, 8, 12, and 16 weeks for EDTA-plasma according to the methods below (see **Blood and Plasma Analysis**). Body weight was also taken at these points. Chow consumption in each cage was measured weekly from weeks 9-13. Pre-determined exclusion criteria include

1) Drop ≥ 20% in body weight between time points.
2) Drop ≥ 25% in cholesterol or triglyceride levels between time points.
3) Less than a 20% increase in body weight at study week 19 (16 weeks of Western Diet plus 3 weeks immunization course) compared to that measured at study week 0.

After study week 19, animals were sacrificed by CO_2 and perfused through the left ventricle with PBS + 10 mM EDTA, then perfusion fixed for 10 minutes in 10% formal/sucrose. We also excluded 2 mice from atherosclerotic analysis (αL, and βL), based on exclusion criteria #3 and #1, respectively.

Atherosclerosis Analysis. The extent of atherosclerosis was quantified by computer-assisted image morphometry (ImageJ, NIH) on Sudan IV-stained *en face* preparations of the thoracic aorta and in cross sections through the aortic outflow tract of paraffin-

embedded hearts, as described[31]. In the *en face* aortas, digital images were taken and Sudan IV-positive lesions were quantified by calibration from pixels into mm^2. For the aortic valve cross-sections, 2-5 μm sections were cut for the same slide, called #1. Slides were prepared with pairs of 5 μm sections until the valve leaflets had been sectioned through and the aorta takes form. Every third section was stained for atherosclerosis analysis. A trichrome stain, consisting of hematoxylin, fuchsin red/picric acid, and aniline blue, was utilized for cross sectional analysis of plaque burden and composition. The quantification of disease in each leaflet began only in fully-formed valve leaflets and 7 consecutive measurements were made of each leaflet. The sum of the lesion area in each leaflet divided by the number of sections measured constitutes the metric used to quantify atherosclerosis in these studies. All animal studies were approved by the Institutional Animal Care and Use Committee of University of California, San Diego Medical School.

Plasma Lipid Analyses. At the pre-determined time point, animals were bled for parallel antibody and plasma lipid analysis. Following a 3-hour fast, mice were anesthetized with Isoflurane and retro-orbital blood was obtained via EDTA-coated micro capillary tubes (at 11 a.m.). Plasma cholesterol and triglycerides levels were determined using automated enzymatic assays (Roche Diagnostics, Indianapolis, IN, USA and Equal Diagnostics, Exton, PA, USA). Fresh plasma samples were pooled according to groups and lipoproteins were fractionized by size using fast protein liquid chromatography (FPLC) equipped with a Superose 6 column, and cholesterol and triglyceride levels were determined in each fraction (250 μL), as described[32].

Plasma sICAM-1, sVCAM-1 Analysis. To assess endothelial damage associated with our group variables, we tested the levels of soluble ICAM-1 (sICAM-1, CD54) and sVCAM-1 (CD106). Plasma samples were diluted 1:50 and tested as per the

manufacturer's instructions of the Quantikine ELISA Kit (R & D Systems).

Statistics. Statistical analysis was performed using Prism v5.0a (GraphPad Software; San Diego, CA).

ACKNOWLEDGEMENTS

These studies would not be possible without the generous help of many members of the Witztum lab and their facilities for morphometric analysis of atherosclerotic lesions. In particular, Joe Witztum, Andrew Li and Jennifer Pattison have been instrumental in helping plan and work-up samples. Florence Casanada and Karen Bowden have also provided invaluable help working up these samples for morphometric analysis. Joe Juliano performed the plasma lipid analyses. Cody Diehl tested the ghost immunized sera for their reactivity against LDL and oxidized epitopes in ELISA.

Initial work on the chimpanzee erythrocyte ghost immunization (Fig. 4-2, pg. 133) was performed with Oliver Pearce. Special thanks are due to Michelle Chung and Michelle Abueg for their help (Fig. 4-8, pg. 141) and tireless dedication to research.

Chapter 4, in part (Fig 4-1, pg. 128), is a reprint of the material as it appears in *Taylor RE, Gregg CJ, Padler-Karavani V, Ghaderi D, Yu H, Huang S, Sorensen RU, Chen X, Inostroza J, Nizet V, & Varki A, J Exp Med 207:1637-1646, 2010*. The dissertation author was the second author on this work and Dr. Ajit Varki directed and supervised the research that forms the basis of this chapter.

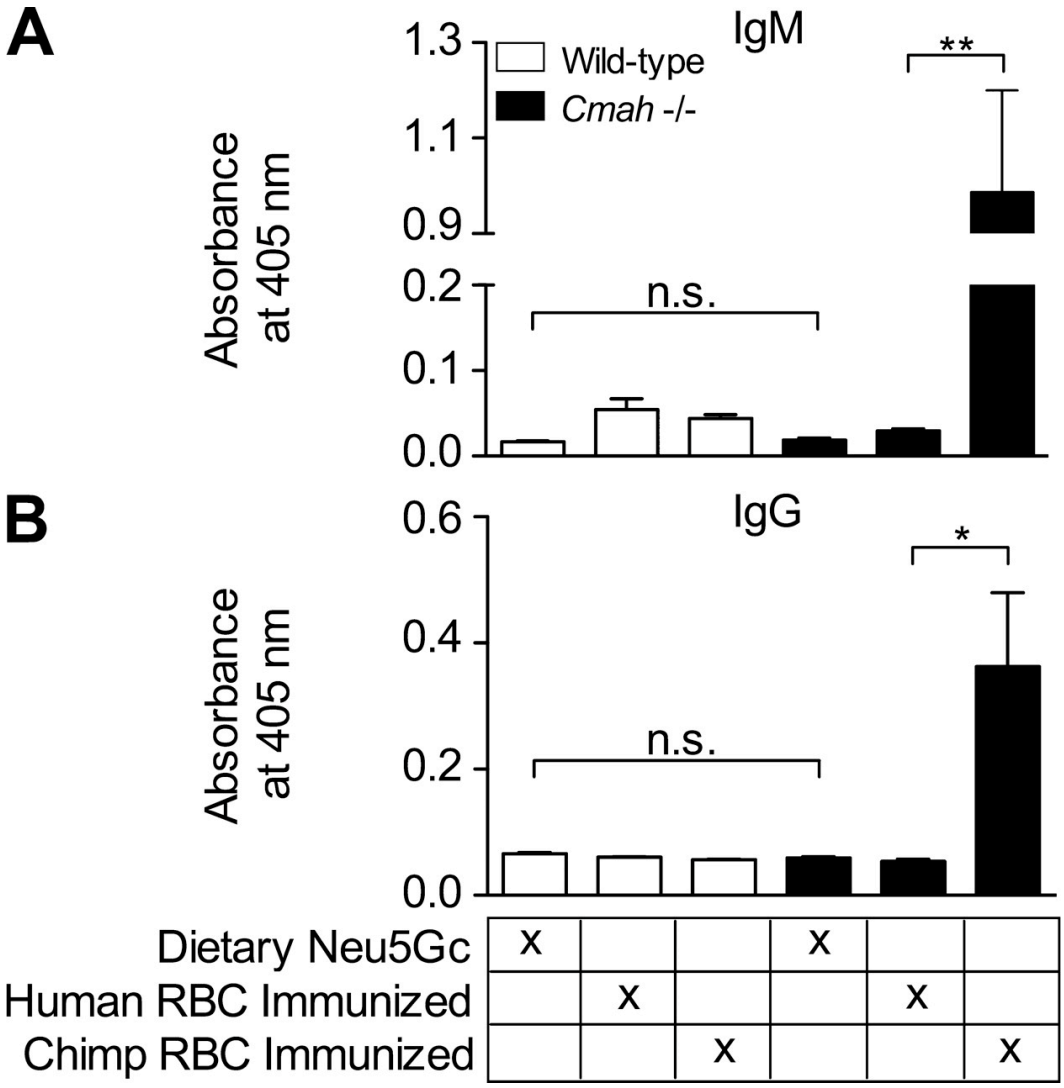

Figure 4-1. Dietary Neu5Gc Does Not Elicit Neu5Gc-specific Antibodies. A, B. Wild-type (open bars, *n*=8) and *Cmah*$^{-/-}$ (filled bars, *n*=8) were fed 0.39 mg_{Neu5Gc}/kg*day (from normal chow) after weaning (4–6 weeks total), immunized with human RBC ghosts (Wild-type *n*=4, *Cmah*$^{-/-}$*n*=4), or immunized with chimpanzee RBC ghosts (Wild-type *n*=4, *Cmah*$^{-/-}$ *n*=4). Sera were analyzed by ELISA for IgM (A, note the broken y-axis) and IgG. **B.** Antibodies against Neu5Gcα-PAA and shown as mean absorbance values at OD_{405} ± SEM. Statistical analysis was performed using an unpaired two-tailed Student's *t*-test. n.s, not significant, *, $P < 0.05$ and **, $P < 0.01$. Data are representative of at least three independent experiments.

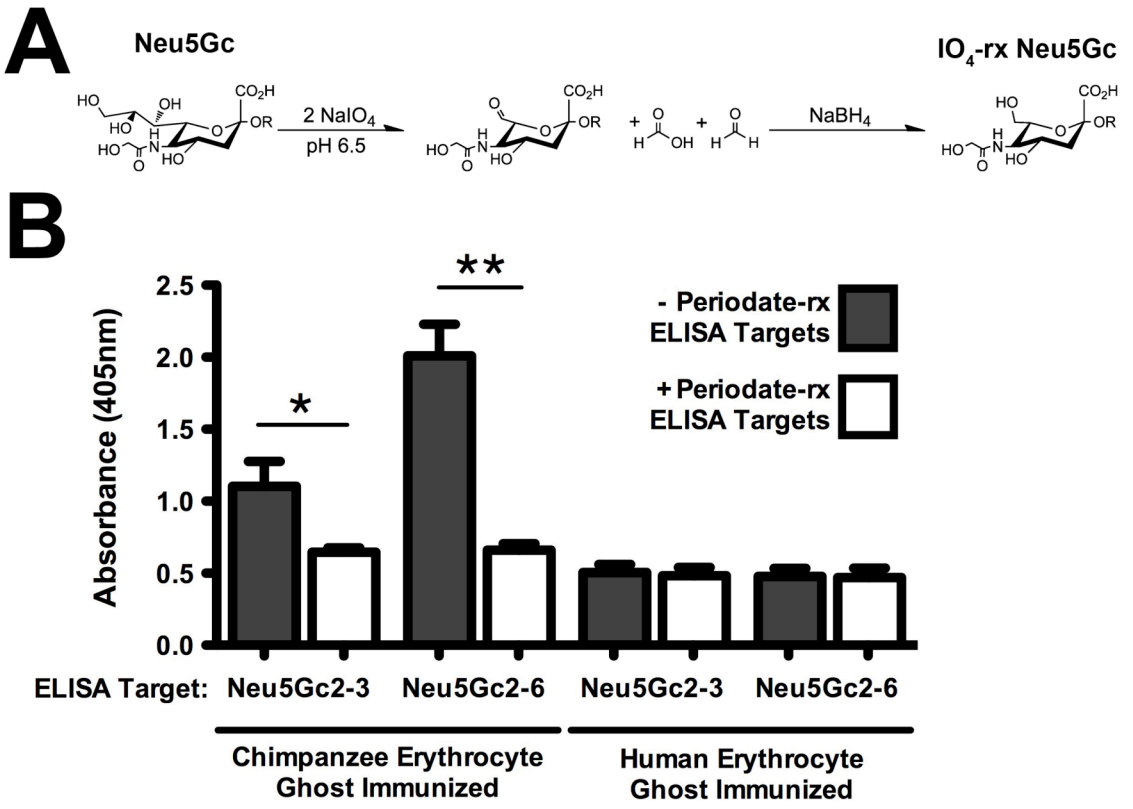

Figure 4-2. Representative Neu5Gc-specific IgG Response from *Cmah*$^{-/-}$ Animals Immunized with Chimpanzee Erythrocyte Ghosts. A. The reaction scheme showing the mild periodate (2 mM $NaIO_4$) oxidation attacking the vicinal hydroxyls at C-8 and C-9, releasing formaldehyde and formic acid. In the final step a strong reducing agent, $NaBH_4$, was used to reduce the truncated side chain on Neu5Gc into a alcohol, thus forming IO_4-rx-Neu5Gc. **B.** *Cmah*$^{-/-}$ animals were immunized against Neu5Gc using chimpanzee erythrocyte ghosts in a Freund's adjuvant-based immunization with a primary immunization a two semi-weekly boosts. 7 days after the last boost, the animals were bled for serum. The Neu5Gc-specific reactivity (IgG titers) of these sera was tested in an ELISA format using Neu5Gcα2-3LacNAc-HSA Neu5Gcα2-6LacNAc-HSA as the target for IgG binding (black bars), which showed Neu5Gc reactivity in chimpanzee erythrocyte ghost immunized mouse sera which preferred Neu5Gcα2-6. To control for the specificity of IgG binding, the ELISA target glycans were periodate treated to destroy Neu5Gc (white bars), which abolished all binding. As a control, littermates were immunized against human erythrocyte ghosts. Because human ghosts lack Neu5Gc, these animals mounted no response against Neu5Gc-containing glycans.

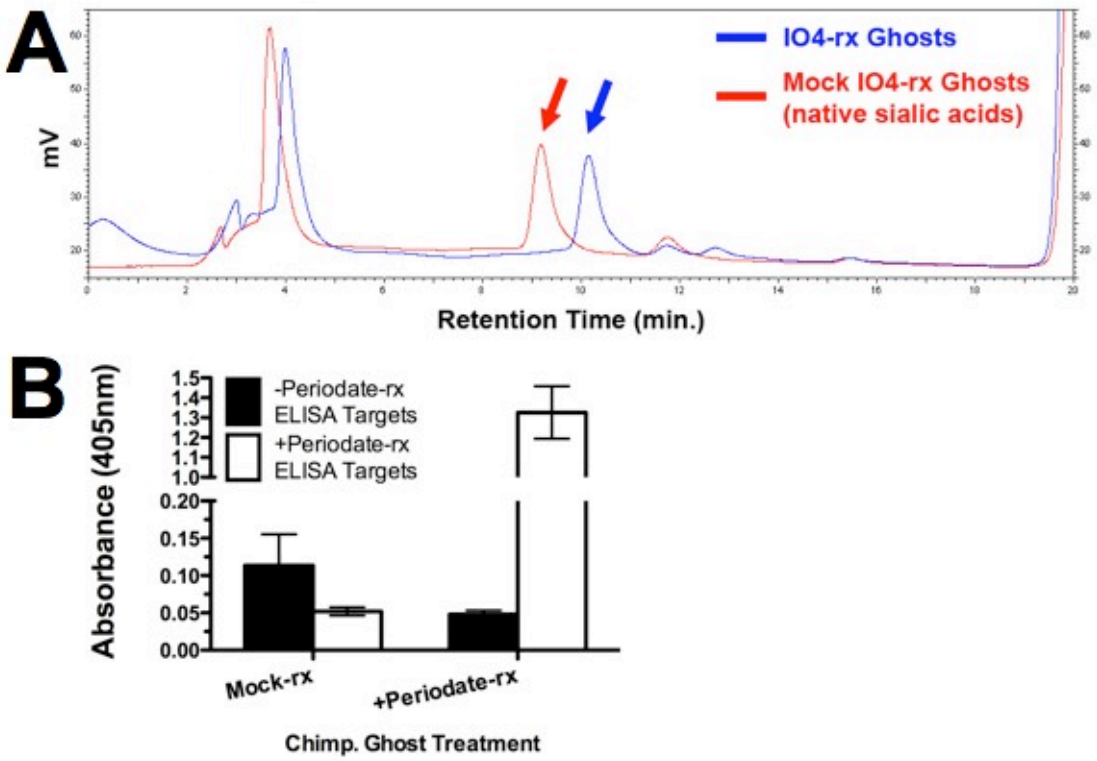

Figure 4-3. Periodate Treatment of Chimpanzee Erythrocyte Ghosts is a Control Antigen for Neu5Gc Immunizations. A. DMB-HPLC chromatogram showing complete oxidation of native Neu5Gc (red trace with red arrow marking Neu5Gc peak) and periodate-rx Neu5Gc (blue trace with blue arrow marking IO_4-rx Neu5Gc). The slight increase in retention time of IO_4-rx Neu5Gc to native Neu5Gc makes it possible to use this method to separate the two species and asses the completion of periodate oxidation on the chimpanzee erythrocyte ghosts. **B.** ELISA with sera from mice immunized with mock-rx chimpanzee erythrocyte ghosts or with periodate-rx chimpanzee erythrocyte ghosts. As expected, the sera from mock-rx ghost-immunized animals binds to Neu5Gcα2-3LacNAc-HSA and is sensitive to periodate treatment of the ELISA target glycans. Sera from animals immunized with periodate-rx ghosts exhibits a strong response, but only when the ELISA target glycans are periodate treated to generate the antigen with which the animals were immunized.

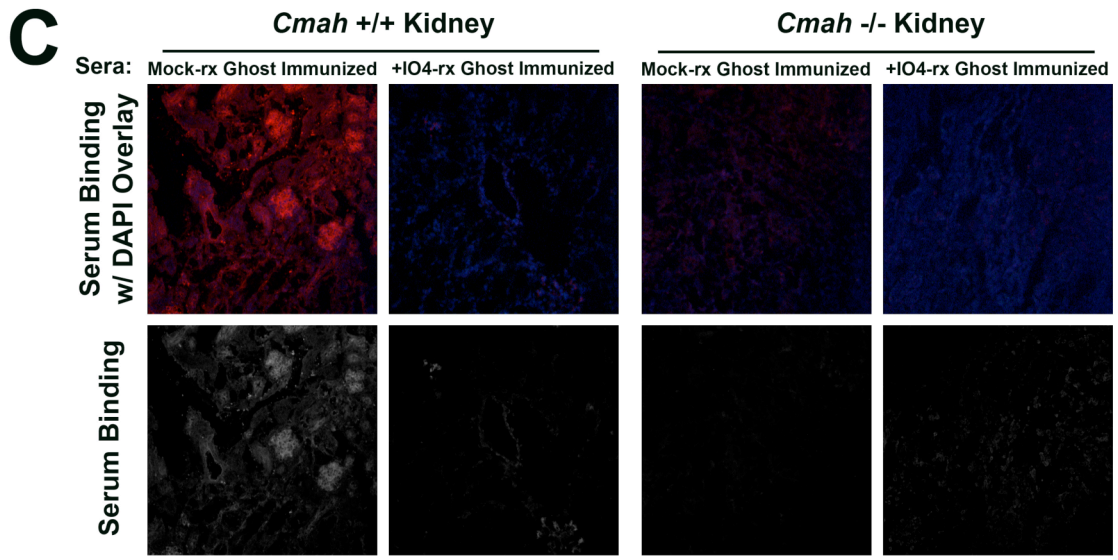

Figure 4-3, cont'd. Periodate Treatment of Chimpanzee Erythrocyte Ghosts is a Control Antigen for Neu5Gc Immunizations. C. Comparison of tissue reactivity of sera from mice immunized with mock-rx chimpanzee erythrocyte ghosts or with periodate-rx chimpanzee erythrocyte ghosts. The top row shows overlaid immunofluorescence images of sera binding (red channel) and nuclei (blue channel). The bottom row shows just the sera binding channel in grayscale. As expected the sera from mock-rx ghost-immunized animals binds to mouse kidney sections in a *Cmah*-dependent fashion. Importantly, the sera from periodate-rx ghost-immunized animals does not bind to mouse kidney section in a non-specific or off-target way.

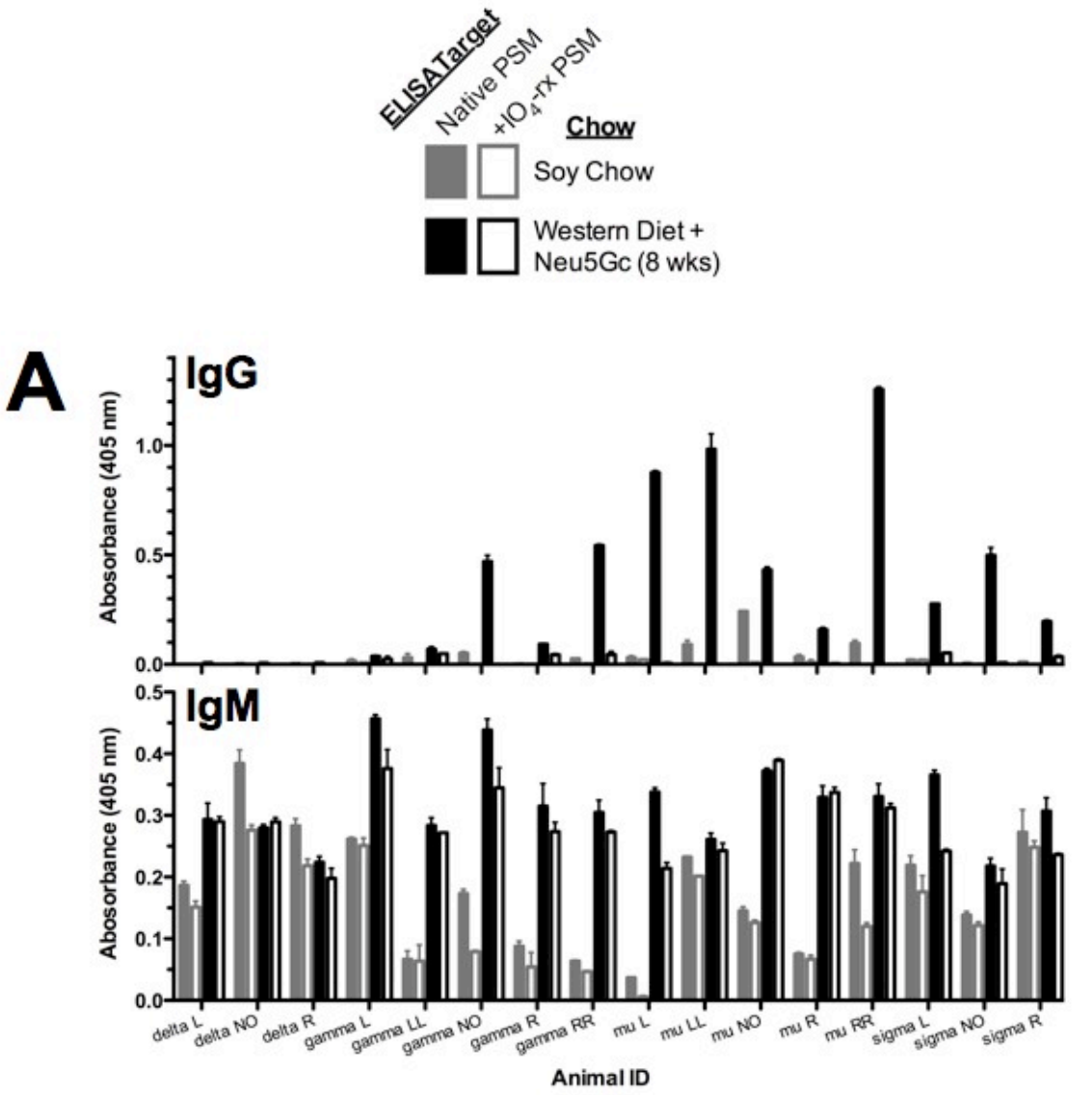

Figure 4-4. Dietary Neu5Gc Boosts Existing Neu5Gc-specific Antibody Responses. In this study, Cmah, Ldlr DKO animals were immunized against Neu5Gc using chimpanzee erythrocyte ghosts, while control groups were immunized against periodate-rx chimpanzee erythrocyte ghosts over the course of three weeks. Prior to and during immunization, animals were maintained on a Neu5Gc-free "Soy Chow". After immunization, animals began a 16 week course on a Western Diet containing Neu5Gc-glycoproteins ("Western Diet + Neu5Gc-glycoproteins"). **A.** IgG levels (top panel) and IgM levels (bottom panel) in individual animals immunized against chimpanzee erythrocyte ghosts before (gray bars) and 8 weeks after (black bars) introduction of dietary Neu5Gc. Dietary Neu5Gc boosts IgG levels. IgGs are sensitive to periodate treatment in every animal, confirming the Neu5Gc-dependence of these responses. Dietary Neu5Gc also boosts IgM levels in some individuals, although the effect less prominent than in the IgG isotype. The periodate sensitivity of Neu5Gc-specific IgMs is poor. This phenomenon has been observed in Neu5Gc-specific IgM responses in mice (see Appendix I) and is believed to be due to a lower stringency of IgMs for antigen binding, as well as the increased avidity conferred by decavalence of IgM structure.

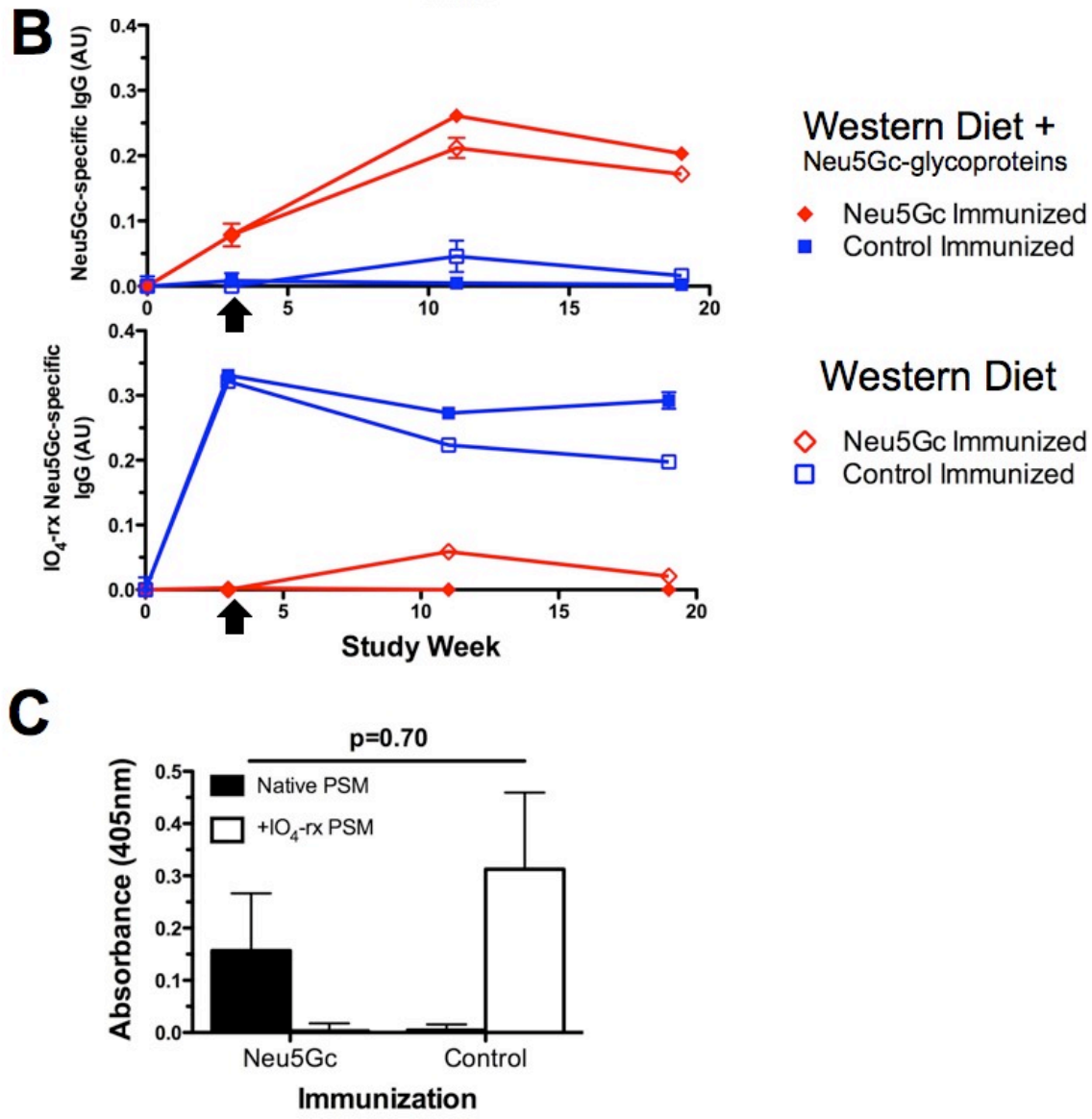

Figure 4-4, cont'd. Dietary Neu5Gc Boosts Existing Neu5Gc-specific Antibody Responses. B. Pooled Neu5Gc-specific IgG (top panel) and IO_4-rx-Neu5Gc-specific IgG (bottom panel) antibody levels were followed in animals immunized against chimpanzee erythrocyte ghosts ("Neu5Gc Immunized", red diamonds) or IO_4-rx chimpanzee erythrocyte ghosts ("Control Immunized", blue squares) that were either eating the Western Diet (open shapes) or the Western Diet + Neu5Gc-glycoproteins (closed shapes). Antibody levels were sampled at 0 weeks (pre-immune), 3 weeks (post-immune), 11 weeks (8 weeks after switch to Western Diet ± Neu5Gc-glycoproteins), 19 weeks (16 weeks after chow switch). Introduction of dietary Neu5Gc is marked by a black arrow on the x-axis just after the 3 week time point. Mice immunized against native chimpanzee erythrocyte ghosts exhibit Neu5Gc-specific titers that are boosted in the presence of dietary Neu5Gc, whereas animals immunized against IO_4-rx chimpanzee erythrocyte ghosts exhibit IO_4-rx-Neu5Gc-specific IgGs that are strong, but not boosted by dietary Neu5Gc. **C.** Average IgG titers from Neu5Gc Immunized and Control Immunized animals against native PSM (filled bars) and IO_4-rx-PSM (open bars) at the conclusion of this study showing that the Neu5Gc-specific IgG response is not statistically different ($p = 0.70$) than the anti-IO_4-rx-Neu5Gc IgG response at this point.

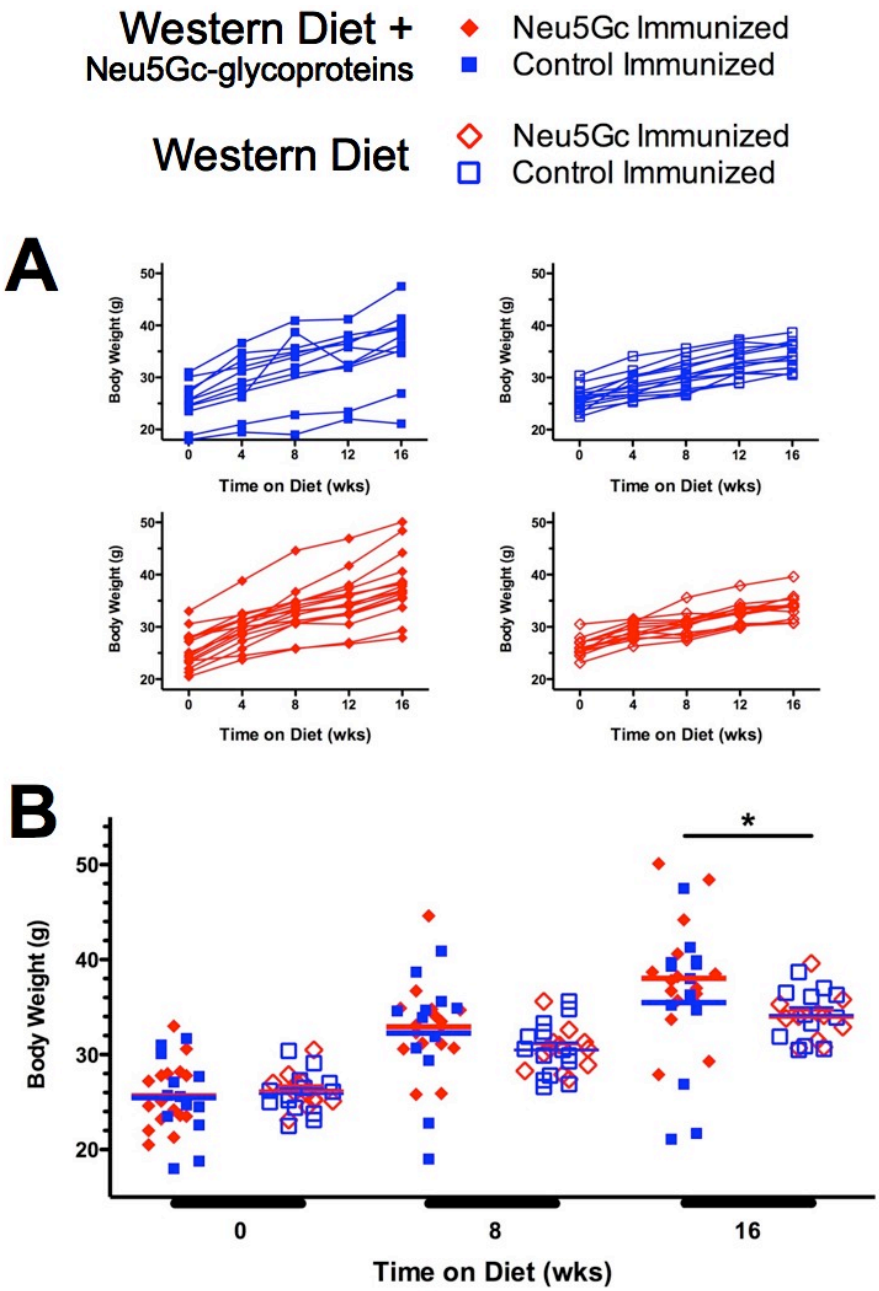

Figure 4-5. Body Weight is Increased in Mice Eating Dietary Neu5Gc, Regardless of Immunization. Neu5Gc-immunized mice (red diamonds) ingested Neu5Gc (filled diamonds) or not (open diamonds). Control-immunized mice (blue squares) ingested Neu5Gc (filled squares) or not (open squares). **A.** Panels show the body weight progression of each animal in the study. Mice that exhibit significant losses of body weight between time points were candidates for exclusion (see **Atherosclerosis Study Parameters)**. **B.** Shows the average cohort body weight of animals throughout the course of this study. The mean body weight is marked by the color-coded line at each time point. Animals ingesting Western Diet + Neu5Gc-glycoproteins exhibited a significant increase in body weight at 16 weeks of diet, compared to animals eating Western Diet alone (p=0.044: open blue squares versus closed red diamonds; p=0.038: open red diamonds versus closed red diamonds).

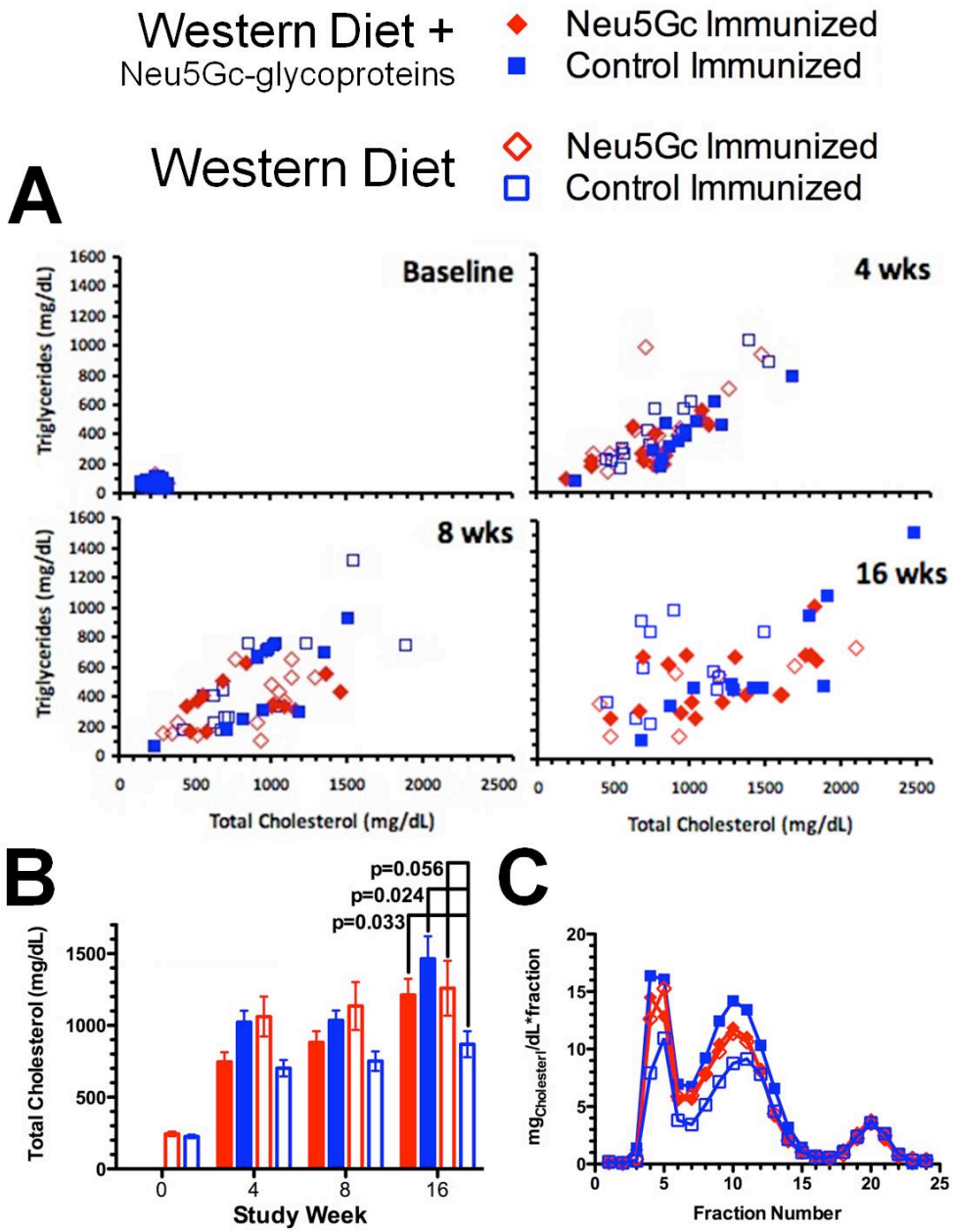

Fig 4-6. Dietary Neu5Gc and Neu5Gc Immunization Do Not Influence Plasma Lipid Profiles. Neu5Gc-immunized mice (red diamonds) ingested Neu5Gc (filled diamonds) or not (open diamonds). Control-immunized mice (blue squares) ingested Neu5Gc (filled squares) or not (open squares). **A.** Scatter plots of fasting lipid profiles. Each panel presents the indicated time point of Western Diet, Baseline, 4, 8, and 16 weeks. Total Cholesterol (mg/dL) is plotted on the x-axis and Triglycerides (mg/dL) are plotted on the y-axis. Both axes on all panels have the same range. **B.** Mean + Standard Deviation of total cholesterol levels of animals in the indicated groups are plotted as a function of time on the diet. Animals on Western Diet and control immunized exhibited a blunted total cholesterol levels at week 16 compared to all groups, thus was excluded from further analysis. **C.** FPLC separation of 50 µL of plasma lipoproteins from pooled fasting plasma samples on a Superose 6 column with subsequent quantification of cholesterol levels in fractions, which showed no change in lipoprotein profiles between groups.

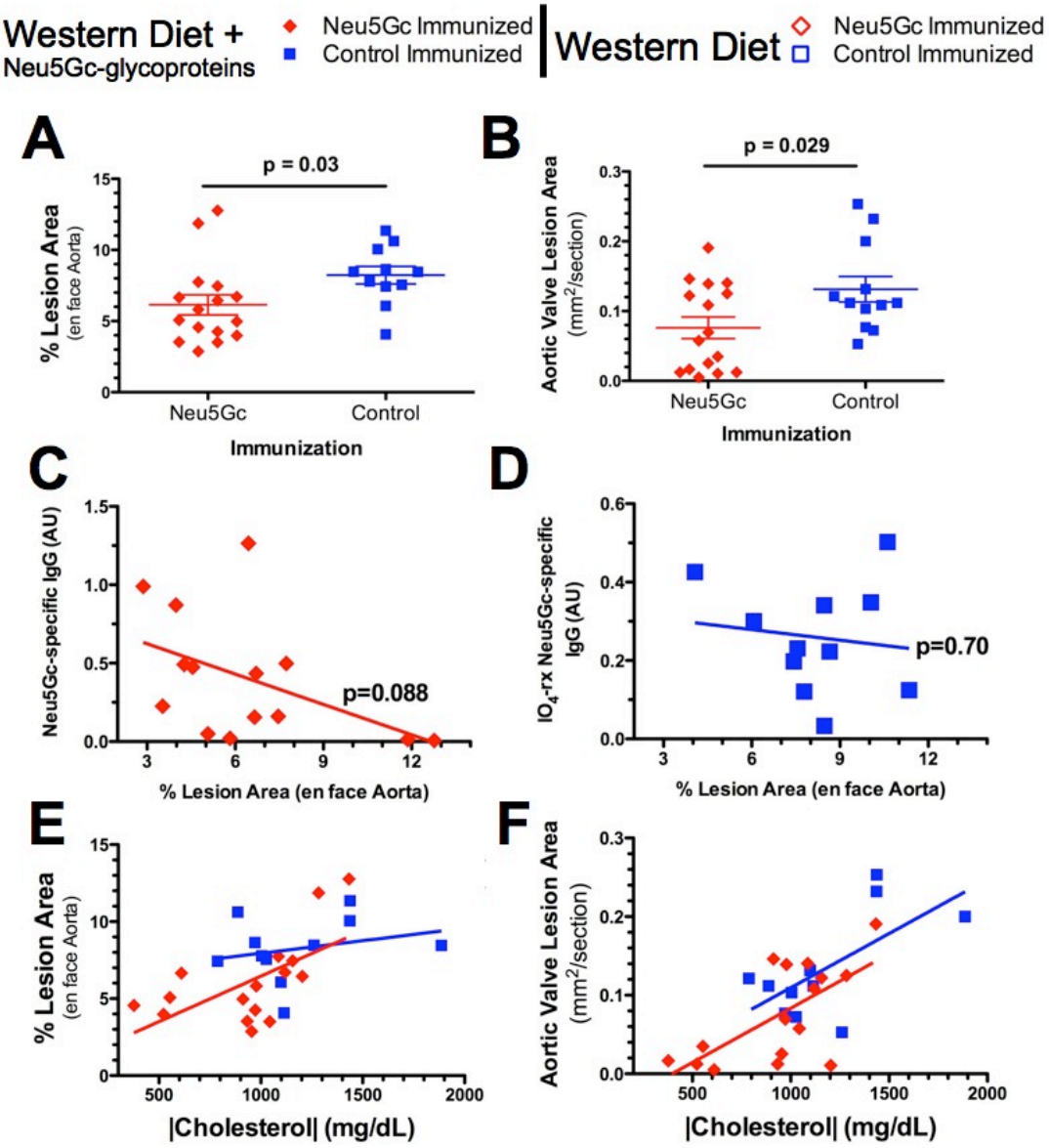

Figure 4-7. Neu5Gc-specific Antibodies Appear Atheroprotective in the Presence of Dietary Neu5Gc. Neu5Gc-immunized mice (red diamonds) ingested Neu5Gc (filled diamonds) or not (open diamonds). Control-immunized mice (blue squares) ingested Neu5Gc (filled squares) or not (open squares). **A,B.** Lesion area of the *en face* aorta (A). Cross-sectional lesion area measured in the aortic valve leaflets (B). Neu5Gc-immunized groups on dietary Neu5Gc exhibited reduced atherosclerosis at both sites compared to control-immunized groups on the same diet (A, p=0.03; B, p=0.029 based on a Student's t test). **C,D.** Plot of the correlation between Neu5Gc-specific antibody titer (C) or the anti-IO_4-rx Neu5Gc antibody titer (D) and lesion area in the *en face* aorta. A negative correlation exists between Neu5Gc-specific antibody titers and lesion area (C, p=0.088 based on the simple correlation test), but little correlation exists between anti-IO_4-rx Neu5Gc antibodies and lesion area (D, p=0.70). **E,F.** Using |Cholesterol| (average cholesterol at 4, 8, 16 weeks of the western diet in mg/dL) as a metric of an animal's cholesterol burden in this study, we plotted the comparison with atherosclerosis in the en face aorta (E) and the aortic valve (F) as well as the trend lines describing this comparison. Notably, Neu5Gc immunization does not affect this relationship in the aortic valve.

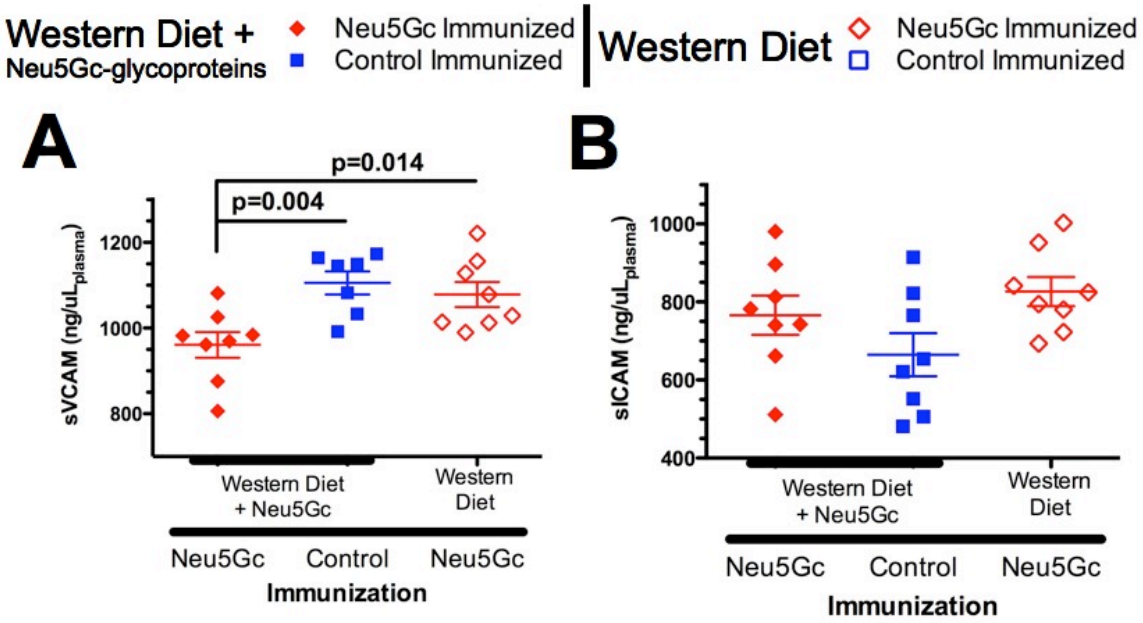

Figure 4-8. Neu5Gc-specific Antibodies Reduce Biomarkers of Inflammation in the Presence of Dietary Neu5Gc. Neu5Gc-immunized mice (red diamonds) ingested Neu5Gc (filled diamonds) or not (open diamonds). Control-immunized mice (blue squares) ingested Neu5Gc (filled squares) or not (open squares). Plasma was tested for soluble VCAM1 (A, sVCAM) and soluble ICAM1 (B, sICAM) levels at sacrifice in *Cmah*, *Ldlr* mice that had been ingesting dietary Neu5Gc (closed shapes) and were immunized against chimpanzee erythrocyte ghosts ("Neu5Gc Immunization", red diamonds) or IO4-rx chimpanzee erythrocyte ghosts ("Control Immunization", blue squares). Although no statistically significant differences were observed in sICAM levels between groups (B), there was a significant reduction in sVCAM levels in animals ingesting dietary Neu5Gc and immunized against Neu5Gc (A, closed red diamonds).

Table 4-1. Binding Preferences of Mock-rx/Periodate-rx Ghost Immunized Mouse Sera to LDL and Oxidized LDL Epitopes in ELISA. ELISAs were performed (by Cody Diehl, Witztum Lab) using malondialdehyde-modified LDL (MDA-LDL), copper-oxidized LDL (Cu-ox LDL), and native LDL as ELISA targets to investigate serum binding of periodate-rx erythrocyte ghost immunized mouse sera compared with mock-rx erythrocyte ghost immunized mouse sera. Binding of IgM, IgG1, IgG2c isotypes were tested. 4 serum dilutions (1:50, 1:500, 1:5,000, 1:50,000) were tested against each epitope for each isotype. Statistically significant ($p<0.05$) increases in binding in 3/4 of the dilutions are reported below for the indicated antigen.

LDL Epitope	Immunoglobulin Isotype		
	IgM	IgG1	IgG2c
MDA-LDL	No Difference	Mock-rx Ghost	Periodate-rx Ghost
Cu-ox LDL	No Difference	Mock-rx Ghost	Periodate-rx Ghost
Native LDL	No Difference	No Difference	No Difference

REFERENCES

1. Roger, V. L. et al. Heart Disease and Stroke Statistics--2011 Update: A Report From the American Heart Association. *Circulation* (2010).
2. Hartvigsen, K. et al. The role of innate immunity in atherogenesis. *J Lipid Res* **50 Suppl**, S388-93 (2009).
3. Shi, G. P. Immunomodulation of vascular diseases: atherosclerosis and autoimmunity. *Eur J Vasc Endovasc Surg* **39**, 485-494 (2010).
4. Steinberg, D., Glass, C. K. & Witztum, J. L. Evidence mandating earlier and more aggressive treatment of hypercholesterolemia. *Circulation* **118**, 672-677 (2008).
5. Miller, Y. I., Choi, S. H., Fang, L. & Harkewicz, R. Toll-like receptor-4 and lipoprotein accumulation in macrophages. *Trends Cardiovasc Med* **19**, 227-232 (2009).
6. Plosch, T., Kosters, A., Groen, A. K. & Kuipers, F. The ABC of hepatic and intestinal cholesterol transport. *Handb Exp Pharmacol* 465-482 (2005).
7. Glass, C. K. & Witztum, J. L. Atherosclerosis. the road ahead. *Cell* **104**, 503-516 (2001).
8. Foley, E. M. & Esko, J. D. Hepatic heparan sulfate proteoglycans and endocytic clearance of triglyceride-rich lipoproteins. *Prog Mol Biol Transl Sci* **93**, 213-233 (2010).
9. Mansbach, C. M. & Siddiqi, S. A. The biogenesis of chylomicrons. *Annu Rev Physiol* **72**, 315-333 (2010).
10. Dallinga-Thie, G. M. et al. The metabolism of triglyceride-rich lipoproteins revisited: new players, new insight. *Atherosclerosis* **211**, 1-8 (2010).
11. Lammey, M. L. et al. Interstitial myocardial fibrosis in a captive chimpanzee (Pan troglodytes) population. *Comp Med* **58**, 389-394 (2008).
12. Varki, N. et al. Heart disease is common in humans and chimpanzees, but is caused by different pathological processes. *Evolutionary Applications* **2**, 101-112 (2009).
13. Finch, C. E. Evolution in health and medicine Sackler colloquium: Evolution of the human lifespan and diseases of aging: roles of infection, inflammation, and nutrition. *Proc Natl Acad Sci U S A* **107 Suppl 1**, 1718-1724 (2010).
14. Herndon, J. G. & Tigges, J. Hematologic and blood biochemical variables of captive chimpanzees: cross-sectional and longitudinal analyses. *Comp Med* **51**, 60-69 (2001).
15. Hanlon, C. S. & Rubinsztein, D. C. Arginine residues at codons 112 and 158 in the apolipoprotein E gene correspond to the ancestral state in humans. *Atherosclerosis* **112**, 85-90 (1995).
16. Ishibashi, S., Goldstein, J. L., Brown, M. S., Herz, J. & Burns, D. K. Massive xanthomatosis and atherosclerosis in cholesterol-fed low density lipoprotein receptor-negative mice. *J Clin Invest* **93**, 1885-1893 (1994).
17. Plump, A. S. et al. Severe hypercholesterolemia and atherosclerosis in apolipoprotein E-deficient mice created by homologous recombination in ES cells. *Cell* **71**, 343-353 (1992).

18. Altheide, T. K. et al. System-wide genomic and biochemical comparisons of sialic acid biology among primates and rodents: Evidence for two modes of rapid evolution. *J Biol Chem* **281**, 25689-25702 (2006).
19. Taylor, R. E. et al. Novel mechanism for the generation of human xeno-autoantibodies against the nonhuman sialic acid N-glycolylneuraminic acid. *J Exp Med* **207**, 1637-1646 (2010).
20. Saito, M., Sugano, K. & Nagai, Y. Action of arthrobacter ureafaciens sialidase on sialoglycolipid substrates. *J Biol Chem* **254**, 7845-7854 (1979).
21. Parthasarathy, S., Steinberg, D. & Witztum, J. L. The role of oxidized low-density lipoproteins in the pathogenesis of atherosclerosis. *Annu Rev Med* **43**, 219-225 (1992).
22. Khallou-Laschet, J. et al. Atheroprotective effect of adjuvants in apolipoprotein E knockout mice. *Atherosclerosis* **184**, 330-341 (2006).
23. Hansen, P. R. et al. Freunds adjuvant alone is antiatherogenic in apoE-deficient mice and specific immunization against TNFalpha confers no additional benefit. *Atherosclerosis* **158**, 87-94 (2001).
24. Verhasselt, V. Oral tolerance in neonates: from basics to potential prevention of allergic disease. *Mucosal Immunol* **3**, 326-333 (2010).
25. Sherer, Y. & Shoenfeld, Y. Mechanisms of disease: atherosclerosis in autoimmune diseases. *Nat Clin Pract Rheumatol* **2**, 99-106 (2006).
26. Spronk, P. E., Bootsma, H., Huitema, M. G., Limburg, P. C. & Kallenberg, C. G. Levels of soluble VCAM-1, soluble ICAM-1, and soluble E-selectin during disease exacerbations in patients with systemic lupus erythematosus (SLE); a long term prospective study. *Clin Exp Immunol* **97**, 439-444 (1994).
27. Bernstein, A. M. et al. Major dietary protein sources and risk of coronary heart disease in women. *Circulation* **122**, 876-883 (2010).
28. Yu, H., Chokhawala, H. A., Varki, A. & Chen, X. Efficient chemoenzymatic synthesis of biotinylated human serum albumin-sialoglycoside conjugates containing O-acetylated sialic acids. *Org Biomol Chem* **5**, 2458-2463 (2007).
29. Padler-Karavani, V. et al. Diversity in specificity, abundance, and composition of anti-Neu5Gc antibodies in normal humans: potential implications for disease. *Glycobiology* **18**, 818-830 (2008).
30. Hayashi, H., Plishker, G. A., Vaughan, L. & Penniston, J. T. Energy-dependent endocytosis in erythrocyte ghosts. IV. Effects of Ca2+, Na+ +K+, and 5'-adenylylimidodiphosphate. *Biochim Biophys Acta* **382**, 218-229 (1975).
31. Tangirala, R. K., Rubin, E. M. & Palinski, W. Quantitation of atherosclerosis in murine models: correlation between lesions in the aortic origin and in the entire aorta, and differences in the extent of lesions between sexes in LDL receptor-deficient and apolipoprotein E-deficient mice. *J Lipid Res* **36**, 2320-2328 (1995).
32. Li, A. C. et al. Peroxisome proliferator-activated receptor gamma ligands inhibit development of atherosclerosis in LDL receptor-deficient mice. *J Clin Invest* **106**, 523-531 (2000).

CHAPTER 5

Conclusion & Future Plans

The original goal of the research in this dissertation was to study the role of dietary Neu5Gc and Neu5Gc-specific antibodies in human diseases associated with red meat consumption, such as atherosclerosis. When I embarked with this goal, several unknowns (e.g., dietary incorporation of Neu5Gc and generating a human-like Neu5Gc-specific antibody response *in vivo*) hampered developing complex animal models. Before considering murine atherosclerosis, extensive work addressed physiologic mechanisms underlying dietary incorporation of Neu5Gc (Chapter 2).

In vivo gastrointestinal studies showed that Neu5Gc-containing glycoproteins are handled very differently than free Neu5Gc monosaccharide. Differences in intestinal absorption lead to different circulatory and excretion kinetics. Moreover, feeding Neu5Gc-containing glycoproteins allows Neu5Gc to enter endogenous biosynthetic pools and be available for glycosylation of self glycans. Long-term feeding of adult animals leads to tissue incorporation of Neu5Gc in a human-like pattern, such as endothelium of the vasculature, intestinal epithelium, and peri-vascular tissues in the kidney and liver. Moreover, feeding Neu5Gc-containing glycoproteins during pregnancy leads to *in utero* loading of pups, a scenario that is relevant to human pregnancies as multiple studies have found Neu5Gc in placental and fetal tissues[1]. Given the cellular composition of Neu5Gc-containing foods, dietary Neu5Gc likely is eaten as comes in glycoproteins and glycolipids. Thus, current feeding strategies using PSM as a candidate Neu5Gc-rich glycoprotein are arguably a physiologic strategy for modeling the human condition. It is important that this supposition be validated through a comprehensive analysis of Neu5Gc content by weight of common foods. It is equally important to understand the relative abundance of free- versus glycosidically-bound Neu5Gc, as well as the type of biological molecules to which

Neu5Gc is bound (glycoprotein, glycolipid, GPI-anchored glycoproteins) as these factors likely influece the extent of Neu5Gc tissue incorporation from the diet.

The observation that dietary Neu5Gc can incorporate into a developing organism during pregnancy brings up interesting questions about the role of sialic acids during development. Although produced endogenously throughout all stages of development, dietary sialic acid supplementation seems to play a positive role in mammalian brain development. For instance, sialic acid supplementation improves learning metrics in rat[2] and pig models[3]. Moreover, human breast milk has higher sialic acid content than other primate breast milk, which are all generally sialic acid-rich compared to rodent breast milk. Thus, there is a general mammalian trend for high breast milk sialic acid content in organisms with larger brains and higher cognitive functions. Interestingly, emerging epidemiological evidence has shown that human breast milk (as opposed to formula) is richer in sialic acid content[4,5] and that breastfed children develop higher IQ levels than formula-fed children[6]. Although IQ is a complex phenotype that is dependent on more than dietary sialic acid intake, the question of whether or not dietary sialic acid is beneficial in development and adulthood should be studied. We are taking one approach to study this question with a murine Aging Study (discussed below).

Despite the success of Neu5Gc-glycoprotein feeding, the mechanism underlying transport of dietary Neu5Gc through the circulation to target tissues is poorly understood. Although DMB-HPLC can detect Neu5Gc in acid-hydrolyzed serum from Neu5Gc-glycoprotein-fed mice, αNeu5Gc IgY does not detect a conventional Neu5Gc-containing serum glycoprotein (Chapter 2). Moreover, Neu5Gc is not carried on lipoproteins, although feeding Neu5Gc-glycoproteins with dietary fat increases circulating Neu5Gc levels. Neu5Gc is present in the liver during short feeding

timepoints, but then is detected on tissues such as endothelium and epithelium in long term fed mice. Although a circulating transport mechanism is likely, passive transfer of syngeneic *Cmah*$^{+/+}$ serum into *Cmah*$^{-/-}$ mice did not result in tissue incorporation.

Understanding the mechanism underlying transport of dietary Neu5Gc through the circulation to target tissues will explain the characteristic pattern of human and *Cmah*$^{-/-}$ mouse tissues that are loaded by dietary Neu5Gc. One potential mechanism could be that dietary Neu5Gc is transported through the circulation on a GPI-anchored protein. GPI-anchored proteins can be spontaneously transferred between erythrocyte membranes in circulation or between an erythrocyte and an endothelial cell[7]. Thus a Neu5Gc-rich GPI-anchored protein could be carried thorugh circulation on erythrocytes and circulating plasma Neu5Gc detected in DMB-HPLC could be irrelevant or could represent cross contamination from the erythrocyte fraction during separation of plasma. Another possibility is that circulating Neu5Gc is actually CMP-Neu5Gc, the high energy donor form of Neu5Gc used by sialyltransferases in glycosylation. There is little precedent for such a mechanism, but several cell types (hepatocytes included) secrete active sialylatransferases into the extracellular space where the concentration of the CMP-sialic acid is very low[8]. The relevance of this observation is unclear, but if dietary sialic acid is circulated as CMP-Sialic Acid, secreted sialyltransferases could act extracellularly to immediately sialylate self-glycans with dietary sialic acid on the cell surface. In the case of Neu5Gc, it could then gain access to cytoplasmic biosynthetic pools through autophagy.

Simultaneous studies (Appendix I) investigated generating Neu5Gc-specific antibodies in mice. *Cmah*$^{-/-}$ mice do not spontaneously develop Neu5Gc-specific responses throughout life, but can mount human-like responses to Neu5Gc, if

immunized. Although several immunization strategies exist, the best and most rigorously controlled is the erythrocyte ghost-based immunization (Chapter 4). This strategy generates a robust response in multiple isotypes in a high percentage of animals. Importantly, several control immunization strategies have been studied to generate a modified erythrocyte ghost without the Neu5Gc component. Control strategies include Neu5Gc-free related (human) erythrocyte ghosts, periodate-treated erythrocyte ghosts, and sialidase-treated erythrocyte ghosts.

Despite this progress, there is important work to be done with mucins and with novel multi-component antigens that are currently being synthesized. Although PSM/OSM immunizations have been successful in generating robust Neu5Gc-specific Ig responses *in vivo*, control immunization strategies have not been pursued. Possible control strategies for mucin immunizations include immunizing with Neu5Gc-free avian submaxillary mucin ("EBN"), as well as periodate- or sialidase-treating the mucin itself. These strategies do not obviate the potential drawback of mucin-based immunizations, as PSM-based feeding is not likely to change in the near future. Despite a wide search for another source of Neu5Gc-rich glycoproteins (serum, protease-digested serum, casein glycomacropeptide, goat sweet whey), PSM has at least 10-fold more Neu5Gc by weight than any other known source. Thus it will be difficult to reconcile the Neu5Gc-dependence of phenomena in PSM-fed/PSM-immunized mice without extensive control experiments.

Finally, novel multi-component antigens should be tested as soon as they are received (collaboration with Geert Jan Boons and Xi Chen). Here Neu5Gc is being glycosidically linked to the antigen through α2-3 and α2-6 linkages. Given the bioactive properties of the polypeptide and lipid-tail portion of this antigen, it is important to immunize with a Neu5Ac-containing antigen in control immunizations.

Related work addressed the immunologic interplay between Neu5Gc exposure in development and subsequent immune responses in adulthood. *In utero* Neu5Gc exposure (through standard mouse chow) or exposure to Neu5Gc in early life (through Neu5Gc-containing mouse milk) does not tolerize subsequent adult immunizations and may play a sensitizing role by boosting existing Neu5Gc-specific responses (Appendix I). Indeed, existing Neu5Gc-specific titers in adult *Cmah*$^{-/-}$ mice are boosted specifically by dietary Neu5Gc (Chapter 4). Progress with Neu5Gc feeding now allows for *in utero* and early life exposure models to be repeated, this time with higher levels of exposure to Neu5Gc, to test if such exposure to an immature immune system will have more definitive immunologic effects in adulthood.

My work has established the foundations for a large, multi-pronged murine Aging Study that is recently underway (Table 5-1). This study is using lifespan, hematology, and biomarkers of inflammation as metrics to assess the lifelong impact of dietary Neu5Gc and Neu5Gc-specific antibodies *in vivo.* (It should be noted that this study also involves humanizing aspects of Siglec biology [SiglecE -/-] to simultaneously study roles of Siglecs in aging.) In the Aging Study, all animals will ingest a soy chow (sialic acid-free) background to which Neu5Gc- (PSM) or Neu5Ac-containing (avian) submaxillary mucin (EBN) can be added, thus allowing us to precisely control intake of dietary sialic acid and asses any detriments associated with lifelong dietary Neu5Gc. By utilizing porcine (and human control) erythrocyte ghost immunizations, we will be able to test for boosting responses in animals on PSM chow versus EBN chow or soy chow alone. Although the dietary boosting response was first discovered in this work (Chapter 4), it will be important to abstract dietary Neu5Gc from other components of the ‘western diet’ to discern a Neu5Gc-specific boosting response. The soy-based

chow strategy in the Aging Study is an improvement in this regard as this chow is Neu5Gc-free and is not confounded by high-fat/high-cholesterol content. Although, the Aging Study will be able to compare animals on soy chow plus PSM with Neu5Gc- (porcine ghost-) or control- (human ghost-) immunization (Table 5-1, Groups 11 vs. 12), thus will be able to establish the need for a pre-existing Neu5Gc immune response in this boosting response, there is one missing aspect that should be pursued in parallel of the Aging Study. That is, immunizing two cohorts of *Cmah*$^{-/-}$ animals on soy chow, then maintaining in one cohort on soy chow while moving the second to soy chow plus PSM. This experimental setup will test the requirement of dietary Neu5Gc exposure in the boosting phenomenon.

Based on our cumulative data, the over-arching hypothesis is that the combination of dietary Neu5Gc and the Neu5Gc-specific antibody response plays a role in uniquely human disease predispositions[9]. Indeed, human lymphocytes seem to be over-reactive in head to head experiments with chimpanzee lymphocytes independent of the Neu5Gc-specific antibodies[10]. From an evolutionary context, humans are unusually susceptible to atherosclerosis, carcinomas, rheumatoid arthritis, and HIV progression to AIDS[11]. These diseases have definitive inflammatory components and human specific mechanisms for inflammation are particularly interesting in this context.

Interestingly, humans (Chapter 3), and now mice (Chapter 2), incorporate dietary Neu5Gc into vascular endothelium. We hypothesized that human Neu5Gc-specific antibodies interact with vascular Neu5Gc to promote vasculitis and play a role in the human predisposition to atherosclerosis. Experiments *in vitro* showed that Neu5Gc incorporates into vascular endothelial cells, which provides Neu5Gc-

containing antigens that bind human Neu5Gc-specific antibodies (Chapter 3). The antibodies are necessary and sufficient to drive a cell-independent inflammation of endothelium that deposits classical complement, engenders novel cell adhesion molecule expression, and leukocyte binding. Applied *in vivo*, these studies suggest that dietary Neu5Gc incorporation into vascular endothelium could initiate and/or propagate vascular inflammation and potentially exacerbate atherosclerosis.

To test the relevance of this mechanism *in vivo*, we exploited progress in Chapter 2 and Appendix I, to establish a mouse model of atherosclerosis in the *Cmah*, *Ldlr* DKO background. Surprisingly, Neu5Gc immunization conferred an atheroprotective effect in animals eating Neu5Gc-glycoprotein chow and the extent of atheroprotection correlated with Neu5Gc-specific IgG levels (Chapter 4). Although particularly unexpected, these results suggest two mutually exclusive possibilities. First, the atheroprotective role of Neu5Gc-specific antibodies in mouse is not physiologically relevant in humans. This could be due to an off target effect of the control (IO_4-rx chimpanzee erythrocyte ghost) immunization on atherosclerosis by generating some sort of cross-reactive response, although data on immunized mouse serum shows that it behaves in a predictable way. Alternatively, this result could be an artifact of the Neu5Gc-specific antibody response generated by the chimpanzee erythrocyte ghosts. Perhaps the chimpanzee erythrocyte ghost immunization failed to generate antibodies that have atherosclerosis relevance in humans? If so, one can envision swapping the chimpanzee erythrocyte immunization with another immunization strategy with more human-like properties.

If the human Neu5Gc-specific response is so complicated that a particular disease is correlated only with a subpopulation of antibodies, it may be advantageous to verify that human Neu5Gc-specific antibodies have relevance in a particular disease

context through epidemiological approaches before embarking on a complex mouse experiment. For atherosclerosis, it would be important that future work redress our EPIC-Norfolk cohort to study atherosclerotic relevance of Neu5Gc-specific antibodies. Complex populations of Neu5Gc-specific antibodies can be measured simultaneously in 2,625 patient serum samples using a glycan microarray approach (under development). In using this microarray, we would cast a wide net of Neu5Gc-containing glycans and we hope to associate subpopulations of antibodies with atherosclerosis in humans.

The second mutually exclusive possibility is that the result is relevant and indicates an incomplete understanding of Neu5Gc biology in atherosclerotic lesions. Intriguingly, atherosclerotic lesions are the only vascular sites in humans where Neu5Gc incorporates in a sub-endothelial pattern throughout the lesion. My dissertation has focused on the effects of dietary Neu5Gc incorporation and Neu5Gc-specific antibodies in endothelium, thus we have been biased in considering our mechanism as important in exacerbating the initiation or progression of atherosclerosis. Given my data, it is completely possible that dietary Neu5Gc incorporation into a lesion and/or the antibodies could have a dualistic role and actually inhibit development of advanced atherosclerotic lesions.

Interestingly, sialic acids on receptor tyrosine kinases (like TLR2 and TLR4) can affect receptor signal transduction, through a cell surface Neu1 sialidase mechanism[12,13]. That TLRs require sialidases to signal properly is particularly interesting because of the role the TLRs play in binding and uptake of LDL and oxidized LDL particles in lesion macrophages. It is plausible that dietary Neu5Gc incorporation onto these receptors is inefficiently processed by sialidases during signaling[14], which would impair proper TLR-based signal transduction. To model this

scenario *in vitro*, we used peritoneal macrophages from *Cmah*, *Ldlr* DKO mice, loaded them with Neu5Ac or Neu5Gc, and incubated them with aggregated human LDL to model the transition of macrophages to foam cells within an atherosclerotic lesion. Binding and uptake of LDL by macrophage TLR4 is associated with a pro-inflammatory response[15] that propagates lesion development by attracting more monocyte-derived macrophages to the lesion. As expected, *Cmah*, *Ldlr* DKO macrophages can incorporate Neu5Gc onto self-glycans if they encounter the sugar (Fig. 5-1B, solid black trace). Surprisingly, Neu5Gc-loaded (Fig. 5-1A, solid black trace) *Cmah*, *Ldlr* DKO macrophages sustain a weak proinflammatory TNFα response to aggregated LDL, compared to non-loaded (Fig. 5-1A, dotted gray trace) or Neu5Ac-loaded (Fig. 5-1A, solid gray trace) macrophages.

Although this example is difficult to fit into my current story, it is a perfect example of our ignorance of the effects of Neu5Gc incorporation and Neu5Gc-specific antibodies on other aspects of atherosclerotic lesion pathophysiology. Potential studies in this area could start by attempting to determine whether lesion Neu5Gc is present on macrophages, lipoproteins, or another cell type to help formulate hypotheses on how the Neu5Gc-specific antibodies would slow lesion development. *In vitro* pilot studies could include determining how Neu5Gc-specific antibodies affect lipoprotein uptake and/or oxidized LDL-based stimulation of Neu5Gc-loaded macrophages. It would be interesting if the Neu5Gc-specific antibody interaction with macrophages leads to reduced inflammatory activation and/or an impaired foam cell transition.

Although interesting, the results in Chapter 4 constitute an incomplete story about the role of dietary Neu5Gc and Neu5Gc-specific antibodies in atherosclerosis. Much work and repeated experiments need to be done to come to a firm conclusion with this animal model. Regardless, this dissertation establishes, for the first time, an animal model of the human condition with respect to Neu5Gc. Thus, the value of this work lies in generating this model of the human condition, where dietary Neu5Gc incorporation and Neu5Gc-specific immune responses can be combined in a controlled fashion *in vivo* to test the role of these variables in a variety of disease contexts.

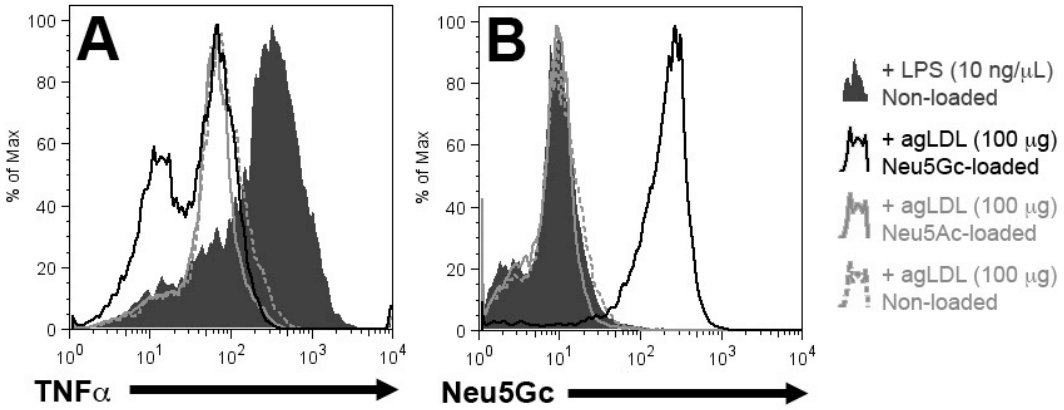

Figure 5-1. Cellular Neu5Gc Incorporation Dysregulates Biology Independent of Neu5Gc-specific Antibodies. Peritoneal *Cmah*, *Ldlr* DKO macrophages were isolated by injection of 3% Thioglycollate and peritoneal lavage 72 hours later. Cells were counted and cultured in RPMI + 10% human serum with 1 mM of the indicated sialic acid for 2 days. To stimulate, cells were incubated in 10 ng/μL LPS or 100 μg aggregated human LDL (aggregated by 2 minute vortex) for 2 days. **A.** Cells were stained with APC-conjugated anti-mouse TNFα antibody by intracellular staining using the Ctyofix/Cytoperm Kit (Becton Dickenson) according to the manufacturer's instructions. TNFα production in LPS-stimulated cells (shaded gray trace) shows a typical LPS-induced pro-inflammatory response. TNFα production in Neu5Gc-loaded cells shows the emergence of a $TNF\alpha^{lo}$ population. **B.** Cells were stained with αNeu5Gc IgY to visualize Neu5Gc incorporation onto cells. Neu5Gc-loaded cells (black trace) show extensive Neu5Gc incorporation, compared to non-loaded or Neu5Ac-loaded cells.

Table 5-1. Organization of an Aging Study to Investigate Lifelong Detriments Associated with Dietary Neu5Gc, Neu5Gc-specific antibodies and Siglec Loss. This table shows the group-based organization of a cohort of animals that is currently underway to study aging-related phenotypes of dietary Neu5Gc intake, Neu5Gc-specific antibodies, and Siglec E loss. For the purposes of this dissertation, interesting group comparisons will involve antibody responses (11 vs. 12 vs. 17, 14 vs. 15 vs. 16), mortality (11 vs. 12 vs. 17), effects of chronic dietary sialic acid (1 vs. 2, 5 vs. 6, 9 vs. 10, 13 vs. 14), effects of dietary Neu5Gc (9 vs. 10, 9 vs. 11, 13 vs. 14, 13 vs. 15).

Group #	Genotype	Diet	Immunization
1	Cmah +/+, SiglecE +/+	Soy Chow	Control
2	Cmah +/+, SiglecE +/+	Soy Chow + EBN	Control
3	Cmah +/+, SiglecE +/+	Soy Chow + PSM	Control
4	Cmah +/+, SiglecE +/+	Soy Chow + PSM	Neu5Gc
5	Cmah +/+, SiglecE -/-	Soy Chow	Control
6	Cmah +/+, SiglecE -/-	Soy Chow + EBN	Control
7	Cmah +/+, SiglecE -/-	Soy Chow + PSM	Control
8	Cmah +/+, SiglecE -/-	Soy Chow + PSM	Neu5Gc
9	Cmah -/-, SiglecE +/+	Soy Chow	Control
10	Cmah -/-, SiglecE +/+	Soy Chow + EBN	Control
11	Cmah -/-, SiglecE +/+	Soy Chow + PSM	Control
12	Cmah -/-, SiglecE +/+	Soy Chow + PSM	Neu5Gc
13	Cmah -/-, SiglecE -/-	Soy Chow	Control
14	Cmah -/-, SiglecE -/-	Soy Chow + EBN	Control
15	Cmah -/-, SiglecE -/-	Soy Chow + PSM	Control
16	Cmah -/-, SiglecE -/-	Soy Chow + PSM	Neu5Gc
17	Cmah -/-, SiglecE +/+	Soy Chow + PSM (0.1x reg. dose)	Neu5Gc

REFERENCES

1. Tangvoranuntakul, P. et al. Human uptake and incorporation of an immunogenic nonhuman dietary sialic acid. *Proc Natl Acad Sci U S A* **100**, 12045-12050 (2003).
2. Bode, L. Human milk oligosaccharides: prebiotics and beyond. *Nutr Rev* **67 Suppl 2**, S183-91 (2009).
3. Wang, B. et al. Dietary sialic acid supplementation improves learning and memory in piglets. *Am J Clin Nutr* **85**, 561-569 (2007).
4. Wang, B., Brand-Miller, J., McVeagh, P. & Petocz, P. Concentration and distribution of sialic acid in human milk and infant formulas. *Am J Clin Nutr* **74**, 510-515 (2001).
5. Morgan, B. L. & Winick, M. A possible relationship between brain N-acetylneuraminic acid content and behavior. *Proc Soc Exp Biol Med* **161**, 534-537 (1979).
6. Anderson, J. W., Johnstone, B. M. & Remley, D. T. Breast-feeding and cognitive development: a meta-analysis. *Am J Clin Nutr* **70**, 525-535 (1999).
7. Sloand, E. M. et al. Transfer of glycosylphosphatidylinositol-anchored proteins to deficient cells after erythrocyte transfusion in paroxysmal nocturnal hemoglobinuria. *Blood* **104**, 3782-3788 (2004).
8. Kitazume, S. et al. In vivo cleavage of alpha2,6-sialyltransferase by Alzheimer beta-secretase. *J Biol Chem* **280**, 8589-8595 (2005).
9. Varki, A. Colloquium paper: uniquely human evolution of sialic acid genetics and biology. *Proc Natl Acad Sci U S A* **107 Suppl 2**, 8939-8946 (2010).
10. Soto, P. C., Stein, L. L., Hurtado-Ziola, N., Hedrick, S. M. & Varki, A. Relative over-reactivity of human versus chimpanzee lymphocytes: implications for the human diseases associated with immune activation. *J Immunol* **184**, 4185-4195 (2010).
11. Varki, A. & Altheide, T. K. Comparing the human and chimpanzee genomes: searching for needles in a haystack. *Genome Res* **15**, 1746-1758 (2005).
12. Amith, S. R. et al. Dependence of pathogen molecule-induced toll-like receptor activation and cell function on Neu1 sialidase. *Glycoconj J* **26**, 1197-1212 (2009).
13. Amith, S. R. et al. Neu1 desialylation of sialyl alpha-2,3-linked beta-galactosyl residues of TOLL-like receptor 4 is essential for receptor activation and cellular signaling. *Cell Signal* **22**, 314-324 (2010).
14. Kitajima, K., Nomoto, H., Inoue, Y., Iwasaki, M. & Inoue, S. Fish egg polysialoglycoproteins: circular dichroism and proton nuclear magnetic resonance studies of novel oligosaccharide units containing one sialidase-resistant N-glycolylneuraminic acid residue in each molecule. *Biochemistry* **23**, 310-316 (1984).
15. Wiesner, P. et al. Low doses of lipopolysaccharide and minimally oxidized low-density lipoprotein cooperatively activate macrophages via nuclear factor kappa B and activator protein-1: possible mechanism for acceleration of atherosclerosis by subclinical endotoxemia. *Circ Res* **107**, 56-65 (2010).

APPENDIX I

Mouse Models that Mimic the Human *N*-glycolylneuraminic Acid-specific Xenoautoantibody Response

ABSTRACT

Work presented in Chapter 2 establishes that human-like incorporation of dietary Neu5Gc is experimentally possible *in vivo*. Although important, the human condition carries a second component: a diverse, polyclonal, sometimes high Neu5Gc-specific immune response. To more completely model the human condition in mice, it is necessary to combine both dietary Neu5Gc and Neu5Gc-specific responses, which will open up a variety of experimental avenues to investigate the role of Neu5Gc in complex pathophysiology. To date, scattered work has focused on mechanisms to generate and characterize Neu5Gc-specific immune responses in mice. This Appendix seeks to synthesize existing information on *Cmah*$^{-/-}$ Neu5Gc-specific antibody responses, describe recent progress with novel Neu5Gc-containing antigens, and discuss the pros and cons of all approaches to help future experimenters choose the best approach. This appendix will discuss the following strategies: Neu5Gc-loaded *Haemophilus influenza*; immunization with Neu5Gc-containing glycoproteins like mucins; immunization with Neu5Gc-expressing cells like thymocytes or erythrocytes; and immunization with novel Neu5Gc-KLH conjugates. This Appendix will discuss experiments designed to investigate the immunology underlying the murine Neu5Gc-specific response and touch upon assays to quantify these responses at the bench.

INTRODUCTION

All human adults have varying levels of circulating IgM, IgG and IgA antibodies against Neu5Gc[1,2]. At the same time, dietary Neu5Gc from foods such as red meat or milk products can be metabolically incorporated into human tissues, particularly epithelia and endothelia (Chapter 3, and [3-5]), through a mechanism likely involving macropinocytosis and delivery of Neu5Gc from the lysosome to the cytosol via a lysosomal transporter[6]. Thus, Neu5Gc-specific antibodies represent novel "xenoautoantibodies", which recognize a non-self, animal-derived xenoautoantigen in the context of "self". Indeed, we have recently demonstrated that human Neu5Gc-specific antibodies interact with metabolically incorporated Neu5Gc to promote chronic inflammation, likely contributing to tumor progression[5] and vascular inflammation (Chapter 3).

Given the progress presented in Chapter 2, we are moving closer to recapitulating the human condition of dietary Neu5Gc incorporation in the mouse. Through a physiologic approach, we have been able to detect incorporation of dietary Neu5Gc into target mouse tissues (Fig. 2-5) and cells (Fig. 2-6) after 3 and 4 week feeding periods with admittedly high dietary doses. Despite the difficulties associated with maintaining high doses of dietary Neu5Gc, it is now possible to design more complex animal models of human physiology/pathophysiology that include both diet and the immune response. This Appendix seeks to synthesize existing information on murine Neu5Gc-specific antibody responses, describe recent progress with novel Neu5Gc-containing antigens, and discuss the pros and cons of all approaches to help future experimenters choose the best approach. This appendix will discuss Neu5Gc-loaded *Haemophilus influenzae*, Neu5Gc-containing mucins, Neu5Gc-expressing thymocytes/splenocytes/erythrocytes from multiple species, Neu5Gc-KLH conjugates,

and advanced multi-component antigens on the horizon. This Appendix will touch upon assays to quantify these responses at the bench.

Recent work[7], partially presented in Chapter 4 (Fig. 4-1), investigated non-typeable *Haemophilus influenzae* (NTHi) as potential mechanism to generate Neu5Gc-specific antibodies in humans and in mouse. NTHi is a small, Gram-negative, non-encapsulated coccobacillus. Glycolipid molecules called lipooligosaccharides (LOS) are a major component of the outer membrane of NTHi. The non-repeating oligosaccharides found at the terminal ends of LOS include sialic acid attached to Galβ1–4Glc and Galβ1–4GlcNAc moieties, which resemble those found on human cell surface glycans. This molecular mimicry of host sialylated glycans confers protection against host immune defenses[8,9]. In fact, NTHi is dependent on sialic acid expression for human serum resistance[10,11], and for virulence in otitis media models[12]. However, NTHi is incapable of synthesizing its own sialic acid and therefore must scavenge exogenous sialic acid from the host[12]. Because NTHi also lacks a sialidase[11], sialic acid scavenged by NTHi must be present as a monosaccharide. Despite these biosynthetic limitations, NTHi was found to utilize Neu5Gc to sialylate its LOS. This approach combines antigen (Neu5Gc) and adjuvant (LOS) in one package for *in vivo* immunizations.

Chimpanzee erythrocyte ghosts have been previously used[5] as an antigen because of the high level of Neu5Gc on this cell type. Moreover, erythrocytes (or any other Neu5Gc-rich cell type), will contain Neu5Gc on a variety of glycans, glycoproteins, glycolipids, and in a variety of glycosidic linkages. Such antigenic heterogeneity is presumed to be an advantage in modeling the diversity of the human Neu5Gc-specific response. The erythrocyte ghost strategy was improved by implementing rigorous immunization controls, like related Neu5Gc-free (human) erythrocyte ghosts, periodate-treating or sialidase-treating intact chimpanzee

erythrocytes to rid the antigen of its Neu5Gc component. However, the robust response of periodate-rx ghost immunized animals to IO_4-rx-Neu5Gc may confound this control (Figs. 4-3B and 4-4B, bottom panel).

Exploiting the utility of antibodies in biological research has been a boon of progress in many experimental systems. Many groups have used animal immunizations to raise antibodies against a protein, peptide, or glycan of interest for subsequent use *in vitro* and *in vivo*. One heavily-used strategy is to conjugate a peptide of interest to an antigenic carrier protein, such as Keyhole Limpet Hemocyanin from *Megathura crenulata*[13]. The KLH monomer is a high molecular weight protein (~394 kDa) that exhibits an extensive degree of oligomerization and commercially-available KLH preparations approach 8 MDa. Because the native protein is antigenic in mammals, researchers have exploited aldehyde-based amine-amine reactions to conjugate a peptide of interest through the N-terminal end of the peptide to lysines on KLH, thereby conferring the antigenicity of KLH to unrelated peptide structures of interest. We will discuss conjugation of N-linked Neu5Gc-containing glycans to KLH for immunization.

Any antigen must be carefully chosen with an understanding of 1) its antigenic nature and its preparation, 2) the Neu5Gc specificity of a subsequent response, 3) any immunoglobulin isotype class switching of the response, and 4) the responder percentage. Finally, rigorously controlling for a complex physiologic response such as an immunization is equally as important as generating the response itself. Currently, the most successful immunizations are complex antigens (chimpanzee ghosts, porcine ghosts, ovine and porcine mucins), where rigorous controls are even more important.

We will also discuss some aspects of the mouse immunology and development that are important for antibody production. We attempt to model some scenarios involving Neu5Gc exposure (during mouse pregnancy, pup stages, and post-weaning

periods) and look for immunologic tolerization or sensitization of the Neu5Gc-specific response. Finally, we will draw on results presented in this dissertation to gain new perspective on the complex interplay between Neu5Gc exposure, dietary intake, and the Neu5Gc-specific immune response.

RESULTS & DISCUSSION

Although several Neu5Gc-containing antigens have been analyzed thus far, it is difficult to identify "the best antigen". Each strategy comes with pros and cons and it is important to understand them when choosing a strategy in the context of a proposed experiment. Thus far, the best strategies use Neu5Gc-expressing erythrocyte ghosts and porcine/ovine submaxillary mucins.

Dietary Neu5Gc alone is insufficient to elicit Neu5Gc-specific antibodies in *Cmah*$^{-/-}$ mice. The temporal correlation in humans (Fig 4-1A, B) between the appearance of Neu5Gc-specific antibodies and the introduction of animal-derived infant foods suggested that dietary Neu5Gc might represent the antigenic stimulus. However, despite consumption of 0.374 mg_{Neu5Gc}/kg*day in their regular chow, *Cmah*$^{-/-}$ mice did not spontaneously generate Neu5Gc-specific IgM or IgG antibodies after 6–9 months (Fig. 4-1A, B). In fact, as summarized in Table I-1, attempts to immunize *Cmah*$^{-/-}$ mice against Neu5Gc through the diet have been unsuccessful. These include: providing free Neu5Gc in the drinking water at 1 mg/ml for 12 weeks; cross-fostering *Cmah*$^{-/-}$ pups with wild-type mothers whose milk contains Neu5Gc (simulating cow's milk-based formula feeding in human infants); feeding with high-Neu5Gc content mucins; feeding with Neu5Gc-rich goat cheese; and oral gavage with cow's milk.

The Erythrocyte Ghost Immunization. Neu5Gc-expressing erythrocyte ghosts generate robust immune responses in a Freund's adjuvant-based immunization (Chapter 4 and [5]). The responses are polyclonal, of multiple isotypes, and have strict

Neu5Gc-binding specificity. The specificity of this response is demonstrated in antibody-antigen interactions that can be competed out with Neu5Gc, not Neu5Ac (not shown), and are sensitive to mild periodate treatment of targets in ELISA assays (Fig. 4-2B). Although chimpanzee erythrocytes have received the most attention, porcine erythrocytes also elicit a robust, class-switching response *in vivo* (Fig. I-1, A-IgM, B-IgG). Equine, rhesus monkey, and bovine ghosts did not elicit a class-switching response. Porcine blood is also commercially available in large volumes, which can be an important factor for large cohorts like the Aging Study (Chapter 5, pg. 154). Direct comparison of chimpanzee erythrocyte ghost and porcine erythrocyte ghost immunizations has not been performed and the subsequent immune responses are supposed to be similar. On a small scale the percentage of IgG responders is similar (around 60-75%) in both immunizations, although no work has looked at the binding specificity of reactivity raised by the porcine erythrocyte immunization.

Control Strategies for Erythrocyte Ghost Immunizations. Control strategies for the chimpanzee erythrocyte ghost immunization have also received the most attention thus far, although the strategies themselves (Neu5Gc-free related antigen, sialidase treatment, periodate-treatment) can often be translated into other antigen systems. The most straightforward strategy is to use human erythrocyte ghosts for control immunization (Fig. 4-2B). Expired human erythrocytes are available from local blood banks in large volumes for large studies. The rigor of the human ghost immunization is greatest for chimpanzee erythrocyte ghost immunizations because of the close evolutionary relationship between these two species. The human erythrocyte ghost immunization is being used as a control for the porcine erythrocyte ghost-based Neu5Gc immunization in the Aging Study (Chapter 5, pg. 154). It will be important to confirm that this control strategy does not result in any off-target effects to help guide future decisions about the rigor of the human erythrocyte ghost immunization control.

Sialidase treatment of intact chimpanzee erythrocytes is an option for removing Neu5Gc from the erythrocyte membrane, although pilot studies were unable to remove 100% of erythrocyte sialic acids with *Arthrobacter ureafaciens* sialidase treatment for 3 hours at 37°C (92% Neu5Gc removed). We speculated that remaining, sialidase-insensitive Neu5Gc was largely present on glycolipids, which are generally poor substrates for sialidases[14]. A sialidase-based strategy to remove Neu5Gc from erythrocytes will uncap terminal galactose and could generate anti-galacto-glycan antibodies. Such antibodies could potentially dysregulate galactose-binding proteins like the Galectins[15]. Despite these potential roadblocks, the sialidase strategy could be attractive, as immunization of $Cmah^{-/-}$ mice with the sialidase-treated erythrocyte ghosts described here generated an immune response that was not Neu5Gc-specific (not shown).

Mild sodium periodate treatment of intact erythrocytes is a good way to rid the chimpanzee erythrocyte ghost antigen of its Neu5Gc component. This reaction specifically attacks the C8-C9 carbon side chain of sialic acids and truncates its structure (IO_4-rx-Neu5Gc). IO_4-rx-Neu5Gc is chemically changed, but largely preserved, which has an important advantage in the context of a control immunization by maintaining sialic acid-independent antigenicity of the ghosts. One concern is if the mild periodate treatment is not as specific as we claim and generates other oxidized structures. Notably, immunization with periodate-treated chimpanzee erythrocyte ghosts yields antibody titers against IO_4-rx-Neu5Gc approximately one order of magnitude higher than Neu5Gc titers in parallel mock-treated chimpanzee erythrocyte ghost immunizations (Fig. 4-3B). Despite these observations, periodate-treated ghost-immunized serum has predictable binding patterns (or lack thereof) on healthy mouse tissues (Fig 4-3B, C). Also, immunized animals exhibited little signs of ill effects and no difference in mortality over the course of a 16-week hypercholesterolemic diet. Future

studies should keep a careful eye on ill effects in periodate-treated erythrocyte ghost immunized groups as a sign of off-target interactions.

Although periodate treatment of chimpanzee erythrocytes can oxidize 100% of cell surface Neu5Gc, it is important to note that erythrocytes from different species will yield different oxidization efficiencies. For example with porcine erythrocytes, it is difficult to convert more than 90% of native Neu5Gc into IO_4-rx-Neu5Gc despite reaction optimization. Although fresh periodate reagent and periodate:sample ratios are important tools to optimize oxidization efficiencies, increasing periodate concentration generates dark brown/black ghosts that aggregate. Thus far, longer treatment times and different reaction temperatures (other than room temperature) have been unsuccessful at improving oxidization efficiency for porcine erythrocyte ghosts.

The Neu5Gc-NTHi immunization. NTHi can efficiently scavenge minute amounts of environmental free Neu5Ac via a specific transporter[16,17], and then use an endogenous CMP-Sia synthetase[18] and sialyltransferases[19] to decorate its LOS. These sialylated LOS molecules are critical for NTHi human serum resistance[16,1816,18] and virulence in a chinchilla otitis media model[12,20]. We hypothesized that NTHi might scavenge exogenous Neu5Gc and express it as an immunogenic epitope, providing a mechanism for the generation of Neu5Gc-specific antibodies. To pursue this, we grew the NTHi strain 2019[21] in a sialic acid free medium and analyzed the bacteria by flow cytometry using a αNeu5Gc IgY antibody[22]. When NTHi strain 2019 was grown in sialic acid-free defined media, the αNeu5Gc IgY antibody background staining was similar to the control IgY, confirming the inability of NTHi to synthesize endogenous Neu5Gc (Sia-free NTHi, not shown). However, when exogenous free Neu5Gc (0.1 μM–1 mM) was added to the defined media there was a dose dependent increase in αNeu5Gc IgY binding (Neu5Gc-NTHi, Fig. I-2A).

To further confirm Neu5Gc incorporation by NTHi strain 2019 was grown in 1 mM Neu5Gc, treated with sialidase or heat-inactivated sialidase, and then probed in a whole-cell ELISA with the αNeu5Gc IgY. Sialidase treatment decreased αNeu5Gc IgY staining when compared to treatment with heat-inactivated sialidase, demonstrating sialidase-dependent release of Neu5Gc from NTHi surface glycans (Fig. I-2B).

To assess antigenicity, *Cmah*$^{-/-}$ mice were injected intraperitoneally with heat-killed Sia-free or Neu5Gc-NTHi. No adjuvant was used. Sia-free NTHi represents an ideal negative control because, aside for the absence of Neu5Gc, it is identical to Neu5Gc-NTHi. Indeed, only *Cmah*$^{-/-}$ mice injected with Neu5Gc-NTHi generated Neu5Gc-specific IgM antibodies and underwent class switching to generate Neu5Gc-specific IgG antibodies after 2–3 injections (Fig. I-3A, B). In contrast, *Cmah*$^{-/-}$ mice injected with Sia-free NTHi did not generate Neu5Gc-specific antibodies (Fig. I-3 A, B). Multiple attempts to elicit Neu5Gc-specific antibodies in *Cmah*$^{-/-}$ mice via intranasal administration of Neu5Gc-expressing NTHi have been unsuccessful (data not shown). The Neu5Gc-specific IgG antibodies generated in *Cmah*$^{-/-}$ mice were then tested for human-like specificity in ELISA and were found to be of similar titer and specificity as seen in human infants (Fig. I-3C) and adults[2].

Neu5Gc-NTHi thus appeared to be a great antigen for generating a Neu5Gc-specific immune response in *Cmah*$^{-/-}$ mice. One clear advantage was the lack of need for exogenous adjuvant as the heat-killed bacteria serve as their own adjuvant. Adjuvants introduce toxicity concerns and can affect biological phenomena, like atherosclerosis[23,24], but often cannot be avoided. A second advantage of Neu5Gc-NHTi is that this strategy has an ideal negative control, Sia-free NTHi. A third advantage is the strong, polyclonal Neu5Gc-specific response in multiple isotypes. The biggest problem with this strategy turned out to be its responder percentage. In October/November 2008, Neu5Gc-NTHi immunizations in a cohort of *Cmah*$^{-/-}$ animals

yielded class-switching IgG responses in 65% of animals. This experiment was called "Factory C" and was used as a source of Neu5Gc-specific mouse serum for *in vitro* and *in vivo* experiments. Pooled serum from this experiment forms the positive control bars presented in all ELISA-based Appendix figures. For unexplained reasons in all subsequent future experiments, only 5-25% of animals responded with class-switching to IgG isotypes, although those that responded did so at a similar magnitude to the pooled "Factory C" average. Despite optimizing immunization conditions, routes of administration, use of adjuvant, and decreasing Neu5Gc content of Neu5Gc-NTHi, we were unable to recapitulate earlier responses. In light of this drop-off, Neu5Gc-NTHi immunization is very impractical for most studies, although it is possible to immunize an excess of animals with Neu5Gc-NTHi and only group the responders for subsequent experimentation. In the future, it will be interesting to test if dietary Neu5Gc can induce class switching and a boosting response in animals that initially exhibited solely IgM responses after Neu5Gc-NTHi immunization.

Allogeneic, not syngeneic, thymocytes/splenocytes are weak antigens against Neu5Gc. In light of successes with Neu5Gc-containing cellular antigens (erythrocytes, Neu5Gc-NTHi) and in light of published work showing Neu5Gc-specific IgG and IgM responses in *Cmah*$^{-/-}$ *C57bl6/j* mice immunized against *Cmah*$^{+/+}$ *Balb/c* thymocytes (but not *Cmah*$^{+/+}$ *C57bl6/j* thymocytes) without adjuvant[25], we were interested to explore this strategy. In the published work, the authors reasoned that while both *C57bl6/j* and *Balb/c* thymocytes contained a foreign antigen (Neu5Gc), the syngeneic *C57bl6/j*-background thymocyte tolerized the immune response, whereas an allogeneic *Balb/*c background was different enough to generate a response. Regardless of strain background, immunizing with *Cmah*$^{-/-}$ cells to control for Neu5Gc-specific responses against *Cmah*$^{+/+}$ cells would be an ideal control, as the sole difference between these antigens is Neu5Gc expression. To expand on these data, we chose to repeat

published work, vary adjuvant to improve responses against C*mah*$^{+/+}$ *C57bl6/j* thymocytes, and include splenocyte immunizations to verify that a special cell type (thymocytes) is not required for this strategy.

First, *Cmah*$^{+/+}$ thymocytes/splenocytes (leukocytes) are very rich in Neu5Gc. Flow cytometric analysis of *Cmah*$^{+/+}$ thymocytes/splenocytes using αNeu5Gc IgY showed strong staining for Neu5Gc (Fig. I-4A, black trace). Also noteworthy, the cell isolation methods are gentle, as most of the cells (93.67%) are negative for propidium iodide staining after isolation (Fig. I-4B). However despite high Neu5Gc content, syngeneic C*mah*$^{+/+}$ *C57bl6/j* thymocytes did not elicit any Neu5Gc-specific response, neither with nor without adjuvant (Fig. I-4C). Interestingly, allogeneic C*mah*$^{+/+}$ *Balb/c* thymocytes mice did engender Neu5Gc-specific IgM with adjuvant, but not without adjuvant (Fig. I-4C). 1/4 and 0/4 animals from adjuvant-based immunizations against allogeneic *Balb/c* splenocytes and *Balb/c* thymocytes, respectively, exhibited class switching to IgG isotype (not shown). These results do not agree with published work[25]. This is likely because the assay that was used to detect antibody responses was different. Tahara *et al.* used a flow cytometric assay to detect immunized mouse serum binding to *Cmah*$^{+/+}$ thymocytes (the antigen itself). They reported an increase in binding after immunization as well as more binding than in *Cmah*$^{-/-}$ thymocytes. On the other hand, our assays use a cleaner system to test serum for sialic acid-specific binding using rigorous controls (competitive inhibition with Neu5Gc in ELISA, periodate treatment of ELISA targets). In immunizations, we always see increases in post-immune serum binding to any ELISA target (Neu5Gc or otherwise). It is important to confirm that a specific response exists rather than study a non-specific B-cell stimulation. Despite a relatively weak response seen with *Cmah*$^{+/+}$ *Balb/c* splenocyte immunization, this strategy could be attractive, perhaps with more boost injections or in an experiment where boosting responses through dietary Neu5Gc is expected. The

beauty in a splenocyte strategy lies in an optimal control immunization using *Cmah*$^{-/-}$ *Balb/*c splenocytes. Finally, splenocytes have the advantage of ease of isolation over thymocytes as 1-2*10^8 cells can be isolated from an adult spleen, whereas a thymus yields ~10^7 cells, and even less as animals age and the thymus shrinks.

These experiments gave interesting insight into how different an antigen needs to be to generate a robust immune response against Neu5Gc. In theory, Neu5Gc is foreign in humans and *Cmah*$^{-/-}$ mice, thus should be antigenic. In practice, even adjuvant is insufficient to generate a response against Neu5Gc-containing syngeneic antigens that present Neu5Gc in the context of self. Allogeneic antigens are more antigenic and do generate Neu5Gc-specific IgM, but again only when injected with adjuvant. In fact, the xenogeneic Neu5Gc-containing cellular antigens (chimpanzee/porcine erythrocytes and Neu5Gc-NTHi) generate the best Neu5Gc-specific responses. The general trend is that antigenicity of Neu5Gc-containing antigens increases as the genetic distance between the underlying cellular antigen and self increase.

Neu5Gc-expressing mucin immunizations. Several Neu5Gc-expressing mucins have been used (Darius Ghaderi, Varki Lab) in Freund's-based immunizations to generate a Neu5Gc immune response. These immunizations, with ovine submaxillary mucin (OSM) or porcine submaxillary mucin (PSM), resulted in a robust, periodate-sensitive IgG response against purified porcine submaxillary mucin ELISA targets (Fig. I-5). Moreover, 12/13 (92%) of the animals tested exhibited IgG responses in OSM immunizations, but only 11/13 (85%) were periodate sensitive. PSM and OSM are similar mucins from the submaxillary glands of livestock. Both contain Neu5Gc, but PSM contains 85-95% Neu5Gc whereas OSM is reported to have similar sialic acid content, but only ~10-15% Neu5Gc (D. Ghaderi, personal communication). It is

currently unclear how this difference affects subsequent immune responses as mucin immunization strategies have not received close attention.

Designing a control mucin immunization is straightforward, although untested. A Neu5Ac-rich salivary mucin from avian submaxillary glands (EBN, “Bird’s Nest”) is an excellent biochemical control for mucin structure, sialylation, and molecular weight. Alternatively, one could also envision periodate- or sialidase-treating porcine/ovine mucin to generate a negative control antigen.

Mucin immunizations are an attractive option, but for one drawback, which is that most experimental models will use porcine submaxillary mucin (PSM) to add Neu5Gc to the diet. One could envision unanticipated interactions between feeding a heterogeneous compound and immunizing against the same heterogeneous compound, then claiming the Neu5Gc dependence of any phenotypes. Although it is reassuring that Neu5Gc-specific IgG titers generated in mucin-based immunizations are periodate sensitive, any increase in Neu5Gc-indepdent reactivity in ELISA using the same antigen as an ELISA target would be a cause for concern.

Immunizations with Neu5Gc conjugated to KLH do not generate detectable Neu5Gc-specific responses. Despite the widespread usage of KLH-peptide conjugates for immunization against peptide antigens, several types of Neu5Gc-containing KLH-conjugates failed to elicit a response *in vivo*. Bovine fibrinogen (a bi-antennary Neu5Gcα2-6-containing glycoprotein) was protease digested and subjected to dialysis to retain glycopeptides and remove non-glycosylated peptides or amino acids (1,000 MWCO). Because of the success of the chimpanzee erythrocyte ghost immunization, chimpanzee erythrocyte ghosts were prepared and the protein pellet isolated by lipid extraction. The membrane proteins were protease digested and dialyzed as above. These preparations of Neu5Gc-containing glycopeptides were then conjugated to native KLH at varying stoichiometric ratios (bovine fibrinogen:KLH:: 6:1;

30:1; 300:1; chimp total protein extract:KLH:: 10:1, 100:1) through lysine-specific gluteraldehyde-based chemistry. These stoichiometric ratios were chosen to investigate what if any effect Neu5Gc multi-valence has in an anti-carbohydrate immune response.

We ascertained conjugation efficiency by centrifugal filtration (3,000 MWCO) to be approximately 86% efficient, that is to say only 14% of Neu5Gc was detected in the run-through fraction (Fig. I-6A). We immunized with 10 $\mu g_{conjugate}$ in a Freund's-based immunization, followed by 2 semiweekly boosts. Surprisingly, we detected essentially no immune response against Neu5Gc using Neu5Gcα2-3LacNAc-HSA as an ELISA target, neither IgMs (Fig. I-6B) nor IgGs (Fig. I-6C). The experiment was repeated, the second time immunizing with 50 $\mu g_{antigen}$ using specialty TiterMax adjuvant[26] and intramuscular injections. These variations also failed to yield detectable Neu5Gc-specific immune responses (not shown).

We conclude that Neu5Gc:KLH conjugates are not a good strategy for immunization. We do not appreciate the significance of the association of successful Neu5Gc immunizations and cellular antigens. We hypothesize that cellular Neu5Gc immunizations are successful because they present Neu5Gc in a heterogeneous fashion within an antigenic context of the plasma membrane. On the other hand, mucin-based immunizations are also successful, but are simply an acellular preparation of acid-precipitated mucin from salivary glands. It will be interesting to determine if a proposed, multicomponent antigen Neu5Gcα2-3LacNAc-MUC1(Tn)-Polio-Pam_3CysSK_4 can overcome barriers to immunization. This novel Neu5Gc-containing antigen contains a TLR2 ligand (lipid A) for leukocyte co-stimulation and the glycan is linked to a peptide with optimized bidning to mouse T-cell receptors. This multicomponent antigen has been previously used to generate robust responses against carbohydrates, like O-GlcNAc[27].

Passive serum transfer is an alternative for immunizations in short term animal models. With a successful immunization strategy, it is possible to generate Neu5Gc-specific antibodies in one mouse that can be harvested and purified for use in other mice. A syngeneic preparation of mouse Neu5Gc-specific antibodies can then be re-injected into naïve animals to rapidly introduce Neu5Gc-specific antibodies for various experimental purposes. Reports suggest that syngeneic serum rapidly enters the circulation and has slow turnover rates *in vivo* (Table 1-1). To quantify this turnover, we performed passive transfer of "Factory C"-derived Neu5Gc-specific antibodies (from Neu5Gc-NTHi immunization) in naïve *Cmah*$^{-/-}$ mice. Small bleeds were taken before and at 2, 4, 8, 14 days after passive serum transfer to minimize the loss of blood volume in this kinetic experiment. Neu5Gc-specific IgG were followed in ELISA using Neu5Gcα2-3LacNAc-HSA as an ELISA target because "Factory C" serum prefer Neu5Gcα2-3 and this target yielded the most reproducible results. Kinetics demonstrated a characteristic peak of reactivity in the serum at 2 days after passive transfer and decay thereafter, although detectable Neu5Gc-specific reactivity was present 2 weeks after transfer (Fig. I-7A). Based on these time points, it is unclear when the remaining reactivity at 2 weeks would return back down to initial levels. By normalizing titer variability between animals by the peak reactivity level at 2 days after transfer, we were able to construct a decay curve from which to ascertain the half-life of these antibodies *in vivo*. The half-life of passively transferred syngeneic IgG is about 7.0 days. Passive serum transfer can be a powerful method to experimental models that require temporal and dosing control over Neu5Gc-specific antibodies responses, especially in light of the inter-animal variability of most Neu5Gc immunizations. However, the short half-life of passively transferred serum makes it prohibitive in long and large animal experiments. ~50 mouse*days (1 mouse * 7 day

experiment = 7 mouse*days) is a reasonable upper bound for animal experiments where passive serum transfer is manageable.

Mouse development, antigen exposure, and the Neu5Gc immune response. The maturity of the immune system and the route of antigen exposure can have important consequences to subsequent immune responses. Due to the human fetal[4], placental[28], and now fetal mouse (Chapter 2, pg. 53-54) incorporation of dietary Neu5Gc, there are likely scenarios where a developing fetus encounters Neu5Gc while the immune system is still immature. Thus, it is important to understand what, if any, effect early exposure has on the adult Neu5Gc-specific immune response.

Current efforts to model these scenarios have yielded mixed results. To model fetal Neu5Gc exposure, we bred *Cmah*$^{-/-}$ males with *Cmah*$^{+/-}$ females. Resultant littermates (*Cmah*$^{+/-}$ and *Cmah*$^{-/-}$) phenotype as equally Neu5Gc expressing at birth, showing that pups are exposed to maternal Neu5Gc *in utero*. Nonetheless, *Cmah*$^{-/-}$ mice born to *Cmah*$^{+/-}$ mothers can still mount an Neu5Gc-specific response in Neu5Gc-NTHi immunizations as adults (Fig. I-8A,B). After one immunization and two boosts, *Cmah*$^{-/-}$ mice from *Cmah*$^{-/-}$ mothers generated a statistically similar response as *Cmah*$^{-/-}$ mice from *Cmah*$^{+/-}$ mothers in both IgM (A) and IgG (B) isotypes, suggesting that although *Cmah*$^{-/-}$ from *Cmah*$^{+/-}$ mothers encountered Neu5Gc in early life this is not sufficient to affect the adult immune system. In an evolutionary context, this indicates that *Cmah*$^{-/-}$ born to *Cmah*$^{+/-}$ parents could have immediately mounted an immune response, if challenged. It is unclear what significance this might have had for hominid evolution, although current hypotheses suggest that *Cmah*$^{-/-}$ humans with an active Neu5Gc-specific immune response could have been protected from Neu5Gc-expressing bacteria and viruses. Pathogens can acquire Neu5Gc in Neu5Gc-expressing reservoirs (animals or *Cmah*$^{+/-}$ parents), thus setting up a mechanism

whereby the immune response against Neu5Gc could have protected *Cmah*$^{-/-}$ humans from pathogen transmission.

Cross-fostering experiments, where *Cmah*$^{-/-}$ animals were immunized against chimpanzee erythrocyte ghosts after exposure to Neu5Gc through a surrogate mother's Neu5Gc-expressing milk also showed variable results. While repeating these studies, we observed statistically significant and insignificant sensitization to Neu5Gc immunization in the IgM isotype (Fig. I-8C, $p = 0.04$), but not the IgG isotype (Fig. I-8D, $p = 0.25$) in cross-fostered *Cmah*$^{-/-}$ animals. Although a trend towards sensitization to Neu5Gc immunization in cross-fostered animals was consistent, these data should be interpreted with caution. It is likely that Neu5Gc-exposure through breast feeding is not sufficient to cause immunologic tolerance or sensitization in Neu5Gc immunizations. Although milk does contain Neu5Gc, it is 2-5 times less by weight than in beef[4]. Perhaps immunologic tolerization or sensitization might result from animals on a higher dose of dietary Neu5Gc. Interestingly, feeding studies in developing animals with mothers on Neu5Gc-glycoprotein chow (Fig. 2-8, pg. 56) showed more extensive Neu5Gc incorporation throughout the body than seen in adult animals on the same chow. Thus, comparing Neu5Gc-specific immune responses between animals on a high Neu5Gc- or Neu5Gc-free diet during early life (pregnancy, development, early adulthood) is an interesting future experiment.

Neu5Gc-immunized animals eating a Neu5Gc-rich diet exhibited a strong boosting response of the IgG isotype over the course of the diet (Fig 4-4A). IgM, the only other isotype tested, also exhibited a boosting effect, but to a weaker extent (Fig. 4-4B). It is remains to be tested if other isotypes (IgA, IgE, IgD) and other tissue fluids (uterine fluid, gastrointestinal secretions) exhibit similar trends. Considering a potential sensitization to Neu5Gc immunization in cross-fostered animals, it is tempting to hypothesize that dietary Neu5Gc plays a sensitizing role and may underlie the ubiquity

of Neu5Gc-specific immune responses in humans. Several experiments need to be conducted to confirm this hypothesis, but the mouse model is an attractive avenue to pursue future work. Although it would be ideal to look for Neu5Gc-specific responses in humans who have completely avoided dietary Neu5Gc (e.g., lifetime vegans with mothers that were vegan during pregnancy), these groups are difficult to find and difficult to trust, given the spectrum of food products with trace amounts of Neu5Gc. However in the mouse, it is reasonable to breed and raise *Cmah*$^{-/-}$ animals on a sialic acid-free chow (Soy Chow, #110751/#110951, Dyets, Inc.). Developing pups with immature immune systems can be exposed to dietary Neu5Gc during pregnancy by feeding pregnant animals. Young animals with maturing immune systems can be exposed through the mother's milk during growth and weaning. Finally, adult animals with mature immune systems can be exposed to dietary Neu5Gc through direct feeding. Dietary Neu5Gc can be maintained long term or be pulsed sporadically in any of the above scenarios. Immunizations can be introduced before or after dietary exposure.

Much work could be done in this versatile model to systematically understand the tempo of dietary Neu5Gc on Neu5Gc immune responses *in vivo*, but experiments should be carefully selected with relevance to the human condition. Currently, three topics are particularly interesting. First, it is imperative to understand the variables that lead to immunologic sensitization to Neu5Gc through the diet and both dose and exposure term deserves immediate attention. Well-controlled immunization cohorts on soy chow and Neu5Gc-containing chow (potentially with high and low levels of dietary Neu5Gc) can be followed semi-weekly to assess the kinetics of the response. Once kinetics are established, the experiment can be tweaked to ascertain the minimum amount (dose, term) of dietary antigen to produce a response. Also, the dietary antigen can be removed to observe any changes in the response magnitude.

The second topic of interest involves high levels of dietary Neu5Gc exposure to a developing fetus for subsequent immunization. I hypothesize that if Neu5Gc is present in tissues when leukocytes with reactivity to self antigens are selected for apoptosis, Neu5Gc-reactive clones may be purged from the immune repertoire. The experimental details may be complicated (e.g., correct time point/dose at which to introduce dietary Neu5Gc to a maturing immune system to affect subsequent responses), but it is tempting to start by maintaining dietary exposure to Neu5Gc throughout pregnancy, weaning and early adulthood before Neu5Gc immunization. It will also be interesting to see if dietary exposure to Neu5Gc only during pregnancy engenders an immunologic phenotype in adulthood. If successful, dietary exposure can be changed to investigate changes in immunologic phenotypes.

The final topic involves swapping the order of dietary Neu5Gc exposure and Neu5Gc immunization. In a scenario where immunization comes before dietary Neu5Gc, dietary Neu5Gc sensitizes the response. Currently, I hypothesize introducing dietary Neu5Gc to an adult animal before subsequent immunization will not sensitize the Neu5Gc immune response, compared to animals maintained on a control diet. In fact, it is possible that this scenario could engender tolerization by introducing a novel antigen to the immune system through the diet[29]. Because Neu5Gc is present in infant formula/foods and immunization mechanisms through Neu5Gc-NTHi are possible early in life[7], it is difficult to know which comes first in humans. Both scenarios may have physiologic relevance.

Detecting Neu5Gc-specific antibodies in ELISA format. Regardless of the effort put into determining an optimal immunization strategy, it is important to discuss detection methods for Neu5Gc-specific immune responses. First and foremost, it is crucial to pick an assay and stick with it. This will minimize moving parts in studies with unknown outcomes, thus making the whole body of your work more cohesive and

comparable. Thus, give considerable thought to many aspects including (ELISA format, ELISA targets, antibody binding controls, quantitative standards, positive, and negative controls) and pick wisely.

The first decision to make is between ELISA and glycan microarray formats. The glycan microarray format is a very interesting format to track ~50 physiologic Neu5Gc-containing glycans simultaneously. Moreover, this format is quantifiable through standards that are present on the microarray slide with the glycans. However, there are several drawbacks to the glycan microarray. These include cost per array and time required for analysis. Currently, the glycan microarray is not tailored to exploratory assays (e.g., characterizing individual responses from a cohort of individuals immunized with a novel antigen), but is more of a complete analysis tool once a response needs complete characterization. ELISAs on the other hand are cheap and easier to analyze since the experimenter is restricted by ELISA targets (discussed below). ELISAs are also amenable to periodate-based treatments of ELISA targets to control for antibody binding specificity. In my opinion, ELISAs should be considered as the best assay for characterizing Neu5Gc-specific responses with the glycan microarray serving an adjunct function for in depth analysis of binding specificity.

The second decision to make (if choosing an ELISA format) is 96- versus 384-well ELISA format. All mouse Neu5Gc-specific antibody data presented here (except for Fig. I-2, I-3, and I-5) were carried out in the 384-well format. The 384-well ELISA is superior in many ways to the 96-well format. A well from a 384-well plate has ¼ of the surface area of a well from a 96-well plate. This reduces the amount of ELISA targets that are necessary to saturate the well by 75%. This is crucial only for the Neu5Gc-HSAs, which are not commercially available and likely will not be synthesized by our collaborator (Xi Chen) in the future. Throughout the ELISA protocol, the reagents

needed (including mouse serum) to perform the test are substantially minimized. The 384-well plate allows many samples, time points, conditions to be sampled on *n* 384-well plates, instead *5n* 96-well plates (including quantitative standards to allow for normalization of signals between 96-well plates). New users can find the small wells on the 384-well plate difficult to use at first, although small-motor hand-eye coordination improves over time. Also the use of a solid, off-white contrast surface will greatly help visualizing wells that are empty or filled.

The next decision to make is the ELISA targets to which to test antibody binding. Neu5Gcα2-3LacNAc-HSA and Neu5Gcα2-6LacNAc-HSA are important ELISA targets that have been chemo-enzymatically synthesized to add a physiologic Neu5Gc-containing glycan to a Neu5Gc-free carrier molecule (human serum albumin, HSA). These targets come in α2-3 and α2-6 glycosidic linkages, and are linked to a common disaccharide unit, LacNAc. This preparation has been synthesized to have multiple Neu5Gc-containing glycans per HSA molecule. Stoichiometric analysis determined that Neu5Gcα2-3LacNAc-HSA and Neu5Gcα2-6LacNAc-HSA have ~15 and ~18 glycans/HSA (not shown). Compared to other Neu5Gc-rich ELISA targets, these targets give a relatively low signal, but help ascertain broad specificity of an Neu5Gc-specific response (e.g., “2-3 versus 2-6”).

Two other important ELISA targets are porcine submaxillary mucin and chimpanzee serum. PSM is a high molecular weight, mucin-type O-GalNAc glycan that is dominantly Neu5Gcα2-3GalNAc (Neu5Gc-Tn antigen) with some other more complex glycans[30]. Neu5Gc-specific signals against PSM as an ELISA target are very strong, thus helpful for assaying weak responses. Chimpanzee serum is another high-density Neu5Gc-containing target. Chimpanzee serum will contain Neu5Gc in a variety of physiologic linkages, but mostly Neu5Gcα2-6 on N-glycans. Essentially any Neu5Gc-containing glycan or cell can be considered as an target in ELISA, though a

pilot experiment should be done to determine the saturating concentration of a perspective target using αNeu5Gc IgY to detect a curve of coated target. In general, multivalent targets will improve the sensitivity of a target for weak Neu5Gc-specific responses.

Several necessary antibody specificity controls have been established in the 384-well format. In general, it is important to avoid using related, Neu5Gc-free targets in ELISA (e.g., Bird's Nest as a control for PSM, or human serum as a control for chimp serum) due to unpredictable, non-specific binding of serum samples to the control targets. Periodate-treatment of ELISA targets is the preferred control for Neu5Gc-specific antibody binding specificity. The periodate treatment of ELISA targets has been optimized for use in 384-well plates and is consistent from assay to assay. The periodate treatment can be easily co-opted for use, unchanged, in the 96-well ELISA format. The periodate treatment is an excellent control to knockdown sialic acid-dependent serum binding by chemically destroying Neu5Gc from the ELISA target after the target has been coated on the plate. This control will knockdown 75-95% of IgG signals, but does not commonly knock down IgM signals by more than 50% (sometimes none). We hypothesize that Neu5Gc-specific IgM binding to ELISA targets is less sensitive to periodate treatment due to low affinity, high avidity of IgMs.

Competitive inhibition of serum binding with Neu5Ac and Neu5Gc (or α-2-methyl derivatives Neu5Ac2me and Neu5Gc2me) is another way to confirm Neu5Gc-specific antibody binding. Pilot studies have shown Neu5Gc, not Neu5Ac, will abolish both IgG and IgM binding to background levels (not shown). To accomplish this, free sialic acid monosaccharide must be used high concentrations (10-50 mM) to compete with antibody-antigen interactions, although 10 fold lower concentrations can be used with the α-2-methyl (2me) derivatives. The main drawback to competitive inhibition in ELISA is the cost of using 10-20 $mg_{free\text{-}Neu5Gc}$ (1-2 $mg_{Neu5Gc2me}$) for a single ELISA

experiment. Until Neu5Gc is cheap and essentially unlimited, periodate treatment of ELISA targets before serum incubation should be the gold standard control for Neu5Gc-specific antibody binding.

The only current problem for the 384-well ELISA is working within the standard curve's range of signal development. The IgG standard curve is linear from 0.6 – 20 ng_{IgG}, below which signals are at background levels and above which signals begin to saturate. Despite this saturation at the top of the curve, the standard curve develops slowly and serum signals are often outside of the standard range, especially for signals developed in PSM- or chimpanzee serum-coated wells. To establish the standard in 384-well ELISAs, binding curves must first be done. Second, pilot assays with known sera binding to many targets need to be carried out to determine if standard antibody dilutions need be increased to slow signal development towards that of the standard curves. Today, one can compare 2 384-well plates by running a dilution series of a known, positive control serum on each plate to generate standard curves that have little quantitative meaning but allow signals from different plates to be normalized into one dataset. More in depth information on these types of assays can be found in my notebooks.

MATERIALS AND METHODS

Mice. *Cmah*$^{-/-}$ mice were backcrossed onto a congenic *C57BL6/j* background. Wild-type *C57BL6/j* and *Balb/c* mice were purchased from Harlan Laboratories (Indianapolis, IN). Mice were fed standard chow (LabDiet, PicoLab Rodent Diet 20, #5053) and water *ad libitum* and maintained on a 12-hour light/dark cycle. *Cmah*$^{-/-}$ animals were maintained on a Neu5Gc-free soy chow (Dyets Inc.) as desired to control dietary Neu5Gc exposure. Cross-foster experiments were carried out by fostering a day 1 Cmah$^{-/-}$ pup to a *Balb/*c mother. Foster moms were generally receptive and

would accept 1-5 pups depending on their own litter size. After 21 days, cross- and normal-fostered *Cmah*$^{-/-}$ littermates were weaned back together onto standard chow for eventual immunization at 8-12 weeks of age. All animal work was performed in accordance with The Association for Assessment and Accreditation of Laboratory Animal Care (AAALAC) and under a protocol approved by the Institutional Animal Care & Use Committee of the University of California, San Diego.

The erythrocyte ghost immunization. Erythrocyte immunizations were performed as described previously[5]. Briefly, *Cmah*$^{-/-}$ mice (age 6−9 weeks, male and female) were injected intraperitoneally with 200 μg chimpanzee (Neu5Gc-rich; Yerkes National Primate Research Center), porcine (Neu5Gc-rich; Pelfreeze Biologicals), or human (Neu5Gc-free) erythrocyte membrane ghosts in 100 μl PBS with equal volume Freund's complete adjuvant (Difco), and boosted twice semi-weekly with the same amount of antigen in Freund's incomplete adjuvant (Difco). Serum for antibody analysis was collected 7 d after the second boost as below (in "**The Neu5Gc-NTHi immunization.**").

Chimpanzee erythrocyte ghost preparation. Performed as described previously (Chapter 4, pg. 124 under the above heading). Protocols were not changed significantly to prepare ghosts from rhesus (Yerkes Primate Foundation), porcine, bovine, and equine whole blood (Pel-freeze Biologicals), other than ghosts were spun at 20,000 rcf for 10 minutes during lysis to help pelleting of porcine ghosts.

Bacteria and growth conditions. NTHi strains 2019 and 2019*siaT* were a generous gift from Michael Apicella, Department of Microbiology, University of Iowa. Sialic acid-free bacterial stocks were prepared by passaging 2019 several times in sialic acid-free media: RPMI 1640 media (Sigma) supplemented with 1 μg/ml protoporphyrin IX (Sigma), 1 μg/ml L-histidine (Sigma), 10 μg/ml β-Nicotinamide adenine dinucleotide

(Sigma), 0.1 mg/ml hypoxanthine (Sigma), 0.1 mg/ml uracil (Sigma), and 0.8 mM sodium pyruvate (Gibco). The absence of sialic acid was confirmed by HPLC and mass spectrometry.

Neu5Gc uptake by NTHi. NTHi strain 2019 or 2019*siaT* grown to mid-log (OD_{600}~0.3−0.4) in sialic acid-free media, was grown for 2 h with or without various amounts of Neu5Gc (Inalco), washed twice with PBS, and then incubated for 1 h at RT with chicken anti-Neu5Gc IgY (1:2,000), control chicken IgY (1:2,000; Jackson ImmunoResearch), or PBS alone. After washing once with PBS, bacteria were resuspended in Fluorescein isothiocyanate (FITC) donkey anti-chicken antibody (1:200; Jackson ImmunoResearch) for 1 h at RT and analyzed by flow cytometry (FACSCalibur, BD Biosciences). For uptake of Neu5Gc from baby food, each food was diluted with an equal volume of sialic acid-free media and the particulate matter pelleted by centrifugation. Following filter sterilization, the filtrate was added to an equal volume of mid-log bacteria in sialic acid-free media, incubated shaking (250 RPM) for 2 h at 37°C, washed twice with PBS, and stained for Neu5Gc by flow cytometry, as described above. Sialidase treatment following Neu5Gc loading of NTHi was performed by resuspending 500 μl (OD_{600} 0.4) in 150 μl PBS, pH 6.0 + 9 mM $CaCl_2$ with 10 mU active or heat-inactivated (10 minutes at 100°C) *Vibrio cholerae* sialidase (Sigma) for 3 hours at 37°C. Neu5Gc was detected in a whole-cell ELISA by resuspending the bacteria in Milli-Q water, adding to a 96-well plate (Costar), and evaporating overnight. Wells were washed with Tris Buffered Saline, pH 7.4 + 0.1% Tween (TBST), and then incubated with chicken anti-Neu5Gc IgY (1:1,000), isotype control chicken IgY (1:1,000), or TBST alone for 1 h at RT, 100 μl/well. Wells were then washed three times with 150 μl TBST, incubated with 100 μl/well alkaline phosphatase (AP) donkey anti-chicken IgY (1:5,000; Jackson ImmunoResearch) for 1

h at RT, washed as before and then developed with *p*-nitrophenyl phosphate, with product measured at 405 nm wavelength on a SpectraMax 250 (Molecular Devices).

The Neu5Gc-NTHi immunization. NTHi strain 2019 was grown to mid-log in sialic acid-free media with or without 1 mM Neu5Gc (Inalco), heat-killed, and injected (200 μl of OD_{600} 0.4) intraperitoneally into *Cmah*$^{-/-}$ and wild-type (C57BL/6) mice (age 5−8 weeks, female). All mice were injected a total of three times at two-week intervals. No adjuvant was used with any of the bacterial injections. Serum for antibody analysis was collected 7 d after the second boost via puncture (Goldenrod Animal Lancets) of the right submandibular (cheek) pouch into an uncoated capillary tube (Fisher Scientific) for storage in a serum Microtainer (Becton Dickenson). After clotting, the serum was spun at 10,000 rcf for 2 minutes and the serum was aliquoted and stored at -20°C.

Neu5Gc-KLH Conjugate Immunization. Human and bovine fibrinogen (Sigma Aldrich) was digested in 5 mg/ml proteinase K added twice in 100 mM TrisHCl, pH 8.0 at 56°C over two nights. Also, a total protein extract from human and chimpanzee ghosts was prepared by sequential 10:10:1::$CHCl_3$:MeOH:sample extractions and dried down. The pellet was then digested as above. Digests were boiled to deactivate the protease and dialyzed in a 1,500 MWCO membrane (Spectrum Laboratories) to remove small amino acids and peptides, but retain sialylated glycopeptides. These were lyophilized, then resuspended and quantified by DMB-HPLC, as described previously (Chapter 2, pg. 42, under **Quantification of…Neu5Gc by DMB-HPLC.**).

Keyhole limpet hemocyanin (EMD Biosciences) was maintained in the 10 mM $MgSO_4$ solution for stability and conjugated to a known molar amount of glycopeptides using 0.1% gluteraldehyde. Conjugation efficiency was quantified by DMB-HPLC of retentate and run-through fractions from centrifugal filtration through a 3,000 MWCO filter (Millipore). To immunize, 100 μL of 0.10 μg/μL antigen was mixed with 100 μL Fruend's adjuvant and injected intraperitoneally, as above. Animals were boosted

twice, semi-weekly. A subsequent experiment tried 50 µg antigen for immunization, followed by 2-10 µg boosts semi-weekly, injected intramuscularly. Serum for antibody analysis was collected 7 d after the second boost as above (in "**The Neu5Gc-NTHi immunization.**").

Thymocyte isolation and immunization. Thymocytes and splenocytes were isolated from young (< 6 weeks) *Cmah*$^{+/+}$ *C57bl6/j* and *Cmah*$^{+/+}$ *Balb/c* mice. Thymocytes/splenocytes were isolated from the thymus/spleen by macerating the lymphoid follicle on a 70 µm cell strainer. Cells were washed thrice in warm RPMI by centrifugation at 500 rcf for 5 minutes, counted, and resuspended in PBS for injection at 10^8 cells/mL. 100 µL of cells were emulsified with 100 µL Fruend's adjuvant for injection. Animals were immunized, then boosted regularly. Serum for antibody analysis was collected 7 d after the first and second boost as above (in "**The Neu5Gc-NTHi immunization.**").

Neu5Gc levels of *Balb/c* splenocytes were visualized for flow cytometry, as described previously (Chapter 2, pg. 47, under **Detection of Cell Surface Neu5Gc by Flow Cytometry.**). Cells were stained with propidium iodide using 10 µg, which was added only just prior to running the sample on the cytometer.

Detection of Neu5Gc-specific antibodies in mouse serum. Performed as described previously (Chapter 4, pg. 126) for 384-well ELISAs. Figures I-2, -3, -7A,B were generated with data from 96-well ELISA. Briefly, 96-well plates (Costar 9018) were coated overnight at 4°C with 250 ng/well Neu5Gcα-PAA in 50 mM sodium carbonate-bicarbonate buffer, pH 9.5. Wells were emptied of coating solution and blocked with 200 µl/well TBS + 0.1% Tween, pH 7.4 (TBST) for 2 h at RT. Sera were added to the wells for 2 h at RT in triplicate, diluted 1:200 in 100 µl TBST. After washing three times with 150 µl TBST, wells were incubated with 100 µl alkaline phosphatase conjugated

goat anti-mouse IgM (Calbiochem) or IgG (Jackson ImmunoResearch), diluted 1:5,000 in TBST for 1 h at RT. Wells were washed again, as described, developed with *p*-nitrophenyl phosphate, and absorbance was measured at a 405 nm wavelength on a SpectraMax 250 (Molecular Devices). Alternatively, mouse Neu5Gc-specific antibodies against Neu5Gc α2–6 or α2–3 linked to Galβ1–4Glcβ-HSA, or Galβ1–4GlcNAcβ-HSA (synthesized as described previously[31]) were detected by ELISA, as described above, using pooled sera from mice injected with NTHi strain 2019 grown in 1 mM Neu5Gc, as described above. Antibody levels were quantified after subtracting the readings obtained from coating with HSA alone.

Statistics. Statistical analysis was performed using Prism v5.0a (GraphPad Software; San Diego, CA).

ACKNOWLEDGEMENTS

We thank Dr. Michael Apicella for generously providing the NTHi 2019 strains. Many thanks to Rachel Taylor for our fruitful collaboration to develop the 384-well ELISA, without which I wouldn't have accomplished nearly as much. Chimpanzee blood samples were provided by the Yerkes National Primate Research Center.

Appendix I, in part (Fig. I-2, -3, Table I-1), is a reprint of the material as it appears in *Taylor RE, Gregg CJ, Padler-Karavani V, Ghaderi D, Yu H, Huang S, Sorensen RU, Chen X, Inostroza J, Nizet V, & Varki A, J Exp Med 207:1637-1646, 2010*. The dissertation author was the primary author and Dr. Ajit Varki directed and supervised the research that forms the basis of this chapter.

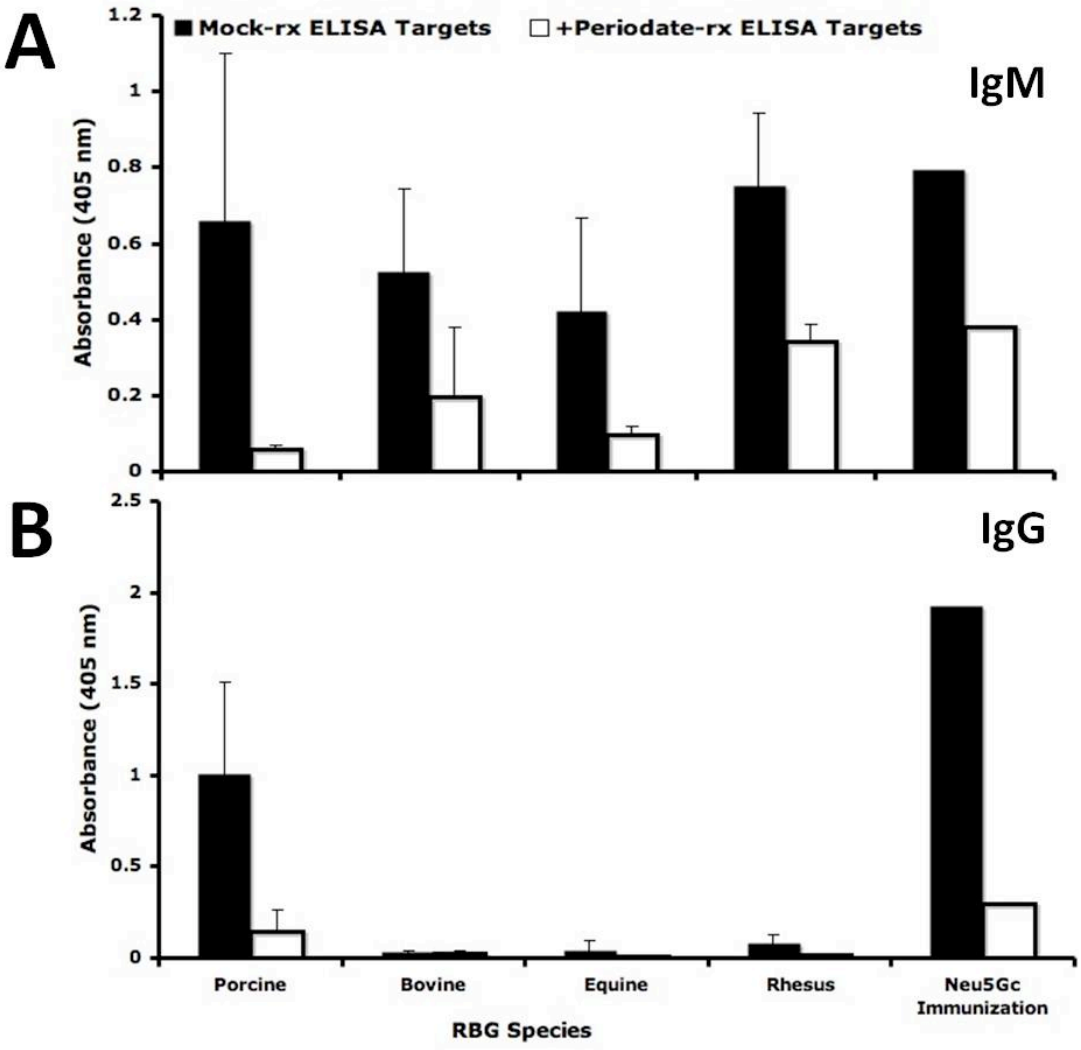

Figure I-1. Immunizing *Cmah*$^{-/-}$ Mice with Erythrocyte Ghosts Lead to Variable Neu5Gc-specific Responses. *Cmah*$^{-/-}$ animals on Neu5Gc-free chow were immunized with the indicated species' erythrocyte ghosts in a Freund's-based immunization, which produced IgM (A) and IgG (B) reactivity to Neu5Gcα2-3LacNAc-HSA. All species' ghost immunizations generate periodate sensitive IgM reactivity to Neu5Gc that were comparable to the positive control levels (see "Neu5Gc immunization" which is Neu5Gc-NTHi immunization). Only porcine (and chimpanzee, not shown here) ghosts result in IgG class switching. Data are representative of a single pilot experiment and show the mean of quadruplicate absorbance values at OD_{405} +/- standard deviation.

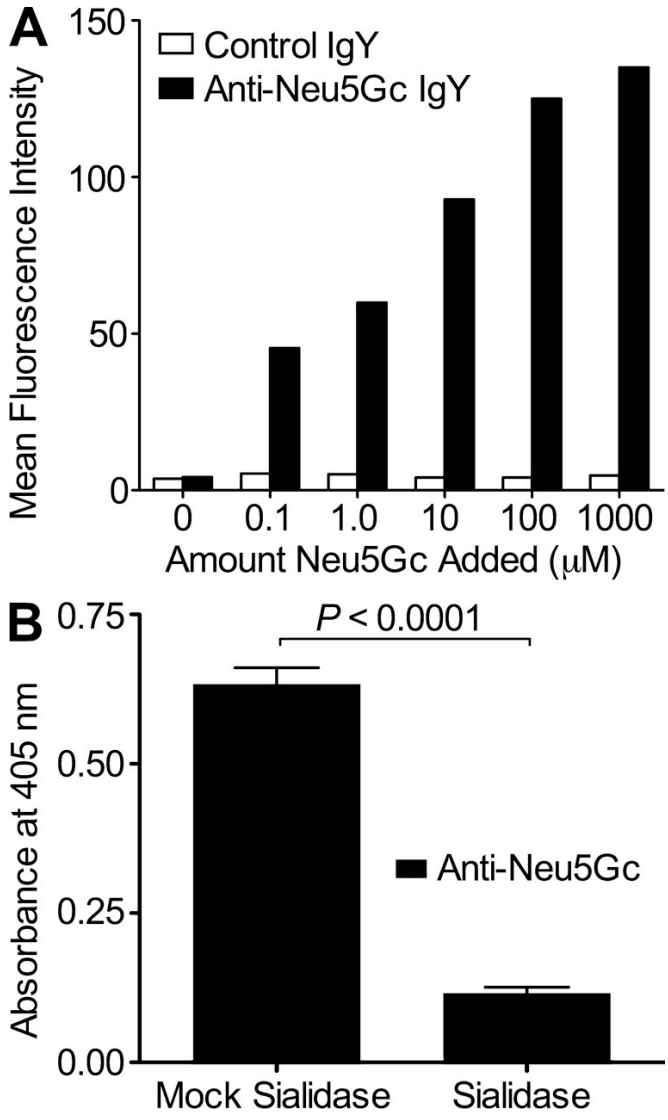

Figure I-2. NTHi can Efficiently Take Up and Incorporate Neu5Gc. A. Dose dependent uptake and expression of NTHi (2019) grown in a sialic acid-free defined media with 0.1 μM–1 mM Neu5Gc. Neu5Gc was detected by flow cytometry analysis using a chicken anti-Neu5Gc IgY antibody. **B.** 2019 grown in 1 mM Neu5Gc were treated with sialidase (sialidase) or heat-inactivated sialidase (mock sialidase) and probed with a chicken anti-Neu5Gc IgY antibody in a whole cell ELISA. Data are representative of at least three independent experiments and show the mean of triplicate absorbance values at OD_{405}. Error bars represent standard deviation. Experiment performed by Rachel E Taylor[7].

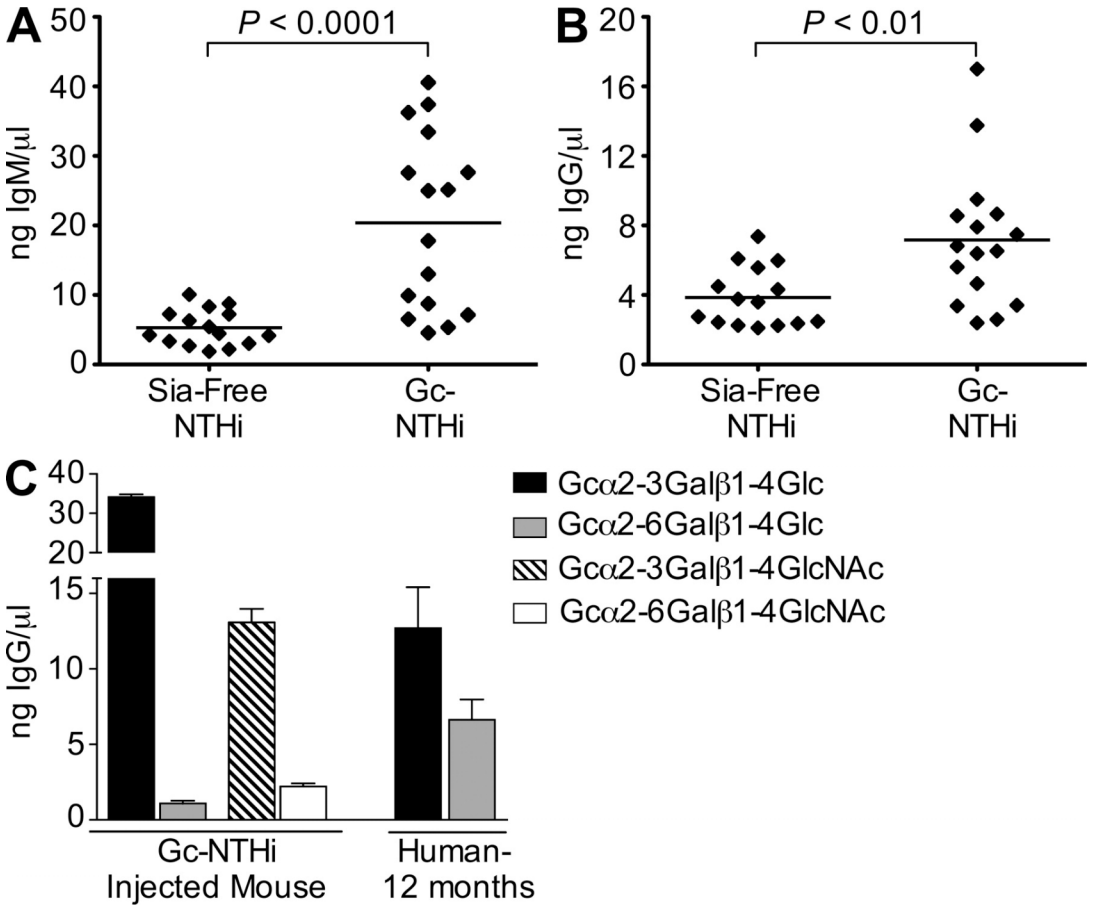

Figure I-3. Neu5Gc Expressed on NTHi Induces Neu5Gc-specific Antibodies in *Cmah*$^{-/-}$ Mice. A,B. *Cmah*$^{-/-}$ mice were injected intraperitoneally with heat-killed NTHi (without adjuvant) which had been grown in sialic-acid free media (Sia-free NTHi, *n*=16) or with sialic-acid free media with 1 mM Neu5Gc (Neu5Gc-NTHi, *n*=17). All mice were injected a total of three times at two week intervals. Sera collected following the third injection were analyzed by ELISA for IgM (A) and IgG (B) antibodies against Neu5Gcα-PAA. The highest and lowest value from each group was removed prior to graphing. Horizontal lines represent the mean values. Statistical analysis was performed using an unpaired one-tailed Student's *t*-test. **C.** Pooled mouse serum from mice injected intraperitoneally with heat-killed NTHi grown in sialic-acid free media with 1 mM Neu5Gc was analyzed in an ELISA for levels of Neu5Gc-specific IgG antibodies against Neu5Gcα2–3Galβ1–4Glcβ-HSA (black bar), Neu5Gcα2–6Galβ1–4Glcβ-HSA (gray bar), Neu5Gcα2–3Galβ1–4GlcNAcβ-HSA (white hashed bar), and Neu5Gcα2-6Galβ1-4GlcNAc-HSA (white bar). Values represent mean IgG levels, quantified according to a mouse IgG standard curve. Error bars represent ST. DEV.. For comparison, serum from 12 month old infants (*n*=15) was analyzed for levels of Neu5Gc-specific antibodies against Neu5Gcα2–3Galβ1–4Glcβ-HSA (black bar), Neu5Gcα2–6Galβ1–4Glcβ-HSA (gray bar) (same data as shown in Figure 4-1B). Values represent mean IgG levels, quantified according to a human IgG standard curve. Error bars represent standard error of the mean. Data are representative of at least three independent experiments.

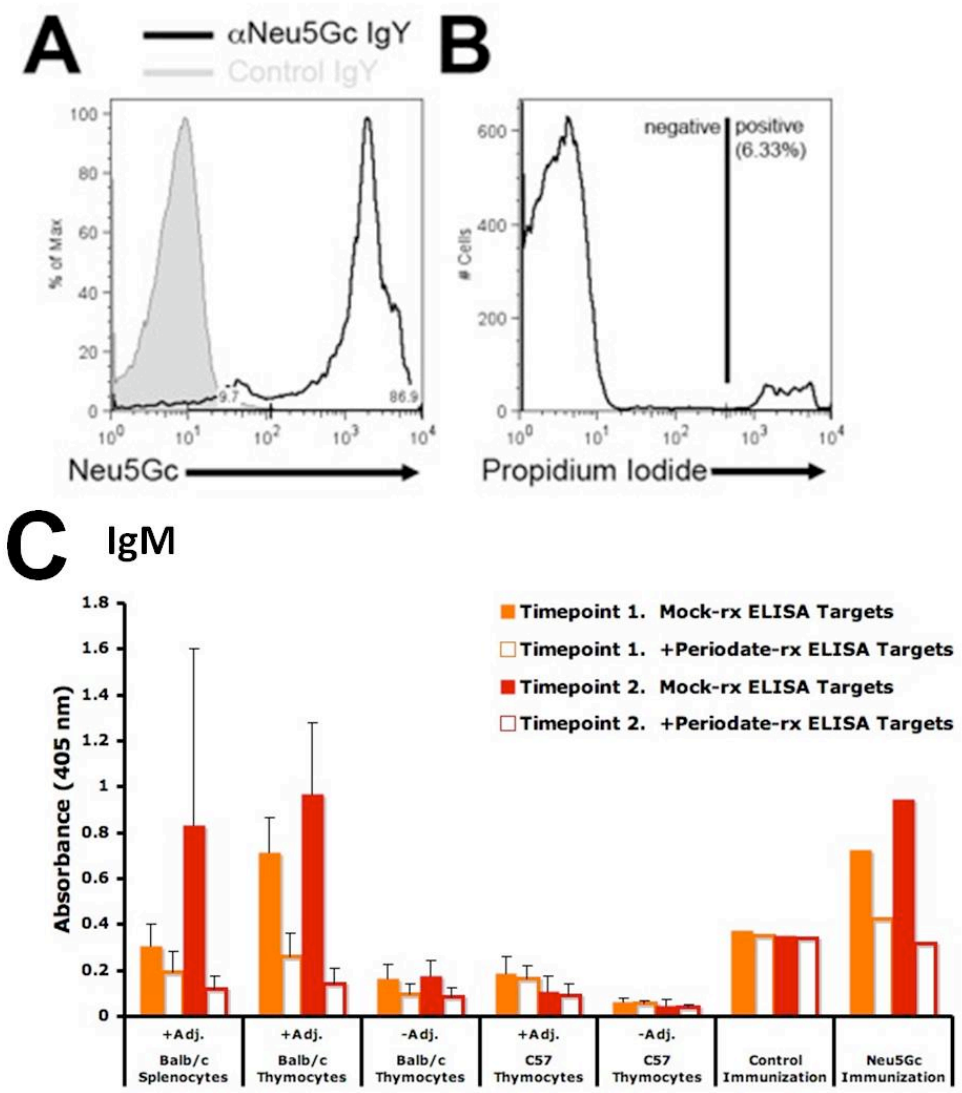

Figure I-4. Syngeneic Neu5Gc-containing Antigens Fail to Generate Neu5Gc-specific Responses. A. Splenocytes (shown) and thymocytes are rich in Neu5Gc, as detected with αNeu5Gc IgY (black trace) in flow cytometry. A control IgY (gray trace) shows the background level of staining in these cells. **B.** Splenocyte isolation is a gentle process. Propidium iodide fluoresces upon DNA intercalation in cells with compromised membranes and only 6.33% of cells stain. Thus the cell isolation procedure does not result in massive cell death or hemorrhaging of intracellular antigens during immunization. **C.** IgM responses detected against Neu5Gcα2,6LacNAc-HSA in ELISA from *Cmah*$^{-/-}$ mice immunized against 10^7 cells (as indicated) and boosted once with 10^7 cells (Timepoint 1) or boosted thrice with 10^7 cells (Timepoint 2). "+/-Adj." indicated whether (+Adj.) or not (-Adj.) Fruend's adjuvant was used during immunization/boosts. –Adj. groups were immunized with the same number and volume of cells, diluted in PBS. The data are cohort averages from groups of 4-5. "Control Immunization" and "Neu5Gc Immunization" are serum from Sia-free NTHi and Neu5Gc-NTHi immunization, respectively. Data are presented as mean +/- standard deviation.

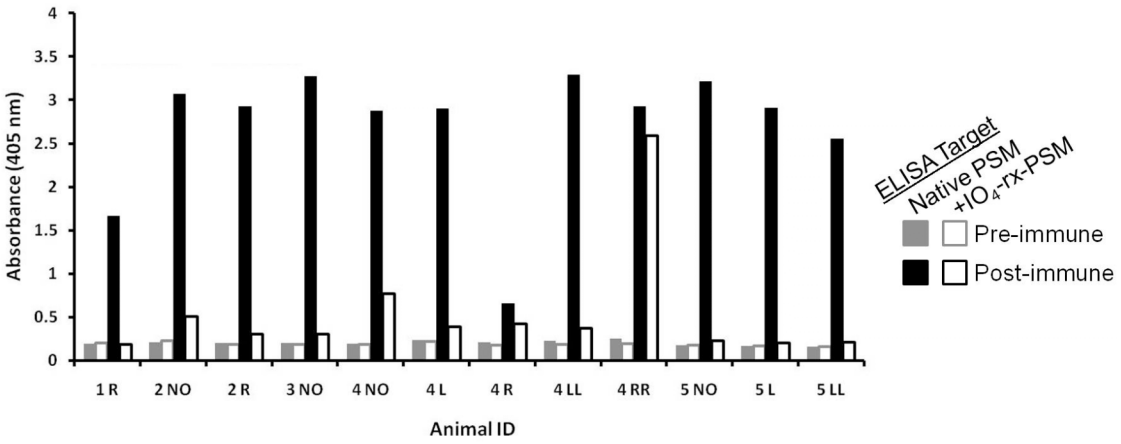

Figure I-5. Neu5Gc-containing Mucins Generate a Neu5Gc-specific Immune Response. *Cmah*$^{-/-}$ animals were injected with 100 µg of ovine submaxillary mucin intraperitoneally in a Freund's-based immunization. Animals were boosted thrice every two weeks. 7 days after the last boost, serum levels of periodate Neu5Gc-specific IgG were easily detectable in almost the entire cohort. 4RR exhibited a perdiodate-insensitive, albeit strong post-immune response. 4R exhibited a weak periodate sensitive post-immune response. The ELISA was repeated twice and this figure is representative. Immunizations and ELISA analysis were performed by Darius Ghaderi.

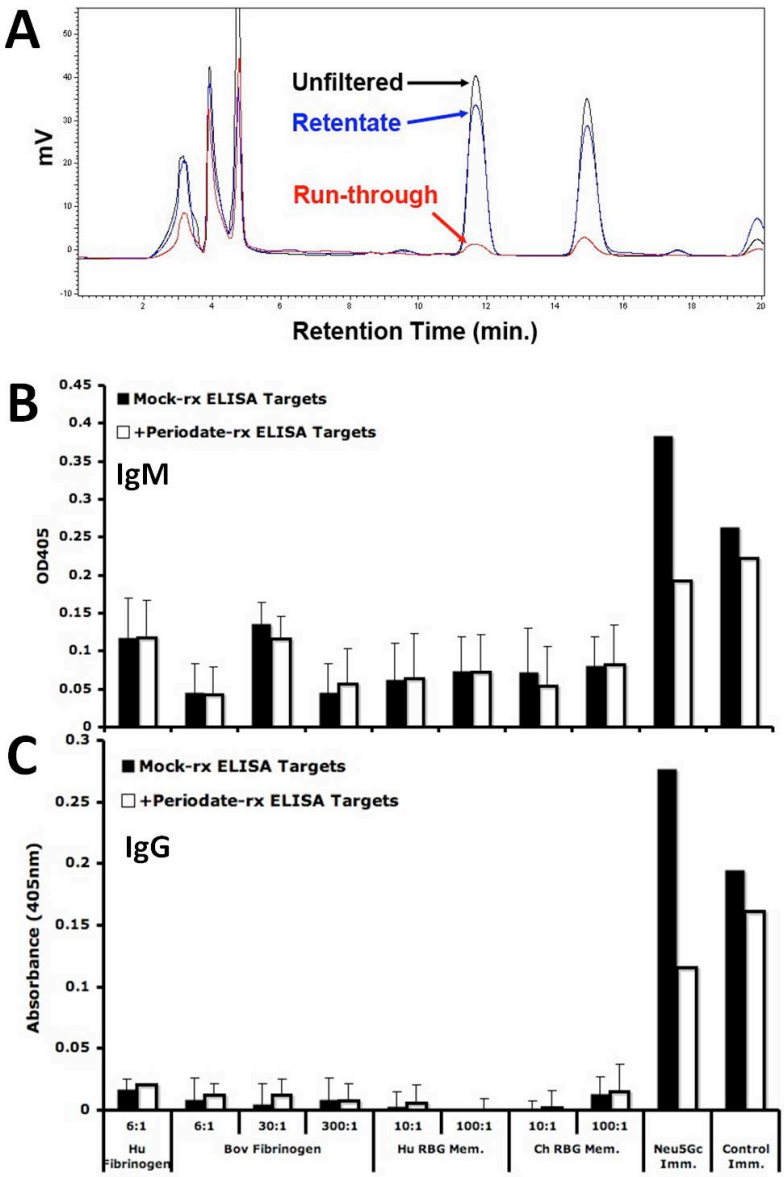

Figure I-6. Neu5Gc-KLH Conjugates Fail to Engender Neu5Gc-specific Immune Responses in Freund's-based Immunization. Glycoproteins were prepared from bovine and human fibrinogen, as well as from total protein extracts of human and chimpanzee RBC membranes. These glycoproteins were conjugated to native KLH for immunization **A.** Centrifugal filtration (3,000 MWCO) was used to assess what percentage of Neu5Gc was unconjugated in the run through (red trace) or conjugated in the retentate (blue trace). Unfiltered sample (black trace) shows the total Neu5Gc content of an equivalent amount of sample before filtration. **B, C.** Subsequent Neu5Gc-specific immune responses against Neu5Gc:KLH conjugates. IgM (B) and IgG (C) titers were tested in animals after an immunization and 2 boosts. There was no evidence of Neu5Gc-specific (e.g., periodate sensitive) antibodies generated by the Neu5Gc:KLH conjugates. "Control Immunization" and "Neu5Gc Immunization" are serum from Sia-free NTHi and Neu5Gc-NTHi immunization, respectively. Data are presented as mean +/- standard deviation. A variation of this experiment was repeated with similar results.

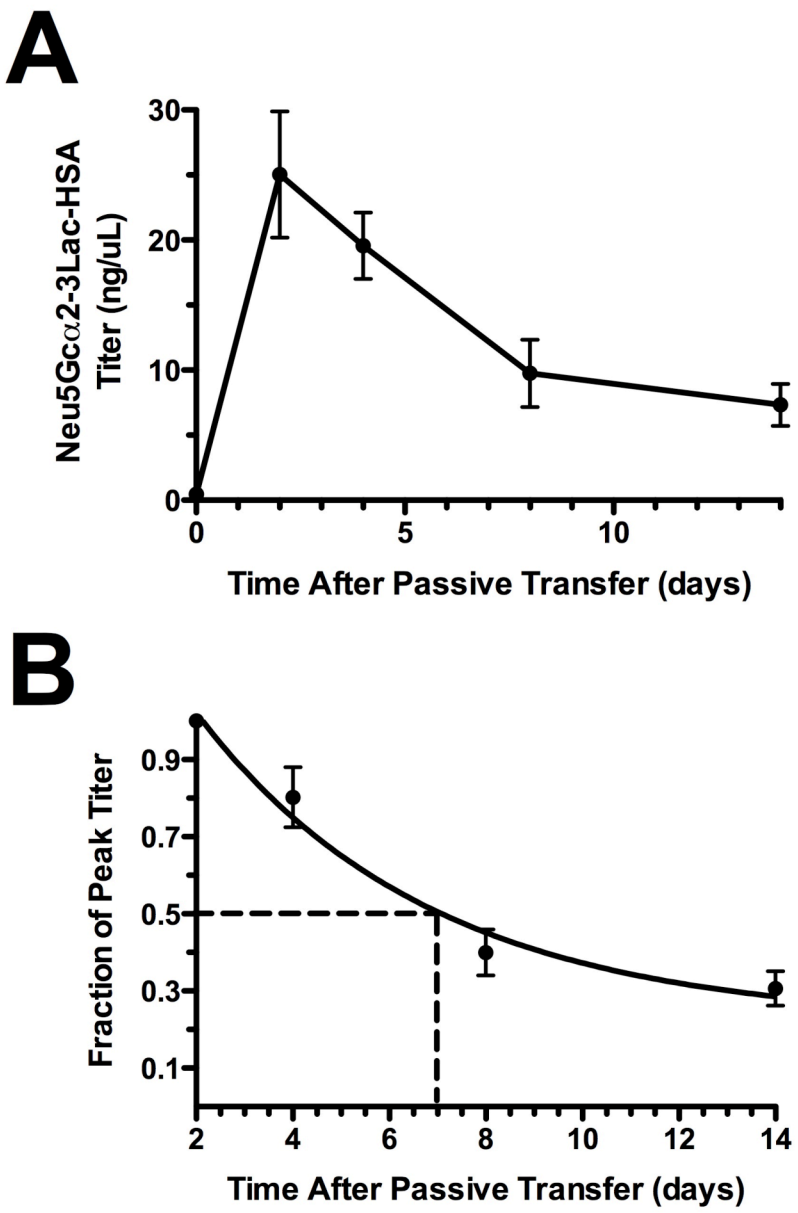

Figure I-7. Kinetics of Passively Transferred Neu5Gc-specific IgG in Naïve *Cmah*$^{-/-}$ Mice. A. ~25 µL of serum (55 $\mu g_{serum}/g_{body\ weight}$) from Neu5Gc-NTHi (Factory C) immunizations were injected intraperitoneally into naïve *Cmah*$^{-/-}$ mice. Small 25-50 µL submandibular bleeds were used to follow Neu5Gc-specific IgG in circulation at 0, 2, 4, 8, and 14 days after passive serum transfer. Serum was tested in triplicate for reactivity against Neu5Gcα2-3LacNAc-HSA in ELISA. Signals were standardized using a linear curve of murine IgG standard in triplicate on the same ELISA plate. Data are presented as a cohort average titer (n=5 animals). **B.** Each animal's peak titer (at 2 days after transfer) was used to normalize subsequent values. The values decay to a similar fraction of peak signal, a background signal that is somewhat variable from mouse to mouse. This decay evinces single exponential kinetics with $t_{1/2}$ ~ 7 days. Data are presented as mean +/- standard deviation.

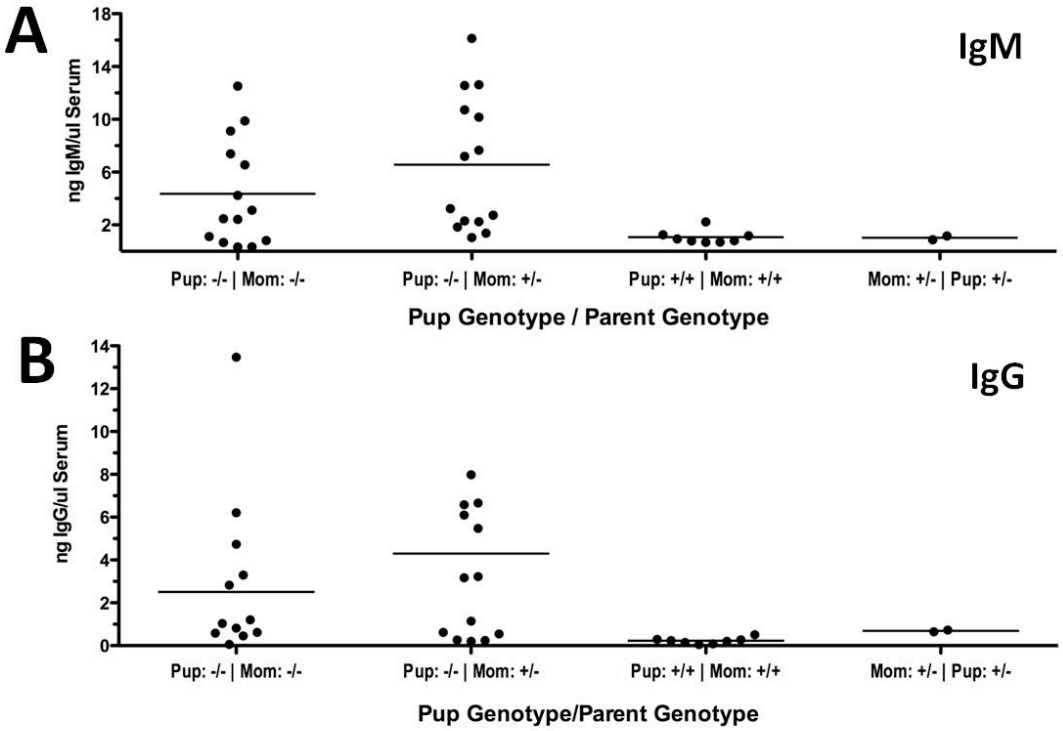

Figure I-8. Neu5Gc Exposure in Early Life and Neu5Gc Immunizations. A,B. *Cmah*$^{-/-}$ pups were born to *Cmah*$^{+/-}$ or *Cmah*$^{-/-}$ moms, thus the former was exposed to Neu5Gc *in utero*. Animals were immunized against Neu5Gc as adults using Neu5Gc-NTHi. After two boosts, serum ELISAs were performed to measure Neu5Gc-specific IgM (A) and IgG (B) against Neu5Gc-PAA as an ELISA target. *Cmah*$^{-/-}$ animals born to *Cmah*$^{+/-}$ pups will mount a response against Neu5Gc. Data are presented as a mean with the scatter visible.

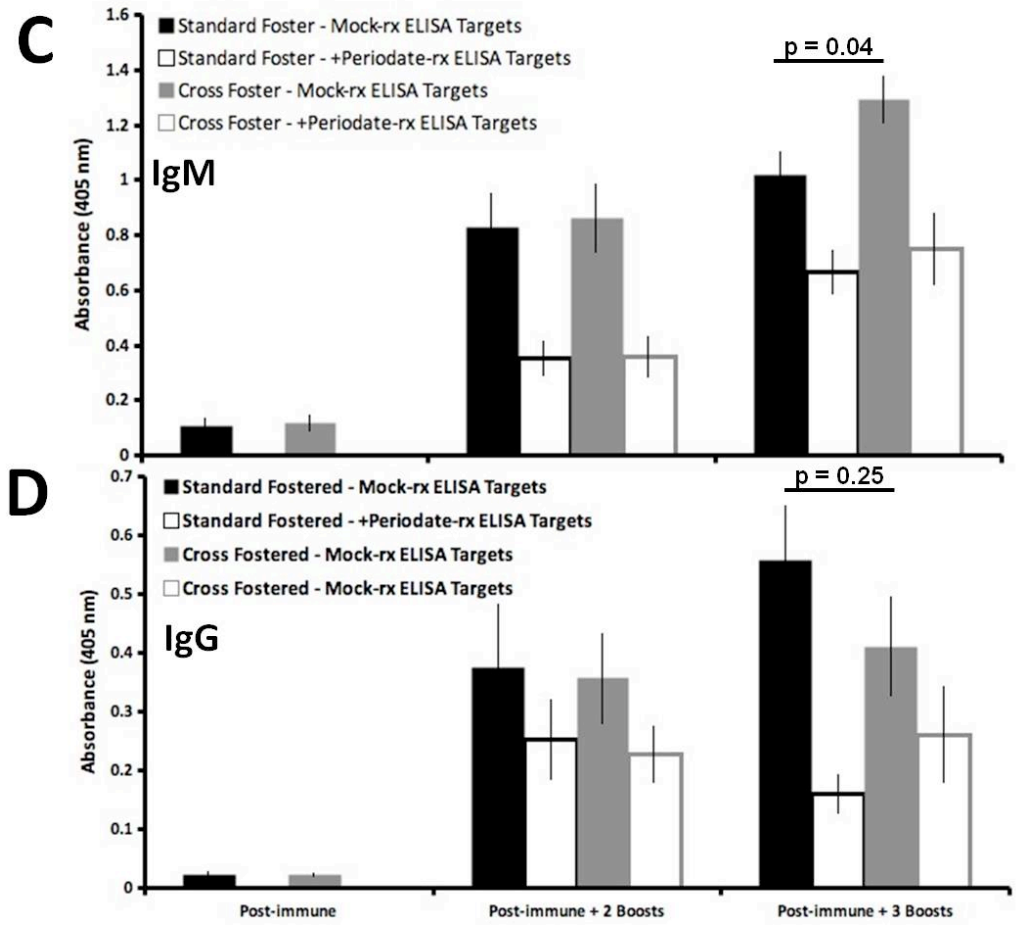

Figure I-8, cont'd. Neu5Gc Exposure in Early Life and Neu5Gc Immunizations. C,D. Day 1, *Cmah*$^{-/-}$ littermates were left intact (standard fostered) or cross-fostered onto a *Balb/c* surrogate mother. The animals were weaned together and maintained on a standard chow. Animals were immunized as adults with chimpanzee erythrocyte ghosts. IgM (C) and IgG (D) levels are shown against Neu5Gcα2-3LacNAc-HSA, 7 days after immunization (left category), 7 days after 2-semiweekly boosts (middle category), or 7 days after 3-semiweekly boosts. The data are presented as cohort averages +/- standard deviation (n=8).

Table I-1. Unsuccessful Attempts at Generating Neu5Gc-specific Antibodies in *Cmah*$^{-/-}$ Mice.

Strategy	Data/Comments
Feeding Standard Mouse Chow	Standard lab diet contains 0.39 mg_{Neu5Gc}/kg*day.
Adding Free Neu5Gc to Drinking Water	Maximum exposure 1 mg/ml*day in drinking water for 12 weeks.
Feeding Cow's Milk	Cow's milk contains ~ 8 μg/g total Neu5Gc[44]. Gavaged 250 μl 5 d/week for 4 weeks.
Feeding Goat Cheese	Rich in Neu5Gc-containing glycolipids, 39.9 μg/g total Neu5Gc[4]
Feeding Mucin	Mixed with standard chow plus 1.25 wt% cholesterol for 8 weeks at ~0.5 mg_{Neu5gc}/day.
Cross-Fostering *Cmah*$^{-/-}$ pups to *Balb/c* females	Wild-type mouse breast milk contains Neu5Gc. Simulates infant exposure to cow's milk/infant formula.
In utero Neu5Gc exposure of *Cmah*$^{-/-}$ pups to *Cmah*$^{+/}$ mother	*Cmah*$^{-/-}$ mice born loaded with Neu5Gc, which clears within 2 weeks. Simulates infant/fetal exposure to Neu5Gc through the mother's diet.

REFERENCES

1. Zhu, A. & Hurst, R. Anti-N-glycolylneuraminic acid antibodies identified in healthy human serum. *Xenotransplantation* **9**, 376-381 (2002).
2. Padler-Karavani, V. et al. Diversity in specificity, abundance, and composition of anti-Neu5Gc antibodies in normal humans: potential implications for disease. *Glycobiology* **18**, 818-830 (2008).
3. Hedlund, M. et al. N-glycolylneuraminic acid deficiency in mice: implications for human biology and evolution. *Mol Cell Biol* **27**, 4340-4346 (2007).
4. Tangvoranuntakul, P. et al. Human uptake and incorporation of an immunogenic nonhuman dietary sialic acid. *Proc Natl Acad Sci U S A* **100**, 12045-12050 (2003).
5. Hedlund, M., Padler-Karavani, V., Varki, N. M. & Varki, A. Evidence for a human-specific mechanism for diet and antibody-mediated inflammation in carcinoma progression. *Proc Natl Acad Sci U S A* **105**, 18936-18941 (2008).
6. Bardor, M., Nguyen, D. H., Diaz, S. & Varki, A. Mechanism of uptake and incorporation of the non-human sialic acid N-glycolylneuraminic acid into human cells. *J Biol Chem* **280**, 4228-4237 (2005).
7. Taylor, R. E. et al. Novel mechanism for the generation of human xeno-autoantibodies against the nonhuman sialic acid N-glycolylneuraminic acid. *J Exp Med* **207**, 1637-1646 (2010).
8. Zola, T. A., Lysenko, E. S. & Weiser, J. N. Natural antibody to conserved targets of Haemophilus influenzae limits colonization of the murine nasopharynx. *Infect Immun* **77**, 3458-3465 (2009).
9. Cober, M. P. & Johnson, C. E. Otitis media: review of the 2004 treatment guidelines. *Ann Pharmacother* **39**, 1879-1887 (2005).
10. Mattos-Guaraldi, A. L., Formiga, L. C. & Andrade, A. F. Trans-sialidase activity for sialic acid incorporation on Corynebacterium diphtheriae. *FEMS Microbiol Lett* **168**, 167-172 (1998).
11. Corfield, T. Bacterial sialidases--roles in pathogenicity and nutrition. *Glycobiology* **2**, 509-521 (1992).
12. Bouchet, V. et al. Host-derived sialic acid is incorporated into Haemophilus influenzae lipopolysaccharide and is a major virulence factor in experimental otitis media. *Proc Natl Acad Sci U S A* **100**, 8898-8903 (2003).
13. MALLEY, A., SAHA, A. & HALLIDAY, W. J. IMMUNOCHEMICAL STUDIES OF HEMOCYANIN FROM THE GIANT KEYHOLE LIMPET (MEGATHURA CRENULATA) AND THE HORSESHOE CRAB (LIMULUS POLYHEMUS). *J Immunol* **95**, 141-147 (1965).
14. Saito, M., Sugano, K. & Nagai, Y. Action of arthrobacter ureafaciens sialidase on sialoglycolipid substrates. *J Biol Chem* **254**, 7845-7854 (1979).
15. Dennis, J. W., Nabi, I. R. & Demetriou, M. Metabolism, cell surface organization, and disease. *Cell* **139**, 1229-1241 (2009).
16. Allen, S., Zaleski, A., Johnston, J. W., Gibson, B. W. & Apicella, M. A. Novel sialic acid transporter of Haemophilus influenzae. *Infect Immun* **73**, 5291-5300 (2005).

17. Severi, E. et al. Sialic acid transport in Haemophilus influenzae is essential for lipopolysaccharide sialylation and serum resistance and is dependent on a novel tripartite ATP-independent periplasmic transporter. *Mol Microbiol* **58**, 1173-1185 (2005).

18. Hood, D. W. et al. Sialic acid in the lipopolysaccharide of Haemophilus influenzae: strain distribution, influence on serum resistance and structural characterization. *Mol Microbiol* **33**, 679-692 (1999).

19. Schilling, B. et al. Biosynthesis of sialylated lipooligosaccharides in Haemophilis ducreyi is dependent on exogenous sialic acid and not mannosamine. Incorporation studies using N-acylmannosamine analogues, N-glycolylneuraminic acid, and 13C-labeled N-acetylneuraminic acid. *Biochemistry* **40**, 12666-12677 (2001).

20. Jurcisek, J. et al. Role of sialic acid and complex carbohydrate biosynthesis in biofilm formation by nontypeable Haemophilus influenzae in the chinchilla middle ear. *Infect Immun* **73**, 3210-3218 (2005).

21. Campagnari, A. A., Gupta, M. R., Dudas, K. C., Murphy, T. F. & Apicella, M. A. Antigenic diversity of lipooligosaccharides of nontypable Haemophilus influenzae. *Infect Immun* **55**, 882-887 (1987).

22. Diaz, S. L. et al. Sensitive and specific detection of the non-human sialic Acid N-glycolylneuraminic acid in human tissues and biotherapeutic products. *PLoS ONE* **4**, e4241 (2009).

23. Khallou-Laschet, J. et al. Atheroprotective effect of adjuvants in apolipoprotein E knockout mice. *Atherosclerosis* **184**, 330-341 (2006).

24. Hansen, P. R. et al. Freunds adjuvant alone is antiatherogenic in apoE-deficient mice and specific immunization against TNFalpha confers no additional benefit. *Atherosclerosis* **158**, 87-94 (2001).

25. Tahara, H. et al. Immunological Property of Antibodies against N-Glycolylneuraminic Acid Epitopes in Cytidine Monophospho-N-Acetylneuraminic Acid Hydroxylase-Deficient Mice. *J Immunol* **184**, 3269-3275 (2010).

26. Bennett, B., Check, I. J., Olsen, M. R. & Hunter, R. L. A comparison of commercially available adjuvants for use in research. *J Immunol Methods* **153**, 31-40 (1992).

27. Teo, C. F. et al. Glycopeptide-specific monoclonal antibodies suggest new roles for O-GlcNAc. *Nat Chem Biol* **6**, 338-343 (2010).

28. Higashi, H. et al. Characterization of N-glycolylneuraminic acid-containing gangliosides as tumor-associated Hanganutziu-Deicher antigen in human colon cancer. *Cancer Res* **45**, 3796-3802 (1985).

29. Verhasselt, V. Oral tolerance in neonates: from basics to potential prevention of allergic disease. *Mucosal Immunol* **3**, 326-333 (2010).

30. Dam, T. K. et al. Binding Studies of {alpha}-GalNAc-specific Lectins to the {alpha}-GalNAc (Tn-antigen) Form of Porcine Submaxillary Mucin and Its Smaller Fragments. *J Biol Chem* **282**, 28256-28263 (2007).

31. Yu, H., Chokhawala, H. A., Varki, A. & Chen, X. Efficient chemoenzymatic synthesis of biotinylated human serum albumin-sialoglycoside conjugates containing O-acetylated sialic acids. *Org Biomol Chem* **5**, 2458-2463 (2007).